Use of Patient-Derived Cellular Models to Investigate the Mechanistic Basis of Circadian Dysfunctions and Chronomodulatory Drugs in Bipolar Disorder

A thesis submitted for the degree of Doctor of Philosophy at the University of Oxford

Trinity Term 2018



Harshmeena Ramesh Sanghani

New College

Department of Pharmacology

Use of Patient-Derived Cellular Models to Investigate the Mechanistic Basis of Circadian Dysfunctions and Chronomodulatory Drugs in Bipolar Disorder

Harshmeena Ramesh Sanghani

A thesis submitted for the degree of Doctor of Philosophy

New College, Department of Pharmacology, University of Oxford

Trinity Term 2018

Abstract

Bipolar disorder is a highly incapacitating neuropsychiatric disorder, where patients exhibit cycling episodes of mania and depression. In addition to these characteristics, sleep and circadian rhythm disruptions are frequently observed through changes in physiology and behaviour. Lithium treatment remains effective in inducing acute and long-term mood stabilisation, yet there is ambiguity as to how it exerts its therapeutic benefits. As lithium induces significant chronomodulatory effects, one possible mechanism may be via the alteration of circadian rhythms. Using virally transduced bipolar patient-derived fibroblasts, we investigated basal circadian rhythms, as well as the cellular responses to chronomodulatory agents in order to identify any aberrancies. We then went on to investigate the mechanism via which lithium induces its chronomodulatory effects.

The use of patient-derived fibroblasts revealed the presence of circadian abnormalities, manifesting as a broad distribution of period lengths. Further, patients with a longer period phenotype exhibited muted chronomodulatory changes following lithium treatment. These changes were not restricted to lithium and were also observed with two novel chronomodulators. Remarkably, these compounds also exhibited changes to circadian rhythms and displayed lithium-like behaviours *in vivo*, highlighting their translational potential. We subsequently went on to confirm that lithium inhibited two major receptor coupled systems: inositol monophosphatase and adenylate cyclase. Using immortalised cell lines, we showed that lithium induces period lengthening predominantly via perturbing the phosphoinositide pathway, which elevates expression of the transcription factor C/EBPα. Whilst we found that adenylate cyclase signalling plays a contributory but subordinate role in mediating period effects, such information may be vital in informing future drug discovery processes, as it could enable the identification of mechanistically novel mood-stabilisers with fewer undesirable side effects. Thus, in this DPhil thesis, we present data highlighting that patient-derived fibroblasts could be instrumental tools which could perpetuate the drug discovery process, and suggest that C/EBPα may be responsible for lithium-induced circadian period lengthening.

Table of Contents

Acknowledgements 7
Abbreviations 8

Chapter 1: General Introduction **11**
1.1 The Discovery of Biological Rhythms 12
1.2 The Mammalian Circadian System 13
1.2.1 The suprachiasmatic nucleus 13
1.2.2 The molecular clock 16
1.2.3 Extra-SCN and peripheral oscillators 19
1.2.4 Photic and non-photic pathways 22
1.2.5 Circadian rhythms in vivo and in vitro 24
1.3 Bipolar Disorder 27
1.4 Sleep and Circadian Rhythm Disruption in Psychiatric Disorders 29
1.4.1 The importance of sleep 29
1.4.2 The consequences of a dysfunctional clock 30
1.4.3 The effects of light on mood 31
1.4.4 Circadian disruptions in bipolar patients 34
1.4.5 Pre-clinical circadian models of bipolar disorder 37
1.5 Pharmacological Treatments for Bipolar Disorder 38
1.5.1 Lithium as a mood-stabiliser 39
1.5.2 Lithium as a therapeutic agent 40
1.5.3 Lithium and circadian rhythms 44
1.6 Aims 48
1.7 References 50

Chapter 2: General Methods **62**
2.1 Cell Culture Techniques 63
2.1.1 Cell culture media 63
2.1.2 Maintenance of cell lines 64
2.2 DNA Cloning with Plasmid Vectors and Bacterial Cell Culture 65
2.2.1 DNA amplification 65
2.2.2 Gateway reaction 66
2.2.3 Bacterial transformation and selection 66
2.2.4 Plasmid preparations 67
2.3 Lentivirus Production 68
2.3.1 Virus detection and concentration 69
2.3.2 Stable cell line generation 70
2.4 ERK ELISA Assay 70
2.5 Luminescence Detection Experiments 71
2.5.1 Transient transfections 71
2.5.2 In vitro siRNA transfections 71
2.5.3 Assessing circadian rhythms 72
2.6 Cellular mRNA Quantification 72
2.6.1 RNA preparation 72
2.6.2 cDNA conversion 73

2.6.3 Real-time PCR 73
2.7 PrestoBlue Assay 74
2.8 Animals 74
2.9 General Data Analysis 74
2.10 General Statistical Analysis 75
2.11 Chapter 3: Methods 76
2.11.1 Growth curves 76
2.11.2 Assessing circadian rhythms 76
2.11.3 Correlograms 76
2.12 Chapter 4: Methods 78
2.12.1 Reagents 78
2.12.2 Assessing circadian rhythms 78
2.12.3 Animal locomotor activity rhythms 78
2.12.4 Open field test and elevated plus maze 79
2.13 Chapter 5: Methods 80
2.13.1 Additional media and reagents 80
2.13.2 Assessing circadian rhythms 82
2.13.3 Analysis of [^{3}H] myo-inositol 82
2.13.4 Cellular mRNA quantification 83
2.13.5 Primers 84
2.13.6 Cignal reporter assay 84
2.13.7 Ex vivo SCN culture 85
2.13.8 Western blotting 86
2.13.9 Mouse brain immunohistochemistry 88
2.14 Chapter 6: Methods 89
2.14.1 Additional media and reagents 89
2.14.2 cAMP-screen chemiluminescence ELISA 90
2.14.3 cAMP::GloSensor assay 90
2.14.4 CRE::*Luc assay* 91
2.14.5 Data analysis 91
2.14.6 Assessing circadian rhythms 91
2.14.7 Cellular mRNA quantification 91
2.14.8 Primers 92

Chapter 3: The Molecular Clocks of Bipolar Patient-Derived Fibroblasts Exhibit Period Length Variability 93
3.1 Introduction 94
3.1.1 The molecular clocks of fibroblasts 94
3.1.2 Bipolar patients and their circadian clocks 97
3.1.3 Aims 99
3.2 Results 100
3.2.1 Subject demographics 100
3.2.2 Optimising lentivirus production 104
3.2.3 Evaluating cellular growth profiles using doubling time 105
3.2.4 Luminometric assessment of circadian parameters via Bmal::Luc expression 109
3.2.5 Patient stratification by Bmal::Luc period length revealed 3 distinct sub-groups 112

3.2.6 Luminometric assessment of Per2::Luc period length 114
3.2.7 Demographic factors cannot account for Per2::Luc period variability 116
3.2.8 Bmal::Luc and Per2::Luc period correlations 118
3.2.9 Correlogram analysis of lithium-treated patients 119
3.2.10 Correlogram analysis of lithium-non-treated patients 121
3.3 Discussion 123
3.3.1 Validity of using bipolar patient fibroblasts and reporter assays 123
3.3.2 Understanding the variability within our subjects 125
3.3.3 The effects of lithium treatment 129
3.3.4 Lithium-treated patients 130
3.3.5 Lithium-non-treated patients 131
3.3.6 Conclusions 132
3.4 References 134

Chapter 4: Pharmacological Modulation of Circadian Rhythms May Influence Mood-Related Behaviours 137
4.1 Introduction 138
4.1.1 Sleep and circadian rhythm disruption in bipolar disorder 138
4.1.2 Pharmacologically targeting circadian genes 140
4.1.3 Lithium 141
4.1.4 Nobiletin and CGS-15943 142
4.1.5 Aims 143
4.2 Results 144
4.2.1 Lithium alters circadian rhythmicity in vitro 144
4.2.2 Lithium does not lengthen period in patients with longer period lengths 146
4.2.3 Lithium increases amplitude in bipolar patient fibroblasts 147
4.2.4 Fibroblasts' lithium response fail to discriminate between lithium-treated and non-treated patients 150
4.2.5 Nobiletin alters circadian rhythmicity in vitro 152
4.2.6 Nobiletin lengthens period in patients with shorter period lengths 153
4.2.7 Nobiletin increases amplitude in bipolar patient fibroblasts 153
4.2.8 CGS-15943 altered circadian rhythmicity in vitro 157
4.2.9 CGS-15943 lengthens period independently of phenotypic period length 158
4.2.10 CGS-15943 increases amplitude in bipolar fibroblasts 159
4.2.11 Changes to circadian rhythmicity are independent of lithium treatment 162
4.2.12 Lithium chloride, nobiletin, and CGS-15943 modulate rhythms in vivo 163
4.2.13 Lithium chloride, nobiletin, and CGS-15943 reduce rearing behaviour 168
4.2.14 Lithium chloride, nobiletin, and CGS-15943 reduce anxiety-related behaviour 170
4.2.15 Period length is correlated with behaviour 172
4.3 Discussion 173
4.3.1 Lithium-induced changes in fibroblast rhythms show the same direction of effect as behavioural changes 173

4.3.2 Fibroblasts can indicate novel drug-induced changes to behavioural rhythms ... 176
4.3.3 Fibroblasts trends associated with lithium sensitivity ... 178
4.3.4 Circadian rhythms as a future biomarker for chronomodulation sensitivity ... 180
4.3.5 Nobiletin and CGS-I5943 modulate rearing behaviours ... 181
4.3.6 Nobiletin and CGS-I5943 modulate anxiety-related behaviours ... 184
4.3.7 Conclusion ... 185
4.4 References ... 187

Chapter 5: Lithium-Induced Perturbations of the Phosphoinositide Cycle Alter Molecular Circadian Rhythms ... 191
5.1 Introduction ... 192
5.1.1 The known circadian consequences of lithium treatment ... 192
5.1.2 Lithium-induced inhibition of inositol monophosphatase ... 193
5.1.3 The inositol depletion hypothesis ... 195
5.1.4 Inositol recycling within the circadian system ... 197
5.1.5 Aims ... 197
5.2 Results ... 198
5.2.1 Cells exhibited differential responses to LiCl treatment ... 198
5.2.2 Inositol-less media potentiated period lengthening ... 199
5.2.3 Inositol-depletion potentiated LiCl-induced period change ... 202
5.2.4 Myo-inositol did not rescue LiCl-induced period effects in vitro ... 204
5.2.5 LiCl reduced cellular myo-inositol entry ... 205
5.2.6 Small molecule IMPase inhibitors partially mimicked the effects of LiCl ... 207
5.2.7 Myo-inositol rescued small molecule induced period lengthening ... 209
5.2.8 L690,488 mimics lithium-induced changes in circadian gene expression ... 210
5.2.9 Impa1 siRNA induced modest period changes in vitro ... 212
5.2.10 Isyna1 siRNA induced modest period changes in vitro ... 213
5.2.11 Understanding the downstream consequences of IMPase inhibition ... 216
5.2.12 Reducing P-ERK does not normalise period lengthening ... 218
5.2.13 C/EBP may play a role in inducing period lengthening ... 220
5.2.14 Myo-inositol reduced LiCl-induced period change in SCN slice cultures ... 223
5.2.15 IMPase is enriched in the master clock ... 225
5.3 Discussion ... 228
5.3.1 Understanding the cell-type specific responses ... 228
5.3.2 Inositol-less media exacerbated period lengthening ... 230
5.3.3 The effects of IMPase inhibition on the molecular clock ... 232
5.3.4 Moderate lithium-like effects observed with Impa1 knockdown ... 233
5.3.5 The role of ERK in modulating rhythms ... 235
5.3.6 The role of C/EBP in modulating rhythms ... 236
5.3.7 Myo-inositol rescue in vitro and ex vivo ... 240
5.3.8 Conclusions ... 241
5.4 References ... 243

Chapter 6: *In Vitro* Modulation of the Adenylate Cyclase Pathway Influences Molecular Circadian Rhythmicity 248

6.1 Introduction 249
6.1.1 The adenylate cyclase pathway 249
6.1.2 The role of adenylate cyclase signalling in regulating circadian rhythms 253
6.1.3 The role of adenylate cyclase signalling in bipolar disorder 254
6.1.4 Aims 256
6.2 Results 257
6.2.1 LiCl reduces cAMP and CREB activity in the MMHD3 cells 257
6.2.2 Vidarabine lengthens period in the U2OS cells 259
6.2.3 Vidarabine lengthens period in the MMHD3 cells 261
6.2.4 2'5'-dideoxyadenosine lengthens period in the U2OS cells 263
6.2.5 2'5'-dideoxyadenosine lengthens period in the MMHD3 cells 265
6.2.6 Adenylate cyclase 6 is responsible for period lengthening in the MMHD3 cells 267
6.2.7 H89 lengthens period in the U2OS cells 269
6.2.8 H89 lengthens period in the MMHD3 cells 271
6.2.9 CBP112 induced period lengthening in the U2OS cells 271
6.2.10 CBP112 induced period lengthening in the MMHD3 cells 273
6.2.11 CBP30 induced period lengthening in the U2OS cells 276
6.2.12 CBP30 induced period lengthening in the MMHD3 cells 276
6.2.13 Increased CREB suppression increases period lengthening 279
6.2.14 Period lengthening is independent of P-ERK activity 280
6.3 Discussion 282
6.3.1 The significance of adenylate cyclase and group III isoforms 282
6.3.2 Modulation of CREB activity 287
6.3.3 The effects of targeting adenylate cyclase signalling in vivo 290
6.3.4 Rhythmicity within the adenylate cyclase pathway 292
6.3.5 Conclusions 293
6.4 References 295

Chapter 7: General Discussion 301

7.1 The Broad View of Bipolar Disorder 302
7.2 The Major Investigative Outcomes 303
7.3 Fibroblasts as Peripheral Clocks 303
7.3.1 Fibroblasts in comparison to the SCN model 304
7.3.2 The 3R's objective 306
7.4 How Chronomodulation can Lead to Mood Modulation 308
7.4.1 Neurotransmitter systems 309
7.4.2 Receptor-coupled signalling pathways 311
7.5 The Mechanistic Pathways of Lithium-Induced Period Lengthening 312
7.5.1 Pre-hepatocytes in comparison to the SCN as model system 312
7.5.2 Lithium concentration in vitro and in vivo 313
7.5.3 IMPase over adenylate cyclase 315
7.6 Future Research Directions 316
7.7 Final Overviews 318
7.8 References 320

Acknowledgements

I would like to extend my appreciation to the NC3Rs for funding this DPhil. Over the last four years, I have received advice and assistance from numerous people, for which I am forever grateful!

I would firstly like to thank my DPhil supervisor, Dr. Sridhar Vasudevan for all his invaluable advice, energy, and patience. A thanks also goes to Sri for teaching me the basic skills required for cellular circadian research. The door to Sri's office was always open whenever I came across any hurdles. His continuous enthusiastic and light-hearted attitude has made this a thoroughly enjoyable few years, for which I feel incredibly fortunate.

I would also like to extend a thanks to Prof. Grant Churchill along with the past and present members of the Vasudevan Lab including: Dr. Dorota Nawrot, Farid Ebrahimjee, Dragos Mosneagu, and Zeinab Wakkaf, for their support and creating a work environment that was filled with laughter. I have also received excellent advice and guidance from Prof. Aarti Jagannath and members of the Jagannath Lab, particularly with the *in vivo* aspects of my DPhil, for which I am very thankful.

On a more personal note, many thanks go to my friends and family in London, Manchester, and Oxford for the laughs, the much needed drinks, and moral support, including (and in no particular order): Anita Valji, Ashvanti Valji, Himanshu Valji, Rhys Pryce, Sonal Varsani, Shaheni Patel, Bhavisha Pethani, Jaina Patel, Roshni Patel, Kavita Kerai, and Jessica Virji.

Last but not least, I would like to thank my mother Lalita, father Ramesh, sisters Aniksha and Shaniya, and grandparents Karsanbhai and Dhanbai for their unwavering support and encouragement throughout my time at Oxford.

Abbreviations

5-HT	serotonin
AC	adenylate cyclase
ADMEM	Advanced Dulbecco's Modified Eagle's Medium
Afh	afterhour
BBB	blood-brain barrier
bHLH	basic helix-loop-helix
BMAL1/2	brain and muscle ARNT-like protein 1/2
BPD	bipolar disorder
BPI	bipolar I disorder
BPII	bipolar II disorder
C/EBP	CCAAT-enhancer binding proteins
cAMP	cyclic adenosine monophosphate
CBP	CREB-binding protein
CLOCK	circadian locomotor output cycles kaput
CRE	cAMP response element
CREB	cAMP response element-binding protein
CRY1/2	cryptochrome 1/2
CSNK1ε/δ	casein kinase 1ε/δ
CT	circadian time
C_T	threshold cycle
DAG	diacylglycerol
DD	constant darkness
DEC1/2	deleted in esophageal cancer 1/2
DMEM	Dulbecco's Modified Eagle's Medium
DSM-V	Diagnostic and Statistical Manual of Mental Disorders V
EPM	elevated plus maze
ERK	extracellular signal–regulated kinase
FBS	fetal bovine serum
FBXL3	F-box/LRR-repeat protein 3
GABA	γ-aminobutyric acid
GFP	green fluorescent protein
GSK3β	glycogen synthase kinase 3β
h	hour

HCN	hyperpolarization-activated cyclic nucleotide-gated channels
HPA	hypothalamic-pituitary-adrenal
i.p.	intraperitoneally
ICD-10	International Statistical Classification of Diseases and Related Health Problems 10
IMPase	inositol monophosphatase
IP	inositol monophosphate
IP2	phosphatidylinositol 4,5-bisphosphate
IP3	inositol 1,4,5-trisphosphate
IPPase	inositol polyphosphate 1-phosphatase
ipRGCs	intrinsically photosensitive retinal ganglion cells
ISYNA1	inositol-3-phosphate synthase 1
LD	light-dark
Li-NT	lithium-non-treated
Li-T	lithium-treated
LiCl	lithium chloride
Luc	luciferase
Maoa	monoamine oxidase A
MAPK	mitogen-activated protein kinase
min	minute
NaCl	sodium chloride
NC3Rs	National Centre for the Replacement, Refinement and Reduction of Animals in Research
NPAS2	neuronal PAS domain protein
OFT	open field test
P/S	penicillin-streptomycin
PACAP	pituitary adenylate cyclase-activating polypeptide
PBS	Dulbecco's phosphate-buffered saline
PDT	population doubling time
PEI	polyethyleneimine
PER1/2/3	period 1/2/3
PI	phosphoinositide
PIP2	phosphatidylinositol 4,5-bisphosphate
PKA	protein kinase A
PKC	protein kinase C
PLC	phospholipase C

PMA	phorbol 12-myristate 13-acetate
REV-ERBα	reverse erythroblastosis virus α
RHT	retinohypothalamic tract
RORα	retinoid-related orphan receptor α
RPMI	Roswell Park Memorial Institute
s	second
SAD	seasonal affective disorder
SCN	suprachiasmatic nucleus
SD	standard deviation
SEM	standard error of the mean
SMIT	sodium myo-inositol co-transporters
Th	tyrosine hydroxylase
TTFL	transcriptional translational feedback loops
VIP	vasoactive intestinal polypeptide
WHO	World Health Organisation

Chapter 1: General Introduction

1. General Introduction

The overall purpose of this DPhil thesis was to gain a better understanding of the circadian abnormalities associated with bipolar disorder (BPD) and the mechanism via which lithium induces chronomodulation.

1.1 The Discovery of Biological Rhythms

The predictable nature of the sun rising at dawn and setting at dusk is associated with regular environmental changes and has enabled the generation of biological rhythms. Almost every organism on earth, ranging from cyanobacteria and plants to complex primates, displays some form of a rhythm (Bell-Pedersen et al., 2005). Circadian rhythms are one such example; they are a 24-hour (h) phenomenon adapted from the earth's rotation upon its axis resulting in two discrete time periods- daytime and night-time. This light-dark (LD) cycle is associated with regular and anticipated changes in light intensity, temperature, and food availability, allowing organisms to optimise physiological functions in a time-dependent manner. Remarkably, the circadian system is not limited to modulating sleep-wake behaviour; it exerts an effect on a plethora of physiological and metabolic functions, including blood pressure, body temperature, hormones, and mood (Hastings et al., 2003).

A daily pattern has a circadian rhythm if it meets the following criteria: 1) the fluctuations observed repeats every 24h at the same approximate time of day, 2) the rhythm is generated endogenously and therefore persists in the absence of external time cues (*zeitgebers*) such as light, and 3) the rhythm is entrainable, meaning it has a determined phase relationship with external

settings and can be re-set upon exposure to stimuli, thereby giving a true representation of the environment (Bünning, 1971, Daan and Pittendrigh, 1976).

The following criteria were established following decades of research, although the initial observations occurred in 1729, by Jean Jacques d'Ortous de Mairan. De Mairan visually observed the presence of recurring 24h changes in the *Mimosa pudica* plant, where the leaves opened during the day and closed at night. Moreover, these patterns persisted under constant darkness, revealing the presence of an endogenous timekeeper in plants (DeMairan, 1729). Consequently, by accurately monitoring leaf movements through the use of a kymograph, Erwin Bünning in the 1930s confirmed the existence of a plant-based 'biological clock' and indeed coined the term itself (Bünning, 1971, Todman, 2007). Subsequently, between the 1950s-1960s, pioneering work by Colin Pittendrigh and Jürgen Aschoff culminated in the understanding that mammals including humans have biological clocks, and that circadian rhythms are entrainable (Daan and Pittendrigh, 1976, Aschoff, 1965).

1.2 The Mammalian Circadian System

1.2.1 The suprachiasmatic nucleus

The complex biological nature of mammals has resulted in the formation of a hierarchical circadian system that helps to maintain bodily rhythmicity. At the heart of this system is the suprachiasmatic nucleus (SCN) of the anterior hypothalamus, the master mammalian pacemaker (Weaver, 1998). Lying above the optic chiasm and lateral to the third ventricle, the SCN is formed of bilateral symmetrical nuclei, as seen in *Figure 1.1A*. Whilst the human SCN contains

approximately 45,000-50,000 densely packed neurones, the rodent SCN comprises 15,000-20,000 neurones, each around 10μM in diameter, and it is these neurones which form the robust and self-sufficient master clock (Hofman et al., 1988, Welsh et al., 2010, van den Pol, 1980).

The localised function of the master clock was established when bilateral ablation of the nuclei deteriorated rhythms in activity, drinking, and corticosterone (Moore and Eichler, 1972, Stephan and Zucker, 1972). As only the nuclei of the SCN were lesioned, this provided the foundations of what we now understand to be the role of the master clock. Subsequent experiments by Ralph et al., showed the restoration of behavioural circadian rhythms in hamsters with ablated SCN through neural transplantation from a foetal donor. Moreover, they established that periodicity of the animal was dependent upon the cells in the newly transplanted SCN tissue, highlighting the autonomy and strength of the SCN oscillators (Ralph et al., 1990). The SCN was then confirmed to ensure a survival advantage as a lesioned circadian clock rendered animals at a greater risk of mortality from predator attack due to inappropriately timed activity (DeCoursey et al., 1997, DeCoursey et al., 2000).

In vivo electrophysiological techniques revealed that when comparing spontaneous hypothalamic electrical activity within and outside the SCN, they were diametrically opposite (Inouye and Kawamura, 1979). This was further supported by *ex vivo* and *in vitro* findings, which showed that SCN rhythmic electrical activity peaked during the subjective day whilst the animal would have slept and troughed at night (Green and Gillette, 1982, Shibata et al., 1982, Ding et al., 1994). Whilst this is specific to nocturnal animals, it is not surprising given

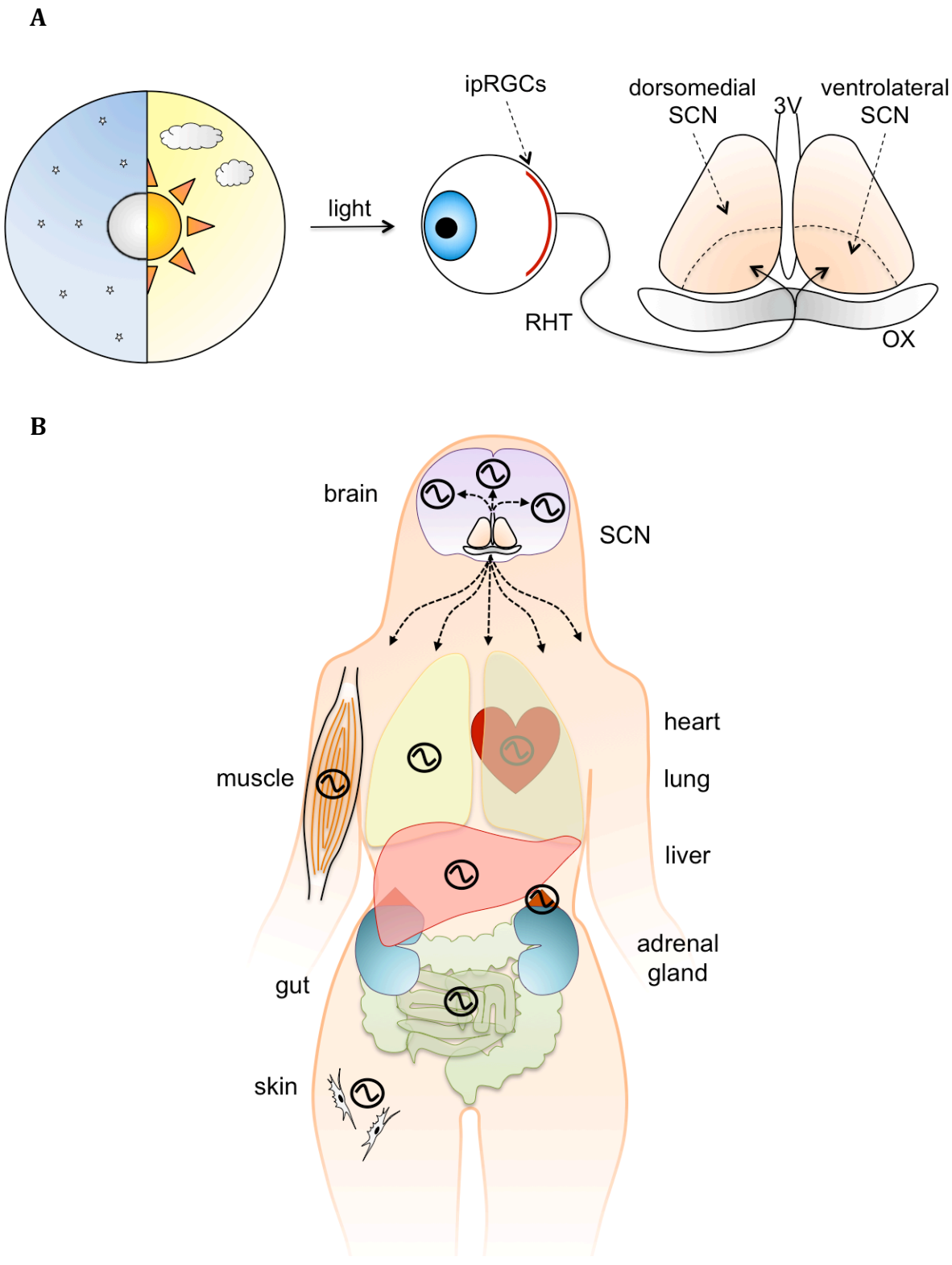

***Figure 1.1*. Schematic representation of the photic input pathway. A)** Light from the environment enters the retina where the ipRGCs transmit this information via the RHT to the SCN. **B)** The SCN then relays time-of-day information to multiple extra-SCN neural and peripheral oscillations, including the heart, liver, and lungs. OX: optic chiasm, 3V: third ventricle, : clock-containing organ, other abbreviations can be found in the text.

that light depolarises SCN cells through the synaptic release of glutamate (Castel et al., 1993). Interestingly, analysis of cultured SCN neurones revealed that the cells were intimately synchronised as the application of tetrodotoxin, a sodium channel blocker, was capable of destroying cell-cell communication resulting in asynchronous rhythm generation without altering individual cellular rhythms (Shibata and Moore, 1993). This confirmed that whilst each neurone has the capability of being self-sustainable, communication via action potentials is vital for coupling and generation of a coherent rhythmic output. Indeed, glial cells also contribute towards circadian timekeeping as recent evidence found that SCN astrocytes displayed antiphasic activity to SCN neurones as a means of regulating extracellular glutamate concentrations (Brancaccio et al., 2017).

1.2.2 The molecular clock

The SCN neurones display cell-autonomous circadian properties as they contain individual pacemakers capable of generating 24h rhythms. Daily changes in clock gene expression underlie the uniform mechanism found throughout the brain and body and are thought to drive circadian rhythms through the formation of multiple interlocking transcriptional translational feedback loops (TTFL) (Takahashi, 2017). The importance surrounding the molecular clockwork was recently acknowledged as the 2017 Nobel Prize in Physiology or Medicine was awarded to Hall, Rosbash, and Young for uncovering similar mechanisms in *Drosophila melanogaster*, which led to the understanding of the mammalian clock as we know it (Dibner and Schibler, 2018).

The primary TTFL is composed of four key components: circadian locomotor output cycles kaput (CLOCK), brain and muscle ARNT-like protein 1/2

(BMAL1/2) (also known as aryl hydrocarbon receptor nuclear translocator like or ARNTL), period 1/2/3 (PER1/2/3), and cryptochrome 1/2 (CRY1/2). During the day CLOCK and BMAL1 heterodimerise and bind to E-box elements of target genes at the canonical recognition sequence CACGTG (King et al., 1997b, Gekakis et al., 1998). This is functionally achievable as these components belong to the basic helix-loop-helix (bHLH)-PAS transcription factor family, allowing both protein-DNA and protein-protein interactions (Shearman et al., 1999). The dimer where CLOCK is constitutively expressed and BMAL1 is rhythmically expressed then induce the rhythmic transcription of multiple genes including the repressors of the clock, the *Per* and *Cry* genes (Gekakis et al., 1998, Kume et al., 1999, Sato et al., 2006). Transcript *Per* and *Cry* mRNA levels rise during the day, followed by subsequent translation and translocation to the nucleus. These elements then form PER-PER or PER-CRY dimers and inhibit the actions of the CLOCK-BMAL1 complex (Takahashi, 2017). Interestingly, 43% of the mammalian protein-coding transcriptome is under the control of the clock, showing 24h oscillatory patterns in a tissue specific manner, highlighting its power in regulating multiple bodily functions (Zhang et al., 2014). In order for the cycle to start anew every 24h, the PER and CRY proteins are phosphorylated and ubiquitinated by casein kinase 1ε/δ (CSNK1ε/δ) or F-box/LRR-repeat protein 3 (FBXL3) respectively, such that proteosome-mediated degradation can occur (*Figure 1.2*) (Lowrey et al., 2000, Akashi et al., 2002, Godinho et al., 2007).

An interlocking secondary TTFL controls the expression of *Bmal1* through the nuclear receptors reverse erythroblastosis virus α (REV-ERBα) (also known as nuclear receptor subfamily 1, group d, member 1 or NR1D1) and retinoid-

related orphan receptor α (RORα), as seen in *Figure 1.2*. These proteins competitively bind to retinoic acid-related orphan receptor response elements in the *Bmal1* promoter region, inducing gene repression or gene transcription respectively (Akashi and Takumi, 2005, Guillaumond et al., 2005). Moreover, both *Rev-ervbα* and *Rorα* possess E-box elements and are thus under the control of CLOCK-BMAL1 mediated transcription. Their mRNA levels oscillate temporally to boost or suppress *Bmal1* in a manner congruent with the core clock (Sato et al., 2004, Guillaumond et al., 2005).

Finally, the tertiary TTFL consists of the bHLH-PAS transcription factor deleted in esophageal cancer 1/2 (DEC1/2) (also known as basic helix-loop-helix family member E40/E41 or BHLHE40/41). *Dec1/2* are also under the control of the CLOCK-BMAL complex, as well as RORα-mediated gene transcription, and therefore show rhythmic expression patterns which peak during the light phase (Honma et al., 2002, Ozaki et al., 2012). These additional TTFL proteins contribute to the molecular clock by suppressing CLOCK-BMAL1 mediated gene transcription of *Per* through both E-box competition and BMAL1 protein binding (Honma et al., 2002). Such accessory loops are vital in enabling the clock to be more durable and resilient to perturbations from external influencers.

Use of genetically modified mice, whereby one or more of the core clock genes were deleted has revealed functional redundancy amongst the genes. Deletion of either the *Per1* or *Per2* gene resulted in a gradual loss of rhythmicity, however the behavioural circadian rhythm appeared unaltered in *Per3* deficient mice (Shearman et al., 2000, Bae et al., 2001). However, deletion of both *Per1* and *Per2* resulted in immediate arrhythmicity, suggesting that the *Per1* and *Per2*

genes are partially functionally redundant (Bae et al., 2001). Similarly, removal of the *Cry1* and *Cry2* genes resulted in a shorter circadian period of 22.5h or longer period of 24.6h respectively. As double knockout studies showed immediate arrhythmicity, the *Cry* genes also exhibit partial redundancy (van der Horst et al., 1999, Vitaterna et al., 1999).

Interestingly, no functional redundancy was observed with *Bmal1*, as removal of this gene rendered the animal totally arrhythmic. Whilst there is a gene encoding *Bmal2*, its expression levels are 20% lower and also under the control of BMAL1 (Bunger et al., 2000). Therefore, abnormalities in *Bmal1* will have a consequential effect on *Bmal2*. *Clock* deficient mice however, display grossly normal behavioural circadian rhythms. It is currently believed that CLOCK and the sequence similar bHLH-PAS transcription factor neuronal PAS domain protein (NPAS2), are functionally redundant as NPAS2 deficient mice also displayed regular rhythmic behaviour and double knockout mice display immediate arrhythmicity (DeBruyne et al., 2007, Landgraf et al., 2016).

1.2.3 Extra-SCN and peripheral oscillators

As previously mentioned, the molecular clock is not unique to the cells of the SCN but is found in extra-SCN neuronal and peripheral tissues, as seen in *Figure 1.1B*. The hierarchical organisation of the circadian system allows us to divide such oscillators into 2 categories: master and slave oscillators (Balsalobre, 2002). Subordinate oscillators have been identified in most bodily regions including the cornea, liver, pineal gland, pituitary glands, kidneys, lungs, heart, muscle, and skin. Indeed, cultured cell lines also display circadian rhythms,

highlighting the highly conserved nature of the clock (Abe et al., 2002, Yoo et al., 2004, Balsalobre et al., 1998).

Interestingly, cell and tissue specific differences in circadian rhythms have been observed. For example, despite the presence of a molecular clock, many peripheral tissues oscillate for fewer cycles than the SCN and become asynchronous without regular input from a synchronising agent such as the SCN. This is because, whilst the clocks within cells are still oscillating with a 24h pattern, there is a lack of cell-to-cell communication aiding organ-specific synchrony (Balsalobre et al., 1998). Furthermore, knocking down the core clock genes (*Clock, Npas2*, *Bmal*, *Per, Cry)* or the accessory genes (*Rev-erbα/β*, *Fbxl3*) induced differential circadian effects in cultured murine NIH-3T3 fibroblasts, murine 3T3-L1 adipocytes, murine MMHD3 hepatocytes, and human U2OS osteosarcoma cells (Ramanathan et al., 2014). This information, together with the evidence noting phase differences in clock gene expression within different cultured tissues, suggests that whilst many cells contain the molecular clock machinery, cell-to-cell differences are apparent and may indicate differences in cellular functions (Yoo et al., 2004).

The molecular clock machinery can act to optimise organ-specific functions to the appropriate time-of-day, thereby allowing the conservation of resources. It was found that 3-16% of protein-coding transcripts have circadian expression profiles in any single tissue, where the liver contained the highest number of oscillating genes (Zhang et al., 2014). Indeed, numerous genes and proteins regulating neurotransmitter synthesis and behaviour such as monoamine oxidase A (*Maoa)*, tyrosine hydroxylase (*Th*), and tryptophan

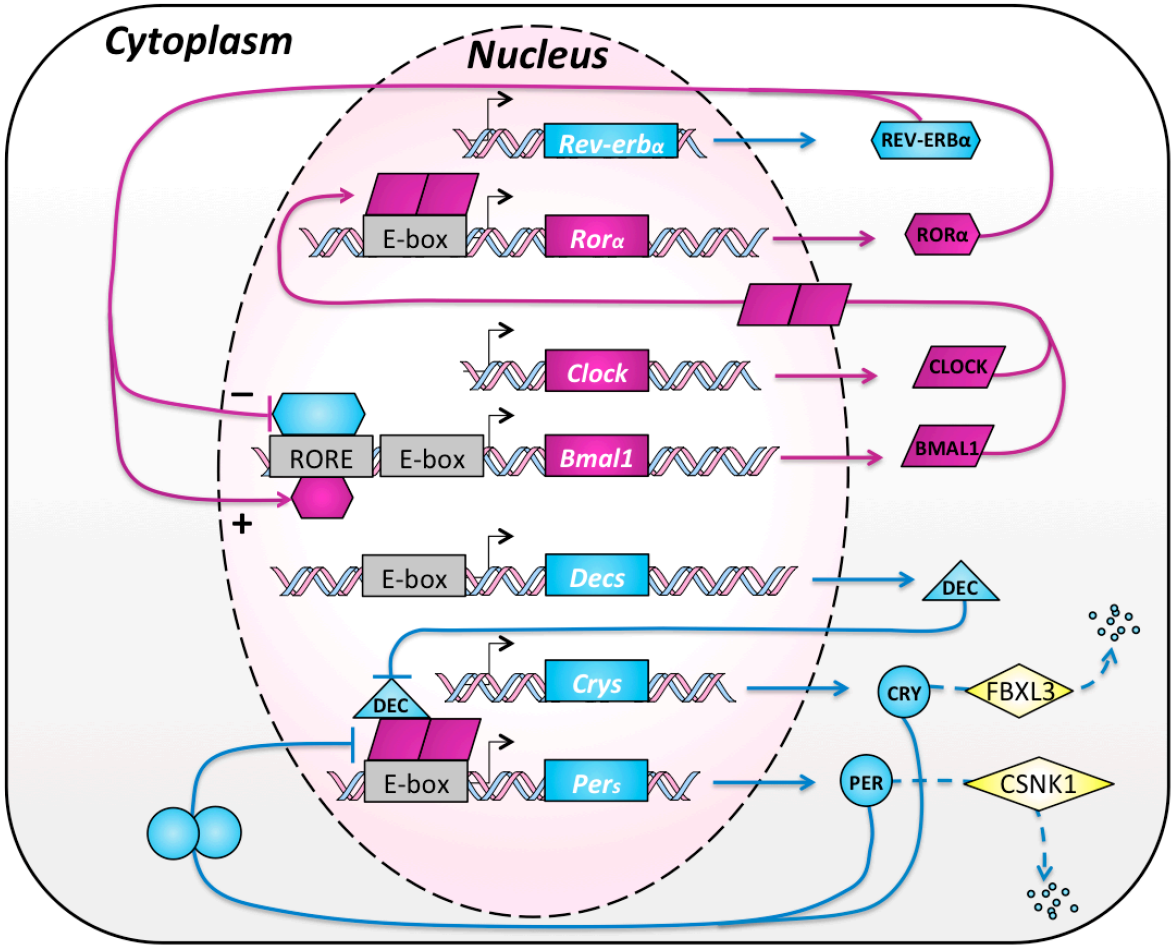

***Figure 1.2*. Schematic representation of the molecular clock.** The core TTFL is composed of CLOCK and BMAL1 binding to E-box elements and driving the transcription of its own repressors, *Per* and *Cry*. In order for the cycle to continue, the PER and CRY proteins are phosphorylated and then ubiquitinated by CSNK1δ and FBXL3 respectively, to enable proteasome-mediated degradation. A secondary loop consists of RORα and REV-ERBα activating or repressing *Bmal1* gene transcription respectively. Finally, DEC proteins function via repression of *Per* gene transcription. This is a simplification of the mechanism is found in all clock containing cells, where cell-type specific differences are apparent. Abbreviations can be found in the text.

hydroxylase, as well as humoral factors such as glucocorticoids and melatonin, show rhythmic expression patterns (Cahill and Ehret, 1981, Hampp et al., 2008, Weitzman et al., 1971, Lewy and Markey, 1978). These rhythms are all consequences of the master clock and the cellular TTFLs, emphasising the role of the clock in maintaining physiology.

1.2.4 Photic and non-photic pathways

The endogenous circadian period of most organisms is genetically predetermined and is ~24h. However, humans have a true period that runs longer at 24.5h, and mice have a clock that is shorter at 23.5h (Czeisler et al., 1999, Carskadon et al., 1999, Yoo et al., 2004). *Zeitgebers* exist in the form of any daily fluctuating exogenous cue that has the potential to entrain circadian rhythms. Due to deviations of organismal periods from the 24h day, *zeitgebers* are vital in ensuring daily entrainment and transduce their effects on the SCN through distinct well-characterised pathways (van Esseveldt et al., 2000).

The photic input pathway is of principal importance as light is a dominant *zeitgeber*. As seen in *Figure 1.1A*, photic information from the external environment is received by the intrinsically photosensitive retinal ganglion cells (ipRGCs) (Berson et al., 2002). This distinct population, comprising only 1-2% of all RGCs is unique as the cells contain the novel photopigment melanopsin, a pigment predominantly sensitive to blue wavelengths of light (λ_{max} =~480nm) (Provencio et al., 1998, Lucas et al., 2003). Labelling of these ipRGC populations revealed that their cellular axons converge at the optic disc to form the retinohypothalamic tract (RHT), establishing the input route to the non-vision forming visual system (Hattar et al., 2002, Lucas et al., 2003).

Many cells from the RHT then monosynaptically innervate neurones of the SCN through the release of synaptic glutamate and pituitary adenylate cyclase-activating polypeptide (PACAP) (Castel et al., 1993, Chen et al., 1999). The SCN is anatomically and functionally divided into two regions: the ventrolateral or core SCN and the dorsomedial or shell SCN. Neurochemical heterogeneity suggests that the two regions serve opposing purposes (Abrahamson and Moore, 2001, Mai et al., 1991). Being ideally situated close to the optic chiasm, many core neurones are retino-recipient. An important neuropeptide involved in the transmission of photic information and circadian entrainment is vasoactive intestinal polypeptide (VIP) and is found in approximately 10% of all SCN neurones (Tanaka et al., 1993, Welsh et al., 2010). VIP exerts its actions predominantly via VPAC2, a cognate receptor found in a third of the VIP expressing core neurones. VIP is involved with relaying time-of-day information to subsequent brain regions including the dorsomedial SCN, thereby facilitating photic entrainment (Kallo et al., 2004, Piggins et al., 1995, Reed et al., 2001). Up to 50% of the shell neurones that predominantly express arginine vasopressin also express the VPAC2 receptor and therefore provide a means for aiding intra-SCN communication (Kallo et al., 2004). The vasopressin neurones serve as one of the output signals of the clock and communicate with subsequent brain regions, as a means of synchronising bodily cells, tissues, and organs (Kalsbeek et al., 2010).

Two subordinate input routes to the SCN form the non-photic input pathways. Non-photic *zeitgebers* can vary from food, sound, and temperature to exercise and social events (Sharma and Chandrashekaran, 2005). Neurones of

the intergeniculate leaflet of the visual thalamus form the geniculohypothalamic tract and innervate SCN neurones through the release of neuropeptide Y and γ-aminobutyric acid (GABA) (Swanson et al., 1974, Francoisbellan and Bosler, 1992, Biello et al., 1994). Additionally, cells from the median raphe innervate the SCN through the release of serotonin (5-HT) (Bosler and Beaudet, 1985, Francoisbellan and Bosler, 1992). Unlike the neurones of the RHT that are predominantly excitatory, input via the non-photic pathway induces hyperpolerisation, thereby suppressing neuronal activity (Schaap and Meijer, 2001, Biello et al., 1997). Thus, it stands to reason that depolarising stimuli are more effective when the cells are hyperpolarised (night-time) and vice versa. It should also be noted that additional input pathways to the SCN exist, for example from the dopaminergic neurones of the ventral tegmental area, a region implicated in mediating reward responses, adding a further layer of complexity to the maintenance of *in vivo* rhythms (Grippo et al., 2017).

1.2.5 Circadian rhythms in vivo and in vitro

The actions of the molecular clock can be observed through both *in vivo* and *in vitro* means. Typically rodent behavioural assessments are performed through the analysis of wheel-running locomotor activity as this is one of the most precise overt rhythms which accurately represents the endogenous rhythms set by the SCN (Jud et al., 2005). Mice present as valuable species for such tests due to their size, similarities in circadian anatomy, and means of genetic manipulation. However, as such rodents are nocturnal, the majority of their locomotor activity occurs during the dark phase of the LD cycle, yet the molecular phase of the circadian clock is consistent with diurnal species

(Mrosovsky et al., 2001, Caldelas et al., 2003, Ripperger et al., 2011). The discovery of peripheral clocks along with progressions in molecular genetic technologies has resulted in the production of bioluminescent clock gene reporters. Components of the molecular clock such as *Per2* are tagged to the luciferase (*Luc*) gene to form a novel construct (*Per2::Luc*) (Ueda et al., 2002, Izumo et al., 2003). Through monitoring the emission of photons across the 24h day for multiple days in transfected cell lines, this visible reporter system has created an excellent marker for observing gene expression changes in cultured cells (Izumo et al., 2003). Moreover, the PER2::LUC fusion protein mouse model whereby the original *Per* gene was replaced with a luciferase flagged *Per* gene, has allowed analysis of clock proteins within the SCN and indeed all clock containing cells and tissues (Yoo et al., 2004). The use of whole animals, explant tissues, and cultured cells has allowed us to analyse key circadian parameters with greater ease (summarised in *Figure 1.3B*).

As mentioned previously, the period of circadian rhythms is typically 24h. This can be assessed *in vivo* through the monitoring of daily locomotor activity onset under constant darkness (DD), an environmental condition where the animals do not experience the light portion of the LD cycle. Under DD, animals show free-running behaviour; an indirect measure of the true endogenous period without manipulation from *zeitgebers* (Jud et al., 2005). *In vitro*, this is denoted by the time between two peaks (or troughs) of an oscillation, as this is the time taken for one complete TTFL cycle (Izumo et al., 2003).

The second parameter of interest is amplitude which denotes the strength of the rhythm, where a large amplitude is indicative of strong day-night

differences. *In vivo*, this is observed through the regularity of activity onset, where arrhythmic animals would have varying onset times and therefore lower amplitudes (Siepka and Takahashi, 2005). *In vitro* observations of changes in the peak to trough of an oscillation show rhythm amplitude, where cultures containing stronger oscillators have larger amplitudes (Izumo et al., 2003).

The final feature is phase, which denotes the relationship between the endogenous rhythms and external *zeitgebers*. The relationship between light and phase becomes apparent under DD when animals are exposed to inappropriately timed light. A pulse of light introduced during the early subjective night (a time which corresponds to the night phase of the LD cycle under constant conditions) induces a phase delay; the animal starts its activity later the following day as the clock has been informed of the presence of light at a later time than anticipated. Similarly, a late night light pulse induces a phase advance, where light during the subjective day induces no effect (Watanabe et al., 2001, Best et al., 1999, Takahashi et al., 1984). Non-photic *zeitgebers* on the other hand show the opposite effects. The presence of arousal stimuli during the latter half of subjective day result in phase advances, as the clock recognises that the resting phase has ended early, where stimuli during the active phase show no effect (Mrosovsky et al., 1992). Such experiments have allowed the construction of the phase response curve, illustrating the importance of SCN gating properties, as clock resetting is phase-dependent. *In vitro* observations of phase advances and delays are seen through leftward and rightward shifts in the oscillations respectively (Brown et al., 2008). Together, these parameters allow a means of in depth analysis of circadian rhythms from a cell culture to whole animal level.

1.3 Bipolar Disorder

BPD is a chronic, heterogeneous, and highly heritable mood disorder currently thought to affect approximately 1-2% of the global population and is declared the 12th leading cause of disability by the World Health Organisation (WHO) (Craddock and Sklar, 2013, Merikangas et al., 2011, World Health Organisation, 2008). The disorder costs the United Kingdom National Health Service over £300 million a year, emphasising that this is a disorder which not only affects quality of life, but is also a substantial economic burden (Young et al., 2011). The disorder is primarily distinguished from other psychiatric disorders by the dual nature of the illness; it is composed of manic and depressive phases. The manic pole consists of abnormally elevated mood and energy including feeling of grandeur and euphoria, as well as hyperactivity and increased risk-taking behaviour, along with reduced anxiety and sleep needs (Cassidy et al., 1998, Young et al., 2007). The depressive phase is the extreme opposite and is associated with low mood including feelings of irritability, anxiety, and anhedonia with daily bouts of insomnia or hypersomnia (American Psychiatric Association, 2013, World Health Organisation, 2014, Phillips and Kupfer, 2013). Moreover, psychosis, which can manifest as hallucinations, delusions, or thought disorders is a phase-independent trait present in 50% patients and if left unaddressed could result in hospitalisation (Dunayevich and Keck, 2000). Cycling between extreme emotions can vary from days to weeks and months, where mood episodes often cycle with euthymia, a period of mood stability (Phillips and Kupfer, 2013).

The Diagnostic and Statistical Manual of Mental Disorders V (DSM-V) produced by the American Psychiatric Association is a fundamental tool used by psychiatrists for diagnostic purposes. As BPD is a spectrum of disorders, heterogeneity has resulted in difficulties identifying the underlying biological issues and subsequently resulted in treatment difficulties. Thus, patients have been subcategorised based on disease severity, phenotype, and symptomology in order to provide better treatments. The manual divides BPD into multiple distinct subclasses where the majority of individuals fall under bipolar I disorder (BPI) or bipolar II disorder (BPII), with prevalence rates of 0.6% or 0.4% respectively (Merikangas et al., 2011, American Psychiatric Association, 2013). BPI diagnosis is distinguished by the presence of a single major manic episode followed by bouts of major depressive episodes, where BPII is associated with major depressive episodes which cycle with periods of hypomania, a less debilitating form of mania (American Psychiatric Association, 2013). This general classification is also found in the International Statistical Classification of Diseases and Related Health Problems 10 (ICD-10), a system used by the WHO (World Health Organisation, 2014).

BPD is unique when compared to other neuropsychiatric conditions, as it is also associated with very high mortality rates as a result of suicidal ideation and action. It was found that up to 60% of patients have suicidal thoughts where an epidemiological study revealed that 29% of patients have attempted suicide at least once in their lifetime, a figure which doubles the rates associated with unipolar depression (Chen and Dilsaver, 1996, Valtonen et al., 2005). This may be due to the complex nature of the disorder. Patients not only attempt suicide

when experiencing major depressive episodes as seen with unipolar depression, but also during extreme manic phases (Valtonen et al., 2005). Mania is associated with behavioural abnormalities including risk-taking and impulsivity, where actions are performed without forethought, both of which can influence suicidality (Swann et al., 2003, Michaelis et al., 2004). Thus, BPD is potentially lethal despite the phase of the disorder, emphasising the need to maintain euthymia through effective acute and long-term treatment options.

The neurobiology thought to underlie BPD is multifaceted and complex. Whilst the behavioural symptoms associated with BPD are well characterised, there is still a lack of understanding surrounding the core pathophysiology. This has resulted in a lack of novel treatment options as well as BPD biomarkers, increasing the difficulty associated with diagnosis. Along with genetic risk factors, many significant components include: changes in cellular mechanisms, the role of second messenger systems, neurotransmitter systems, and advanced biological processes such as the hypothalamic-pituitary-adrenal (HPA) axis, and importantly for the purposes of this thesis, sleep and circadian rhythm modulation.

1.4 Sleeps and Circadian Rhythm Disruption in Psychiatric Disorders

1.4.1 The importance of sleep

The role sleep has to play in neuropsychiatric disorders has been acknowledged since 1883, where the German psychiatrist Emil Kraepelin first scripted this occurrence (Kraepelin, 1883). It is now understood that alternations between wake and sleep are composed of two intersecting processes, named the opponent process model. Firstly, for every moment spent

awake, there is an increased propensity to sleep, where sleep reduces this load, forming the homeostatic component (Borbely and Achermann, 1999). Although the exact cause of the increased sleep drive is unknown, the sleep regulatory molecule adenosine is heavily implicated as it accumulates throughout the day in sleep governing brain regions such as the basal forebrain, and dissipates during sleep (Porkka-Heiskanen et al., 1997). The second SCN-dependent process facilitates the initiation and maintenance of wakefulness, thus opposing the homeostatic sleep load which builds throughout the day (Borbely and Achermann, 1999). Interestingly, sleep can also feedback onto the clock as sleep deprivation studies found elevated cortical *Per1* and *Per2* expression in mice (Wisor et al., 2008). Therefore, given that sleep is a global brain event involving multiple nuclei and neurotransmitter systems, perturbations to either the sleep or circadian systems could have far-reaching consequences on brain function.

1.4.2 The consequences of a dysfunctional clock

A dysfunctional clock, as found in neuropsychiatric disorders, could induce physiological abnormalities by impacting the overall temporal synchrony of extra-SCN neuronal oscillators implicated in sleep and general physiology such as the ventrolateral preoptic area and the lateral hypothalamus (Abe et al., 2002). Additionally, given that such regions also contain molecular clocks responsible for tissue specific transcription of more than just *Per* and *Cry*, the downstream consequences on metabolism, physiology, and behaviour could be instrumental in disease pathophysiology (Zhang et al., 2014). Consequently, as circadian rhythm disruptions can impact sleep, sleep can then impact emotions

and behaviour, and eventually the clock itself, this strengthens the idea of targeting the molecular clock as a novel treatment option.

Although it is not fully understood how sleep and circadian rhythm disruptions can influence mental health, the current model suggests that an overlapping feature is the role of the circadian clock, as depicted in *Figure 1.3A* (Jagannath et al., 2013). Abnormalities in the clock can impact both sleep regulation and mental health, where a bi-directional relationship is present. Poor sleep quality can cause hypercortisolism, cognitive regression as well as general health problems, all of which can impact mental well-being (Vgontzas et al., 2001, Fortier-Brochu and Morin, 2014, Taylor et al., 2007). Similarly, psychiatric disorders can induce glucocorticoid production, patients may be prescribed sleep modifying medications, or struggle to maintaining social relationships, which can then impact sleep duration and quality (Cervantes et al., 2001, Wirz-Justice et al., 2001, Mushtaq et al., 2014). The cyclical nature of these events highlights the potential detrimental impact of a dysfunctional clock. The comorbid nature of sleep and mood is now well established such that the DSM-V and ICD-10 recognise sleep disturbances as part of the diagnosing criteria for neuropsychiatric disorders including BPD, depression, and anxiety disorders (American Psychiatric Association, 2013, World Health Organisation, 2014).

1.4.3 The effects of light on mood

There is accumulating evidence which suggests that light itself can impact temperament, an interesting idea given that circadian disruptions are implicated in psychiatric disorders. Mood was shown to closely align to circadian phase in

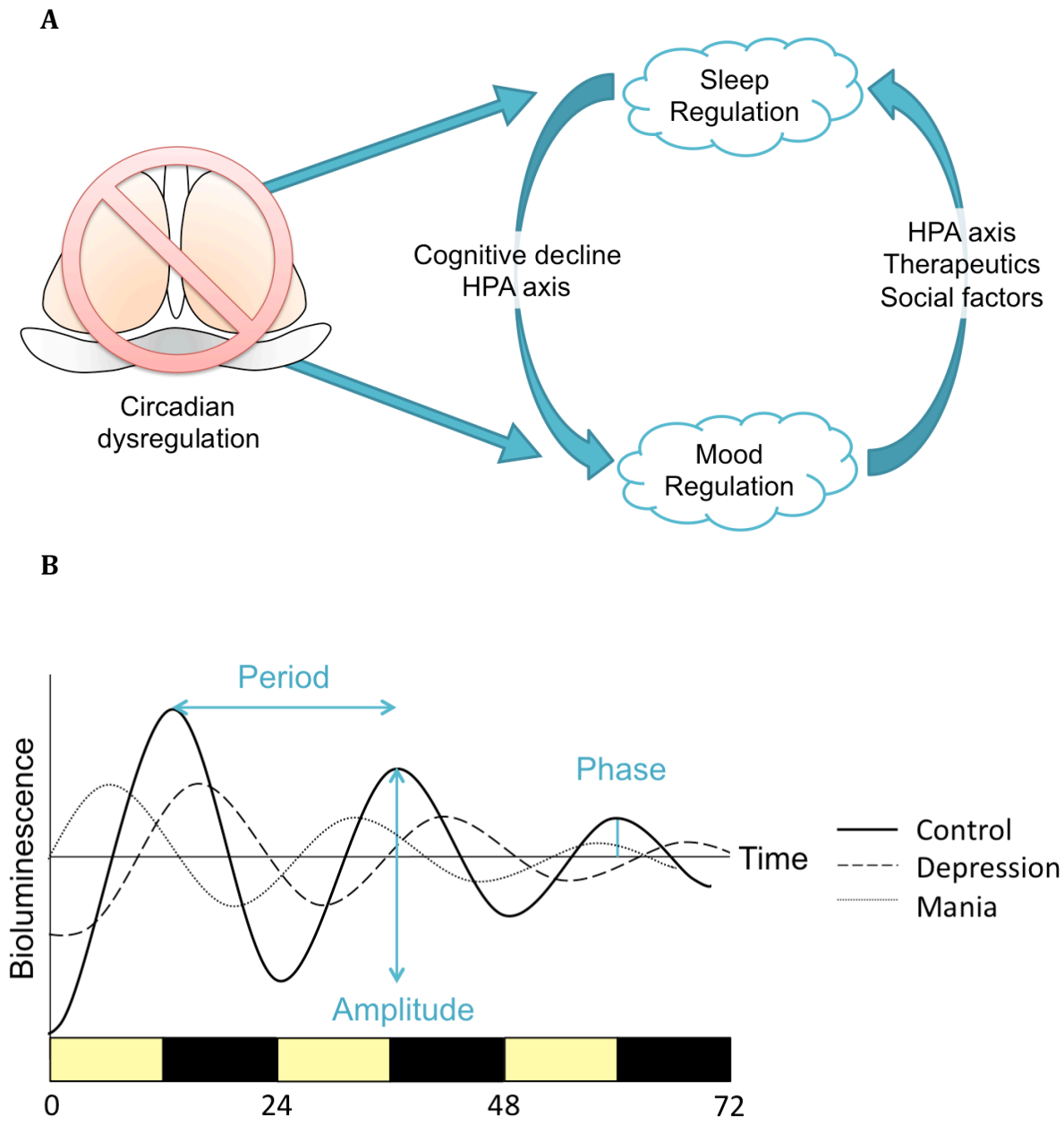

Figure 1.3. **Sleep and circadian rhythm disruptions in psychiatric disorders.** **A)** A model suggesting the role of circadian disruptions in psychiatric disorders. A dysfunctional clock can impact both sleep and mood, which may augment disease states. Adapted from Jagannath et al., 2013. **B)** Based on the current literature, the predicted circadian changes to be observed in BPD patients include a lengthened period, observed through increases in the oscillatory peak-to-peak distance, amplitude reductions, seen by a reduction in the height of oscillations and state-dependent phase advances or delays, observed by changes in peak activity relative to the LD cycle. Abbreviations can be found in the text.

healthy subjects, where a rise or fall in core body temperature was associated with increasing or decreasing levels of mood respectively (Boivin, 2000). Furthermore, healthy subjects exposed to higher intensity daytime light displayed elevated mood (Hoaki et al., 2011). This relationship was strengthened when looking at the impact of light on neuropsychiatric disorders, the most obvious of which is seasonal affective disorder (SAD). Patients suffering from SAD experience recurrent depression only during the winter months, behaviour which is seemingly normalised during the summer months (Rosenthal et al., 1984). During winter, both photoperiod and light intensity are significantly reduced, factors which may precipitate low mood (Lam and Levitan, 2000).

The theories that have dominated in trying to explain SAD all encompass the circadian system. Firstly, the potent effects of bright light therapy in curbing depression has been noted since 1984 (Rosenthal et al., 1984). As reduced photoperiods are a major contributory factor to SAD, exposing patients with up to 10,000 lux of light for as little as 15minutes (min) during the morning has proven to effectively control depressive symptoms (Partonen, 1994, Eastman et al., 1998, Lam et al., 2006). Moreover, studies have also found that exposing patients to 464-468nm blue light alone can improve symptoms of depression (Glickman et al., 2006, Anderson et al., 2009). This is quite predictable as the mechanism via which light therapy is believed to be effective is through the activation of the melanopsin containing ipRGCs, which provide a direct means of communication to the SCN and other emotion modulating retino-recipient brain regions, such as the lateral habenula and medial amygdala (Hattar et al., 2006). Indeed, patients with mutations in *OPN4* encoding melanopsin were 5.6 times

more likely to have SAD (Roecklein et al., 2009). Thus, by fooling the master clock into believing the photoperiod has been extended, summer-like day lengths can be mimicked, a period where remission is usually observed.

Further, the phase delayed hypothesis of the circadian clock suggests that chronic abnormalities in melatonin production result in patients having an evening preference- waking up and sleeping later, where light therapy functions by advancing the clock (Lewy et al., 1988, Lewy et al., 1998). Whilst night-time production of this neurohormone occurs at a time observed in healthy controls, melatonin offset in the morning is delayed (Wehr et al., 2001). This results in an extended period of melatonin production and ultimately a shorter internal representation of photoperiod. Therefore, this may also provide an explanation as to why morning light therapy is efficient, as it curbs melatonin release and extends the photoperiod experienced by the SCN.

1.4.4 Circadian disruptions in bipolar patients

There is a wealth of evidence highlighting the impact of light variation on BPD, where the aetiology of BPD could be associated with a dysfunctional circadian system. Notably, clinical studies have found that BPD patients display abnormalities in many 24h rhythms. Firstly, sleep patterns appear to be grossly disrupted across BPI and BPII patients, where sleep abnormalities provide a reliable prodromal indication of mania (Jackson et al., 2003). Furthermore, studies have found that 69-99% of manic patients have reductions in sleep requirements, and 60% of bipolar depressed patients exhibit an increased sleep onset latency by up to 80min (Loudon et al., 1977, Serretti and Olgiati, 2005, Casper et al., 1985, Demaertelaer et al., 1987, Benedetti et al., 2007). Moreover,

this sleep deprivation phenotype is coupled with fragmented sleeping patterns in euthymic patients and can be detected through increased dark phase movements in actigraphy studies (Jones et al., 2005, Rock et al., 2014). It could be argued that this indicates patients have lower amplitude rhythms, as the internal representation of day and night are less distinguished, and this is indeed what has been found (Rock et al., 2014, Yang et al., 2009). Additionally, as such abnormalities are observed in mood-stable euthymic patients, this implies that dysfunction in the circadian machinery is an intrinsic part of BPD and not merely a phase-dependent phenomenon.

The evidence regarding the presence of circadian period abnormalities appears to be varied in BPD. McCarthy and colleagues found period elongation by 25min when observing *Per2* rhythms, suggesting a deceleration in the molecular clockwork (McCarthy et al., 2013). Moreover, similar luminometric studies reported a trend for lengthened *Bmal1* rhythms by 40min relative to controls (Bamne et al., 2013). Further, when observing total activity through actigraphy studies, sleep period was reduced in BPD patients, suggesting that the active period was elongated by 25min (Rock et al., 2014). However, qPCR detection of *BMAL1*, *PER1*, *PER2*, *REV-EVBα*, and *DEC2* showed no period effects relative to controls, albeit in 12 patient cell lines (Yang et al., 2009).

Much like SAD, there is a phase delay hypothesis associated with BPI and BPII. Along with the presence of increased sleep latency, studies using 81-190 patients indicated that euthymic patients preferred to wake and sleep later (Falsin Giglio et al., 2010, Wood et al., 2009). This suggested that regardless of BPD sub-type many patients exhibited a delay in their circadian clocks.

Intriguingly, a recent study suggested the presence of state-dependent circadian phase variability. Of the manic episodes examined, 88% showed a 7h phase advance in buccual *PER1* expression and salivary cortisol. Additionally, all the depressive episodes showed a 5h delay in these rhythmic parameters (Moon et al., 2016). Whilst the replicability of these findings needs to be validated on a larger scale (only 31 mood episodes were analysed), they did associate recovery from mood episodes with a complimentary 7h delay or 5h advance in manic or depressed patients respectively (Moon et al., 2016). This suggests that circadian phase may be a valid indicator of disease states and that drugs which stabilise circadian phase shifting may also stabilise mood.

This idea of mood-dependent phase shifting has also been endorsed when looking at jet-lag studies - transmeridian travel induced circadian misalignment. Travelling across multiple time zones in pre-disposed individuals can precipitate mania when traveling east or depression when travelling west (Inder et al., 2016). Indeed, travelling east requires the clock to phase advance and travelling west requires a delay, corresponding with the previous study showing that advancements and delays are associated with mania and depression respectively (Moon et al., 2016). This suggests that the SCN may be more malleable in BPD as additional gross circadian disturbances may occur when switching from a manic to depressive phase.

In accordance with this evidence it could be hypothesised that exposing predisposed patients to light therapy could induce symptoms of mania. This is indeed what has been found in a subset of patients with SAD, depression, or BPD. Of the side effects reported with light therapy, hypomania and irritability were

common occurrences found in around 20-30% of subjects (Wirzjustice et al., 1986, Schwitzer et al., 1990, Meesters and Van Houwelingen, 1998, Leibenluft et al., 1995). Such reports also highlight that light therapy should be regarded as equivalent in importance to pharmaceutical treatments as diagnosis, dosage, and time of exposure can have detrimental consequences. Similarly, curtailing the photophase patients experience during the summer months should in theory normalise symptoms of mania. A preliminary case study suggested this might be true. By stabilising the sleep phase of a patient suffering from rapid cycling BPD to 10-14h enforced bed rest, the experimenters were able to stabilise his mood (Wehr et al., 1998). Subsequently, a pilot study by Barbini et al., provided a controlled assessment to confirm this finding. They exposed manic patients to a 10:14h LD cycle for 3 consecutive days as an adjunct therapy. It was found that extending the period of darkness was sufficient to improve clinical outcomes for acutely manic patients, and also showed that lower doses of mood-stabilisers were efficacious (Barbini et al., 2005). Overall, therapies involving routines of stable photoperiods and sleep can prove effective for mood-stabilisation. This adds to the compilation of evidence demonstrating the influence of light on emotions, and further suggests that chronobiotic interventions may be key to treating BPD.

1.4.5 Pre-clinical circadian models of bipolar disorder

There is accumulating pre-clinical evidence highlighting the importance of circadian rhythms in psychiatry, as rodent models displaying abnormalities in their circadian genes present mania-like phenotypes, akin to those displayed in humans (Landgraf et al., 2014). Some of the valuable models used include the

Clock∆19 and the *Afterhours* (*Afh*) mutants, where the former possesses a truncated CLOCK protein and the latter, a mutation that renders the FBXL3 protein unable to target CRY1/2 for ubiquitin-mediated degradation (Gekakis et al., 1998, Godinho et al., 2007). Such models presented with useful behavioural phenotypes parallel to human mania, including reduced anxiety and depression-like behaviours, with elevated risk-taking behaviours (Roybal et al., 2007, Keers et al., 2012). When analysing the circadian phenotype of the *Clock∆19* and *Afh* mutants, additional irregularities were observed as their molecular clocks had decelerated to 27h (King et al., 1997a, Godinho et al., 2007). Moreover, mutants displayed enhanced phase shifting responses showing advances and delays of up to 12h in response to a light pulse, where wild-type mice can typically only advance by 3h and delay by 6h (Vitaterna et al., 2006, Guilding et al., 2013). This ability to shift may be due to the low amplitude inducing nature of the mutations as this could render the SCN more susceptible to perturbations by *zeitgebers*.

Thus, there is an overwhelming accumulation of clinical and pre-clinical information highlighting the role of circadian rhythms in BPD. This validates further exploring the circadian abnormalities in the human population, in order to provide effective pharmacological or chronotherapeutic interventions.

1.5 Pharmacological Treatments for Bipolar Disorder

Due to the complex nature of BPD, treatment options vary depending on diagnosis specifications. Aside from chronotherapeutics (light and dark therapy), treatments include antidepressants as well as lithium, antipsychotics, and anticonvulsant drugs, where the latter pharmacological agents typically fall under the term 'mood-stabilisers' (Sie, 2014). Ranging from monotherapy to

multiple combined drug therapies, the aim of such mood-stabilising agents is to induce a state of acute and long-term euthymia.

It was found that half of all the top selling drugs targeted genes with circadian expression patterns, suggesting that the timing of drug administration may be crucial in mediating health benefits, whilst reducing the chances of off-target side effects (Zhang et al., 2014). Further, preliminary evidence suggests that pharmacological manipulation of the molecular clock may improve mood instability. By using cognitive behavioural therapy to treat insomnia in psychiatric patients, Myers et al. were able to reduce episodes of otherwise treatment-resistant persecutory delusions in 50% of their cohort (Myers et al., 2011). Moreover, the melatonergic agonist agomelatine normalised a spectrum of depressive symptoms and enhanced sleep quality in patients (Kennedy and Emsley, 2006, Olie and Kasper, 2007). This therefore suggests that targeting the circadian system may be a new therapeutic avenue in the treatment of BPD.

1.5.1 Lithium as a mood-stabiliser

Of the array of mood-stabilising agents available today, the metallic element lithium is not only the oldest compound, but remains a first-line therapy for BPD (Sie, 2014). The psychiatrist John Cade serendipitously discovered its properties in 1949. Cade believed that mania might have been linked with excessive uric acid within the urine. However, to test the theory he needed to increase the solubility of uric acid and so formulated lithium urate. When injected into guinea pigs he observed a reduction in excitation, where he then found similar effects with lithium administered to manic patients (Cade, 1949).

Today, we understand that 2 weeks of lithium monotherapy can effectively stabilise mood in 70-80% of BPD patients (Okusa and Crystal, 1994). The first meta-analytical study examining five data sets found that lithium prevented relapse in up to 60% of patients by reducing symptoms of mania (Geddes et al., 2004). A subsequent update from seven trials found that it was also effective at normalising depressive episodes, rendering it a *bona fide* mood-stabiliser (Severus et al., 2014). It is a unique molecule as to date it is the only drug known to reduce suicidality by up to 5 fold (Goodwin et al., 2003, Gonzalez-Pinto et al., 2006, Cipriani et al., 2013). Despite knowledge of its mood-stabilising properties for almost 70 years, we still do not fully understand how lithium induces therapeutic benefits.

1.5.2 Lithium as a therapeutic agent

Lithium, a naturally occurring ion, appears to drastically impact mood, but has no known physiological functions in a healthy human. Where low levels of potassium, sodium, calcium, or chloride ions are associated with disease states, there is a lack of known lithium deficiency disorders (Aral and Vecchio-Sadus, 2008). Adults typically consume 1mg of lithium per day through grains, vegetable, dairy products, and meat although variability is observed based on the lithium content of regional agricultural conditions (Aral and Vecchio-Sadus, 2008). However, for lithium to be effective at stabilising mood, blood plasma concentrations within the narrow band of 0.6-1.5mM must be achieved (Timmer and Sands, 1999). Due to the narrow therapeutic index associated with lithium treatment, toxicity is achieved above 1.5mM, resulting in numerous undesirable side effects, including: tremors, nausea, vomiting, diarrhoea, weight gain,

polydipsia, polyuria, renal failure, hair loss, and reduced sexual desire (Dols et al., 2013). Unfortunately, this has resulted in over 50% of patients showing long-term issues with covert non-compliance, which can also manifest due to poor disease insight, disorganised lifestyles, disease severity, or comorbid issues (Schou, 1997, Okusa and Crystal, 1994, Keck et al., 1996). Such details highlight the need for equally efficacious drugs with fewer side effects.

Unlike other group1 alkali metals such as sodium and potassium, which are 0.95Å and 1.33Å respectively, lithium has half the ionic radii at 0.60Å. As magnesium ions are 0.65Å, the current hypothesis states that due to similarities in ionic radii, lithium competitively displaces magnesium on magnesium-dependent enzymes resulting in inhibition and alterations to multiple signal transduction cascades (Diamond and Wright, 1987, De Freitas et al., 2006). Supporting this, chronic lithium application increased cytoplasmic magnesium levels in multiple human relevant cells lines, suggesting the presence of a competitive mechanism (Abukhdeir et al., 2003, Layden et al., 2003, Ramasamy and Defreitas, 1989). Lithium functions via uncompetitive inhibition, whereby it binds and inhibits enzymes only if the magnesium co-factor is bound, thus increasing the drug selectivity profile (Nahorski et al., 1991). Several enzymes are inhibited through the displacement of magnesium, notably inositol monophosphatase, adenylate cyclase, and glycogen synthase kinase 3β (GSK3β) (York et al., 1995, Mork and Geisler, 1987, Ryves and Harwood, 2001).

Following oral consumption of 300mg lithium carbonate, absorption is rapid and complete within 8h, peaking after 2-4h. As lithium is water-soluble, it is not protein bound and thus circulates freely in the total volume of bodily

water, with the exception of the cerebrospinal fluid due to higher levels of transporter-mediated efflux (Okusa and Crystal, 1994, Schou, 1968). The negative membrane potential for cells would imply that there would be greater lithium concentrations inside the cell. However, as there is no significant ionic gradient (such as those found with potassium and sodium), it is suggested that lithium is actively transported out of cells (Timmer and Sands, 1999).

Importantly, being an ion, lithium is blood-brain barrier (BBB) permeable and so has the capacity to affect neurological systems. Rodent studies found that lithium showed double the serum concentrations in the white matter and hypothalamus, a noteworthy finding as this is where the master clock resides (Edelfors, 1975). More detailed analysis found that the basal ganglia, which controls motor movements and hedonic behaviours; the pituitary which controls neuroendocrine function; the hippocampus, implicated in learning and memory; and the olfactory cortex, involved with processing smell and reward, also exhibited significantly elevated lithium concentrations (Ebadi et al., 1974). It is understood that lithium accrues and leaves the brain at a slower rate relative to the muscles, where this delay may account for the 2 week treatment time required to observe lithium's therapeutic benefits (Schou, 1958, Edelfors, 1975). Within the body, lithium accumulates to the greatest degree in bones, muscle, and large intestine, followed by the brain and kidneys (Edelfors, 1975, Schou, 1958, Ebadi et al., 1974). This suggests that modern day *in vitro* analysis of lithium may show high cell-to-cell variability.

Lithium is excreted predominantly by the kidneys as an unmetabolised ion. The plasma half-life shows great inter-individual variability depending on

the administered dose, volume of distribution, renal function, and therefore the rate of clearance (Goodnick et al., 1981, Schou, 1968). Where a single dose typically has a half-life of 16-28h, this can be doubled taking 53-58h in populations where lithium has been taken for over a year (Goodnick et al., 1981).

Whilst mechanisms of lithium cellular entry are not fully understood, four key mechanisms have emerged predominantly using erythrocytes (Ehrlich and Diamond, 1979). Firstly, as lithium is an analogue of sodium, it was suggested that flux occurred via sodium-dependent transporters and pumps. However, use of ouabain, a sodium-potassium ATPase inhibitor, had a limited effect on lithium flux in erythrocytes, as the sodium binding pocket showed a low affinity for lithium binding, but may play more of a role in fibroblasts (Ehrlich and Diamond, 1979, Smith and Rozengurt, 1978). The pump however, does create a large sodium gradient required for the sodium-lithium countertransporter. Thus, the presence of high extracellular sodium resulted in sodium influx down its electrochemical gradient in exchange for lithium. Phloretin inhibited transporter activity and suggested that it was responsible for ~75% of lithium efflux (Ehrlich and Diamond, 1979, Duhm et al., 1976). Passive leak is the process through which ions freely move across membranous pores. Approximately 25% of efflux, and 70% of lithium influx is due to leak where high influx is believed to be due to the negative membrane potential (-10mV) within cells (Ehrlich and Diamond, 1979). Finally, the presence of bicarbonate ions was responsible for 30% of lithium influx, due to stimulation of monovalent ion entry (Ehrlich and Diamond, 1979, Duhm and Becker, 1977). Whilst there is limited research assessing flux mechanisms in different cell types, the assumption that influx is dominated by

passive permeability and efflux via sodium-lithium exchange is generally accepted (Timmer and Sands, 1999, Moore et al., 2002, Smith and Rozengurt, 1978).

1.5.3 Lithium and circadian rhythms

As significant circadian abnormalities are observed in BPD, it is not surprising that mood-stabilisers may have an effect on this system. The promiscuous nature of lithium and the obscurity surrounding its efficacious mood-stabilising properties makes it plausible to suggest that lithium may function via actions upon sleep and the circadian system. A recent large-scale study confirmed that lithium improved sleep quality in euthymic BPI but not BPII patients, observed through longer night-time sleep durations and greater sleep efficiency (Geoffroy et al., 2016).

Lithium has also been shown to alter circadian rhythms by increasing the amplitude and period of rhythms. The amplitude effects are predictable as patients exhibit low amplitude rhythms. However, despite trends for a longer period emerging in patients, lithium appears to further lengthen the clock. Nevertheless, as we do not know how lithium functions, both chronomodulatory effects may be implicated in inducing and maintaining euthymia.

Lithium has been shown to consistently lengthen circadian period in multiple organisms, including plants, rodents, primates, and humans by 1-1.5h (Engelmann, 1972, Kripke and Wyborney, 1980, Welsh and Mooreede, 1990, Klemfuss, 1992, Johnsson et al., 1979). Both rats and mice, being popular models for assessing circadian rhythms show period lengthening by ~0.3-1h under

constant conditions when provided with lithium containing chow (Kripke and Wyborney, 1980, Li et al., 2012). These findings have also been validated on an electrophysiological level. Abe et al., showed that lithium dose-dependently lengthened the firing rate rhythms of SCN neurones in a dispersed culture, where 3mM lithium induced lengthening by 1h and 6mM by 3h (Abe et al., 2000). Interestingly, prior studies found that lithium supressed SCN spontaneous firing rate rhythms, and so this may be the mechanism via which deceleration is achieved (Mason and Biello, 1992). This suggests that behavioural period lengthening may be due to the direct actions of lithium upon the SCN.

This idea is further supported by biological assays looking at gene and protein expression patterns. In healthy rodents, 2mM lithium treated SCN sections took 1h longer to complete a single oscillation, when assessing PER2::LUC rhythms (Li et al., 2012). Moreover, a recent study found that lithium induced period changes in a region-specific manner, where lengthening was also found in the olfactory bulb, median eminence, and substantia niagra, an interesting finding considering that lithium preferentially accumulates in the hypothalamus, basal ganglia, and olfactory regions (Yoshikawa and Honma, 2016, Ebadi et al., 1974). This period phenotype was also found in non-neuronal tissues, where 5mM lithium induced a 45min change in lung slices, 10mM induced a 1h change in healthy human fibroblasts, and 20mM induced a 1h change in rodent skin and lung fibroblasts (Li et al., 2012, McCarthy et al., 2013). Immortalised cells also showed increased *Per2* period when assessing gene expression changes (Osland et al., 2011). This suggests that the molecular oscillations in most clock-containing tissues are altered upon lithium treatment.

Robust evidence also highlights the amplitude enhancing phenotype associated with lithium. Mouse luminometric assays have shown a 2.5 fold increase in circadian amplitude when 2mM, 5mM, or 20mM lithium is applied to SCN explants, lung tissues, or lung fibroblasts respectively (Li et al., 2012). Curiously, 1mM lithium also showed modest increases in *Per2* amplitude when looking at control subject fibroblasts, but not BPD patient cells. The authors also found that lithium was able to act as a re-synchronising agent thereby increasing amplitude by promoting a coherent rhythmic output (McCarthy et al., 2013). This is further supported by the analysis of gene expression in NIH-3T3 cells (immortalised mouse fibroblasts), which found that 20mM lithium augmented *Per2* and *Cry1* expression, with opposing or no effects on multiple other genes including *Per1/3* and *Cry2* (Osland et al., 2011). Interestingly, *Rev-erbα* expression and protein content is supressed following treatment with 20mM lithium in the NIH-3T3 cells with an associative doubling of *Bmal1* expression. This led to the finding that lithium-induced inhibition of GSK3β reduces its ability to phosphorylate and stabilise REV-ERBα, which renders it susceptible to degradation, ultimately elevating *Bmal1* expression (Yin et al., 2006). This suggests that lithium may function by targeting both the positive and negative arms of the clock in order to manipulate circadian rhythm generation. Although the effects of lithium on behavioural amplitude do not appear to have a significant effect in wild-type mice, these effects may emerge in models with disrupted amplitude rhythms (Li et al., 2012, Kripke and Wyborney, 1980). However, such effects are yet to be explored and published.

A recent study assessed the effects of 1mM lithium on BPD patient lymphoblastic cell lines and supports the evidence collected from immortalised cells. Two days after treatment, they found that when compared to non-responders, the lithium-responsive patients displayed increases in *RORα* and reductions in *REV-ERBα*, with consequential augmentation of *BMAL1.* Elevated levels of the negative components *PER1*, *CRY2*, *DEC1/2*, and *CSNK1δ* were also observed, providing the first detailed genetic insight into the effects of lithium on lithium sensitive and resistant patient clocks (Geoffroy et al., 2017). By increasing the biological difference between day and night-time activities, patients will presumably experience fewer sleep disruptions and abnormal gating of normal physiology, all of which may help to stabilise affect.

Indeed, evidence is emerging suggesting lithium's chronomodulatory effects are exerted through independent pathways. The amplitude enhancing effects of 20mM lithium are believed to be via GSK3β inhibition. This is because more targeted inhibition of GSK3β via the drug BIO resulted in a non-additive 2-fold amplitude increase in rat fibroblasts, with period shortening effects. Moreover, the mechanism of action is believed to be through increased *Per2* transcription, which doubled upon treatment with lithium or BIO, with no effect on PER2 degradation properties (Li et al., 2012). Moreover, Noguchi et al., found that circadian period was lengthened by 1h in SCN sections treated with 1mM lithium from control, $Cry1^{-/-}$, and $Cry2^{-/-}$ mice, albeit with variable baseline periods. They also found that 10mM lithium had no effect on wild-type or $Cry2^{-/-}$ fibroblast period but increased the amplitude 2.5 times. This suggests that the amplitude and lengthening effects are independent of CRY function, as lithium-

induced chronomodulatory changes were not altered (Noguchi et al., 2016). It also suggests that period and amplitude effects are independent of each other as lower concentrations resulted in the modulation of amplitude and not period.

1.6 Aims

The overall aims of this thesis can be divided into two sections. The first part aimed to gain a better understanding of circadian rhythm disruptions and modifications in BPD patient cells. Being a project funded by the National Centre for the Replacement, Refinement, and Reduction of Animals in Research (NC3Rs), we hoped to identify whether human fibroblasts could replace the use of animals at the initial stages of the drug discovery process. The second section aimed to identify the potential mechanism via which the mood-stabilising agent lithium induces chronomodulation. Therefore, this thesis will address the following:

1. *Are there circadian rhythm differences between well-characterised BPD patients and control subjects?*

The first chapter investigates the circadian rhythms in BPD patients by assessing both *Bmal1* and *Per2* gene expression, with the aim of assessing and validating previous findings on a larger scale. We also assess whether any differences are apparent between lithium-treated and non-treated patients.

2. *Are the fibroblasts susceptible to perturbation by lithium and novel repurposed compounds in a similar manner to in vivo observations?*

The effects of lithium as well as two additional rhythm-modulating compounds will be assessed *in vitro* on our patient-derived fibroblasts and *in vivo* through

mouse circadian (wheel-running) and behavioural (open field test, elevated plus maze) assays. This will help identify whether: 1) our fibroblasts model *in vivo* drug effects, and 2) whether pharmacological modulation of circadian rhythms can modulate behavioural changes.

3. *Does lithium induce period lengthening via inositol monophosphatase inhibition?*

As the mechanism via which period lengthening occurs is still elusive, this chapter provides evidence suggesting that rhythm alterations may be via inhibition of inositol monophosphatase, a key enzyme in the phosphoinositide pathway.

4. *Can adenylate cyclase inhibition play a role in modulating circadian rhythmicity in vitro?*

Initial investigations into lithium's mechanism of action also led to the analysis of the adenylate cyclase pathway. This chapter aims to show that pharmacological modification of this pathway also results in chronomodulatory changes, providing a route to identify additional mood-modulating compounds.

1.7 References

ABE, M., HERZOG, E. D. & BLOCK, G. D. 2000. Lithium lengthens the circadian period of individual suprachiasmatic nucleus neurons. *Neuroreport,* 11**,** 3261-3264.

ABE, M., HERZOG, E. D., YAMAZAKI, S., STRAUME, M., TEI, H., SAKAKI, Y., MENAKER, M. & BLOCK, G. D. 2002. Circadian rhythms in isolated brain regions. *Journal of Neuroscience,* 22**,** 350-356.

ABRAHAMSON, E. E. & MOORE, R. Y. 2001. Suprachiasmatic nucleus in the mouse: retinal innervation, intrinsic organization and efferent projections. *Brain Research,* 916**,** 172-191.

ABUKHDEIR, A. M., LAYDEN, B. T., MINADEO, N., BRYANT, F. B., STUBBS, E. B. & DE FREITAS, D. M. 2003. Effect of chronic Li+ treatment on free intracellular Mg2+ in human neuroblastoma SH-SY5Y cells. *Bipolar Disorders,* 5**,** 6-13.

AKASHI, M. & TAKUMI, T. 2005. The orphan nuclear receptor ROR alpha regulates circadian transcription of the mammalian core-clock Bmal1. *Nature Structural & Molecular Biology,* 12**,** 441-448.

AKASHI, M., TSUCHIYA, Y., YOSHINO, T. & NISHIDA, E. 2002. Control of intracellular dynamics of mammalian period proteins by casein kinase I epsilon (CKI epsilon) and CKI delta in cultured cells. *Molecular and Cellular Biology,* 22**,** 1693-1703.

AMERICAN PSYCHIATRIC ASSOCIATION 2013. *Diagnostics and Statisitcal Manual of Mental Disorders (DSM) 5th edition,* Washington.

ANDERSON, J. L., GLOD, C. A., DAI, J., CAO, Y. & LOCKLEY, S. W. 2009. Lux vs. wavelength in light treatment of Seasonal Affective Disorder. *Acta Psychiatrica Scandinavica,* 120**,** 203-212.

ARAL, H. & VECCHIO-SADUS, A. 2008. Toxicity of lithium to humans and the environment - A literature review. *Ecotoxicology and Environmental Safety,* 70**,** 349-356.

ASCHOFF, J. 1965. A self-sustained oscillator with an inherent frequency underlies human 24-hour periodicity. *Science,* 148**,** 1427-&.

BAE, K., JIN, X. W., MAYWOOD, E. S., HASTINGS, M. H., REPPERT, S. M. & WEAVER, D. R. 2001. Differential functions of mPer1, mPer2, and mPer3 in the SCN circadian clock. *Neuron,* 30**,** 525-536.

BALSALOBRE, A. 2002. Clock genes in mammalian peripheral tissues. *Cell and Tissue Research,* 309**,** 193-199.

BALSALOBRE, A., DAMIOLA, F. & SCHIBLER, U. 1998. A serum shock induces circadian gene expression in mammalian tissue culture cells. *Cell,* 93**,** 929-937.

BAMNE, M. N., PONDER, C. A., WOOD, J. A., MANSOUR, H., FRANK, E., KUPFER, D. J., YOUNG, M. W. & NIMGAONKAR, V. L. 2013. Application of an ex vivo cellular model of circadian variation for bipolar disorder research: a proof of concept study. *Bipolar Disorders,* 15**,** 694-700.

BARBINI, B., BENEDETTI, F., COLOMBO, C., DOTOLI, D., BERNASCONI, A., CIGALA-FULGOSI, M., FLORITA, M. & SMERALDI, E. 2005. Dark therapy for mania: a pilot study. *Bipolar Disorders,* 7**,** 98-101.

BELL-PEDERSEN, D., CASSONE, V. M., EARNEST, D. J., GOLDEN, S. S., HARDIN, P. E., THOMAS, T. L. & ZORAN, M. J. 2005. Circadian rhythms from multiple oscillators: Lessons from diverse organisms. *Nature Reviews Genetics,* 6**,** 544-556.

BENEDETTI, F., DALLASPEZIA, S., FULGOSI, M. C., LORENZI, C., SERRETTI, A., BARBINI, B., COLOMBO, C. & SMERALDI, E. 2007. Actimetric evidence that CLOCK 3111 T/C SNP influences sleep and activity patterns in patients affected by bipolar depression. *American Journal of Medical Genetics Part B-Neuropsychiatric Genetics,* 144B**,** 631-635.

BERSON, D. M., DUNN, F. A. & TAKAO, M. 2002. Phototransduction by retinal ganglion cells that set the circadian clock. *Science,* 295**,** 1070-1073.
BEST, J. D., MAYWOOD, E. S., SMITH, K. L. & HASTINGS, M. H. 1999. Rapid resetting of the mammalian circadian clock. *Journal of Neuroscience,* 19**,** 828-835.
BIELLO, S. M., GOLOMBEK, D. A. & HARRINGTON, M. E. 1997. Neuropeptide Y and glutamate block each other's phase shifts in the suprachiasmatic nucleus in vitro. *Neuroscience,* 77**,** 1049-1057.
BIELLO, S. M., JANIK, D. & MROSOVSKY, N. 1994. Neuropeptide-y and behaviorally induced phase-shifts. *Neuroscience,* 62**,** 273-279.
BOIVIN, D. B. 2000. Influence of sleep-wake and circadian rhythm disturbances in psychiatric disorders. *Journal of Psychiatry & Neuroscience,* 25**,** 446-458.
BORBELY, A. A. & ACHERMANN, P. 1999. Sleep homeostasis and models of sleep regulation. *Journal of Biological Rhythms,* 14**,** 557-568.
BOSLER, O. & BEAUDET, A. 1985. VIP neurons as prime synaptic targets for serotonin afferents in rat suprachiasmatic nucleus - a combined autoradiographic and immunocytochemical study. *Journal of Neurocytology,* 14**,** 749-763.
BRANCACCIO, M., PATTON, A. P., CHESHAM, J. E., MAYWOOD, E. S. & HASTINGS, M. H. 2017. Astrocytes Control Circadian Timekeeping in the Suprachiasmatic Nucleus via Glutamatergic Signaling. *Neuron,* 93**,** 1420-+.
BROWN, S. A., KUNZ, D., DUMAS, A., WESTERMARK, P. O., VANSELOW, K., TILMANN-WAHNSCHAFFE, A., HERZEL, H. & KRAMER, A. 2008. Molecular insights into human daily behavior. *Proceedings of the National Academy of Sciences of the United States of America,* 105**,** 1602-1607.
BUNGER, M. K., WILSBACHER, L. D., MORAN, S. M., CLENDENIN, C., RADCLIFFE, L. A., HOGENESCH, J. B., SIMON, M. C., TAKAHASHI, J. S. & BRADFIELD, C. A. 2000. Mop3 is an essential component of the master circadian pacemaker in mammals. *Cell,* 103**,** 1009-1017.
BÜNNING, E. 1971. Symptoms, problems, and common features of circadian rhythms in plants and animals. Proc Int Symp Circadian Rhythmicity, Wageningen, 11-31.
CADE, J. F. J. 1949. Lithium salts in the treatment of psychotic excitement. *Medical Journal of Australia,* 2**,** 349-352.
CAHILL, A. L. & EHRET, C. F. 1981. Circadian variations in the activity of tyrosine-hydroxylase, tyrosine aminotransferase, and tryptophan-hydroxylase - relationship to catecholamine metabolism. *Journal of Neurochemistry,* 37**,** 1109-1115.
CALDELAS, I., POIREL, V. J., SICARD, B., PEVET, P. & CHALLET, E. 2003. Circadian profile and photic regulation of clock genes in the suprachiasmatic nucleus of a diurnal mammal Arvicanthis ansorgei. *Neuroscience,* 116**,** 583-591.
CARSKADON, M. A., LABYAK, S. E., ACEBO, C. & SEIFER, R. 1999. Intrinsic circadian period of adolescent humans measured in conditions of forced desynchrony. *Neuroscience Letters,* 260**,** 129-132.
CASPER, R. C., REDMOND, D. E., KATZ, M. M., SCHAFFER, C. B., DAVIS, J. M. & KOSLOW, S. H. 1985. Somatic symptoms in primary affective-disorder - presence and relationship to the classification of depression. *Archives of General Psychiatry,* 42**,** 1098-1104.
CASSIDY, F., MURRY, E., FOREST, K. & CARROLL, B. J. 1998. Signs and symptoms of mania in pure and mixed episodes. *Journal of Affective Disorders,* 50**,** 187-201.
CASTEL, M., BELENKY, M., COHEN, S., OTTERSEN, O. P. & STORMMATHISEN, J. 1993. Glutamate-like immunoreactivity in retinal terminals of the mouse suprachiasmatic nucleus. *European Journal of Neuroscience,* 5**,** 368-381.
CERVANTES, P., GELBER, S., KIN, F., NAIR, V. N. P. & SCHWARTZ, G. 2001. Circadian secretion of cortisol in bipolar disorder. *Journal of Psychiatry & Neuroscience,* 26**,** 411-416.

CHEN, D., BUCHANAN, G. F., DING, J. M., HANNIBAL, J. & GILLETTE, M. U. 1999. Pituitary adenylyl cyclase-activating peptide: A pivotal modulator of glutamatergic regulation of the suprachiasmatic circadian clock. *Proceedings of the National Academy of Sciences of the United States of America,* 96**,** 13468-13473.

CHEN, Y. W. & DILSAVER, S. C. 1996. Lifetime rates of suicide attempts among subjects with bipolar and unipolar disorders relative to subjects with other axis I disorders. *Biological Psychiatry,* 39**,** 896-899.

CIPRIANI, A., HAWTON, K., STOCKTON, S. & GEDDES, J. R. 2013. Lithium in the prevention of suicide in mood disorders: updated systematic review and meta-analysis. *Bmj-British Medical Journal,* 346**,** f3646.

CRADDOCK, N. & SKLAR, P. 2013. Bipolar Disorder 1 Genetics of bipolar disorder. *Lancet,* 381**,** 1654-1662.

CZEISLER, C. A., DUFFY, J. F., SHANAHAN, T. L., BROWN, E. N., MITCHELL, J. F., RIMMER, D. W., RONDA, J. M., SILVA, E. J., ALLAN, J. S., EMENS, J. S., DIJK, D. J. & KRONAUER, R. E. 1999. Stability, precision, and near-24-hour period of the human circadian pacemaker. *Science,* 284**,** 2177-2181.

DAAN, S. & PITTENDRIGH, C. S. 1976. Functional-analysis of circadian pacemakers in nocturnal rodents .2. Variability of phase response curves. *Journal of Comparative Physiology,* 106**,** 253-266.

DE FREITAS, D. M., CASTRO, M. & GERALDES, C. 2006. Is competition between Li+ and Mg2+ the underlying theme in the proposed mechanisms for the pharmacological action of lithium salts in bipolar disorder? *Accounts of Chemical Research,* 39**,** 283-291.

DEBRUYNE, J. P., WEAVER, D. R. & REPPERT, S. M. 2007. CLOCK and NPAS2 have overlapping roles in the suprachiasmatic circadian clock. *Nature Neuroscience,* 10**,** 543-545.

DECOURSEY, P. J., KRULAS, J. R., MELE, G. & HOLLEY, D. C. 1997. Circadian performance of suprachiasmatic nuclei (SCN)-lesioned antelope ground squirrels in a desert enclosure. *Physiology & Behavior,* 62**,** 1099-1108.

DECOURSEY, P. J., WALKER, J. K. & SMITH, S. A. 2000. A circadian pacemaker in free-living chipmunks: essential for survival? *Journal of Comparative Physiology a-Sensory Neural and Behavioral Physiology,* 186**,** 169-180.

DEMAERTELAER, V., HOFFMAN, G., LEMAIRE, M. & MENDLEWICZ, J. 1987. Sleep spindle activity changes in patients with affective-disorders. *Sleep,* 10**,** 443-451.

DEMAIRAN, J. J. D. 1729. Observation Botanique. Paris: Hist. Acad. Roy. Sci. 35 –36.

DIAMOND, J. & WRIGHT, E. 1987. Citation-classic - biological-membranes - the physical basis of ion and non-electrolyte selectivity. *Current Contents/Life Sciences***,** 18-18.

DIBNER, C. & SCHIBLER, U. 2018. Body clocks: time for the Nobel Prize. Acta Physiol, 222, e13024.

DING, J. M., CHEN, D., WEBER, E. T., FAIMAN, L. E., REA, M. A. & GILLETTE, M. U. 1994. Resetting the biological clock - Mediation of nocturnal circadian shifts by glutamate and NO. *Science,* 266**,** 1713-1717.

DOLS, A., SIENAERT, P., VAN GERVEN, H., SCHOUWS, S., STEVENS, A., KUPKA, R. & STEK, M. L. 2013. The prevalence and management of side effects of lithium and anticonvulsants as mood stabilizers in bipolar disorder from a clinical perspective: a review. *International Clinical Psychopharmacology,* 28**,** 287-296.

DUHM, J. & BECKER, B. F. 1977. Studies on lithium transport across red-cell membrane .2. Characterization of ouabain-sensitive and ouabain-insensitive Li+ transport - effects of bicarbonate and dipyridamole. *Pflugers Archiv-European Journal of Physiology,* 367**,** 211-219.

DUHM, J., EISENRIED, F., BECKER, B. F. & GREIL, W. 1976. Studies on lithium transport across red-cell membrane .1. Li+ uphill transport by Na+-dependent Li+ counter-transport system of human erythrocytes. *Pflugers Archiv-European Journal of Physiology,* 364**,** 147-155.

DUNAYEVICH, E. & KECK, P. E. 2000. Prevalence and description of psychotic features in bipolar mania.: *Current psychiatry reports*, 2, 286-290.

EASTMAN, C. I., YOUNG, M. A., FOGG, L. F., LIU, L. W. & MEADEN, P. M. 1998. Bright light treatment of winter depression - A placebo-controlled trial. *Archives of General Psychiatry,* 55**,** 883-889.

EBADI, M. S., SIMMONS, V. J., HENDRICKSON, M. J. & LACY, P. S. 1974. Pharmacokinetics of lithium and its regional distribution in rat-brain. *European Journal of Pharmacology,* 27**,** 324-329.

EDELFORS, S. 1975. Distribution of sodium, potassium and lithium in brain of lithium-treated rats. *Acta Pharmacologica Et Toxicologica,* 37**,** 387-392.

EHRLICH, B. E. & DIAMOND, J. M. 1979. Lithium fluxes in human-erythrocytes. *American Journal of Physiology,* 237**,** C102-C110.

ENGELMANN, W. 1972. LITHIUM SLOWS DOWN KALANCHOE CLOCK. *Zeitschrift Fur Naturforschung Part B-Chemie Biochemie Biophysik Biologie Und Verwandten Gebiete,* B 27**,** 477-+.

FALSIN GIGLIO, L. M., MAGALHAES, P. V. S., ANDERSEN, M. L., WALZ, J. C., JAKOBSON, L. & KAPCZINSKI, F. 2010. Circadian preference in bipolar disorder. *Sleep and Breathing,* 14**,** 153-155.

FORTIER-BROCHU, E. & MORIN, C. M. 2014. Cognitive Impairment in Individuals with Insomnia: Clinical Significance and Correlates. *Sleep,* 37**,** 1789-1800.

FRANCOISBELLAN, A. M. & BOSLER, O. 1992. Convergent serotonin and GABA innervation of VIP neurons in the suprachiasmatic nucleus demonstrated by triple labeling in the rat. *Brain Research,* 595**,** 149-153.

GEDDES, J. R., BURGESS, S., HAWTON, K., JAMISON, K. & GOODWIN, G. M. 2004. Long-term lithium therapy for bipolar disorder: Systematic review and meta-analysis of randomized controlled trialls. *American Journal of Psychiatry,* 161**,** 217-222.

GEKAKIS, N., STAKNIS, D., NGUYEN, H. B., DAVIS, F. C., WILSBACHER, L. D., KING, D. P., TAKAHASHI, J. S. & WEITZ, C. J. 1998. Role of the CLOCK protein in the mammalian circadian mechanism. *Science,* 280**,** 1564-1569.

GEOFFROY, P. A., CURIS, E., COURTIN, C., MOREIRA, J., MORVILLERS, T., ETAIN, B., LAPLANCHE, J. L., BELLIVIER, F. & MARIE-CLAIRE, C. 2017. Lithium response in bipolar disorders and core clock genes expression.: *The World Journal of Biological Psychiatry*, 18, 1–14.

GEOFFROY, P. A., SAMALIN, L., LLORCA, P. M., CURIS, E. & BELLIVIER, F. 2016. Influence of lithium on sleep and chronotypes in remitted patients with bipolar disorder. *Journal of Affective Disorders,* 204**,** 32-39.

GLICKMAN, G., BYRNE, B., PINEDA, C., HAUCK, W. W. & BRAINARD, G. C. 2006. Light therapy for seasonal affective disorder with blue narrow-band light-emitting diodes (LEDs). *Biological Psychiatry,* 59**,** 502-507.

GODINHO, S. I. H., MAYWOOD, E. S., SHAW, L., TUCCI, V., BARNARD, A. R., BUSINO, L., PAGANO, M., KENDALL, R., QUWAILID, M. M., ROMERO, M. R., O'NEILL, J., CHESHAM, J. E., BROOKER, D., LALANNE, Z., HASTINGS, M. H. & NOLAN, P. M. 2007. The after-hours mutant reveals a role for Fbxl3 in determining mammalian circadian period. *Science,* 316**,** 897-900.

GONZALEZ-PINTO, A., MOSQUERA, F., ALONSO, M., LOPEZ, P., RAMIREZ, F., VIETA, E. & BALDESSARINI, R. J. 2006. Suicidal risk in bipolar I disorder patients and adherence to long-term lithium treatment. *Bipolar Disorders,* 8**,** 618-624.

GOODNICK, P. J., FIEVE, R. R., MELTZER, H. L. & DUNNER, D. L. 1981. Lithium elimination half-life and duration of therapy. *Clinical Pharmacology & Therapeutics,* 29**,** 47-50.

GOODWIN, F. K., FIREMAN, B., SIMON, G. E., HUNKELER, E. M., LEE, J. & REVICKI, D. 2003. Suicide risk in bipolar disorder during treatment with lithium and divalproex. *Jama-Journal of the American Medical Association,* 290**,** 1467-1473.

GREEN, D. J. & GILLETTE, R. 1982. Circadian-rhythm of firing rate recorded from single cells in the rat suprachiasmatic brain slice. *Brain Research,* 245**,** 198-200.

GRIPPO, R. M., PUROHIT, A. M., ZHANG, Q., ZWEIFEL, L. S. & GULER, A. D. 2017. Direct Midbrain Dopamine Input to the Suprachiasmatic Nucleus Accelerates Circadian Entrainment. *Current Biology,* 27**,** 2465-+.

GUILDING, C., SCOTT, F., BECHTOLD, D. A., BROWN, T. M., WEGNER, S. & PIGGINS, H. D. 2013. Suppressed cellular oscillations in after-hours mutant mice are associated with enhanced circadian phase-resetting. *Journal of Physiology-London,* 591**,** 1063-1080.

GUILLAUMOND, F., DARDENTE, H., GIGUERE, V. & CERMAKIAN, N. 2005. Differential control of Bmal1 circadian transcription by REV-ERB and ROR nuclear receptors. *Journal of Biological Rhythms,* 20**,** 391-403.

HAMPP, G., RIPPERGER, J. A., HOUBEN, T., SCHMUTZ, I., BLEX, C., PERREAU-LENZ, S., BRUNK, I., SPANAGEL, R., AHNERT-HILGER, G., MEIJER, J. H. & ALBRECHT, U. 2008. Regulation of monoamine oxidase a by circadian-clock components implies clock influence on mood. *Current Biology,* 18**,** 678-683.

HASTINGS, M. H., REDDY, A. B. & MAYWOOD, E. S. 2003. A clockwork web: Circadian timing in brain and periphery, in health and disease. *Nature Reviews Neuroscience,* 4**,** 649-661.

HATTAR, S., KUMAR, M., PARK, A., TONG, P., TUNG, J., YAU, K. W. & BERSON, D. M. 2006. Central projections of melanopsin-expressing retinal ganglion cells in the mouse. *Journal of Comparative Neurology,* 497**,** 326-349.

HATTAR, S., LIAO, H. W., TAKAO, M., BERSON, D. M. & YAU, K. W. 2002. Melanopsin-containing retinal. ganglion cells: Architecture, projections, and intrinsic photosensitivity. *Science,* 295**,** 1065-1070.

HOAKI, N., TERAO, T., WANG, Y. M., GOTO, S., TSUCHIYAMA, K. & IWATA, N. 2011. Biological aspect of hyperthymic temperament: light, sleep, and serotonin. *Psychopharmacology,* 213**,** 633-638.

HOFMAN, M. A., FLIERS, E., GOUDSMIT, E. & SWAAB, D. F. 1988. Morphometric analysis of the suprachiasmatic and paraventricular nuclei in the human-brain - sex-differences and age-dependent changes. *Journal of Anatomy,* 160**,** 127-143.

HONMA, S., KAWAMOTO, T., TAKAGI, Y., FUJIMOTO, K., SATO, F., NOSHIRO, M., KATO, Y. & HONMA, K. 2002. Dec1 and Dec2 are regulators of the mammalian molecular clock. *Nature,* 419**,** 841-844.

INDER, M. L., CROWE, M. T. & PORTER, R. 2016. Effect of transmeridian travel and jetlag on mood disorders: Evidence and implications. *Australian and New Zealand Journal of Psychiatry,* 50**,** 220-227.

INOUYE, S. T. & KAWAMURA, H. 1979. Persistence of circadian rhythmicity in a mammalian hypothalamic island containing the suprachiasmatic nucleus. *Proceedings of the National Academy of Sciences of the United States of America,* 76**,** 5962-5966.

IZUMO, M., JOHNSON, C. H. & YAMAZAKI, S. 2003. Circadian gene expression in mammalian fibroblasts revealed by real-time luminescence reporting: Temperature compensation and damping. *Proceedings of the National Academy of Sciences of the United States of America,* 100**,** 16089-16094.

JACKSON, A., CAVANAGH, J. & SCOTT, J. 2003. A systematic review of manic and depressive prodromes. *Journal of Affective Disorders,* 74**,** 209-217.

JAGANNATH, A., PEIRSON, S. N. & FOSTER, R. G. 2013. Sleep and circadian rhythm disruption in neuropsychiatric illness. *Current opinion in neurobiology,* 23**,** 888-94.

JOHNSSON, A., PFLUG, B., ENGELMANN, W. & KLEMKE, W. 1979. Effect of lithium-carbonate on circadian periodicity in humans. *Pharmakopsychiatrie Neuro-Psychopharmakologie,* 12**,** 423-425.

JONES, S. H., HARE, D. J. & EVERSHED, K. 2005. Actigraphic assessment of circadian activity and sleep patterns in bipolar disorder. *Bipolar Disorders,* 7**,** 176-186.

JUD, C., SCHMUTZ, I., HAMPP, G., OSTER, H. & ALBRECHT, U. 2005. A guideline for analyzing circadian wheel-running behavior in rodents under different lighting conditions. *Biological Procedures Online,* 7**,** 101-116.

KALLO, I., KALAMATIANOS, T., WILTSHIRE, N., SHEN, S. B., SHEWARD, W. J., HARMAR, A. J. & COEN, C. W. 2004. Transgenic approach reveals expression of the VPAC(2) receptor in phenotypically defined neurons in the mouse suprachiasmatic nucleus and in its efferent target sites. *European Journal of Neuroscience,* 19**,** 2201-2211.

KALSBEEK, A., FLIERS, E., HOFMAN, M. A., SWAAB, D. F. & BUIJS, R. M. 2010. Vasopressin and the Output of the Hypothalamic Biological Clock. *Journal of Neuroendocrinology,* 22**,** 362-372.

KECK, P. E., MCELROY, S. L., STRAKOWSKI, S. M., STANTON, S. P., KIZER, D. L., BALISTRERI, T. M., BENNETT, J. A., TUGRUL, K. C. & WEST, S. A. 1996. Factors associated with pharmacologic noncompliance in patients with mania. *Journal of Clinical Psychiatry,* 57**,** 292-297.

KEERS, R., PEDROSO, I., BREEN, G., AITCHISON, K. J., NOLAN, P. M., CICHON, S., NOETHEN, M. M., RIETSCHEL, M., SCHALKWYK, L. C. & FERNANDES, C. 2012. Reduced Anxiety and Depression-Like Behaviours in the Circadian Period Mutant Mouse Afterhours. *Plos One,* 7**,** e38263.

KENNEDY, S. H. & EMSLEY, R. 2006. Placebo-controlled trial of agomelatine in the treatment of major depressive disorder. *European Neuropsychopharmacology,* 16**,** 93-100.

KING, D. P., VITATERNA, M. H., CHANG, A. M., DOVE, W. F., PINTO, L. H., TUREK, F. W. & TAKAHASHI, J. S. 1997a. The mouse Clock mutation behaves as an antimorph and maps within the W-19H deletion, distal of Kit. *Genetics,* 146**,** 1049-1060.

KING, D. P., ZHAO, Y. L., SANGORAM, A. M., WILSBACHER, L. D., TANAKA, M., ANTOCH, M. P., STEEVES, T. D. L., VITATERNA, M. H., KORNHAUSER, J. M., LOWREY, P. L., TUREK, F. W. & TAKAHASHI, J. S. 1997b. Positional cloning of the mouse circadian Clock gene. *Cell,* 89**,** 641-653.

KLEMFUSS, H. 1992. Rhythms and the pharmacology of lithium. *Pharmacology & Therapeutics,* 56**,** 53-78.

KRAEPELIN, E. 1883. Compendium der Psychiatrie zum Gebrauch fuer Studierende und Aerzte.

KRIPKE, D. F. & WYBORNEY, V. G. 1980. Lithium slows rat circadian activity rhythms. *Life Sciences,* 26**,** 1319-1321.

KUME, K., ZYLKA, M. J., SRIRAM, S., SHEARMAN, L. P., WEAVER, D. R., JIN, X. W., MAYWOOD, E. S., HASTINGS, M. H. & REPPERT, S. M. 1999. mCRY1 and mCRY2 are essential components of the negative limb of the circadian clock feedback loop. *Cell,* 98**,** 193-205.

LAM, R. W. & LEVITAN, R. D. 2000. Pathophysiology of seasonal affective disorder: a review. *Journal of Psychiatry & Neuroscience,* 25**,** 469-480.

LAM, R. W., LEVITT, A. J., LEVITAN, R. D., ENNS, M. W., MOREHOUSE, R., MICHALAK, E. E. & TAM, E. M. 2006. The can-SAD study: A randomized controlled trial of the effectiveness of light therapy and fluoxetine in patients with winter seasonal affective disorder. *American Journal of Psychiatry,* 163**,** 805-812.

LANDGRAF, D., MCCARTHY, M. J. & WELSH, D. K. 2014. The Role of the Circadian Clock in Animal Models of Mood Disorders. *Behavioral Neuroscience,* 128**,** 344-359.

LANDGRAF, D., WANG, L. L., DIEMER, T. & WELSH, D. K. 2016. NPAS2 Compensates for Loss of CLOCK in Peripheral Circadian Oscillators. *Plos Genetics,* 12**,** e1005882.

LAYDEN, B. T., ABUKHDEIR, A. M., WILLIAMS, N., FONSECA, C. P., CARROLL, L., CASTRO, M., GERALDES, C., BRYANT, F. B. & DE FREITAS, D. M. 2003. Effects of Li+ transport and Li+ immobilization on Li+/Mg2+ competition in cells: implications for bipolar disorder. *Biochemical Pharmacology,* 66**,** 1915-1924.

LEIBENLUFT, E., TURNER, E. H., FELDMANNAIM, S., SCHWARTZ, P. J., WEHR, T. A. & ROSENTHAL, N. E. 1995. Light therapy in patients with rapid cycling bipolar disorder: Preliminary results. *Psychopharmacology Bulletin,* 31**,** 705-710.

LEWY, A. J., BAUER, V. K., CUTLER, N. L., SACK, R. L., AHMED, S., THOMAS, K. H., BLOOD, M. L. & JACKSON, J. M. L. 1998. Morning vs evening light treatment of patients with winter depression. *Archives of General Psychiatry,* 55**,** 890-896.

LEWY, A. J. & MARKEY, S. P. 1978. Analysis of melatonin in human-plasma by gas-chromatography negative chemical ionization mass-spectrometry. *Science,* 201**,** 741-743.

LEWY, A. J., SACK, R. L., SINGER, C. M., WHITE, D. M. & HOBAN, T. M. 1988. Winter Depression and the Phase-Shift Hypothesis for Bright Light's Therapeutic Effects: History, Theory, and Experimental Evidence. *Journal of Biological Rhythms,* 3**,** 121-134.

LI, J., LU, W.-Q., BEESLEY, S., LOUDON, A. S. I. & MENG, Q.-J. 2012. Lithium Impacts on the Amplitude and Period of the Molecular Circadian Clockwork. *Plos One,* 7**,** e33292.

LOUDON, J. B., BLACKBURN, I. M. & ASHWORTH, C. M. 1977. Study of symptomatology and course of manic illness using a new scale. *Psychological Medicine,* 7**,** 723-729.

LOWREY, P. L., SHIMOMURA, K., ANTOCH, M. P., YAMAZAKI, S., ZEMENIDES, P. D., RALPH, M. R., MENAKER, M. & TAKAHASHI, J. S. 2000. Positional syntenic cloning and functional characterization of the mammalian circadian mutation tau. *Science,* 288**,** 483-491.

LUCAS, R. J., HATTAR, S., TAKAO, M., BERSON, D. M., FOSTER, R. G. & YAU, K. W. 2003. Diminished pupillary light reflex at high irradiances in melanopsin-knockout mice. *Science,* 299**,** 245-247.

MAI, J. K., KEDZIORA, O., TECKHAUS, L. & SOFRONIEW, M. V. 1991. Evidence for subdivisions in the human suprachiasmatic nucleus. *Journal of Comparative Neurology,* 305**,** 508-525.

MASON, R. & BIELLO, S. M. 1992. A neurophysiological study of a lithium-sensitive phosphoinositide system in the hamster suprachiasmatic (SCN) biological clock in vitro. *Neuroscience Letters,* 144**,** 135-138.

MCCARTHY, M. J., WEI, H., MARNOY, Z., DARVISH, R. M., MCPHIE, D. L., COHEN, B. M. & WELSH, D. K. 2013. Genetic and clinical factors predict lithium's effects on PER2 gene expression rhythms in cells from bipolar disorder patients. *Translational Psychiatry,* 3**,** e318.

MEESTERS, Y. & VAN HOUWELINGEN, C. A. J. 1998. Rapid mood swings after unmonitored light exposure. *American Journal of Psychiatry,* 155**,** 306-306.

MERIKANGAS, K. R., JIN, R., HE, J. P., KESSLER, R. C., LEE, S., SAMPSON, N. A., VIANA, M. C., ANDRADE, L. H., HU, C. Y., KARAM, E. G., LADEA, M., MEDINA-MORA, M. E., ONO, Y., POSADA-VILLA, J., SAGAR, R., WELLS, J. E. & ZARKOV, Z. 2011. Prevalence and Correlates of Bipolar Spectrum Disorder in the World Mental Health Survey Initiative. *Archives of General Psychiatry,* 68**,** 241-251.

MICHAELIS, B. H., GOLDBERG, J. F., DAVIS, G. P., SINGER, T. M., GARNO, J. L. & WENZE, S. J. 2004. Dimensions of impulsivity and aggression associated with suicide attempts among bipolar patients: A preliminary study. *Suicide and Life-Threatening Behavior,* 34**,** 172-176.

MOON, J. H., CHO, C. H., SON, G. H., GEUM, D., CHUNG, S., KIM, H., KANG, S. G., PARK, Y. M., YOON, H. K., KIM, L., JEE, H. J., AN, H., KRIPKE, D. F. & LEE, H. J. 2016. Advanced Circadian Phase in Mania and Delayed Circadian Phase in Mixed Mania and Depression Returned to Normal after Treatment of Bipolar Disorder. *Ebiomedicine,* 11**,** 285-295.

MOORE, C. M., DEMOPULOS, C. M., HENRY, M. E., STEINGARD, R. J., ZAMVIL, L., KATIC, A., BREEZE, J. L., MOORE, J. C., COHEN, B. M. & RENSHAW, P. F. 2002. Brain-to-serum lithium ratio and age: An in vivo magnetic resonance spectroscopy study. *American Journal of Psychiatry,* 159**,** 1240-1242.

MOORE, R. Y. & EICHLER, V. B. 1972. Loss of a circadian adrenal corticosterone rhythm following suprachiasmatic lesions in rat. *Brain Research,* 42**,** 201-&.

MORK, A. & GEISLER, A. 1987. Mode of action of lithium on the catalytic unit of adenylate-cyclase from rat-brain. *Pharmacology & Toxicology,* 60**,** 241-248.

MROSOVSKY, N., EDELSTEIN, K., HASTINGS, M. H. & MAYWOOD, E. S. 2001. Cycle of period gene expression in a diurnal mammal (Spermophilus tridecemlineatus): Implications for nonphotic phase shifting. *Journal of Biological Rhythms,* 16**,** 471-478.

MROSOVSKY, N., SALMON, P. A., MENAKER, M. & RALPH, M. R. 1992. Nonphotic phase-shifting in hamster clock mutants. *Journal of Biological Rhythms,* 7**,** 41-49.

MUSHTAQ, R., SHOIB, S., SHAH, T. & MUSHTAQ, S. 2014. Relationship between loneliness, psychiatric disorders and physical health? A review on the psychological aspects of loneliness.: *Journal of clinical and diagnostic research*, 8, WE01.

MYERS, E., STARTUP, H. & FREEMAN, D. 2011. Cognitive behavioural treatment of insomnia in individuals with persistent persecutory delusions: A pilot trial. *Journal of Behavior Therapy and Experimental Psychiatry,* 42**,** 330-336.

NAHORSKI, S. R., RAGAN, C. I. & CHALLISS, R. A. J. 1991. Lithium and the phosphoinositide cycle - an example of uncompetitive inhibition and its pharmacological consequences. *Trends in Pharmacological Sciences,* 12**,** 297-303.

NOGUCHI, T., LO, K., DIEMER, T. & WELSH, D. K. 2016. Lithium effects on circadian rhythms in fibroblasts and suprachiasmatic nucleus slices from Cry knockout mice. *Neuroscience Letters,* 619**,** 49-53.

OKUSA, M. D. & CRYSTAL, L. J. T. 1994. Clinical manifestations and management of acute lithium intoxication. *American Journal of Medicine,* 97**,** 383-389.

OLIE, J. P. & KASPER, S. 2007. Efficacy of agomelatine, a MT1/MT2 receptor agonist with 5-HT2C antagonistic properties, in major depressive disorder. *International Journal of Neuropsychopharmacology,* 10**,** 661-673.

OSLAND, T. M., FERNO, J., HAVIK, B., HEUCH, I., RUOFF, P., LAERUM, O. D. & STEEN, V. M. 2011. Lithium differentially affects clock gene expression in serum-shocked NIH-3T3 cells. *Journal of Psychopharmacology,* 25**,** 924-933.

OZAKI, N., NOSHIRO, M., KAWAMOTO, T., NAKASHIMA, A., HONDA, K., FUKUZAKI-DOHI, U., HONMA, S., FUJIMOTO, K., TANIMOTO, K., TANNE, K. & KATO, Y. 2012. Regulation of basic helix-loop-helix transcription factors Dec1 and Dec2 by RORa and their roles in adipogenesis. *Genes to Cells,* 17**,** 109-121.

PARTONEN, T. 1994. Effects of morning light treatment on subjective sleepiness and mood in winter depression. *Journal of Affective Disorders,* 30**,** 47-56.

PHILLIPS, M. L. & KUPFER, D. J. 2013. Bipolar Disorder 2 Bipolar disorder diagnosis: challenges and future directions. *Lancet,* 381**,** 1663-1671.

PIGGINS, H. D., ANTLE, M. C. & RUSAK, B. 1995. Neuropeptides phase-shift the mammalian circadian pacemaker. *Journal of Neuroscience,* 15**,** 5612-5622.

PORKKA-HEISKANEN, T., STRECKER, R. E., THAKKAR, M., BJORKUM, A. A., GREENE, R. W. & MCCARLEY, R. W. 1997. Adenosine: A mediator of the sleep-inducing effects of prolonged wakefulness. *Science,* 276**,** 1265-1268.

PROVENCIO, I., COOPER, H. M. & FOSTER, R. G. 1998. Retinal projections in mice with inherited retinal degeneration: Implications for circadian photoentrainment. *Journal of Comparative Neurology,* 395**,** 417-439.

RALPH, M. R., FOSTER, R. G., DAVIS, F. C. & MENAKER, M. 1990. Transplanted suprachiasmatic nucleus determines circadian period. *Science,* 247**,** 975-978.

RAMANATHAN, C., XU, H. Y., KHAN, S. K., SHEN, Y., GITIS, P. J., WELSH, D. K., HOGENESCH, J. B. & LIU, A. C. 2014. Cell Type-Specific Functions of Period Genes Revealed by Novel Adipocyte and Hepatocyte Circadian Clock Models. *Plos Genetics,* 10**,** e1004244.

RAMASAMY, R. & DEFREITAS, D. M. 1989. Competition between Li+ and Mg-2+ for ATP in human-erythrocytes - A P-31 NMR and optical spectroscopy study. *Febs Letters,* 244**,** 223-226.

REED, H. E., MEYER-SPASCHE, A., CUTLER, D. J., COEN, C. W. & PIGGINS, H. D. 2001. Vasoactive intestinal polypeptide (VIP) phase-shifts the rat suprachiasmatic nucleus clock in vitro. *European Journal of Neuroscience,* 13**,** 839-843.

RIPPERGER, J. A., JUD, C. & ALBRECHT, U. 2011. The daily rhythm of mice. *Febs Letters,* 585**,** 1384-1392.

ROCK, P., GOODWIN, G., HARMER, C. & WULFF, K. 2014. Daily rest-activity patterns in the bipolar phenotype: A controlled actigraphy study. *Chronobiology International,* 31**,** 290-296.

ROECKLEIN, K. A., ROHAN, K. J., DUNCAN, W. C., ROLLAG, M. D., ROSENTHAL, N. E., LIPSKY, R. H. & PROVENCIO, I. 2009. A missense variant (P10L) of the melanopsin (OPN4) gene in seasonal affective disorder. *Journal of Affective Disorders,* 114**,** 279-285.

ROSENTHAL, N. E., SACK, D. A., GILLIN, J. C., LEWY, A. J., GOODWIN, F. K., DAVENPORT, Y., MUELLER, P. S., NEWSOME, D. A. & WEHR, T. A. 1984. Seasonal Affective-Disorder - A description of the syndrome and preliminary findings with light therapy. *Archives of General Psychiatry,* 41**,** 72-80.

ROYBAL, K., THEOBOLD, D., GRAHAM, A., DINIERI, J. A., RUSSO, S. J., KRISHNAN, V., CHAKRAVARTY, S., PEEVEY, J., OEHRLEIN, N., BIRNBAUM, S., VITATERNA, M. H., ORSULAK, P., TAKAHASHI, J. S., NESTLER, E. J., CARLEZON, W. A., JR. & MCCLUNG, C. A. 2007. Mania-like behavior induced by disruption of CLOCK. *Proceedings of the National Academy of Sciences of the United States of America,* 104**,** 6406-6411.

RYVES, W. J. & HARWOOD, A. J. 2001. Lithium inhibits glycogen synthase kinase-3 by competition for magnesium. *Biochemical and Biophysical Research Communications,* 280**,** 720-725.

SATO, T. K., PANDA, S., MIRAGLIA, L. J., REYES, T. M., RUDIC, R. D., MCNAMARA, P., NAIK, K. A., FITZGERALD, G. A., KAY, S. A. & HOGENESCH, J. B. 2004. A functional genomics strategy reveals rora as a component of the mammalian circadian clock. *Neuron,* 43**,** 527-537.

SATO, T. K., YAMADA, R. G., UKAI, H., BAGGS, J. E., MIRAGLIA, L. J., KOBAYASHI, T. J., WELSH, D. K., KAY, S. A., UEDA, H. R. & HOGENESCH, J. B. 2006. Feedback repression is required for mammalian circadian clock function. *Nature Genetics,* 38**,** 312-319.

SCHAAP, J. & MEIJER, J. H. 2001. Opposing effects of behavioural activity and light on neurons of the suprachiasmatic nucleus. *European Journal of Neuroscience,* 13**,** 1955-1962.

SCHOU, M. 1958. Lithium studies .3. Distribution between serum and tissues. *Acta Pharmacologica Et Toxicologica,* 15**,** 115-124.

SCHOU, M. 1968. Lithium in psychiatric therapy and prophylaxis. *Journal of Psychiatric Research,* 6**,** 67-&.

SCHOU, M. 1997. The combat of non-compliance during prophylactic lithium treatment. *Acta Psychiatrica Scandinavica,* 95**,** 361-363.

SCHWITZER, J., NEUDORFER, C., BLECHA, H. G. & FLEISCHHACKER, W. W. 1990. Mania as a side-effect of phototherapy. *Biological Psychiatry,* 28**,** 532-534.

SERRETTI, A. & OLGIATI, P. 2005. Profiles of "manic" symptoms in bipolar I, bipolar II and major depressive disorders. *Journal of Affective Disorders,* 84**,** 159-166.

SEVERUS, E., TAYLOR, M. J., SAUER, C., PFENNIG, A., RITTER, P., BAUER, M. & GEDDES, J. R. 2014. Lithium for prevention of mood episodes in bipolar disorders: systematic review and meta-analysis. *International journal of bipolar disorders* 2, 15.

SHARMA, V. K. & CHANDRASHEKARAN, M. K. 2005. Zeitgebers (time cues) for biological clocks. *Current Science,* 89**,** 1136-1146.

SHEARMAN, L. P., JIN, X. W., LEE, C. G., REPPERT, S. M. & WEAVER, D. R. 2000. Targeted disruption of the mPer3 gene: Subtle effects on circadian clock function. *Molecular and Cellular Biology,* 20**,** 6269-6275.

SHEARMAN, L. P., ZYLKA, M. J., REPPERT, S. M. & WEAVER, D. R. 1999. Expression of basic helix-loop-helix/PAS genes in the mouse suprachiasmatic nucleus. *Neuroscience,* 89**,** 387-397.

SHIBATA, S. & MOORE, R. Y. 1993. Tetrodotoxin does not affect circadian rhythms in neuronal activity and metabolism in rodent suprachiasmatic nucleus in vitro.: *Brain research*, 606, 259-266.

SHIBATA, S., OOMURA, Y., KITA, H. & HATTORI, K. 1982. Circadian rhythmic changes of neuronal-activity in the suprachiasmatic nucleus of the rat hypothalamic slice. *Brain Research,* 247**,** 154-158.

SIE, M. 2014. Mood stabilisers in the management of bipolar affective disorder.: *Progress in Neurology and Psychiatry*, 18, 22-32.

SIEPKA, S. M. & TAKAHASHI, J. S. 2005. Methods to record circadian rhythm wheel running activity in mice. *Circadian Rhythms,* 393**,** 230-239.

SMITH, J. B. & ROZENGURT, E. 1978. Lithium transport by fibroblastic mouse cells - characterization and stimulation by serum and growth-factors in quiescent cultures. *Journal of Cellular Physiology,* 97**,** 441-449.

STEPHAN, F. K. & ZUCKER, I. 1972. Circadian-rhythms in drinking behavior and locomotor activity of rats are eliminated by hypothalamic-lesions. *Proceedings of the National Academy of Sciences of the United States of America,* 69**,** 1583-&.

SWANN, A. C., PAZZAGLIA, P., NICHOLLS, A., DOUGHERTY, D. M. & MOELLER, F. G. 2003. Impulsivity and phase of illness in bipolar disorder. *Journal of Affective Disorders,* 73**,** 105-111.

SWANSON, L. W., COWAN, W. M. & JONES, E. G. 1974. Autoradiographic study of efferent connections of ventral lateral geniculate-nucleus in albino-rat and cat. *Journal of Comparative Neurology,* 156**,** 143-163.

TAKAHASHI, J. S. 2017. Transcriptional architecture of the mammalian circadian clock. *Nature Reviews Genetics,* 18**,** 164-179.

TAKAHASHI, J. S., DECOURSEY, P. J., BAUMAN, L. & MENAKER, M. 1984. Spectral sensitivity of a novel photoreceptive system mediating entrainment of mammalian circadian-rhythms. *Nature,* 308**,** 186-188.

TANAKA, M., ICHITANI, Y., OKAMURA, H., TANAKA, Y. & IBATA, Y. 1993. The direct retinal projection to VIP neuronal elements in the rat SCN. *Brain Research Bulletin,* 31**,** 637-640.

TAYLOR, D. J., MALLORY, L. J., LICHSTEIN, K. L., DURRENCE, H. H., RIEDEL, B. W. & BUSH, A. J. 2007. Comorbidity of chronic insomnia with medical problems. *Sleep,* 30**,** 213-218.

TIMMER, R. T. & SANDS, J. M. 1999. Lithium intoxication. *Journal of the American Society of Nephrology,* 10**,** 666-674.

TODMAN, D. 2007. A History Of Sleep Medicine. The Internet Journal of Neurology.

UEDA, H. R., CHEN, W. B., ADACHI, A., WAKAMATSU, H., HAYASHI, S., TAKASUGI, T., NAGANO, M., NAKAHAMA, K., SUZUKI, Y., SUGANO, S., IINO, M., SHIGEYOSHI, Y. & HASHIMOTO, S. 2002. A transcription factor response element for gene expression during circadian night. *Nature,* 418**,** 534-539.

VALTONEN, H., SUOMINEN, K., MANTERE, O., LEPPAMAKI, S., ARVILOMMI, P. & ISOMETSA, E. I. 2005. Suicidal ideation and attempts in bipolar I and II disorders. *Journal of Clinical Psychiatry,* 66**,** 1456-1462.

VAN DEN POL, A. N. 1980. The hypothalamic suprachiasmatic nucleus of rat - intrinsic anatomy. *Journal of Comparative Neurology,* 191**,** 661-702.

VAN DER HORST, G. T. J., MUIJTJENS, M., KOBAYASHI, K., TAKANO, R., KANNO, S., TAKAO, M., DE WIT, J., VERKERK, A., EKER, A. P. M., VAN LEENEN, D., BUIJS, R., BOOTSMA, D., HOEIJMAKERS, J. H. J. & YASUI, A. 1999. Mammalian Cry1 and Cry2 are essential for maintenance of circadian rhythms. *Nature,* 398**,** 627-630.

VAN ESSEVELDT, K. E., LEHMAN, M. N. & BOER, G. J. 2000. The suprachiasmatic nucleus and the circadian time-keeping system revisited. *Brain research. Brain research reviews,* 33**,** 34-77.

VGONTZAS, A. N., BIXLER, E. O., LIN, H. M., PROLO, P., MASTORAKOS, G., VELA-BUENO, A., KALES, A. & CHROUSOS, G. P. 2001. Chronic insomnia is associated with nyctohemeral activation of the hypothalamic-pituitary-adrenal axis: Clinical implications. *Journal of Clinical Endocrinology & Metabolism,* 86**,** 3787-3794.

VITATERNA, M. H., KO, C. H., CHANG, A. M., BUHR, E. D., FRUECHTE, E. M., SCHOOK, A., ANTOCH, M. P., TUREK, F. W. & TAKAHASHI, J. S. 2006. The mouse Clock mutation reduces circadian pacemaker amplitude and enhances efficacy of resetting stimuli and phase-response curve amplitude. *Proceedings of the National Academy of Sciences of the United States of America,* 103**,** 9327-9332.

VITATERNA, M. H., SELBY, C. P., TODO, T., NIWA, H., THOMPSON, C., FRUECHTE, E. M., HITOMI, K., THRESHER, R. J., ISHIKAWA, T., MIYAZAKI, U., TAKAHASHI, J. S. & SANCAR, A. 1999. Differential regulation of mammalian period genes and circadian rhythmicity by cryptochromes 1 and 2. *Proceedings of the National Academy of Sciences of the United States of America,* 96**,** 12114-12119.

WATANABE, K., DEBOER, T. & MEIJER, J. H. 2001. Light-induced resetting of the circadian pacemaker: Quantitative analysis of transient versus steady-state phase shifts. *Journal of Biological Rhythms,* 16**,** 564-573.

WEAVER, D. R. 1998. The suprachiasmatic nucleus: A 25-year retrospective. *Journal of Biological Rhythms,* 13**,** 100-112.

WEHR, T. A., DUNCAN, W. C., SHER, L., AESCHBACH, D., SCHWARTZ, P. J., TURNER, E. H., POSTOLACHE, T. T. & ROSENTHAL, N. E. 2001. A circadian signal of change of season in patients with seasonal affective disorder. *Archives of General Psychiatry,* 58**,** 1108-1114.

WEHR, T. A., TURNER, E. H., SHIMADA, J. M., LOWE, C. H., BARKER, C. & LEIBENLUFT, E. 1998. Treatment of a rapidly cycling bipolar patient by using extended bed rest and darkness to stabilize the timing and duration of sleep. *Biological Psychiatry,* 43**,** 822-828.

WEITZMAN, E. D., FUKUSHIMA, D., NOGEIRE, C., ROFFWARG, H., GALLAGHER, T. F. & HELLMAN, L. 1971. 24 hour pattern of episodic secretion of cortisol in normal subjects. *Journal of Clinical Endocrinology & Metabolism,* 33**,** 14-+.

WELSH, D. K. & MOOREEDE, M. C. 1990. Lithium lengthens circadian period in a diurnal primate, Saimiri-sciureus. *Biological Psychiatry,* 28**,** 117-126.

WELSH, D. K., TAKAHASHI, J. S. & KAY, S. A. 2010. Suprachiasmatic Nucleus: Cell Autonomy and Network Properties. *Annual Review of Physiology,* 72**,** 551-577.

WIRZ-JUSTICE, A., HAUG, H. J. & CAJOCHEN, C. 2001. Disturbed circadian rest-activity cycles in schizophrenia patients: An effect of drugs? *Schizophrenia Bulletin,* 27**,** 497-502.

WIRZJUSTICE, A., BUCHELI, C., GRAW, P., KIELHOLZ, P., FISCH, H. U. & WOGGON, B. 1986. Light treatment of seasonal affective-disorder in Switzerland. *Acta Psychiatrica Scandinavica,* 74**,** 193-204.

WISOR, J. P., PASUMARTHI, R. K., GERASHCHENKO, D., THOMPSON, C. L., PATHAK, S., SANCAR, A., FRANKEN, P., LEIN, E. S. & KILDUFF, T. S. 2008. Sleep deprivation

effects on circadian clock gene expression in the cerebral cortex parallel electroencephalographic differences among mouse strains. *Journal of Neuroscience,* 28**,** 7193-7201.

WOOD, J., BIRMAHER, B., AXELSON, D., EHMANN, M., KALAS, C., MONK, K., TURKIN, S., KUPFER, D. J., BRENT, D., MONK, T. H. & NIMGAINKAR, V. L. 2009. Replicable differences in preferred circadian phase between bipolar disorder patients and control individuals. *Psychiatry Research,* 166**,** 201-209.

WORLD HEALTH ORGANISATION 2014. *ICD-10 classification of mental and behavioural disorders: clinical descriptions and diagnostic guidelines; 10th Revision,* Geneva.

WORLD HEALTH ORGANISATION 2008. *The global burden of disease: 2004 update. Part 3 Disease incidence, prevalence and disability*.

YANG, S., VAN DONGEN, H. P. A., WANG, K., BERRETTINI, W. & BUCAN, M. 2009. Assessment of circadian function in fibroblasts of patients with bipolar disorder. *Molecular Psychiatry,* 14**,** 143-155.

YIN, L., WANG, J., KLEIN, P. S. & LAZAR, M. A. 2006. Nuclear receptor Rev-erba is a critical lithium-sensitive component of the circadian clock. *Science,* 311**,** 1002-1005.

YOO, S. H., YAMAZAKI, S., LOWREY, P. L., SHIMOMURA, K., KO, C. H., BUHR, E. D., SIEPKA, S. M., HONG, H. K., OH, W. J., YOO, O. J., MENAKER, M. & TAKAHASHI, J. S. 2004. PERIOD2 :: LUCIFERASE real-time reporting of circadian dynamics reveals persistent circadian oscillations in mouse peripheral tissues. *Proceedings of the National Academy of Sciences of the United States of America,* 101**,** 5339-5346.

YORK, J. D., PONDER, J. W. & MAJERUS, P. W. 1995. Definition of a metal-dependent Li+-inhibited phosphomonoesterase protein family based upon a conserved 3-dimensional core structure. *Proceedings of the National Academy of Sciences of the United States of America,* 92**,** 5149-5153.

YOSHIKAWA, T. & HONMA, S. 2016. Lithium lengthens circadian period of cultured brain slices in area specific manner. *Behavioural Brain Research,* 314**,** 30-37.

YOUNG, A. H., RIGNEY, U., SHAW, S., EMMAS, C. & THOMPSON, J. M. 2011. Annual cost of managing bipolar disorder to the UK healthcare system. *Journal of Affective Disorders,* 133**,** 450-456.

YOUNG, J. W., MINASSIAN, A., PAULUS, M. P., GEYER, M. A. & PERRY, W. 2007. A reverse-translational approach to bipolar disorder: Rodent and human studies in the Behavioral Pattern Monitor. *Neuroscience and Biobehavioral Reviews,* 31**,** 882-896.

ZHANG, R., LAHENS, N. F., BALLANCE, H. I., HUGHES, M. E. & HOGENESCH, J. B. 2014. A circadian gene expression atlas in mammals: Implications for biology and medicine. *Proceedings of the National Academy of Sciences of the United States of America,* 111**,** 16219-16224.

Chapter 2: General Methods

2. General Methods

2.1 Cell Culture Techniques

All cell and tissue culture procedures were performed under sterile conditions using a containment level II biological safety cabinet (Gelaire). Cells were maintained in incubators at 37°C with 5% CO_2 and high humidity (Panasonic) in 75cm^2 or 25cm^2 cell culture flasks (Greiner, Corning). All experiments were performed in 96-well or 384-well clear bottom plates (Greiner) unless otherwise specified.

2.1.1 Cell culture media

DMEM: Dulbecco's Modified Eagle's Medium (DMEM) with high glucose GlutaMAX supplement (ThermoFisher Scientific), 10% fetal bovine serum (FBS) (Sigma), and 1% penicillin-streptomycin (P/S) (Sigma).

ADMEM: Advanced DMEM (ADMEM) (ThermoFisher Scientific) with high glucose 1x GlutaMAX supplement (ThermoFisher Scientific), 10% FBS, and 1% P/S.

RPMI: Roswell Park Memorial Institute (RPMI) media, supplemented with 10% FBS, 1% P/S, 1x GlutaMAX, 16ng/mL insulin-like growth factor (Cambridge Bioscience), 55ng/mL recombinant human epidermal growth factor (R&D systems), and 10µg/mL human insulin (Roche Diagnostics).

Recording Media: Low glucose DMEM (D2902 Powder) (Sigma) was used for the performance of many experiments and will be referred to as recording media. The recording media was supplemented with 9.5mL/L 45% D-

glucose solution (Sigma), 10mM HEPES solution (Sigma), 3.7g/L $NaHCO_3$ solution (Sigma), 0.5% P/S, 1x GlutaMAX and adjusted to pH 7.3 in 1L of water.

2.1.2 Maintenance of cell lines

The two immortalised cell lines of use included the murine MMHD3 pre-hepatocytes and human U2OS osteosarcoma cells with and without stable *Per2::Luc* or *Bmal::Luc* expression, where *Bmal* denotes *Bmal1* specifically throughout. These are promoter driven luciferase genes that allow photon detection following transcription factor binding to the *Per2* or *Bmal* promoter regions. The U2OS-blank cells were obtained from the ATCC, the *Per2::Luc* U2OS cells were gifted from Patrick Nolan (MRC Harwell, UK), MMHD3-blank cells from Marco Tripodi (Sapienza University of Rome, Italy), and the *Bmal::Luc* MMHD3 cells from John Hogenesch (University of Pennsylvania, USA). Cell lines were maintained from passage 2-30, where the U20S cells were grown and maintained in DMEM on standard tissue culture flasks. The MMHD3 cells were maintained in RPMI media and grown on rat tail collagen type 1 (Corning) pre-coated flasks, diluted to 50µg/mL in 0.2M acetic acid for a minimum of 5h.

Primary human dermal fibroblasts were cultured from skin biopsy samples. Cells from 39 bipolar patients and 24 control subjects were obtained from the Oxford StemBANCC (details in Chapter 3, Table 3.2). All fibroblasts were cultured in ADMEM from passage 3-11 in standard tissue culture flasks.

After washing with Dulbecco's phosphate-buffered saline (PBS) without magnesium or calcium (ThermoFisher Scientific), the cells were passaged using TrypLE™ solution (ThermoFisher Scientific). All cells were passaged when 80-90% confluent and subcultured 1-2 times a week.

2.2 DNA Cloning with Plasmid Vectors and Bacterial Cell Culture

2.2.1 DNA amplification

DNA amplification of the *cAMP::GloSensor* plasmid (Promega) was performed to create a lentiviral expression clone. DNA regions of interest were amplified using the NEB Q5 High Fidelity 2x master mix (New England Biolabs). Primers, as seen below, were used to amplify the *cAMP::GloSensor* region from 1ng of plasmid. The primers were designed to fulfil the needs of a BP/LR gateway reaction (ThermoFisher Scientific). The following PCR protocol was set up → initial denaturation: 98°C for 30seconds (s), 30 cycles of: 98°C for 10s, 66°C for 30s, 72°C for 65s, final extension: 72°C for 120s, hold: 4°C indefinitely.

The *cAMP::GloSensor* gateway cloning primers sequences are as follows (5' to 3'):

1. **Forward:**GGGGACAAGTTTGTACAAAAAAGCAGGCTYTTTAATACGACTCACTA TAGGGCTAGC
2. **Reverse:**GGGGACCACTTTGTACAAGAAAGCTGGGTYGAGTTTAAACCCCTTCTG GAGTG

The PCR product was then run on a precast 1% E-gel EX (ThermoFisher Scientific). After confirming that the PCR product was of the correct weight, gel excision and purification was performed using the Wizard SV Gel and PCR Clean-up System (Promega), a kit designed for purification of 100bp-10kb fragments. The excised gel was weighed and an equal volume of membrane binging solution was added (100µL per 100mg gel weight). The gel was then dissolved after incubating the mixture at 50°C. The dissolved gel was then passed through the DNA binding column, centrifuging at 13,000g for 1min. The membrane with the

DNA fragments bound was washed 2 times with membrane wash solution containing ethanol and was centrifuged at 13,000g for 1-5min, and finally eluted in 50µL nuclease-free water. DNA concentrations were measured using the Qubit 2.0 Flurometer (ThermoFisher Scientific).

2.2.2 Gateway reaction

Once the DNA fragments had been isolated, a single step BP/LR gateway reaction was performed. 100ng of DNA was incubated with 150ng of the donor vector pDONR (Invitrogen), 150ng of the destination vector PLX304 (ThermoFisher Scientific), and 2µL of LR ClonaseII (ThermoFisher Scientific) in a final volume of 10µL TE buffer (Qiagen). The cocktail was incubated at room temperature overnight, after which the reaction was terminated with the addition of 1µL proteinase K for 10min at 37°C (ThermoFisher Scientific).

Gateway cloning technology utilises the *att* sites from the *E. coli* genome to provide regions for site-specific recombination in the presence of enzymes, where recombination is specific between *attB* and *attP* sites, and *attL* and *attR* sites. The method is robust in the generation of functional destination plasmids as there are 2 processes of selection. Firstly, antibiotic selection occurs as the transformed bacteria without the correct antibiotic resistance cassette will die, and secondly because of the presence of the *ccdB* gene. This is a gene present in the donor and destination vectors, which ensures that bacteria that did not undergo the process of recombination have stunted growth.

2.2.3 Bacterial transformation and selection

The Gateway cocktail was then used to transform Top10 One Shot competent *E. coli* cells (ThermoFisher Scientific), as these cells are efficient in

propagating cloned plasmids and are sensitive to the effects of the *ccdB* gene. 5µL of the Gateway cocktail was added to 45µL of bacterial cells and incubated on ice for 30min. This was followed by a 30s heat shock at 42°C, a process that creates pores in the bacterial membrane, and a further 2min on ice. After adding 250µL of S.O.C. media (Melford), the bacterial cells were placed in an orbital shaker for 2h at 37°C and then 100µL of cells were spread on pre-warmed selection agar plates and incubated at 30°C overnight. Selection plates were made from Lysogeny broth (LB) by mixing LB powder (20g/L) (Sigma) with sodium chloride (NaCl) (5g/L) in water and autoclaving for sterilisation. 1g agar (Melford) was added to 200mL LB media with either 60µg/mL kanamycin (Sigma), or 100µg/mL carbencillin (Sigma). 24h later 5-6 individual colonies from the carbencillin plate were selected and if successful, would contain the expression clone. Colonies were expanded in antibiotic containing LB media.

2.2.4 Plasmid preparations

Bacterial mini-preps (Qiagen) were then performed on all selected colonies where all centrifugation steps were performed at 13,000g. Bacteria were pelleted and resuspended in 250µL of resuspension buffer. After the addition of 250µL of cell lysing agent for 5min, 350µL of neutralising buffer was added and the mixture was centrifuged for 10min. The DNA containing supernatant was added to the QIAprep spin column and centrifuged for 1min, after which the column with the plasmid DNA bound was washed with 750µL buffer PE and centrifuged for a further minute. The plasmid was finally eluted in nuclease-free water by centrifuging for 1min.

Restriction enzyme digestion of the eluted plasmid followed by E-gel electrophoresis confirmed the presence of the correct plasmid. Double digestion was performed by mixing 1µL of eluted DNA, 1µL Fast Digest buffer (ThermoFisher Scientific), and 1µL of restriction enzyme mix in a final volume of 10µL water. Samples were then incubated at 37°C for 1h followed by 1% E-gel electrophoresis. Final confirmation was executed by sending the plasmid off for sequencing using Sanger sequencing services (Source Bioscience).

2.3 Lentivirus Production

HEK 293 cells (obtained from the ATCC) were seeded to 70% confluence in 10cm dishes (Corning). A calcium phosphate triple transfection method was used. The transfection complex was created by combining 3 plasmids using a 3:2:1 ratio of 12.5µg expression clone, 8.25µg packaging plasmid, and 4.4µg envelope plasmid. psPAX2 and PMD2G were used as the packaging and envelope plasmids respectively for all virus production, and the transfection vectors used included: *Bmal::Luc* (Addgene), *Per2::Luc* (Addgene), and *cAMP::GloSensor* (made in-house). The transfection complex required the addition of 126µL 2M $CaCl_2$ (Melford) to the plasmid cocktail in a final volume of 900µL water, followed by the addition of 900µL 2x HEPES buffered saline (Melford) whilst vortexing the mixture to create a fine precipitate. The mix was then added to the HEK cells in DMEM containing 25µM chloroquine but deficient of P/S for 1h prior to viral plasmid addition. Following 24h of incubation at 37°C, the media was changed to DMEM containing 5mM sodium buterate and incubated for a further 72h at 37°C, after which the media containing the lentivirus was collected and passed through a 0.4µm filter before storing the viral supernatant at -80°C.

Mass production of *Bmal::Luc* and *Per2::Luc* virus was performed in order to infect human fibroblasts with the same batch of lentivirus. HEK 293 cells were seeded to 80% confluence in HYPERflasks (Corning). This specialised flask is designed to equal the surface area of 10x 175cm^2 flasks, where the presence of a gas permeable filter allows the flask to be maximally filled. The aforementioned 3:2:1 ratio of plasmids was used, where the complex included: 60.4µg transfection vector, 40.25µg packaging plasmid, 16.1µg envelope plasmid, in a final volume of 10mL NaCl (150mM) (Sigma). Alternatively, 25kDa polyethyleneimine (PEI) (Polyscience) was the transfection reagent of choice. 1mL of PEI (1mg/mL) in 10mL NaCl (150mM) was added drop-by-drop to the DNA/NaCl solution and incubated at room temperature for 20min. The transfection complex was then added to DMEM + 2% FBS prior to HYPERflask addition and the cells were incubated at 37°C overnight. 16h post transfection, the cellular media was replaced with pre-warmed DMEM + 10% FBS and incubated at 37°C for 48h to allow sufficient virus generation.

2.3.1 Virus detection and concentration

The presence of viral particles was confirmed using Lenti-X™ GoStix (Clontech), where 20µL of viral supernatant was loaded and intensity was assessed after 10min. The C and T regions represent the control and test bands respectively where the presence of the p24 viral capsid protein is detected.

The viral supernatant was then collected and passed through a 0.4µm filter before concentrating using the Vivaspin 20 (100,000 MWCO) (Sartorious) centrifugal filtration devices. The media was centrifuged at 3,000g, 20°C for

40min and the sample was then recovered from the concentrator pocket and stored at -80°C. Overall, the viral media was concentrated ~25 times.

2.3.2 Stable cell line generation

A 1 to 10 ratio of viral supernatant to media was used with the U2OS cells, which were incubated at 37°C for 24h. Only the U2OS cells were selected with puromycin (2µg/mL) for 4 days, followed by single colony selection under a light microscope to create our own *Bmal::Luc* U2OS cell line.

Primary cell lines underwent a spinfection protocol whereby 100,000 cells with 200µL of concentrated viral supernatant (multiplicity of infection ~20) were centrifuged at 3,000g, 25°C for 99min. Cells were then resuspended in the viral media and incubated at 37°C overnight. Mixed colonies were accepted for all experiments.

2.4 ERK ELISA Assay

The ERK1/2 (pT202/Y204) and Total ERK1/2 SimpleStep ELISA kit (Abcam) was used on *Bmal::Luc* MMHD3 cells. Cells were serum starved for 3h with the addition of compounds for 10min and followed by cell lysis. Compounds included: 30mM NaCl, 30mM lithium chloride (LiCl), vehicle, 3µM L690,488, 500nM SCH772984 (MedChem Express), 1mM vidarabine, 30µM H89, or 1µM phorbol 12-myristate 13-acetate (PMA). 50µL of sample was combined with 50µL of capture and detector antibodies on immobilising antibody pre-coated plates and incubated for 1h at room temperature. The wells were then thoroughly washed and incubated with 100µL of TMB - a colour developing substrate and absorbance was detected at 450nm in a plate reader. Values are presented after P-ERK levels were normalised to total (T)-ERK levels.

2.5 Luminescence Detection Experiments

All luminescence detection assays were performed using a plate reader. Readers included: FLUOstar Omega and FLUOstar Optima (BMG Labtech), TriStar^2 LB 942 (Berthold Technologies), Tecan Infinite M200 Pro, and Tecan Infinite F200 (Tecan).

2.5.1 Transient transfections

96-well plates were seeded to 70% confluence and luminescence was detected using a plate reader. Plasmid DNA was diluted to 1µg per 100µL of reduced serum Opti-MEM (ThermoFisher Scientific) with 3µL or 5µL of ViaFect transfection reagent (Promega) for U2OS or MMHD3 cells respectively. 50ng of DNA were transfected per well for 24h prior to use for ensuing cellular assays.

2.5.2 In vitro siRNA transfections

All SMARTpool siRNA (Dharmacon) was assessed on *Bmal::Luc* MMHD3 cells. The siRNA used included: non-targeting control (siControl), *Adcy1-10*, *C/EBPα*, *Csnk1δ*, *Impa1*, and *Isyna1*. All plasmids were resuspended and diluted to 2µM concentrations using nuclease-free siRNA Buffer (Dharmacon). Cells were seeded to 70% confluence in 96-well plates and transfected with 3-50nM siRNA using Dharmafect 1 (Dharmacon) according to the manufacturer's instructions. This required diluting the siRNA in a final volume of 10µL Opti-MEM, and 0.4µL Dharmafect 1 in a final volume of 10µL Opti-MEM per well, as this proved most efficient in prior optimising experiments. By adding the siRNA mix to the transfection reagent, whole complexes (20µL) were incubated at room temperature for 20min and then subsequently combined with 80µL of RPMI media and added to the plated cells. Cells were then incubated at 37°C for 24h

and treated with 200nM dexamethasone treatment to synchronise the cells prior to using them for circadian bioluminescence assays or real-time PCR analysis. RNA extractions occurred 48h after transfection.

2.5.3 Assessing circadian rhythms

Cells were seeded to 100% confluence in 96- or 384-well plates. Dexamethasone, a glucocorticoid receptor agonist synchronises the clocks within individual cells allowing observation of rhythmic patterns. All cells were treated with 200nM dexamethasone (Sigma) in recording media for 1-1.5h, followed by the addition of recording media supplemented with B27 (ThermoFisher Scientific), 400µM D-luciferin potassium salt (Gold Biotechnology), with or without pharmacological compounds of interest. Bioluminescence was recorded for a minimum of 4 days in the plate reader. The U2OS and MMHD3 cells were tested using an array of the aforementioned plate readers, however, all fibroblast assays were performed in the Tecan Infinite M200 Pro/ F200. Period is reported in hours and amplitude in relative light units (RLU) or fold change.

2.6 Cellular mRNA Quantification

2.6.1 RNA preparation

Total RNA was extracted from *Bmal::Luc* MMHD3 cells seeded in 12-well or 96-well plates and lysed respectively with 350µL or 100µL/well RLT buffer (Qiagen) supplemented with 1% β-mercaptoethanol (Sigma), a reducing agent which denatures RNAases released as a consequence of cell lysis. Whole-cell RNA extractions were performed using the RNeasy plus mini kit (Qiagen), where all centrifugation steps were performed at 12,000g. Cells were immediately centrifuged in the gDNA eliminator for 30s. One volume of 100% ethanol (sigma)

was added to the flow-through to precipitate the RNA and then transferred to the RNeasy mini elute spin column and centrifuged for 15s. The column with the RNA bound was then washed with RWI and RPE (wash buffers) prior to the addition of 80% ethanol all of which required centrifugation for 15s, 15s, and 2min respectively. The RNA was finally eluted in 30µL RNase-free water after centrifuging for 1min. RNA concentration was measured using the Nanodrop 2000 (ThermoFisher Scientific) prior to cDNA conversion.

2.6.2 cDNA conversion

RNA to cDNA conversion was performed using the qScript cDNA Synthesis kit (Quanta Biosciences). 300ng of RNA were converted per sample, requiring 2µL 5x qScript reaction mix and 0.5µL qScript RT enzyme in a final volume of 10µL water. The PCR protocol, which in theory generates 1 copy of cDNA for 1 molecule of RNA, involved 1 cycle of: 22°C for 5min, 42°C for 30min, 85°C for 5min, before holding at 4°C indefinitely. cDNA samples were diluted to 2ng/µL in water and stored at -80°C until real-time PCR was performed.

2.6.3 Real-time PCR

SYBR green master mix (ThermoFisher Scientific) real-time PCR was performed using the StepOne Real-Time PCR system (ThermoFisher Scientific). The SYBR green intercalating dye binds preferentially to dsDNA, and the exponential increase in DNA can be interpreted through fluorescence measurements. 10ng of cDNA were loaded per well (96-well plate). This was followed by the addition of 10µL of master mix consisting of 7.5µL 2x SYBR green, 0.15µL forward primer, 0.15µL reverse primer, and 2.2µL water. However, when Bio-Rad pre-validated primers were used, 0.75µL of the primer

mix was required and the water content was adjusted appropriately. Primer lists can be found in the respective chapter methods. The PCR protocol, which ran for 40 cycles, required an initial holding temperature of 95°C for 5min to activate the Taq polymerase, followed by 30 cycles of 95°C for 10s, 60°C for 30s, and 72°C for 12s, followed by the production of a melt curve.

2.7 PrestoBlue Assay

A PrestoBlue™ cell viability assay (ThermoFisher Scientific) was used after the termination of experiments. The PrestoBlue reagent was diluted to 1x in the respective cell culture media where 20-50µL were added per well for 1h at 37°C. The fluorescence was then measured in a plate reader with the excitation and emission filters set at 544nm and 590nm respectively. The fluorescence of wells with no cells was used as the negative control. This is a resazurin-based assay where the reducing environment of live cells alters the non-fluorescent blue resazurin molecule into a very fluorescent resorufin molecule. Values were compared to vehicle treatment to detect changes in cell viability.

2.8 Animals

Mice of all genotypes were reared and maintained under 12:12h LD cycles, under a controlled ambient temperature of 20-22°C and 40% humidity with standard food and water available *ad libitum*. All animal experiments were performed in accordance with the United Kingdom Animals (Scientific Procedures) Act of 1986.

2.9 General Data Analysis

With regards to the cell-based circadian analysis, data from a full 384-well plate, read once an hour for 4 days resulted in over 35,000 data points.

Therefore, due to the sheer enormity of the data generated, a specialised software, MultiCycle (ActiMetrics) was used to calculate the circadian period and amplitude of oscillations, unless otherwise specified. Both cell and tissue data were analysed using MultiCycle. The software calculates a baseline subtracted 24h running average of the raw luminescence data which is then smoothed by 4h such that waveforms oscillate around Y=0, enabling well-to-well comparison of different circadian parameters (fibroblasts were smoothed by 10h). Smoothing enables the detection of subtle changes, particularly in low amplitude oscillating tissues and cells. A dampened sine wave is then fitted to the data using a Levenberg-Marquardt algorithm, which is used to provide data on the circadian parameters of interest. For immortalised cell lines, parameters were calculated by excluding the first 12-16h followed by the analysis of 3 oscillations. Primary cell lines were analysed using 2 oscillations, due to the rapid rate of dampening.

Real-time PCR data was analysed through the relative gene quantification method, which compares threshold cycle (C_T) values to a housekeeping gene. The C_T values of genes were converted to relative gene amount and normalised to the housekeeping gene using the following equation: $\mathcal{X} = 2^{-C_T}$.

2.10 General Statistical Analysis

Statistical analysis was performed using GraphPad Prism 6, where results are presented in the form of average ± standard error of the mean (SEM). An unpaired two-tailed t-test was performed when comparing two parameters. A one-way ANOVA with a Tukey or a Dunnett's post hoc test was used when comparing multiple parameters, unless otherwise specified. The threshold for significance was set at $P<0.05$. *$P<0.05$, **$P<0.01$, ***$P<0.001$, ****$P<0.0001$.

2.11 Chapter 3: Methods

2.11.1 Growth curves

Human fibroblasts were grown and seeded at 15,000 cells/well in 6-well plates (Corning). The cells were then trypsinised in triplicates and counted on days 1, 4, and 8 to assess the population doubling time (PDT). A selection of cell lines were trypsinised and counted every day to confirm the pattern represented was indicative of standard growth curves. Cell counting was performed using the Countess Automated Cell Counter (Invitrogen) and PDT was calculated using the formula below. $\mathcal{T}$: incubation time in days, $\mathcal{Xb}$: cell number on day 1, $\mathcal{Xe}$: cell number on day 8.

$$\mathcal{PDT} = \mathcal{T}\frac{\ell n2}{\ell n(\mathcal{Xe} \div \mathcal{Xb})}$$

2.11.2 Assessing circadian rhythms

All fibroblasts were seeded in 96-well plates, treated with dexamethasone, and bioluminescence was recorded. Period values for each cell line were characterised by averaging data obtained from six individual samples.

2.11.3 Correlograms

The statistical programme R was used to generate correlograms. These are correlation matrices where multiple parameters are compared simultaneously in order to identify correlative patterns. The graphical representation portrays two key pieces of information. Firstly, the correlation coefficient is analysed using a Pearson parametric correlation test from a scale of +1 to -1, where the presence of a correlation is represented along a spectrum of blue to red and by the size of the circle. Blue is indicative of a positive

correlation, and red of a negative correlation, where a larger circle also represents a stronger correlation. Secondly, the significance of the relationship between the two parameters is indicated by the presence of an asterisk. Significance is indicated and assessed using a two-tailed t-test in bottom left corner, where the top right-hand corner indicated significance following adjustments for multiple comparisons using the Holm-Bonferroni test. Only data from patient-derived fibroblasts transduced with both the *Bmal::Luc* and *Per2::Luc* virus were tested in the correlation matrices.

Example scripts

1. Import the data file into R and assign it a name.

```
> LithiumResponse
```

2. Use the 'corr' function to create the correlation matrix (Pearson parametric test).

```
> CorLithResponse=cor(LithiumResponse)
```

3. Use the 'corr.test' function to calculate the probability values for the correlation matrix (t-test, Holm-Bonferroni test).
   The numbers indicate the columns to be included in the analysis.

```
> CorLithResponseSig=Corr.test(LithiumResponse[,c(2,3,4,
5,8,9,11,15,16,20,36,3,7,38,22,23,24,25,26,27,28,29,30)])
```

4. Use the 'corrplot' function to output the correlation matrix as a correlogram with desired visual aids.

p.mat:	defines the values used to assess significance.
sig.level:	denotes the P-values assigned to the asterisks (1-3).
pch.cex:	defines the size of the asterisk.
label_sig:	allows you to mark the significant differences according to the defined significance levels.
diag:	defines whether diagonal autocorrelation is displayed.
mar:	defines the boundaries of the correlogram image.

```
> corrplot(corLithResponseSig$r, title = "Lithium-
Sensitive", p.mat = corLithResponseSig$p, sig.level =
c(.001, .01, .05), pch.cex = 2.5, insig = "label_sig",
diag = FALSE, mar=c(0,0,1,0))
```

2.12 Chapter 4: Methods

2.12.1 Reagents

Compounds: LiCl (Sigma), nobiletin (Cayman chemical company), CGS-15943 (Sigma), DMSO (Sigma) and nuclease free water (Ambion).

2.12.2 Assessing circadian rhythms

Bmal::Luc fibroblasts were seeded in 96-well plates prior to dexamethasone treatment, and bioluminescence was recorded, as previously described. Drug-induced period and amplitude values for each cell line were characterised by averaging data obtained from 3 individual samples per concentration tested. Period changes were calculated by subtracting values of interest from the vehicle treatment, where amplitude changes were denoted by calculating the fold change.

2.12.3 Animal locomotor activity rhythms

40 male C57BL/6J mice, 8 weeks of age (acquired from Envigo), were housed under 12:12h LD cycles for 3 weeks for entrainment purposes prior to experimental onset. Each animal was then behaviourally tested using a longitudinal study approach. Following entrainment, all mice were housed under DD and injected with a compound of interest at circadian time (CT) 6 every other day for 2 weeks, then allowed to free run for 1 week. This protocol was repeated using the same mice, where the compounds of interest were now injected at CT16 every other day for 10 days, as summarised in *Figure 2.1A*.

Four groups of 10 mice were injected intraperitoneally (i.p.) with either vehicle, 200mg/kg of LiCl, 50mg/kg of nobiletin, or 5mg/kg of CGS-15943. The

drugs were diluted in 0.9% NaCl (Steripod) with 5% kolliphor HS 15 (Sigma) and 5% 2-hydroxypropyl-β-cyclodextrin (Sigma), except for LiCl, which was diluted in 0.9% NaCl alone. Compounds were administered in 300µL volumes per mouse containing 3% vehicle.

Wheel-running activity data was collected and analysed using the ClockLab software (ActiMetrics). Period was analysed using alternative days, whereby the day of drug administration was excluded. Amplitude was analysed by normalising the number of revolutions during the treatment period to vehicle treated mice.

2.12.4 Open field test and elevated plus maze

Following the termination of the wheel-running assessments, the effects of the compounds on behaviour were assessed using the open field test (OFT) and the elevated plus maze (EPM) (*Figure 2.1B*). Animals were administered a final injection of LiCl, nobiletin, CGS-15943, or vehicle at CT14-16 and tested 3h after injection.

The animals were first tested using the Linton AM1053 X, Y, Z IR Activity Monitor (San Diego Instruments), which registers animal movement through the detection of infrared beam breaks. The apparatus consisted of two parallel frames each containing 24 equally spaced beams along the X and Y (8 x 16) axis. The experiment was performed under dim red light conditions, where cage light levels ranged between 0.7-1.5 lux. Animal activity was scored in 1min time bins for 20min. Animals were assessed in clear Perspex cages 36 x 20 x 15cm in size where all mice were placed in the same corner of the cage prior to the onset of activity monitoring. The parameters of interest were analysed using a built-in

software which included: % time the animal is active, % time spent rearing, and the number of centre-rears. Activity was registered if the animal broke any beam on the lower level, where rearing (vertical exploratory activity) was detected if the animals broke any beam on the upper grid.

Following the OFT, animals were placed in their home cage environments for 1.5-2h prior to commencing the EPM. The experiment was performed using a maze elevated 47cm off the ground. The apparatus consisted of a central platform (5 x 5 cm) with two opposing open arms (28 x 5 cm) lit to 290 lux and two opposing closed arms (28 x 5 x 30 cm) under 50 lux. The mouse was placed on the central platform facing the closed arms and animal activity was recorded for 10min. Any mice that fell off the apparatus were excluded from the analysis. Analysis was performed using ANY-maze 5.3 (Stoelting Co.). The software monitors the movement of an animal in specific pre-defined regions. The variables of interest included: distance travelled, % time spent active, the frequency of open arm entries, and % time spent in the open arms of the maze.

2.13 Chapter 5: Methods

2.13.1 Additional media and reagents

Inositol-less media: Inositol-less DMEM Eagle High Glucose without L-glutamine (USBiological life sciences) supplemented with 1x GlutaMAX, 3.7g/L $NaHCO_3$ (Sigma), 10mM HEPES, 0.5% P/S, and adjusted to pH 7.3.

Compounds: LiCl (Sigma), NaCl (Sigma), myo-inositol (Sigma), ebselen (Sigma), L690,488 (Tocris Biosciences), SCH772984, DMSO (Sigma), and nuclease free water (Ambion).

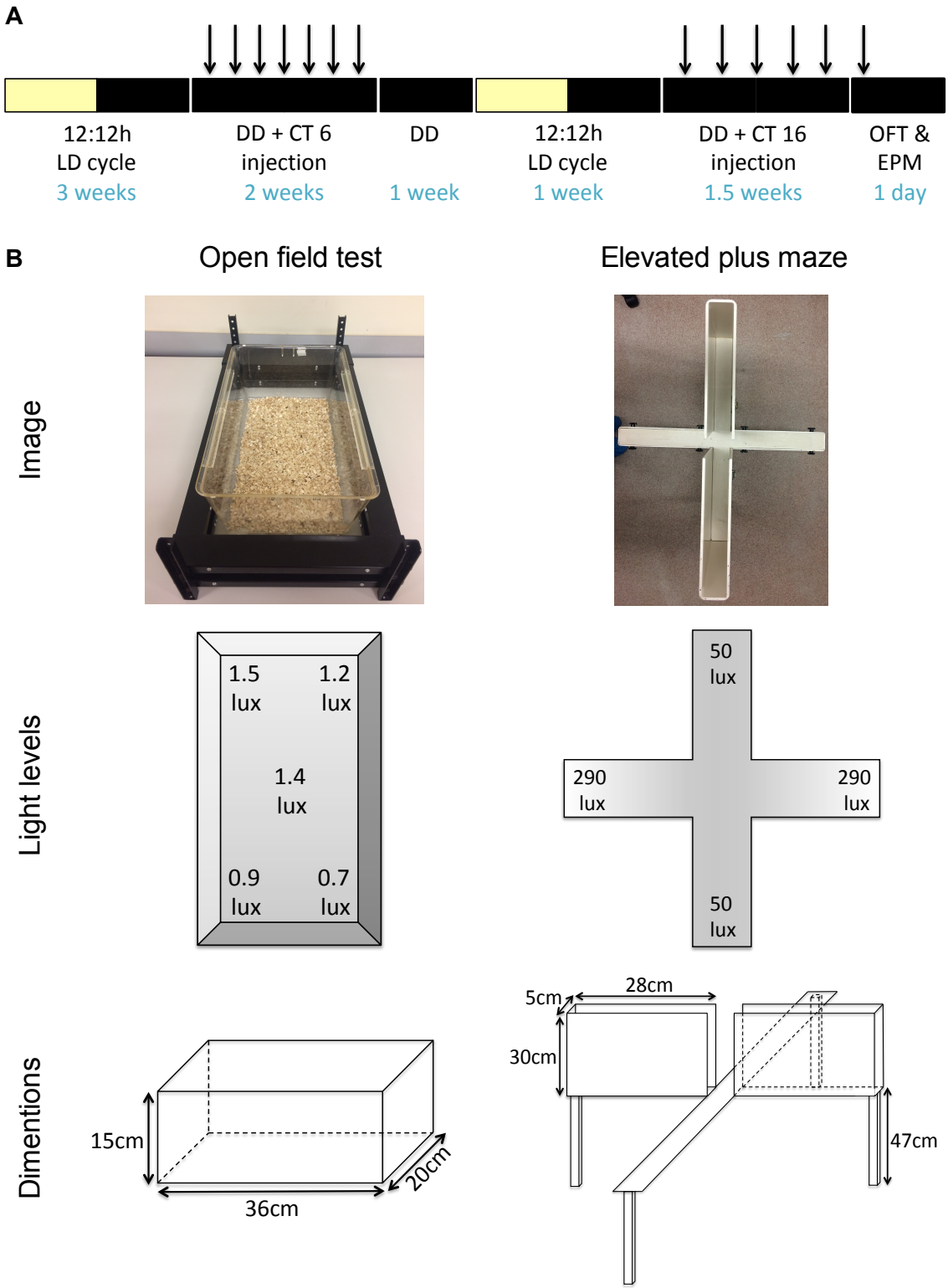

Figure 2.1. **Summary of the *in vivo* methodology used to assess circadian rhythms and behavioural changes. A)** Timeline summarising the experimental protocol implemented when assessing drug-induced locomotor and behavioural changes over 9 weeks. Arrows indicate administration of an i.p. injection. **B)** Photographs captured of the OFT and EPM equipment, with the lux levels measured before experimental onset and apparatus dimensions.

Table 2.1. NMDG-HEPES recovery solution - for SCN culture.

	mM	Molecular weight	g/L
NMDG **(Sigma)**	93	195.2	18.6
HCl	93	36.5	Adjust to pH 7.3
KCl **(VWR International)**	2.5	74.6	0.19
NaH_2PO_4 **(Sigma)**	1.2	138.0	0.17
$NaHCO_3$ **(Sigma)**	30	84.0	2.52
HEPES **(VWR International)**	20	238.3	4.77
Glucose **(Sigma)**	25	180.2	4.51
Sodium ascorbate **(Sigma)**	5	198.0	0.99
Thiourea **(Sigma)**	2	76.1	0.15
Sodium pyruvate **(Sigma)**	3	110.0	0.33
$MgSO_4$ **(Sigma)**	10	246.5	1.20
$CaCl_2$. $2H_20$ **(Merk Millipore)**	0.5	147.0	250µL (2M stock)

Table 2.2. 1x Tris Buffered Saline (TBS) - for immunohistochemistry

	mM	Molecular weight	g/L
Tris base **(Promega)**	19.8	121.1	2.4
NaCl **(ThermoFisher Scientific)**	150.7	58.4	8.8
HCl	93	36.5	Adjust to pH 7.6

2.13.2 Assessing circadian rhythms

Bmal::Luc MMHD3 and *Bmal::Luc* U2OS cells were seeded in 96- or 384-well plates prior to dexamethasone treatment, and bioluminescence was recorded, as previously described.

2.13.3 Analysis of [^{3}H] myo-inositol

Bmal::Luc MMHD3 cells were treated with vehicle or 30mM LiCl. 48h later the cells were washed with inositol-less media before adding RPMI with 34nM [^{3}H] myo-inositol (0261A Inositol, myo-[1, 2 -3H(N)]; 60 Ci/mmol; 1mCi/mL in water) (American Radiolabeled Chemicals Inc.). The cells were then lysed at 1, 3, and 10min intervals. At the time of cell lysis, cellular reactions were quenched with the addition of 40mM myo-inositol, followed by a 3x wash in ice cold PBS

containing 40mM myo-inositol. Lysis was performed by using 500µL Solvable (Perkin Elmer) per well, and incubating cells for at 60°C for 1h.

A micro BCA protein assay kit (ThermoFisher Scientific) was used to determine protein concentrations following the manufactures instructions. 5µL of radioactive sample were mixed with 145µL water. This was followed by the addition of 150µL working reagent/well. Samples were transferred to 37°C for 2h before reading the absorbance at 562nm. Final concentrations were determined from a standard curve prepared from bovine serum albumin.

Liquid scintillation counting which allows quantitative detection of radioactive material was performed using 300SL Liquid Scintillation Counter (LabLogic). 100µL of radioactive sample was mixed with 4.4mL Ultima-flo scintillation fluid. Radioactive measurement assays were set to record for 500s/sample. Counts per minute were normalised to protein content.

2.13.4 Cellular mRNA quantification

Bmal::Luc MMHD3 cells were seeded to 100% confluence for time-point based RNA extractions in 12-well plates. Following 1h of 200nM dexamethasone treatment, the recording media was changed to contain B27. 24h after treatment and incubation at 37°C was defined as time 0 for all cellular mRNA quantification experiments. After 0h, 24h, or 48h of treatment with 30mM LiCl, 30mM NaCl, 3µM L690,488, DMSO, or nothing, the cells were lysed and gene expression levels were analysed with real-time PCR.

2.13.5 Primers

Primers for mRNA quantification of gene expression and siRNA-induced gene knockdown are found in *Table 2.3*.

Table 2.3. List of the primer sequences used throughout this investigation. Use of commercially available primers are also indicated.

Species:	Gene:	Forward/ Reverse:	Primer Sequence (5'-3'):
M. musculus	*Bmal*	Forward	GAGGTGCCACCAACCCATAC
M. musculus	*Bmal*	Reverse	AGTCAAACAAGCTCTGGCCAA
M. musculus	*C/EBPα*		Bio-Rad primer- qMmuCED0002368
M. musculus	*Csnk1δ*	Forward	TCGAACACCACGGCAAGTAG
M. musculus	*Csnk1δ*	Reverse	TGAAGACCACTGGAAGCCA
M. musculus	*Gapdh*	Forward	TGCACCACCAACTGCTTAG
M. musculus	*Gapdh*	Reverse	GATGCAGGGATGATGTTC
M. musculus	*Impa1*	Forward	TTCTGTGGTGCTGGAGACTG
M. musculus	*Impa1*	Reverse	AAACCCCTAAAAAGGGCTGA
M. musculus	*Isyna1*	Forward	GTGGACGACATGGTTCACAG
M. musculus	*Isyna1*	Reverse	CAGCACTAGGTCCAGCATGA
M. musculus	*Per1*	Forward	AGTTCCTGACCAAGCCTCGTTAG
M. musculus	*Per1*	Reverse	CCTGCCCTCTGCTTGTCATC
M. musculus	*Per2*	Forward	GGGGTGAGATTCGTCATTGAACTTG
M. musculus	*Per2*	Reverse	AGGACATTGGCACACTGGAAAGAG
M. musculus	*Slc5a3*		Bio-Rad primer- qMmuCED0051355

2.13.6 Cignal reporter assay

MMHD3-blank cells were assessed with the Cignal 45 reporter assay kit (Qiagen). Cells were co-transfected with 45 luciferase tagged transcriptional response elements and renilla luciferase under a CMV promoter (200ng/well in a 40:1 ratio). A reverse transfection protocol (where the DNA and viafect complex are added to the cell culture plates prior to the cells) with a standard DNA:optimen:viafect ratio was used, where complexes were incubated for 20min. The positive control contained luciferase and green fluorescent protein

(GFP) each under their own CMV promoters allowing visualisation of transfections. The negative control contained the luciferase gene without the CMV promoter. 24h after transfection the cells were serum starved in RPMI media for 6h. Subsequently, recording media containing 400μM luciferin was added and baseline luminescence measurements were taken. This was followed by the addition of either 30mM LiCl, 3μM L690,488, or vehicle, and the effects of drugs on luciferase tagged transcription factors were detected for 16h. Cells were then lysed using repeated freeze-thaw cycles and the renilla substrate was added to detect renilla luciferase. Comparing peak luminescence vales to baseline levels assessed transcriptional activity. Transcription factor-luciferase levels were normalised to renilla luciferase, an internal control indicating transfection efficiency. Values are presented as a percentage of luminescence activity normalised between the positive (100%) and negative (0%) controls, where significance indicates a difference from the negative control.

2.13.7 Ex vivo SCN culture

Ex vivo experiments using SCN slice culture were performed using homozygous male and female *mPer2*^{Luc} knockin mice (PER2::LUC) bred on a C57BL/6J background belonging to the University of Oxford, Foster Lab breeding colony. Adult mice between 10-14 weeks of age were used for all experiments.

Mice were culled via cervical dislocation and decapitation followed by enucleation and removal of the whole brain. The caudal brain was then glued onto the stage and fixed using 3% low melt agar (Sigma) before coronal slices were obtained using the Compresstome VF-200 semi-automatic slicer (Precision Instruments). 250μm serial brain sections were sliced in NMDG-HEPES recovery

solution (*Table 2.1*) where 2 mid-SCN brain sections were collected per mouse (~0.22mm posterior to Bregma). The slices of interest were then microdissected to contain the bilaterally intact SCN (~2mm in diameter).

Microdissected SCN sections were transferred to 0.6cm^2 Millicell cell culture inserts (Merk Millipore) placed a 24-well plate (Perkin Elmer). The insert was placed in 500µL recovery media, a cocktail of recording media supplemented with 2.5mM AP-V (Tocris Biosciences), 100nM MK-801 maleate (Abcam), and 3mM glutathione reduced ethyl ester (Sigma) and incubated at 37°C for 30min. The inserts were then placed in fresh recording media supplemented with B27, 400µM luciferin, and 5% FBS and inserted into the TriStar^2 plate reader for luminescence detection.

SCN slice cultures were recorded for 4 days after which a full media change was performed and the sections were treated with various reagents and assessed for a further 4 days. Over this time, data was collected once an hour by averaging photon emissions every 150s. Period and amplitude change was calculated by comparing oscillation pre- and post-treatment.

2.13.8 Western blotting

Protein extraction

Proteins from whole mouse brain, *Bmal::Luc* MMHD3, and *Bmal::Luc* U2OS cells were extracted for western blot analysis, where all steps were performed on ice unless otherwise stated. 1x 14-week-old male C57BL/6J mouse brain (Envigo) was removed and immediately placed in PBS without magnesium or calcium. The brain was Dounce homogenised in 10mL RIPA buffer (Sigma) supplemented with 100µL Halt Protease and Phosphatase Inhibitor Cocktail

(ThermoFisher Scientific) and 100µL 0.5M EDTA (ThermoFisher Scientific) and incubated for 1h. The protease and phosphatase inhibitors are critical as cell lysis results in the mass release of unregulated proteases and phosphatases, which result in protein modification, denaturation, or proteolysis. Similarly, the divalent cation chelator EDTA reduces DNAse and proteases activity, as many require magnesium co-activation to function. The sample was then centrifuged at 13,000g, 20min at 4°C after which the supernatant containing whole brain proteins was stored at -20°C.

Similarly, cell-based protein extraction samples were washed with PBS without magnesium or calcium. This was followed by a 30min incubation period on ice with 2mL RIPA buffer containing 20µL of the inhibitor mix and 20µL EDTA. The samples were then centrifuged at 13,000g, 20min at 4°C after which the protein containing supernatant was stored at -20°C. A BCA protein assay was performed to calculate protein concentrations.

SDS-PAGE gel electrophoresis

Protein lysates were separated using gel electrophoresis, where pure human IMPase was used as a positive control. The SDS-PAGE gel required loading 100ng-20µg of protein per well, along with 5µL/well of chameleon-duo prestained protein ladder (LI-COR) as the molecular weight marker. All samples were diluted in 10% β-mercaptoethanol and 4x Laemmli buffer (Bio-Rad), and boiled at 95°C for 5min before loading into the Novex WedgeWell 10-20% Tris-Glycine gel (Invitrogen). Gels were loaded into the Mini Gel Tank (Invitrogen) containing Novex 1x Tris-Glycine SDS running buffer (Invitrogen), and ran for 30min, 225V.

Immunoblotting

The Trans-Blot Turbo Transfer system (Bio-Rad) was then used for gel to membrane protein transfer. The Immobilon-FL PVDF (Merk, Millipore) with a 0.4µm filter was activated by briefly soaking the sheets in methanol (ThermoFisher Scientific) before transferring them to the Turbo-blot transfer buffer (Bio-Rad). Stacks were then formed with an ion reservoir stack, the Immobilon-FL PVDF, the gel, and a final ion reservoir stack. The system ran at 1.3A, 25V, for 9min. The membrane was washed in *Odyssey Blocking Buffer-TBS* (LI-COR)-Tween 20 (0.5%) (Promega) before blocking in *Odyssey Blocking Buffer-TBS* for 1h. All antibodies were diluted in *Odyssey Blocking Buffer-TBS.* The membrane was then incubated at 4°C in the primary antibody overnight. Antibodies included anti-IMPA1 (ab184165, Abcam) and anti-β-actin (ab8227, Abcam) both of which required a 1 in 4,000 dilution. After a 4x wash with *Odyssey Blocking Buffer-TBS*-Tween 20, the membrane was incubated with the secondary antibody, goat-anti rabbit IRDye 800CW (1 in 10,000) (LI-COR) for 1h at room temperature. The membrane was washed 4x in *Odyssey Blocking Buffer-TBS*-Tween 20 before imaging with the Odyssey Infrared Imaging System (LI-COR). The LI-COR Image studio was used to report optical density values.

2.13.9 Mouse brain immunohistochemistry

Immunohistochemistry on free-floating brain sections was performed using 14-week-old male C57BL/6J mice (Envigo). The whole brain was incubated in 4% paraformaldehyde in PBS (ChemCruz) for 4h prior to slicing 50µm sections using the Compresstome. The tissue was washed 3x in 1% TBS (*Table 2.2*)-Triton X100 (VWR International) prior to blocking with 4% goat-

serum (Sigma) diluted in 1% TBS-Triton X100 for 1h. The anti-IMPA1 antibody was diluted to 1 in 2,000 in 0.1% TBS-Triton X100 and 2.5% goat serum and incubated overnight at 4°C. Brain slices were then washed 4x with 0.05% TBS-Tween 20 prior to the addition of goat-anti rabbit IRDye or Alexa Fluor 488 antibodies (ThermoFisher Scientific) diluted to 1 in 5,000 or 1 in 500 respectively in 0.05% TBS-Tween 20 and 2.5% goat serum. Control sections were incubated in the secondary antibody alone. After 4x TBS-Tween 20 washes, the sections were ready for mounting on microglass slides (75 x 25 mm) (Corning). SlowFade Diamond Antifade mount with or without DAPI (ThermoFisher Scientific) was added to the brain slices with a cover slip (22 x 22 mm) (VWR International) placed on top.

Where the IRDye antibody was used, imaging was performed with the LI-COR Odyssey Infrared Imaging System. An Olympus FV1000 laser-scanning microscope with an Argon laser and 488nm excitation line was used to image brain sections incubated with Alexa Fluor 488. The objectives were as follows: 10x, 0.4 NA, UPlanSApo (air), 60x, 1.35, Oil UPlanSApo, and 60x magnified.

2.14 Chapter 6: Methods

2.14.1 Additional media and reagents

CO_2 independent media: CO_2 independent media (ThermoFisher Scientific) supplemented with 1x GlutaMAX.

Compounds: vidarabine (LKT laboratories), 2'5'-didioxyadenosine (Enzo life sciences), H89 (Sigma), KT5720 (Cayman chemical company), CBP112 (Structural Genomics Consortium), CBP30 (Structural Genomics Consortium), LiCl (Sigma), forskolin (Cayman chemical company), PMA (Abcam), DMSO

(Sigma), and nuclease free water (Ambion).

2.14.2 cAMP-screen chemiluminescence ELISA

A highly sensitive cAMP-screen chemiluminescence ELISA kit (Applied Biosystems) was used to detect cAMP concentrations. MMHD3-blank cells were seeded in 96-well plates and treated with vidarabine, 2'5'-didioxyadenosine, or LiCl for 6h. Cells were then lysed and transferred to an assay plate coated in a goat anti-rabbit secondary antibody. Subsequently, rabbit anti-cAMP antibody, cAMP-AP conjugate, and the chemiluminescence substrate CSPD/Sapphire-II solutions were added. An inverse relationship existed between cAMP and bioluminescence signals; as cellular cAMP levels rise, there is a greater chance that they will displace the cAMP-AP conjugate binding to the primary antibody, and so bioluminescence detection will fall. cAMP alterations were inferred through comparison against a standard curve created from pure cAMP.

2.14.3 cAMP::GloSensor assay

The pGloSensor™ 22F cAMP plasmid (Promega) enables high-sensitivity detection of changes in intracellular cAMP. The plasmid contains a mutant luciferase biosensor from the firefly (*P. pyralis*) joined to cAMP binding domains. Therefore, following cAMP binding, the protein undergoes conformational changes resulting in detectable photon emissions. The U2OS cells were infected with *cAMP::GloSensor* lentivirus, where mixed colonies were used for all experiments. The U2OS-blank cells were serum-starved in CO_2 independent media with 5mM luciferin and various reagents for 2h at room temperature. Following baseline measurements, the cells were treated with 10μM forskolin and luminescence was recorded for 1h at 25°C.

2.14.4 CRE::*Luc assay*

The CRE::*Luc* plasmid (created by the Vasudevan Lab) enables the detection of CREB transcription factor activity. The CRE DNA sequence is fused to a firefly luciferase gene, such that following CREB binding to CRE, increases in luminescence are detected. Following 24h of transfection, the U2OS-blank and MMHD3-blank cells were serum-starved in recording media with 400μM luciferin and various reagents for 6h. Following baseline recordings, cells were treated with 100μM forskolin and luminescence was recorded at 37°C for 16h.

2.14.5 Data analysis

All *cAMP::GloSensor* and CRE::*Luc* transfection data was analysed by calculating drug-induced fold changes, comparing baseline measurements with peak luminescence values. Values were then normalised to give a percentage change between the positive control (forskolin) and negative control (vehicle). Significance was assessed by comparing drug responses to the positive control.

2.14.6 Assessing circadian rhythms

Circadian experiments were performed on *Bmal::Luc* U2OS or *Bmal::Luc* MMHD3 cells as previously described. Data analysis occurred using Kaiseki Ninja (Churitsu Electric Co.), an alternative high throughput analysis software.

2.14.7 Cellular mRNA quantification

Bmal::Luc MMHD3 cells were seeded to 100% confluence for real-time PCR in 96-well plates. Following 1h of 200nM dexamethasone treatment, recording media containing B27 was added. The cells were incubated at 37°C for 24h, after which the cells were lysed.

2.14.8 Primers

Primers for mRNA quantification of gene expression and siRNA-induced gene knockdown are found in *Table 2.4*.

Table 2.4. List of primer sequences used throughout this investigation. Use of commercially available primers are also indicated below.

Species:	Gene:		Forward/ Reverse:	Primer Sequence (5'-3'):
M. musculus	*Adcy1*	AC1	Forward	CCAGCCAAGAGGATGAAGTT
M. musculus	*Adcy1*	AC1	Reverse	AATGCCCTCCGCTTGTC
M. musculus	*Adcy2*	AC2	Forward	TGTGTGAAAATGGGACTGGA
M. musculus	*Adcy2*	AC2	Reverse	GAGAAATGCAGCTCCAAAGG
M. musculus	*Adcy3*	AC3	Bio-Rad primer- qMmuCED0044117	
M. musculus	*Adcy4*	AC4	Bio-Rad primer- qMmuCED0022405	
M. musculus	*Adcy5*	AC5	Bio-Rad primer- qMmuCED0045483	
M. musculus	*Adcy6*	AC6	Forward	GAGGCAAACAACGAGGGC
M. musculus	*Adcy6*	AC6	Reverse	GCCATGTAGGTGCTACCG
M. musculus	*Adcy7*	AC7	Forward	AAGGGCTTTGAGCGTGAGTA
M. musculus	*Adcy7*	AC7	Reverse	CCAAAGGACACACCCAGAGT
M. musculus	*Adcy8*	AC8	Bio-Rad primer- qMmuCED0045484	
M. musculus	*Adcy9*	AC9	Forward	ATGGGCGGCTTGAAGAAATA
M. musculus	*Adcy9*	AC9	Reverse	GCAGGGGTGAGCTTGGA
M. musculus	*Adcy10*	AC10	Forward	CCTGCTTCTCCTTGCTGTG
M. musculus	*Adcy10*	AC10	Reverse	GCAGGAGTAAAGTCCCAGG
M. musculus	*Csnk1δ*		Forward	TCGAACACCACGGCAAGTAG
M. musculus	*Csnk1δ*		Reverse	TGAAGACCACTGGAAGCCA
M. musculus	*Gapdh*		Forward	TGCACCACCAACTGCTTAG
M. musculus	*Gapdh*		Reverse	GATGCAGGGATGATGTTC

Chapter 3: The Molecular Clocks of Bipolar Patient-Derived Fibroblasts Exhibit Period Length Variability

3.1 Introduction

Almost every organism has adapted to life on earth by the development of circadian rhythms. Much like the conductor of an orchestra, in mammals, the SCN is a structure devoted to ensuring coherent rhythmicity of the body as a whole (Weaver, 1998). However, it is not unique in its capacity to maintain rhythmicity. There are multiple neuronal and non-neuronal tissues which contain the molecular clockwork responsible for driving cell-autonomous rhythm generation (summarised in Chapter 1, *Figure 1.2*) (Yoo et al., 2004, Guilding et al., 2010).

3.1.1 The molecular clocks of fibroblasts

Of the array of extra-SCN and peripheral oscillators present within the body, an organ of current exploration is the skin, owning to the ease of obtaining biopsy samples and investigating the inherent self-sustaining circadian clocks (Sandu et al., 2012). Fibroblasts are cells that function to generate components of the extracellular matrix and maintain structural frameworks (Tracy et al., 2016). They were, in fact, the first non-neuronal cell type reported to display *in vitro* rhythmic patterns of clock gene expression (Balsalobre et al., 1998, Yagita et al., 2001). The highly accessible nature of skin cells relative to the internal organs such as the brain and their ability to multiply to sustain populations, make fibroblasts a promising tool for assessing human circadian rhythmicity.

Initial studies by the Schibler group over a decade ago validated the use of fibroblasts to assess circadian rhythmicity. They found that Rat-1 fibroblasts and NIH-3T3 mouse fibroblasts were capable of maintaining rhythmic *Bmal::Luc* expression for multiple days *in vitro* (Nagoshi et al., 2004). Whilst individual cells

are capable of generating rhythmicity, a synchronising agent in the form of a serum shock or the glucocorticoid analogue dexamethasone, is required to observe coherent luminometric reporter outputs (Balsalobre et al., 1998, Balsalobre et al., 2000). Nagoshi and colleagues found that through the creation of lentiviral vectors where the *Bmal* promoter drives the expression of luciferase, an elegant and sophisticated bioluminescence photon detection assay was formulated (Nagoshi et al., 2004). The use of such reporter-based techniques appeared superior over the classical time point based mRNA assays, as the method provided considerably higher time resolved data.

Subsequently, Brown and colleagues assessed lentiviral-mediated generation of stable primary human fibroblast lines. After obtaining biopsy samples from 19 subjects, assessment of *Bmal::Luc* rhythmicity revealed that healthy humans had an average period of 24.5h (Brown et al., 2005). This corroborated previous findings, where isolating humans in environments devoid of external time cues revealed a similar endogenous period (Czeisler et al., 1999, Carskadon et al., 1999).

Importantly, it was found that period, denoted by the assessment of *Bmal::Luc* fibroblast rhythms, represented the endogenous rhythms set by the SCN. By characterising mouse fibroblast rhythms in conjunction with physiological wheel-running activity from genetic mutants with known period variability, a strong correlation emerged. Mice with behavioural period lengthening displayed decelerated rhythms in their fibroblast-based molecular clocks, mice with shorter wheel-running periods displayed faster fibroblast oscillations, and behaviourally arrhythmic mice did not display any *Bmal*

oscillations within their fibroblast clocks (Brown et al., 2005). Moreover, the fibroblasts displayed heightened responses relative to wheel-running behaviour, as period change was 2-4 times greater in the fibroblast model (Brown et al., 2005). Although many translational factors could account for this, it does suggest that whilst fibroblasts do not fully mimic the state of the SCN, they do provide a clear indication about the functioning's of the master molecular clock.

Indeed, these correlations can also be translated to humans. Chronotype, the behavioural manifestation defining an individual's circadian rhythm, is largely variable in the human population. The two extremes are the so-called 'larks' and 'owls', which describe people with extreme early or late shifted activity patterns (Roenneberg et al., 2003). It is generally believed that subjects with longer periods tend to have stronger evening preferences, where subjects with shorter periods display the opposite (Brown et al., 2008). With this in mind, Brown et al., demonstrated that longer or shorter fibroblast periods correlated with evening or morning preferences respectively, where chronotype was assessed via a questionnaire (Brown et al., 2008). This relationship was further established by inferring chronotype from physiological parameters. Period assessed by examining salivary melatonin was closely associated with fibroblast periods from 3 distinct populations (Pagani et al., 2010). Thus, human subject-derived fibroblasts provide a valid representation of circadian rhythmicity *in vivo*, and could therefore serve as a biomarker of human molecular rhythms when examining both healthy human clocks, as well as disorders associated with circadian dysfunction.

3.1.2 Bipolar patients and their circadian clocks

One disorder associated with prominent sleep and circadian rhythm disruptions is BPD. In fact, these symptoms are so frequently observed, that they are included in the BPD diagnostic criteria, where the chronomodulator lithium remains as a first line mood-stabilising agent for the disorder (American Psychiatric Association, 2013, World Health Organisation, 2014). The vast majority of patients exhibit significantly reduced sleep needs during their manic phases, where depression can be associated with insomnia, delayed sleep onset or hypersomnia (Harvey, 2008). Moreover, behavioural assessments revealed that patients exhibited fragmented patterns of sleep indicating low amplitude rhythms (Jones et al., 2005, Rock et al., 2014).

As rhythm strength is impaired, this suggests that the molecular clock is more susceptible to perturbations from external influences such as light, a dominant *zeitgeber*. This has been found with animal models of mania-like behaviour such as the *Clock*Δ19 and *Afh* mice. Such models display abnormal phase shifting responses in the form of exaggerated behavioural compensation (Vitaterna et al., 2006, Guilding et al., 2013). Indeed, seasonality and transmeridian travel can also precipitate episodes of mood instability in BPD patients (Akhter et al., 2013, Inder et al., 2016). Additionally, patients exhibit a stronger evening preference, which as we have mentioned can be indicative of lengthened circadian periods (Wood et al., 2009, Falsin Giglio et al., 2010). Whether circadian disruption is a cause or consequence of BPD is still up for questioning, yet a current applicable model suggests that both are entangled in the pathophysiology of BPD (summarised in Chapter 1, *Figure 1.3A*).

Table 3.1. Summary of previous fibroblast bioluminescence reporter studies assessing molecular rhythmicity from healthy controls or bipolar patients.

Subject	n	Gene	Period (h)	Variability (h)	Publication
Control	19	*Bmal*	24.5±0.75 (SD)	4	Brown et al., 2005
Control	28	*Bmal*	24.5±0.75 (SEM)	2	Brown et al., 2008
Control	9 11 8	*Bmal*	24.71±0.38 (SEM) 24.77±0.42 (SEM) 24.46±0.48 (SEM)	1.1 1.4 1.4	Pagani et al., 2010
Control **BPI**	19 19	*Per2*	25.10±0.20 (SEM) 25.50±0.20 (SEM)*	? ?	McCarthy et al., 2013
Control **BPI**	12 13	*Bmal*	25.50±0.60 (SD) 26.30±1.20 (SD)	? ?	Bamne et al., 2013

**: significant difference, SEM: standard error of the mean, SD: standard deviation*

As it is acknowledged that skin cells can provide an indication of human circadian rhythmicity, preliminary studies used fibroblasts to examine the molecular clocks of BPD patients. Initial studies were performed by examining mRNA transcript expression profiles which allowed the examination of both period and amplitude. Whilst no significant period differences were observed between BPD and control subjects, BPD patients presented with lower amplitude *BMAL* expression, with similar trends identified with *PER2* (Yang et al., 2009). Interestingly, luminometric studies where subject cell lines were transduced with *Per2::Luc,* found that period was significantly elongated by 25min in BPD patients relative to healthy controls (McCarthy et al., 2013). A subsequent study assessing the positive arm of the clock via analysis of *Bmal::Luc* rhythms supported these findings. It was shown that BPD patients-derived fibroblasts presented with non-significant trends for period lengthening by 40min relative to controls (summarised in *Table 3.1*) (Bamne et al., 2013). Despite the variability observed, the advanced resolution of bioluminescence analysis, afforded by an increased frequency in measurements, may enable the

identification of more subtle changes that may otherwise be missed when assessing rhythmicity using classic real-time PCR techniques.

3.1.3 Aims

Thus, it is known that BPD patients, along with mood instability also exhibit great sleep and circadian rhythm abnormalities and that fibroblasts display molecular rhythms which strongly correlate with the rhythms presented by the SCN. As initial studies have indicated that BPD fibroblast period is in line with the human behavioural assessments, the aim of this investigation was to delve deeper into the analysis of patient-derived fibroblasts. Using a larger cohort of well characterised BPD patients, we aimed to validate whether patients do in fact exhibit abnormalities in their molecular clocks. Moreover, we sought to determine, for the first time, whether lithium treatment, or to a lesser extent, sex, age, diagnosis, the age where depression or mania first caused impairment, or psychosis may account for the variability within our patient samples. This information, as well as helping to understand the circadian rhythms status associated with BPD, may also validate whether fibroblasts can be used as a valid tool to replace the use of whole animals and murine SCN tissues at the initial stages of drug discovery and future assessments of pharmacological perturbations on the molecular clock.

3.2 Results

3.2.1 Subject demographics

A total of 39 BPD patient-derived fibroblasts and 24 control subject-derived fibroblasts were used in this study, where all demographic data was obtained from the Oxford StemBANCC. As summarised in *Table 3.2*, the BPD participants had an average age of 43 years, 74% were female, 82% were diagnosed with BPI disorder, 67% presented with psychotic symptoms, and the age where depression first caused impairment was on average 4.3 years earlier than the age where mania first caused impairment. The BPD patients were further divided into those who were lithium-treated (Li-T) and lithium-non-treated (Li-NT). The criteria for Li-T included patients who were taking lithium at the time of the biopsy. 77% of the patients were Li-T and their sub-demographics closely resembled those found with the overall cohort. However, the age at which depression first caused impairment was 4.7 years earlier in the Li-NT sub-group relative to Li-T group. With regards to the control subjects, 55% were female with an average age of 53.56±3.18 years.

Further details of the Li-T cohort (*Table 3.3*) show that the patients had been taking lithium for an average of 10 years. Lithium functioned as a *bona fide* mood-stabiliser in 80% of patients, its effectiveness was undetermined in the remaining 20%, and only 1 patient had a compliance rate of <2 years. Qualitative assessment of the effectiveness of lithium as a mood-stabiliser (on a scale from 1-10) was 6, where only 20% of patients were consuming lithium alone. This suggests that the majority of patients were on combined therapies. When dividing the Li-T cohort by sex these variables closely matched overall patterns.

Table 3.2. Demographic summary of the bipolar subjects used in the current investigation.

			Sex:		Diagnosis:		BPD/ subsyndromal:		Age of first impairment: (years)		
Subject	**n**	**Age (years)**	**Female**	**Male**	**BPI**	**BPII**	**Parents**	**Siblings**	**Depression**	**Mania**	**Psychotic symptoms**
All BPD	39	43.10 ±1.97	29 (74%)	10 (26%)	32 (82%)	7 (18%)	16	11	18.74±1.30	23.03±1.57	26 (67%)
Li-T	30	43.03±2.39	21 (70%)	9 (30%)	25 (83%)	5 (17%)	15	11	19.83±1.56	23.10±1.72	20 (67%)
Li-NT	9	43.33±3.94	8 (89%)	1 (11%)	7 (78%)	2 (22%)	1	0	15.11±1.84	22.78±3.84	6 (67%)

Table 3.3. An expansion of the features associated with Li-T patients.

				Lithium prevents mood episodes:		>2 years compliance:			Lithium monotherapy:	
Subject	**Age (years)**	**Currently on lithium**	**Consistent time on lithium (years)**	**Yes**	**Not sure**	**Yes**	**No**	**Effectiveness of lithium (1 to 10)**	**Yes**	**No**
Li-T	43.03±2.39	30 (100%)	10.19±0.24	24 (80%)	6 (20%)	29 (97%)	1 (3%)	6.00±0.49	6 (20%)	24 (80%)
Female	41.71±2.68	21 (100%)	8.25±1.99	16 (76%)	5 (24%)	20 (95%)	1 (5%)	6.00±0.60	4 (19%)	17 (81%)
Male	46.11±5.02	9 (100%)	14.67±4.13	8 (89%)	1 (11%)	9 (100%)	0 (0%)	6.00±0.88	2 (22%)	7 (78%)

The patients were consuming an assortment of 1-6 drugs in order to control mood instability. As seen in *Table 3.4*, the drugs were divided into 5 classes by indication.

Table 3.4. The medications consumed by patients were categorised by indication.

Class	Medications
Mood-stabilisers	lithium, lamotrigine, valproate
Antipsychotics	aripiprazole, chlorpromazine, olanzapine, quetiapine, risperidone
Antidepressants	amitriptyline, citalopram, escitalopram, mirtazapine, sertraline
Anxiolytics	diazepam, lorazepam
Hypnotics	zolpidem, zopiclone

The average patient was consuming a combination of 2-3 compounds across all the aforementioned drug classes. As seen in *Table 3.5*, mood-stabilisers followed by antipsychotics were the medications most frequently consumed. Antidepressants, anxiolytics, and hypnotic agents were the least favourable compounds forming 21% of all the total drugs consumed by our cohort. The Li-T patients were twice as likely to be consuming compounds from the mood-stabiliser class than Li-NT patients. Whilst Li-T patients appeared to show similar trends to the overall cohort, the Li-NT sub-group presented subtle differences. As well as consuming fewer drugs overall, there was no longer a discrepancy between the number of mood-stabilisers or antipsychotics consumed, and the amount of anxiolytic and hypnotic agents was 2-3 times greater.

Table 3.5. Summary of the bipolar patient pharmacological treatments.

Subject	Total number of drugs	Mood-stabilisers	Antipsychotics	Antidepressants	Anxiolytics	Hypnotics
All BPD	**92** 2.35±0.21	**50 (54%)** 1.28±0.11	**23 (25%)** 0.59±0.10	**8 (9%)** 0.21±0.08	**6 (7%)** 0.15±0.04	**5 (5%)** 0.13±0.05
Li-T	**76** 2.53±0.24	**45 (59%)** 1.50±0.10	**18 (24%)** 0.60±0.11	**6 (8%)** 0.20±0.09	**4 (5%)** 0.13±0.06	**3 (4%)** 0.10±0.06
Li-NT	**16** 1.78±0.36	**5 (31%)** 0.56±0.18	**5 (31%)** 0.56±0.18	**2 (13%)** 0.22±0.15	**2 (13%)** 0.22±0.15	**2 (13%)** 0.22±0.15

3.2.2 Optimising lentivirus production

In order to perform luminometric recordings and analysis of circadian rhythms *in vitro*, the DNA encoding the circadian reporters needed to be introduced to all the individual cell lines of interest. This is typically performed via transient transfections or viral transduction. As the former is difficult in primary cells, we focused on the generation of lentiviral vectors as the delivery method for our fibroblasts. In order to generate sufficient quantities of lentivirus, the HYPERflasks were used. This allowed all the cells to be treated with a lentiviral solution that contained the same number of virally infective particles, and minimised variability due to viral transduction itself.

Prior to generating the lentivirus where luciferase expression was driven by activity at the *Bmal* (*Bmal::Luc*) or *Per2* (*Per2::Luc*) promoters, the transfection technique was modified. This was because the standard triple transfection techniques required 12.5μg of the expression clone to generate 10mL of concentrated viral media. Therefore, to generate 550mL of viral media, 687.5μg of DNA would have been required. On the other hand, use of PEI, an economical transfection agent with a similar methodological complexity to calcium phosphate was found to only require 60.4μg of DNA, an 11 fold difference. We therefore decided to assess the transfection efficiency of both techniques on a smaller scale using a lentivirus containing GFP. As seen in *Figure 3.1A,* visual assessment of the HEK 293 cells using the EVOS FLoid Cell Imaging Station (ThermoFisher Scientific) revealed that both techniques resulted in similar levels of GFP expression. This confirmed that both PEI and the calcium phosphate transfection methods displayed equal transfection efficiency.

The HYPERflasks were then used to generate the viral vectors containing the circadian reporters. As displayed by *Figures 3.1B-C*, the generation of virus was established by using the Lenti-X GoStixs. The presence of the p24 protein was assessed 24h post transfection, to confirm the initiation of virus production, and after 48h prior to viral media collection. Visually, the colours of the test bands were similar to the control bands after 48h, a band that represents ~$5x10^5$ infectious units/mL. The presence of viral units was then verified after concentration, to confirm that the particles were not filtered out in the process.

Finally, the Lenti-X GoStixs confirm the presence of viral surface proteins. Therefore, to confirm the lentivirus contained functional expression clones, one control and one BPD patient cell line was infected with both the *Bmal::Luc* and *Per2::Luc* virus to confirm that circadian oscillations were detectable. Indeed, both cell lines (*Figures 3.1D-E*), displayed near 24h oscillations in *Bmal* and *Per2*, which appeared to cycle in antiphasic directions as predicted.

3.2.3 Evaluating cellular growth profiles using doubling time

In order to assess the general health and growth characteristics of the fibroblasts used in this study that may contribute to any circadian deviations, and to help plan future experiments, growth curves were created to assess the PDT prior to stable cell line generation. As seen in *Figures 3.2A-B*, cell confluence increased over a period of 1 to 7 days and reached confluence on day 8.

It is acknowledged that the cell cycle is temporally gated by the circadian clock, and inhibition of cell cycle progression can impact circadian period length (Bieler et al., 2014). Therefore, given that cell division is a constant, deviations in

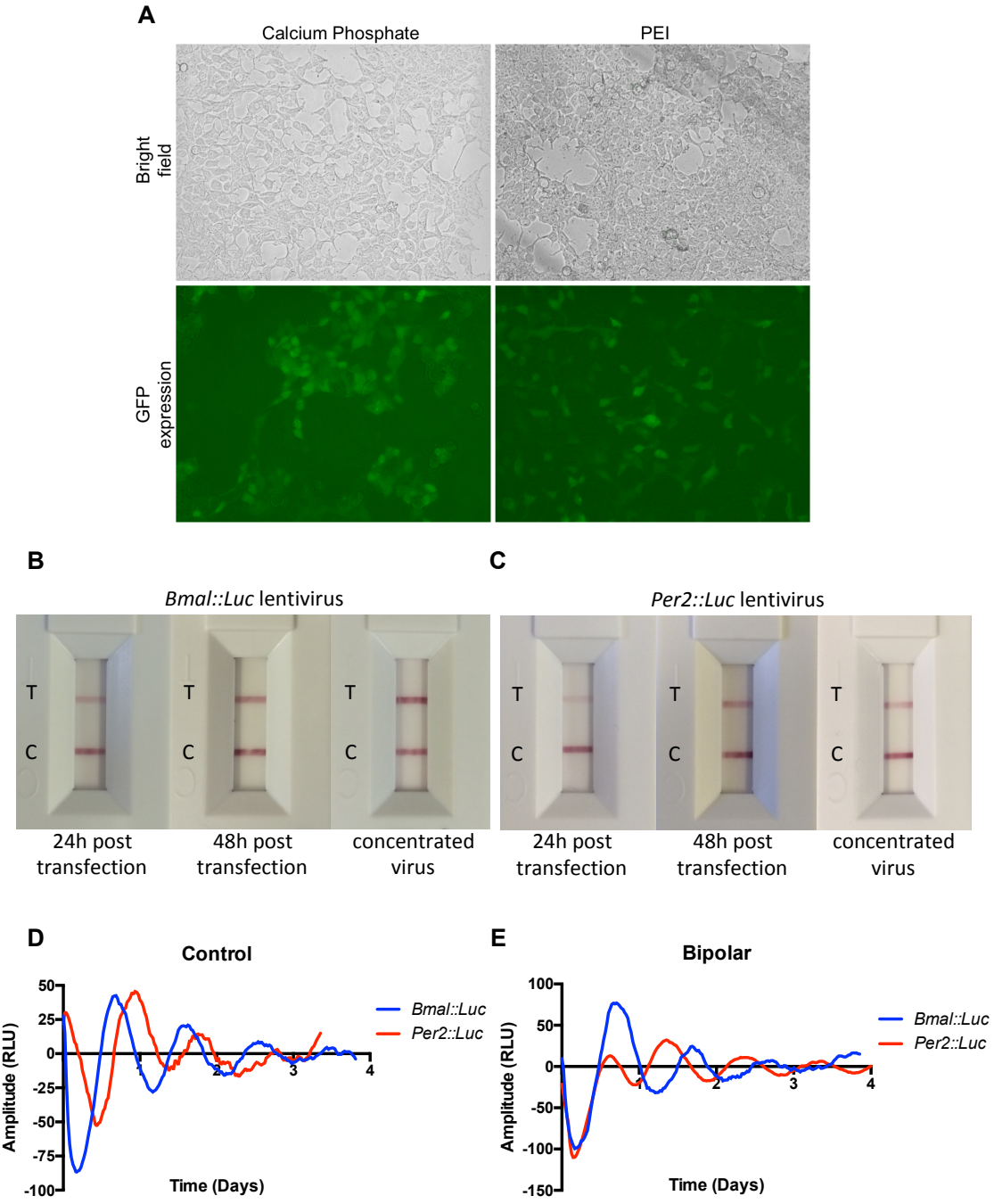

Figure 3.1. **Successful *Bmal::Luc* and *Per2::Luc* lentivirus production using the HYPERflasks. A)** Bright field and fluorescence images of HEK 293 cells containing the GFP viral vector. Lentivirus was produced using either calcium phosphate or PEI-mediated transfections. The Lenti-X GoStixs assessing p24 viral protein production 24h and 48h after transfection in the HYPERflasks, and after concentration of the *Bmal::Luc* lentivirus **(B)** or *Per2::Luc* lentivirus **(C)**. Functionality of the viral supernatants was assessed on one control **(D)** and one BPD patient **(E)** cell line. The representative traces confirm that *Bmal* and *Per2* cycle in antiphase.

growth rates could indicate fundamental differences between the cells, and not just their circadian rhythms. When comparing the overall PDT of the control and BPD fibroblasts, no significant differences emerged. The cell lines had an overall average PDT of 3.24±0.10 and 3.37±0.14 days respectively (*Figure 3.2C*). Moreover, the PDT of BPD patients exhibited great variability ranging between 2.26 and 6.21 days. We therefore assessed whether any disease-related factors could account for these changes. Whilst the number of participants belonging to each group varied, dividing the BPD cohort by sex (female: 3.26±0.16, male: 3.68±0.31 days) (*Figure 3.2D*), lithium treatment (Li-T: 3.44±0.17, Li-NT: 3.12±0.18 days) *(Figure 3.2F),* diagnosis (BPI: 3.39±0.16, BPII: 3.25±0.26 days) *(Figure 3.2G)*, the age depression first caused impairment (never: 2.60, 5-14: 3.59±0.46, 15-19: 3.36±0.17, 20-24: 3.24±0.40, 25-34: 3.45±0.24, 35-46: 3.46±0.43 days) *(Figure 3.2H)*, or the age mania first caused impairment (never: 2.86±0.36, 15-19: 3.49±0.30, 20-24: 3.74±0.32, 25-29: 3.10±0.24, 30-34: 2.81±0.19, 35-46: 3.31±0.21 days) *(Figure 3.2I)* did not impact PDT.

Significant differences emerged when assessing the age of the patients at the time of the biopsy *(Figure 3.2E)*. The overall PDT was significantly longer for patients between 20-29 years of age by 1.5 and 1.2 days when compared to those between 30-39 and 40-49 years respectively. Moreover, similar trends were observed for patients between 50-59 and 60-69 years, where PDT was on average 1 and 1.3 days longer respectively (20-29: 4.35±0.58, 30-39:2.93±0.09, 40-49: 3.18±0.17, 50-59: 3.35±0.19, 60-69: 3.07±0.20 days). This is interesting, as the greatest variability was observed in the youngest population, an age where BPD onset is most prominent.

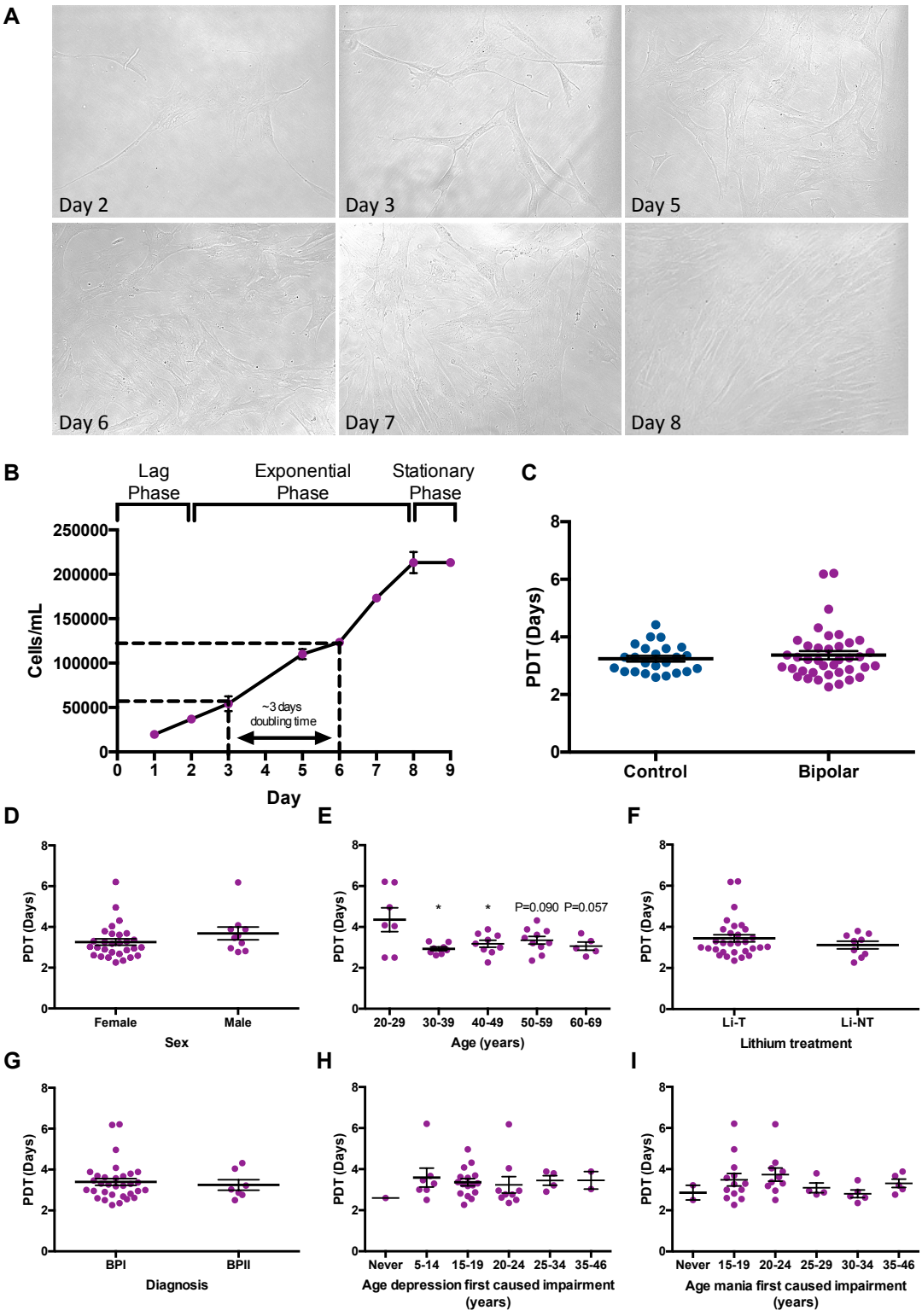

Figure 3.2. **The population doubling time for participant fibroblasts. A)** Example bright field images of cell growth on days 2-8. **B)** Representative growth curve assessing PDT during the exponential growth phase. **C)** The overall PDT for control (n=24) and BPD (n=39) subject cells. Bipolar patients were further stratified in order to identify the source of variability, by assessing the impact of sex **(D)**, age **(E)**, lithium treatment **(F)**, diagnosis **(G)**, and the ages where depression or mania first caused impairment **(H-I)**.

3.2.4 Luminometric assessment of circadian parameters via Bmal::Luc expression

All control and BPD patient-derived fibroblasts were transduced with the *Bmal::Luc* lentivirus to generate stable cell lines. After seeding the fibroblasts, dexamethasone-induced synchronisation enabled the observation of bioluminescence rhythms for multiple days *in vitro* (summarised in *Figure 3.3A*). As seen in *Figure 3.3B*, there was no overall significant difference when comparing the period length of healthy controls to BPD fibroblasts (control: 24.03±0.20, bipolar: 23.87±0.21 h). Further analysis of the data using the Welch's correction revealed that the BPD cohort exhibited significantly larger period length variability compared to controls, ranging between 20.2h to 26.5h. As period lengths were widely dispersed within this 6h period range, this may provide a rationale for why no significant differences were observed. We then decided to assess whether demographic factors could account for the period variability within our bipolar samples, with the acknowledgement that subdivisions did not contain equal sample numbers.

Firstly, when trying to understand whether sex differences could account for period variability, no significant differences emerged (female: 23.87±0.26, male: 23.86±0.32 h) (*Figure 3.3C*). Unlike the results assessing cellular growth curves, age did not present any significant differences when analysing period (20-29: 23.39±0.71, 30-39: 24.50±0.28, 40-49: 23.78±0.43, 50-59: 24.04±0.42, 60-69: 23.32±0.44 h) (*Figure 3.3D*). Similarly, no differences were found when assessing the effects of lithium treatment, although a trend for longer periods in Li-NT patients was identified (Li-T: 23.77±0.25, Li-NT: 24.18±0.40 h) (*Figure 3.3E*). The next parameter analysed was BPD diagnosis where, interestingly, the

emergent trend suggested that patients diagnosed with BPII had on average a period that was 1.1h shorter than those with BPI (BPI: 24.05±0.19, BPII: 23.00±0.74 h) (*Figure 3.3F*). This was the parameter which came the closest to potentially accounting for some of the variability observed.

Next, we sought to identify whether any relationships existed between circadian period length and the ages at which depression or mania first caused impairments (*Figure 3.3G*). Whilst no significant differences emerged with either parameter, a trend was becoming apparent, where there was greater period lengthening the younger the age at which depression first caused impairment (never: 22.29, 5-14: 24.56±0.55, 15-19: 24.14±0.23, 20-24: 23.06±0.51, 25-34: 24.00±0.83, 35-46: 23.37±0.08 h). Similarly, when assessing the age at which mania first caused impairment, no significant differences were found (*Figure 3.3H*). However, a pattern distinct from the first major depressive episode emerged as subjects who were between 25-29 years exhibited the longest average period, where patients experiencing their first episode of mania at an earlier or later stage presented shorter rhythms (never: 23.78±1.49, 15-19: 24.09±0.29, 20-24: 23.49±0.52, 25-29: 25.14±0.57, 30-34: 23.92±0.52, 35-46: 23.00±0.32 h). As seen in *Figure 3.3I*, those who did or did not experience psychosis had average period lengths of 23.90±0.24h and 23.80±0.43h respectively, and thus no significant differences were identified. Therefore, the disease characteristics analysed could not fully account for the period variability in our BPD patient samples.

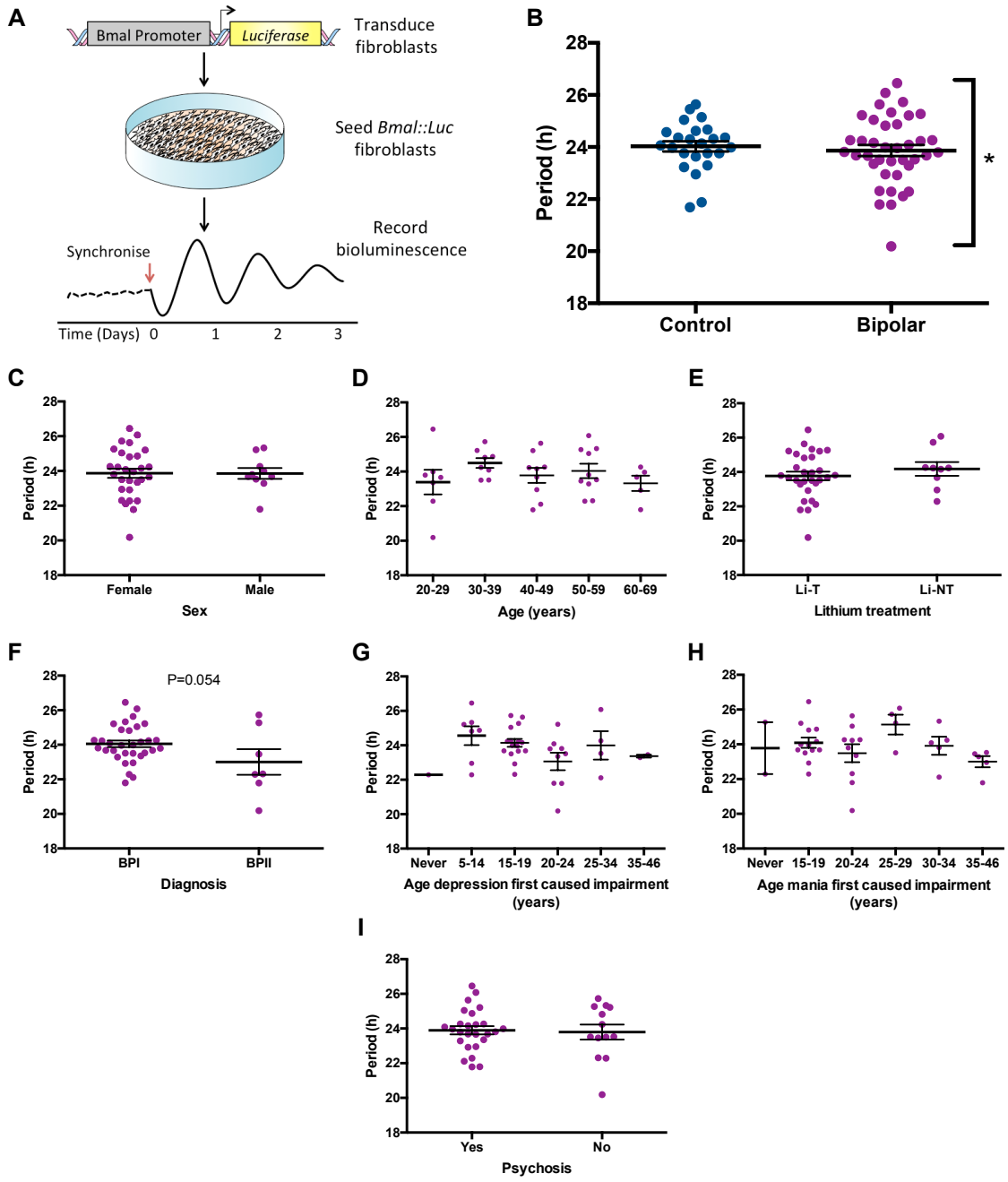

***Figure 3.3. Bmal::Luc* rhythms from bipolar patient fibroblasts display variable period lengths. A)** Schematic representation of the protocol implemented to assess circadian rhythmicity. **B)** The overall *Bmal::Luc* period lengths from control (n=24) or BPD patient (n=39) fibroblasts. Bipolar patients were further sub-divided into various categories in order to identify why period length was so variable. The groups included division by sex **(C)**, age **(D)**, lithium treatment **(E)**, diagnosis **(F)**, the ages where depression or mania first caused impairment **(G-H)**, and whether patients presented symptoms of psychosis **(I)**.

3.2.5 Patient stratification by Bmal::Luc period length revealed 3 distinct sub-groups

Due to the lack of patient phenotypes accounting for circadian periodicity, a different approach was undertaken. As seen in *Figure 3.4A*, the frequency distribution diagram illustrates that period length for BPD patients was normally distributed. The majority of BPD patients had period lengths between 23.00-23.99h. At the extreme ends were 3 patients with periods less than 22.00h and 2 patients with a period greater than 26.00h.

Based on this information, patients were divided into 3 categories, those with: a) **short periods** of 23.49h or under, b) **medium periods** between 23.50h to 24.99h, and c) **long periods** of 25.00h or more. As expected, dividing patients into these new groups resulted in obvious period differences amongst all 3 categories, where period was on average 1.5h different between successive groups (*Figure 3.4B)*. Those classified as short had an average period length of 22.48±0.26h, the medium fibroblasts averaged 24.03±0.10h, and the long as 25.55±0.16h. The representative traces highlight the period variability in example cell lines. The raw luminescence counts highlight the high level of background noise associated with examining fibroblast rhythms and display their rapid rates of dampening for the cells in the short, medium, and long categories (*Figures 3.4C-E*). Following baseline subtraction and smoothing, differences in circadian parameters became more apparent, as seen in *Figure 3.4F*. These representative traces highlight the period variability between cells in these categories.

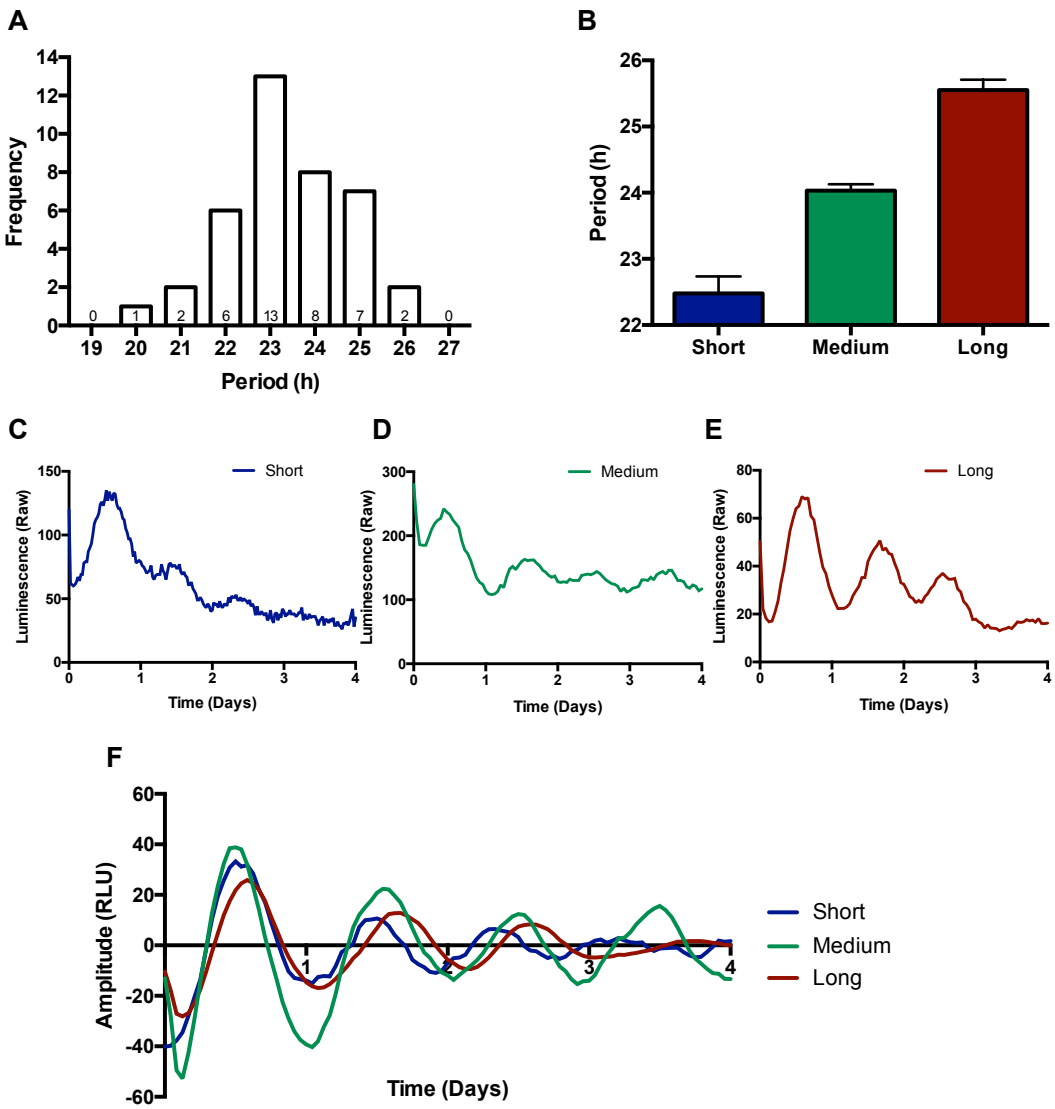

Figure 3.4. **Division of bipolar patient fibroblasts into short, medium, and long *Bmal::Luc* period groups. A)** A frequency distribution diagram highlighting the number of patients belonging to each period category. **B)** Patients were divided into sub-groups based on their *Bmal::Luc* period length. The short category contained patients with period lengths of 23.49h or less (n=13), the medium between 23.50-24.99h (n=17), and the long 25.00h or more (n=9). Raw luminescence traces of example fibroblasts that belong to the short **(C)**, medium **(D)**, or long **(E)** groups. **F)** Normalised traces aiding the identification of period variability amongst the BPD patient fibroblasts.

3.2.6 Luminometric assessment of Per2::Luc period length

To confirm the findings from the previous section, a subset of the control and BPD patient fibroblasts from the short, medium, and long groups were transduced with the *Per2::Luc* lentivirus to create stable cell lines which monitor the negative arm of the molecular clock. Much like the protocol implemented to assess *Bmal::Luc* rhythms, the virally transduced cells were treated with dexamethasone to induce cell synchrony, and *Per2::Luc* luminescence was monitored (*Figure 3.5A*). Whilst no significant differences were observed, the BPD patients exhibited trends for lengthened *Per2::Luc* rhythms by 27min, where variability ranged between 22.5-25.2h (control: 23.48±0.27, bipolar: 23.93±0.23 h) (*Figure 3.5B*). This 3h period distribution was smaller than findings with *Bmal*, however, this may be due to the sample number assessed.

As such, we decided to assess whether patients assigned to the aforementioned categories of short, medium, and long based on their *Bmal* rhythms, would result in significant period differences when assessing their *Per2* rhythms. When categorising patient cells, two things became apparent: 1) the aforementioned criteria for classifying those with short, medium, and long period was applicable, and 2) significant differences emerged between cells within these groupings. Cells within the short category had an average period of 22.75±0.08h, which was 1.6h shorter than those within the medium group, which averaged 24.31±0.13h. Similarly, those within the medium group had a period that was 1h shorter than cells within the long category which had an average period length of 25.16±0.08h (*Figures 3.5C-D*).

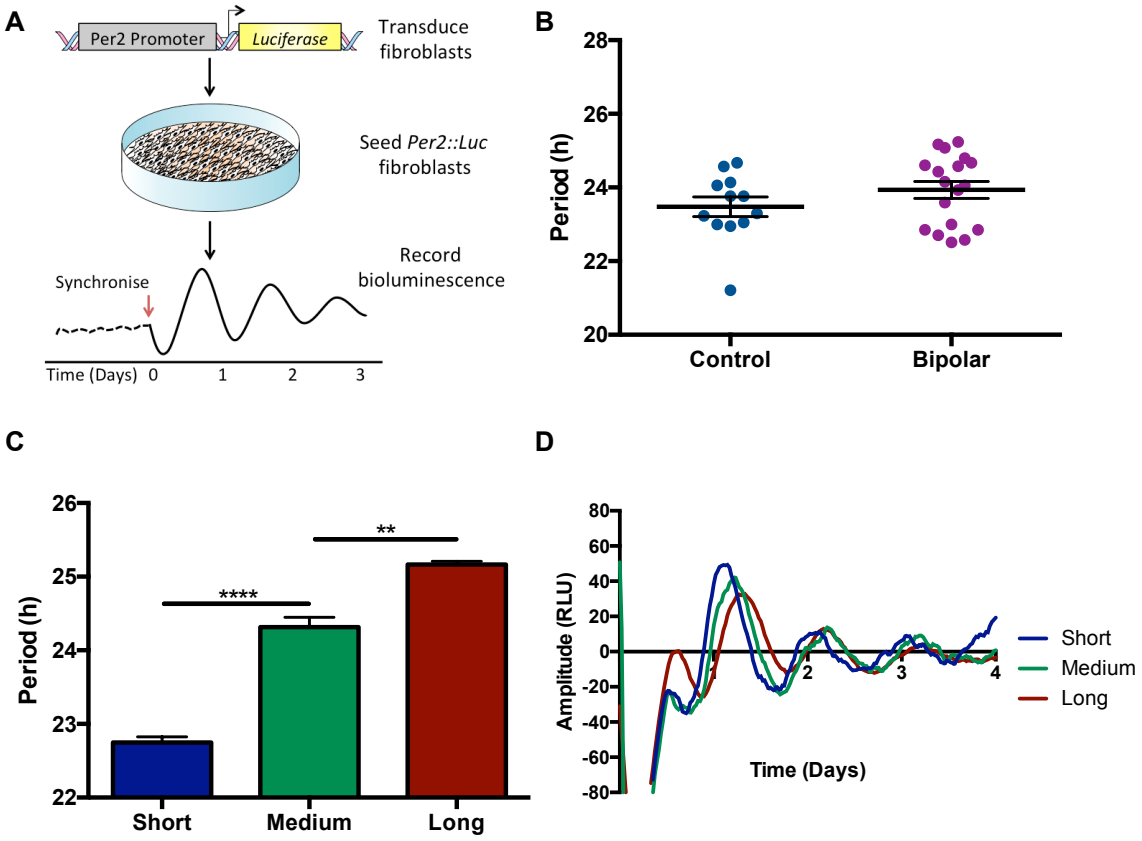

Figure 3.5. **Characterising patients as having a short, medium, or long *Bmal* period resulted in clear *Per2::Luc* period differences. A)** Schematic representation of the protocol implemented to assess circadian rhythmicity. **B)** The overall *Per2::Luc* period lengths from control (n=12) or BPD patient (n=18) fibroblasts. **C)** Patients were assorted into their previously assigned sub-groups based on their *Bmal::Luc* period length. The short category contained patients with period lengths of 23.49h or less (n=6), the medium between 23.50-24.99h (n=9), and the long 25.00h or more (n=3). **D)** Normalised traces aiding the identification of period variability amongst the BPD patient fibroblasts.

3.2.7 Demographic factors cannot account for Per2::Luc period variability

Given the removal of patients with extreme period lengths and reduced period distributions, we decided to investigate whether any bipolar disease characteristics could shed light on the cause of period variability. When analysing whether differences in sex or age could account for period variability, no significant differences were identified (sex → female: 23.90±0.25, male: 24.11±0.63; age → 20-39: 24.02±0.55, 40-49: 24.05±0.37, 50-59: 23.77±0.38 h) (*Figures 3.6A-B*). Whilst no significant differences were observed with lithium treatment, the emergent trend was that of period lengthening by 34min with Li-NT patients (Li-T: 23.71±0.30, Li-NT: 24.28±0.34 h) (*Figure 3.6C*). Moreover, when assessing whether BPD diagnosis could account for period variability, much like *Bmal* rhythms, a trend for greater period lengthening was observed with BPI patients by 36min (BPI: 24.07±0.25, BPII: 23.47±0.51 h) (*Figure 3.6D*).

Subsequently, we analysed whether the age at which depression or mania first caused impairment could account for the period effects. Unlike assessment of *Bmal* rhythms, no significant trends emerged with either category (first major depressive episode → 5-14: 24.10±0.73, 15-24: 23.92±0.30, 25-39: 24.08±0.48 h; first major manic episode → 15-19: 23.92±0.51, 20-24: 24.50±30, 25-34: 24.07±0.47, 35-40: 23.39±0.71 h) (*Figures 3.6E-F*). Finally, the presence of psychotic episodes did not influence circadian period length in our BPD patient cohort (psychotic symptoms: 23.93±0.29, no psychotic symptoms: 23.95±0.38 h) (*Figure 3.6G*). Thus, the BPD features assessed could not fully account for the period variability observed in our BPD patient samples.

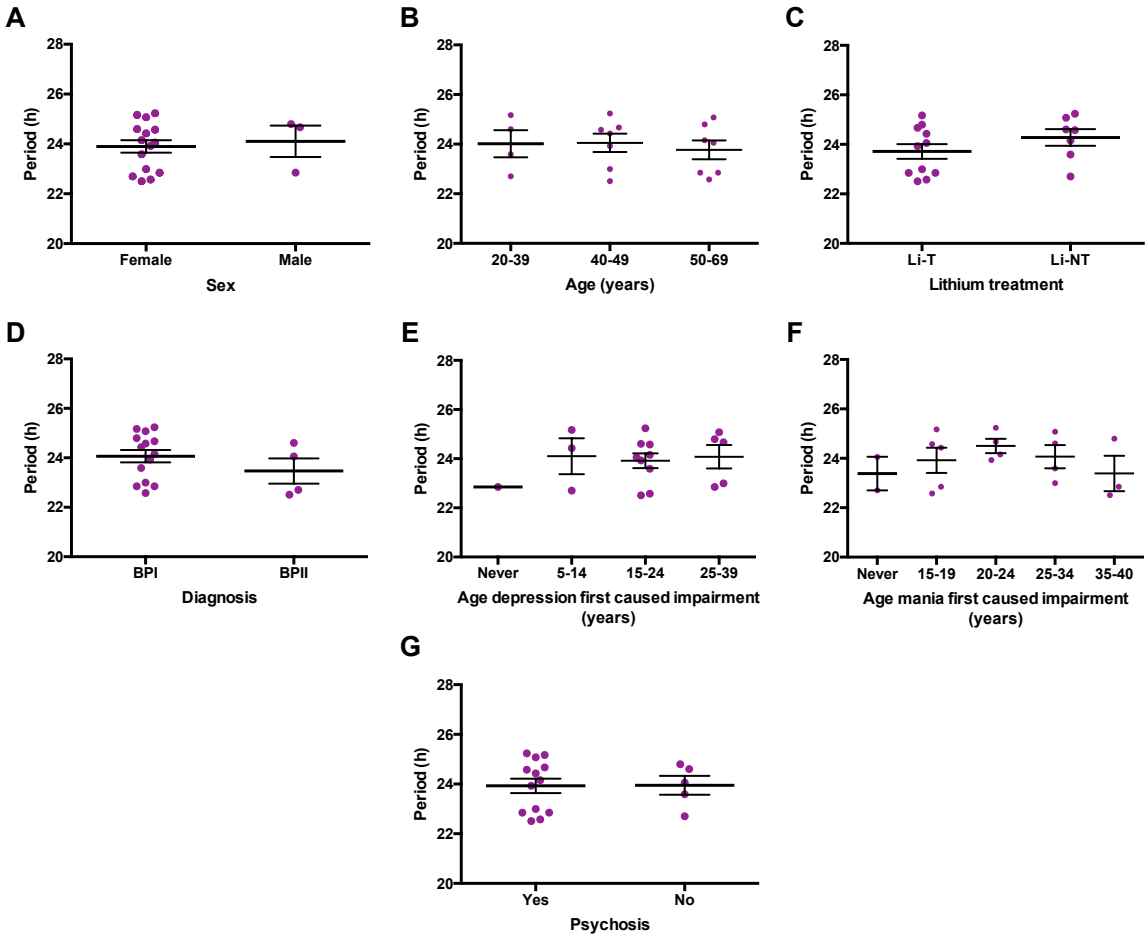

Figure 3.6. **No specific demographic feature could account for the variability in *Per2::Luc* rhythms from bipolar patient fibroblasts.** BPD patients were sub-divided into various categories in order to identify why period length was so variable. The groups included division by sex **(A)**, age **(B)**, lithium treatment **(C)**, diagnosis **(D)**, the ages where depression or mania first caused impairment **(E-F)**, and whether patients presented symptoms of psychosis **(G)**.

.

3.2.8 Bmal::Luc and Per2::Luc period correlations

Subsequently, a regression analysis was performed to see whether there was any correlation between *Bmal* and *Per2* bioluminescence rhythms (*Figure 3.7*). A positive correlation was observed (R^2=0.621), such that patients with longer *Bmal* molecular rhythms were more likely to display longer *Per2* rhythms and vice versa. Therefore, it could be suggested that both the positive and negative arms of the molecular clock exhibit similar period changes in our BPD fibroblasts. This is the first time such a correlation has been observed in BPD patient cells, and suggests that no individual component of the molecular clock is 'broken', but the whole clock mechanism displays a variable phenotype.

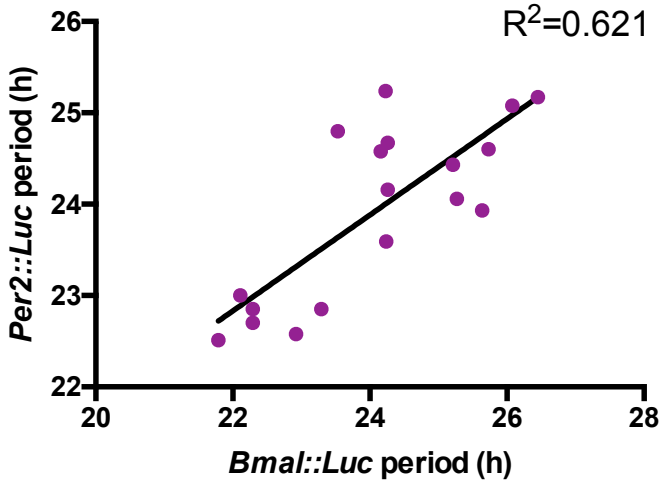

Figure 3.7. **Bipolar patients with longer *Bmal* periods exhibit longer *Per2* periods.** Regression analysis comparing *Bmal::Luc* rhythms with *Per2::Luc* rhythms in BPD patient-derived fibroblasts (n=18).

3.2.9 Correlogram analysis of lithium-treated patients

Due to the potential interest in using the fibroblasts as a model to screen for novel pharmacological mechanisms via which mood stability could be induced, we decided to explore the correlations exhibited by Li-T and Li-NT patients. To this end we created correlograms, as seen in *Figures 3.8-9*. This facilitated the observation of any significant interactions between the known patient disease phenotypes and the newly acquired patient circadian data.

When assessing the Li-T cohort, multiple significant patterns became apparent, as seen in *Figure 3.8*. Firstly, many observations were anticipated and thus served to validate our approach. For example, the time a person was on lithium increased with age. Given that lithium treatment can be a life-long prescription and that patients were on lithium for an average of 10 years, this appeared sensible. Also, as we previously identified, a negative correlation was observed between PDT and age, such that the higher the PDT, the younger the patient, where we also established a positive correlation between *Per2* and *Bmal* period.

With the additional information collected in our investigation, an interesting relationship was found between periodicity and patient medications, where the longer the circadian period, the greater the total number of medications consumed. Furthermore, patients with a shorter circadian period were consuming more mood-stabilisers, an interesting finding given that lithium induces period lengthening. On the other hand, patients with a longer period were consuming more antipsychotics, hypnotics, and anxiolytics, where the latter two classes reached significance after adjusting for multiple comparisons.

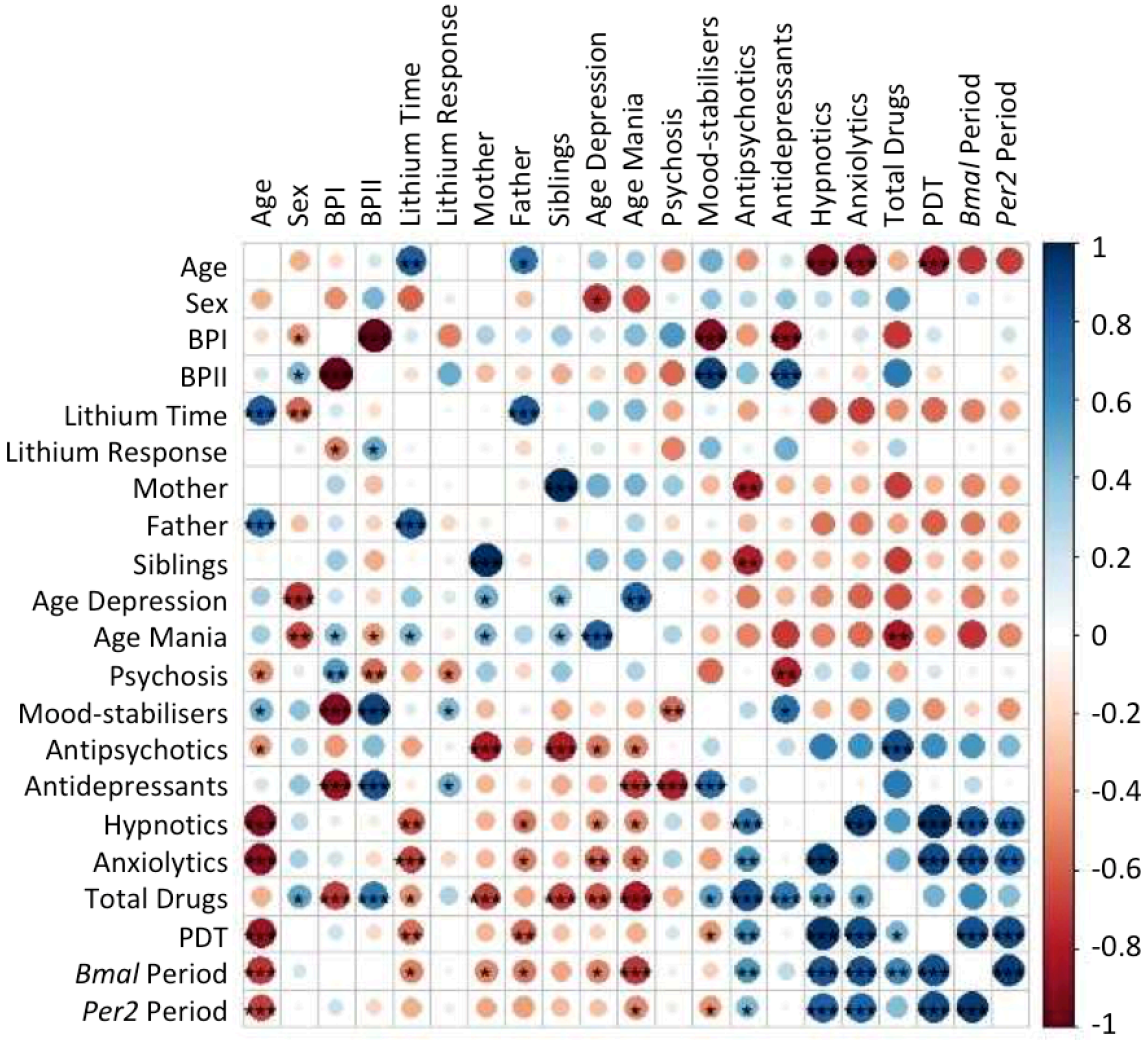

Figure 3.8. **Correlation matrix for lithium-treated bipolar patients.** The correlation matrix revealed patterns and their level of significance when comparing multiple parameters (n=11). The scale (right) signifies the strength of the correlation, where blue indicates a positive correlation, and red a negative correlation. The size of the circle reiterates this. The stars indicate the level of significance: *P<0.05, **P<0.01, ***P<0.001.

3.2.10 Correlogram analysis of lithium-non-treated patients

Analysis of the Li-NT sub-group also revealed some noteworthy patterns, as seen in *Figure 3.9*. Much like the Li-T group, these patients also presented a positive correlation between PDT and periodicity, as well as *Per2* and *Bmal* period. A finding not observed with the Li-T group was the positive correlation between periodicity and the onset of psychotic symptoms, such that the longer the circadian period the more likely patients were to present symptoms of psychosis.

Additionally, interesting discrepancies were identified between the medications consumed and periodicity. Mood-stabilisers still presented a significant negative relationship such that patients with a shorter circadian period were consuming more mood-stabilisers, suggesting that non-lithium based mood-stabilisers may target patients with similar periodicities. However, unique to this subgroup was the positive correlation identified between antidepressants and periodicity, such that the more antidepressants consumed the longer the patient's circadian period. Thus, differences emerged in correlative patterns when assessing lithium sensitivity.

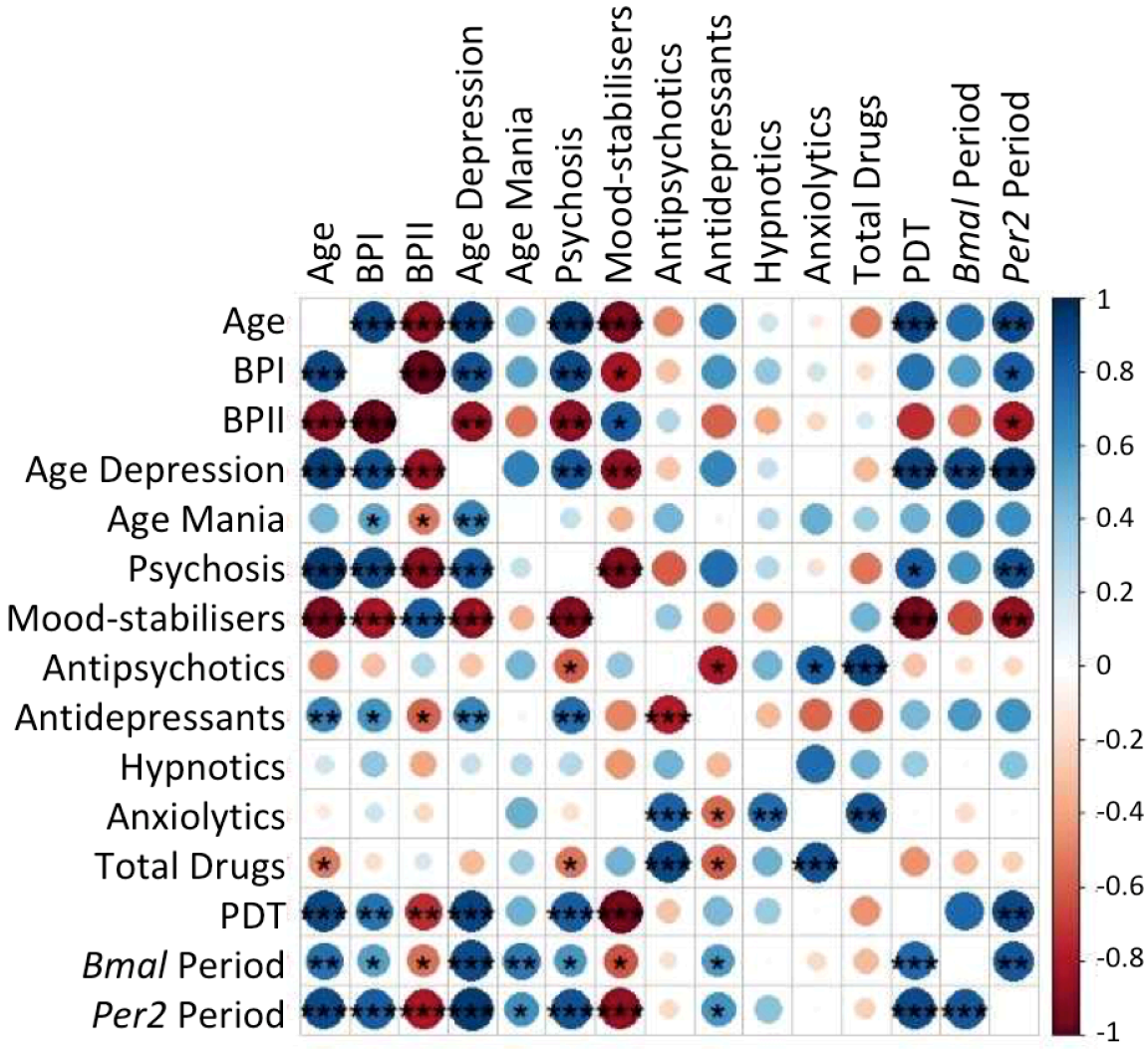

Figure 3.9. **Correlation matrix for lithium non-treated bipolar patients.** The correlation matrix revealed patterns and their level of significance when comparing multiple parameters (n=7). The scale (right) signifies the strength of correlation, where blue indicates a positive correlation, and red a negative correlation. The size of the circle reiterates this. The stars indicate the level of significance: *=P<0.05, **P<0.01, ***P<0.001.

3.3 Discussion

This investigation sought to gain an enhanced understanding of the circadian disturbances associated with BPD via analysis of patient-derived fibroblasts. Whilst no significant period differences were identified, patient fibroblasts exhibited *Bmal::Luc* period variability ranging 6h, where no specific disease characteristics were clearly accountable for these effects. On the other hand, when analysing *Per2* rhythmicity, patient-derived cells presented trends for period lengthening by 27min, effects which could not be correlated with the known demographics. We did however find a strong and significant correlation between *Bmal::Luc* and *Per2::Luc* rhythms in our transduced cell lines, where dividing patients into Li-T and Li-NT groups revealed an interesting association between circadian period and patient medications.

3.3.1 Validity of using bipolar patient fibroblasts and reporter assays

Use of healthy human or murine cells previously validated that the molecular clocks within fibroblasts provide an accurate indication of the master clock within the brain, the SCN (Brown et al., 2005, Pagani et al., 2010). This study assessed rhythms in fibroblasts obtained from a single biopsy per patient, with a single infection per gene of interest, and in a single trial, where 6 technical replicates were averaged to provide period information. This was because Brown and colleagues previously confirmed that doing so was sufficient to provide information regarding the state of the circadian clock. They found that rhythms within the fibroblasts were identical to those within hair-root keratinocytes, suggesting that the period observed was not unique to a specific

cell type, but representative of rhythms in that individual (Brown et al., 2005). Moreover, the standard deviation between their trials was 18min and the standard deviation between biopsies was 6min, suggesting that a single trial from a single biopsy was sufficient to indicate circadian rhythmicity, assuming that all samples underwent similar processes. The highest variability came from different infections, which had a standard deviation of 25min (Brown et al., 2005). However, as we infected all our cells with the same batch of concentrated viral supernatant, we significantly reduced the variability observed due to such technical factors, which suggests that the wide distributions may be associated with the inherent circadian clocks of the subjects themselves. Furthermore, we validated our *Bmal::Luc* period observations by using an alternative reporter system. In doing so a correlation was observed, further validating our findings.

It should be acknowledged that our fibroblast model also possesses certain limitations as a model by nature is a simplification of the true phenomena, which in these circumstances is the capacity to model *in vivo* behavioural effects. For example, *in vivo* biological processes can display homeostatic feedback mechanisms. As well as oscillating with a 24h rhythm, changes in membrane potential can impact and therefore feedback onto the molecular clock, effects which would not be prominent in our fibroblast cultures (Welsh et al., 2010). Furthermore, as well as containing cell-autonomous circadian clocks, neurones within the SCN also display network-level properties, maintaining identical period lengths, specific phase relationships, and strong amplitude rhythms (Welsh et al., 2010). Investigations into understanding SCN

coupling have revealed a key role for the neurotransmitter GABA and the neuropeptide VIP, both of which function to maintain network coupling and thereby resist transient changes (Evans et al., 2013). Indeed, these effects are largely absent in non-SCN tissues including our fibroblasts, an effect highlighted by the need to treat cell cultures with a synchronising agent. Such properties may explain why period change was 2-4 times greater in the cultured fibroblast models relative to wheel-running behaviour in mutant animal models (Brown et al., 2005). Thus, although the fibroblast model has limited ability to recapitulate *in vivo* behaviour, it is capable of giving a reliable readout on the properties of the individual's molecular clock (determined by genetics) and in assessing drug-induced chronomodulatory changes at the level of the molecular clock.

3.3.2 Understanding the variability within our subjects

Much like previous observations of healthy human cells, when characterising the PDT, the *Bmal::Luc* period, or *Per2::Luc* periodicity, large inter-individual variability was observed. Due to the moderate number of fibroblasts used in this study, variables could only be assessed at a superficial level. For example, when looking at age, the sub-groups could not be further divided by sex as the sample sizes would be insufficient to provide statistical power. Therefore, whilst some trends emerged further analysis with a larger cohort may aid in characterising the origins of period variability in BPD.

Firstly, we observed a correlation between PDT and age, where the younger patients had the longest PDT, a finding which was in stark contrast to what we had hypothesised. This was because the use of fibroblasts from healthy older subjects (63-92 years) relative to younger subjects (21-36 years) revealed

not only longer PDTs, but reduced rates of fibroblast migration from skin samples, reduced cell numbers at confluence, and faster onset of cellular senescence, defined by the lack of cellular confluence after 1 week (Schneider and Mitsui, 1976). This appeared sensible as the cellular characteristics modelled the age of the individual from which they originated. Further, findings with dental pulp stem cells showed that the higher the passage number, the longer the PDT (Bressan et al., 2012). When assessing the passage numbers of patients between 20-29 years in our samples, all were between 3-5 passages, with no rudimentary correlation identified. Therefore, whilst future investigations should account for extreme passage variability, this did not seem to be the reason for why younger patients exhibited longer PDTs. It could instead be due to currently unknown disease characteristics.

Secondly, when assessing healthy human fibroblast rhythms, we observed a standard error ranging 0.20-0.27h (12-16min), which was within the same range as previous investigations (*Table 3.1*). Period variability may be due to genetic differences in the pre-determined period lengths. The importance of genotype is highlighted as mutations in single genes can significantly impact periodicity in rodents. For example, the *Tau* mutant hamster, which displays a 20h period, has a mutation in the *Csnk1ε* gene, whilst the *ClockΔ19* mouse with a mutant *Clock* gene exhibits a lengthened period phenotype of 27h (Lowrey et al., 2000, King et al., 1997). Such examples highlight the importance of individual components of the clock in determining period, but also show how small alterations to the genetic code can have large-scale consequences on rhythmicity, emphasising the role of genetics in determining period in a healthy population.

In humans, periodicity is often inferred from differences in chronotype. The strength of the circadian oscillators themselves denoted by amplitude or variability within the photic/non-photic input pathways may also contribute to introducing differences in period (Brown et al., 2008). For example, reductions in light information signalling to the SCN may reduce the effectiveness of this *zeitgeber* to induce corrective phase shifts, and subsequently lead to the subject living under free-running conditions, which in humans runs longer than the 24h day, and would be observed as period lengthening. Indeed, in circadian blind patients, examination of their endogenous period can reveal just this (Sack et al., 1992). Thus, the combined actions of genetics, oscillator amplitude, and the circadian input pathways could act to determine period.

Much like previous studies assessing healthy human rhythms, we found the period lengths of BPD patients to follow a Gaussian distribution. Assessing behavioural rhythms of healthy subjects via a forced desynchrony protocol revealed 36min variability, where the use of fibroblasts revealed variability within the range of 4h (Czeisler et al., 1999, Brown et al., 2005). As period effects have shown to be correlative yet exaggerated in culture, this suggests that *in vitro* models may amplify circadian abnormalities. This can be advantageous as should targeting circadian disturbances provide one means of normalising mood instability, patient cells could be screened to examine their molecular rhythmicity with faster speeds and greater ease than behavioural assessments.

In our investigation the standard error observed for BPD patients was between 0.21-0.23h (13-14min), which was similar to the previous publication assessing *Per2* rhythmicity, possibly as similar sample sizes were assessed, and

smaller when compared to *Bmal* rhythms, where we used 3 times more samples (*Table 3.1*). Moreover, in the current investigation a trend for patient fibroblasts displaying a longer *Per2* period by 27min emerged, where a significant effect has previously been observed by 25min (McCarthy et al., 2013). Similarly, neither the current investigation nor the previous study assessing *Bmal* rhythmicity found significant period effects. Whilst they observed trends for 40min lengthening, such effects were not observed in our investigation (Bamne et al., 2013). This may be because along with the genetically encoded period variability underlying rhythmicity in the human population, there are additional components such as medication, epigenetic influences, genetic factors such as race and random mutations, or currently unknown disease factors which simply add to the complexity of the underlying BPD pathophysiology. Indeed, the strong trend emerging suggests that circadian disturbance may be more prominent with BPI. As there are no studies assessing BPII cellular rhythmicity, this is an interesting avenue for future investigative studies.

Whilst this was an observational study, we had hypothesised observing period lengthening in our patients. This was because along with the indications from preliminary fibroblast studies as mentioned, patients had also been found to exhibit evening preferences, where they would wake up and sleep later, and such activity has been correlated with having a longer circadian period (Wood et al., 2009, Falsin Giglio et al., 2010, Brown et al., 2008). Whilst the true consequences of this are not fully understood, in combination with low amplitude rhythms, patients may fail to fully entrain to the 24h day, which can lead to abnormalities in affect, physiology, and behaviour.

3.3.3 The effects of lithium treatment

One of the aims of this investigation was to gain a deeper understanding into whether there was a relationship between lithium treatment and circadian period. This was because, the mechanism giving rise to lithium sensitivity remains elusive, therefore we were curious to address whether circadian rhythmicity was implicated. The trends identified suggested that the Li-NT group had longer periods when assessing *Bmal* and *Per2* rhythmicity by 25min and 34min respectively. This is interesting as it implies that patients who were treated with lithium may have shorter periods, and this was indeed the correlation observed. As lithium is a chronomodulatory molecule that lengthens circadian period, this suggested that part of lithium's mechanism of action may be to further lengthen circadian period of patients and provides a solid foundation for further investigation (Li et al., 2012).

Moreover, analysing *Bmal* fibroblast rhythms from patients with circadian rhythm sleep disorders revealed that period was significantly longer in patients with non-24-hour sleep-wake disorder. Period differences were also observed based on whether these subjects responded to chronotherapeutic treatments. Patients who did not respond to bright light therapy in combination with melatonin treatment exhibited a longer period phenotype by 37min (Hida et al., 2017). Therefore, much like the indicative patterns observed with our patient data, a longer circadian period may be indicative of poor treatment responses. Further investigations could help clarify whether circadian period could act as a biomarker of lithium responsiveness in the future.

3.3.4 Lithium-treated patients

We divided our patient sample according to lithium treatment in order to investigate the associations between circadian rhythmicity and lithium responsiveness. It should be acknowledged that due to the low sample number, such patterns are only indicative of possible correlations. Therefore, larger scale studies will need to be performed preferably based on a power calculation. Along with the aforementioned negative correlation observed with mood-stabilisers, we found a positive correlation between periodicity and the consumption of antipsychotics, anxiolytics, and hypnotic agents, as greater consumption of these compounds was associated with a longer circadian period.

The strongest correlation was observed with the anxiolytic and hypnotic agents. As the anxiolytic agents consumed were from the benzodiazepine class, an overlapping feature of these two categories was their psychoactive sedative nature. Due to the highly entwined nature of the sleep and circadian systems, the hypnotic abilities of sedatives are likely to impact circadian rhythmicity. Indeed, treatment of insomnia can reduce treatment-resistant persecutory delusions, suggesting that targeting sleep and circadian rhythm disruptions may normalise behavioural abnormalities (Myers et al., 2011).

The model depicted in Chapter 1, *Figure 1.3A*, suggests that circadian dysfunctions are core to neuropsychiatric disorders, and can give rise to both sleep disruptions and mood abnormalities. BPD has a major sleep phenotype, therefore based on this idea, the weaker circadian clocks of BPD patients may give rise to sleep abnormalities, where sedative agents are then prescribed to treat these overt symptoms. There are reasons as to why the consumption of the

drugs themselves may not be responsible for lengthening period. The screening of drug libraries by the Vasudevan Lab found that the benzodiazepines clonazepam and temazepam (10μM, n=4) did not induce any circadian period lengthening (Vasudevan Lab, *unpublished*). Moreover, in patients suffering from psychiatric disorders, gradually reducing their dosage of benzodiazepine consumption did not impact rhythm parameters, although trends for increased day and night-time activity were observed (Baandrup et al., 2016). This suggests that benzodiazepines may not overtly impact rhythmicity in humans. On the other hand, if the prescription of sedative agents was purely a sleep-based phenomenon, then circadian abnormalities should not be detected at the cellular level. Thus, we suggest that circadian abnormalities give rise to sleep disruptions, exemplified by the number of sedative agents prescribed.

3.3.5 Lithium-non-treated patients

When analysing the prominent patterns associated with Li-NT patients, we found both overlapping and distinct observations. A correlation was observed in which shorter circadian periods were associated with the increased consumption of mood-stabilisers. As patients in this category were not consuming lithium, this suggests that lamotragine and valproate may also induce period lengthening. Indeed, the aforementioned in-house drug library screen found that lamotrigine (10μM, n=4) lengthened circadian period (Vasudevan Lab, *unpublished*). Valproate has also been shown to lengthen period to a similar extent as lithium in *Drosophila* (Dokucu et al., 2005). However, when tested on mammalian PER2::LUC SCN sections or fibroblasts, no alterations in period were identified (Johansson et al., 2011). This may be due differences in the gene of

interest as valproate differentially impacted circadian genes, where trends for *Bmal* period lengthening were emerging in NIH-3T3 cells (Griggs et al., 2018).

Additionally, a positive correlation was identified between the use of antidepressants and period lengthening. Given that depressive symptoms are more common in BPII and such patients are less likely to be prescribed lithium, it could be suggested that these correlations may be due to diagnosis type (Baldessarini et al., 2007). However, both the Li-T and Li-NT groups contained an equal number of BPII patients (n=2). The discrepancies may therefore be due to molecular underpinnings. As lithium lengthens period and appeared to be more common in patients with a shorter circadian period length, antidepressants may target patients with longer periods by inducing a shortening effect. The majority of antidepressants consumed were selective-serotonin reuptake inhibitors. Indeed, a study indicated that sertraline, citalopram, fluoxetine, fluvoxamine, and paroxetine all reduced period by up to 1.6h in Rat-1 fibroblasts (Nomura et al., 2008). Overall, much like the findings in Li-T patients, whether there is a true causal link between period and medications requires further validation, however, noteworthy dissimilarities did emerge.

3.3.6 Conclusions

In conclusion, this investigation supports previous findings of period lengthening in *Per2::Luc* rhythms from well-validated BPD patients. Further analysis uncovered that the Li-T patients exhibit stronger relationships with the consumption of anxiolytic and hypnotic agents, where the Li-NT patients showed stronger associations with the consumption of antidepressant medications. Whilst these correlations require further research, they do highlight differences

associated with lithium treatment. Validation of these responses may help to elucidate whether circadian rhythmicity can act as a biomarker for lithium responsiveness, a finding that could help revolutionise patient treatment plans.

Future studies could also look into assessing rhythm amplitude in our patient fibroblasts. This was not feasible in the current investigation as we used lentiviral-mediated transduction, where the number of viral integrations per cell cannot be controlled making it difficult to accurately compare rhythmic amplitude. Amplitude could simply be higher as there were more copies of the *Per2* or *Bmal* gene inserted into the genome. Indeed, lentiviral copy number in fibroblasts could be assessed by analysing DNA content using real-time PCR techniques. Alternatively, a novel method to overcome this issue could be to use dual integrase cassette exchange (DICE) technology (Zhu et al., 2014). DICE first requires the addition of a 'landing pad' containing attP sites through site-specific homologous recombination. The landing pad is then exchanged with the target gene of interest (*Bmal* or *Per2*) flagged by attB sites by phiC31 and Bxb1 integrases. This system is advantageous as it allows site and copy number specificity aiding accurate data comparisons.

Overall, our fibroblast model provides a biologically relevant representation of human physiology when assessing patient molecular clocks. This could therefore help further understand circadian abnormalities in mood disorders and in identifying patient-relevant pharmacological treatments in the future. As patients displayed period variability, it is worth identifying whether our fibroblasts accurately model drug-induced circadian changes, thus validating their use in future drug discovery programmes.

3.4 References

AKHTER, A., FIEDOROWICZ, J. G., ZHANG, T., POTASH, J. B., CAVANAUGH, J., SOLOMON, D. A. & CORYELL, W. H. 2013. Seasonal variation of manic and depressive symptoms in bipolar disorder. *Bipolar Disorders,* 15**,** 377-384.

AMERICAN PSYCHIATRIC ASSOCIATION 2013. *Diagnostics and Statisitcal Manual of Mental Disorders (DSM) 5th edition,* Washington.

BAANDRUP, L., FASMER, O. B., GLENTHOJ, B. Y. & JENNUM, P. J. 2016. Circadian rest-activity rhythms during benzodiazepine tapering covered by melatonin versus placebo add-on: data derived from a randomized clinical trial. *Bmc Psychiatry,* 16**,** 348.

BALDESSARINI, R. J., LEAHY, L., ARCONA, S., GAUSE, D., ZHANG, W. & HENNEN, J. 2007. Patterns of psychotropic drug prescription for US patients with diagnoses of bipolar disorders. *Psychiatric Services,* 58**,** 85-91.

BALSALOBRE, A., BROWN, S. A., MARCACCI, L., TRONCHE, F., KELLENDONK, C., REICHARDT, H. M., SCHUTZ, G. & SCHIBLER, U. 2000. Resetting of circadian time peripheral tissues by glucocorticoid signaling. *Science,* 289**,** 2344-2347.

BALSALOBRE, A., DAMIOLA, F. & SCHIBLER, U. 1998. A serum shock induces circadian gene expression in mammalian tissue culture cells. *Cell,* 93**,** 929-937.

BAMNE, M. N., PONDER, C. A., WOOD, J. A., MANSOUR, H., FRANK, E., KUPFER, D. J., YOUNG, M. W. & NIMGAONKAR, V. L. 2013. Application of an ex vivo cellular model of circadian variation for bipolar disorder research: a proof of concept study. *Bipolar Disorders,* 15**,** 694-700.

BIELER, J., CANNAVO, R., GUSTAFSON, K., GOBET, C., GATFIELD, D. & NAEF, F. 2014. Robust synchronization of coupled circadian and cell cycle oscillators in single mammalian cells. *Molecular Systems Biology,* 10**,** 739.

BRESSAN, E., FERRONI, L., GARDIN, C., PINTON, P., STELLINI, E., BOTTICELLI, D., SIVOLELLA, S. & ZAVAN, B. 2012. Donor Age-Related Biological Properties of Human Dental Pulp Stem Cells Change in Nanostructured Scaffolds. *Plos One,* 7**,** e49146.

BROWN, S. A., FLEURY-OLELA, F., NAGOSHI, E., HAUSER, C., JUGE, C., MEIER, C. A., CHICHEPORTICHE, R., DAYER, J. M., ALBRECHT, U. & SCHIBLER, U. 2005. The period length of fibroblast circadian gene expression varies widely among human individuals. *Plos Biology,* 3**,** 1813-1818.

BROWN, S. A., KUNZ, D., DUMAS, A., WESTERMARK, P. O., VANSELOW, K., TILMANN-WAHNSCHAFFE, A., HERZEL, H. & KRAMER, A. 2008. Molecular insights into human daily behavior. *Proceedings of the National Academy of Sciences of the United States of America,* 105**,** 1602-1607.

CARSKADON, M. A., LABYAK, S. E., ACEBO, C. & SEIFER, R. 1999. Intrinsic circadian period of adolescent humans measured in conditions of forced desynchrony. *Neuroscience Letters,* 260**,** 129-132.

CZEISLER, C. A., DUFFY, J. F., SHANAHAN, T. L., BROWN, E. N., MITCHELL, J. F., RIMMER, D. W., RONDA, J. M., SILVA, E. J., ALLAN, J. S., EMENS, J. S., DIJK, D. J. & KRONAUER, R. E. 1999. Stability, precision, and near-24-hour period of the human circadian pacemaker. *Science,* 284**,** 2177-2181.

DOKUCU, M. E., YU, L. P. & TAGHERT, P. H. 2005. Lithium- and valproate-induced alterations in circadian locomotor behavior in Drosophila. *Neuropsychopharmacology,* 30**,** 2216-2224.

EVANS, J. A., LEISE, T. L., CASTANON-CERVANTES, O. & DAVIDSON, A. J. 2013. Dynamic Interactions Mediated by Nonredundant Signaling Mechanisms Couple Circadian Clock Neurons. *Neuron,* 80**,** 973-983.

FALSIN GIGLIO, L. M., MAGALHAES, P. V. S., ANDERSEN, M. L., WALZ, J. C., JAKOBSON, L. & KAPCZINSKI, F. 2010. Circadian preference in bipolar disorder. *Sleep and Breathing,* 14**,** 153-155.

GRIGGS, C. A., MALM, S. W., JAIME-FRIAS, R. & SMITH, C. L. 2018. Valproic acid disrupts the oscillatory expression of core circadian rhythm transcription factors. *Toxicology and Applied Pharmacology,* 339**,** 110-120.

GUILDING, C., HUGHES, A. T. L. & PIGGINS, H. D. 2010. Circadian oscillators in the epithalamus. *Neuroscience,* 169**,** 1630-1639.

GUILDING, C., SCOTT, F., BECHTOLD, D. A., BROWN, T. M., WEGNER, S. & PIGGINS, H. D. 2013. Suppressed cellular oscillations in after-hours mutant mice are associated with enhanced circadian phase-resetting. *Journal of Physiology-London,* 591**,** 1063-1080.

HARVEY, A. G. 2008. Sleep and circadian rhythms in bipolar disorder: Seeking synchrony, harmony, and regulation. *American Journal of Psychiatry,* 165**,** 820-829.

HIDA, A., OHSAWA, Y., KITAMURA, S., NAKAZAKI, K., AYABE, N., MOTOMURA, Y., MATSUI, K., KOBAYASHI, M., USUI, A., INOUE, Y., KUSANAGI, H., KAMEI, Y. & MISHIMA, K. 2017. Evaluation of circadian phenotypes utilizing fibroblasts from patients with circadian rhythm sleep disorders. *Translational Psychiatry,* 7**,** e1106.

INDER, M. L., CROWE, M. T. & PORTER, R. 2016. Effect of transmeridian travel and jetlag on mood disorders: Evidence and implications. *Australian and New Zealand Journal of Psychiatry,* 50**,** 220-227.

JOHANSSON, A. S., BRASK, J., OWE-LARSSON, B., HETTA, J. & LUNDKVIST, G. B. S. 2011. Valproic Acid Phase Shifts the Rhythmic Expression of PERIOD2::LUCIFERASE. *Journal of Biological Rhythms,* 26**,** 541-551.

JONES, S. H., HARE, D. J. & EVERSHED, K. 2005. Actigraphic assessment of circadian activity and sleep patterns in bipolar disorder. *Bipolar Disorders,* 7**,** 176-186.

KING, D. P., ZHAO, Y. L., SANGORAM, A. M., WILSBACHER, L. D., TANAKA, M., ANTOCH, M. P., STEEVES, T. D. L., VITATERNA, M. H., KORNHAUSER, J. M., LOWREY, P. L., TUREK, F. W. & TAKAHASHI, J. S. 1997. Positional cloning of the mouse circadian Clock gene. *Cell,* 89**,** 641-653.

LI, J., LU, W.-Q., BEESLEY, S., LOUDON, A. S. I. & MENG, Q.-J. 2012. Lithium Impacts on the Amplitude and Period of the Molecular Circadian Clockwork. *Plos One,* 7**,** e33292.

LOWREY, P. L., SHIMOMURA, K., ANTOCH, M. P., YAMAZAKI, S., ZEMENIDES, P. D., RALPH, M. R., MENAKER, M. & TAKAHASHI, J. S. 2000. Positional syntenic cloning and functional characterization of the mammalian circadian mutation tau. *Science,* 288**,** 483-491.

MCCARTHY, M. J., WEI, H., MARNOY, Z., DARVISH, R. M., MCPHIE, D. L., COHEN, B. M. & WELSH, D. K. 2013. Genetic and clinical factors predict lithium's effects on PER2 gene expression rhythms in cells from bipolar disorder patients. *Translational Psychiatry,* 3**,** e318.

MYERS, E., STARTUP, H. & FREEMAN, D. 2011. Cognitive behavioural treatment of insomnia in individuals with persistent persecutory delusions: A pilot trial. *Journal of Behavior Therapy and Experimental Psychiatry,* 42**,** 330-336.

NAGOSHI, E., SAINI, C., BAUER, C., LAROCHE, T., NAEF, F. & SCHIBLER, U. 2004. Circadian gene expression in individual fibroblasts: Cell-autonomous and self-sustained oscillators pass time to daughter cells. *Cell,* 119**,** 693-705.

NOMURA, K., CASTANON-CERVANTES, O., DAVIDSON, A. & FUKUHARA, C. 2008. Selective serotonin reuptake inhibitors and raft inhibitors shorten the period of Period1-driven circadian bioluminescence rhythms in rat-1 fibroblasts. *Life Sciences,* 82**,** 1169-1174.

PAGANI, L., SEMENOVA, E. A., MORIGGI, E., REVELL, V. L., HACK, L. M., LOCKLEY, S. W., ARENDT, J., SKENE, D. J., MEIER, F., IZAKOVIC, J., WIRZ-JUSTICE, A., CAJOCHEN, C., SERGEEVA, O. J., CHERESIZ, S. V., DANILENKO, K. V., ECKERT, A. & BROWN, S. A. 2010. The Physiological Period Length of the Human Circadian Clock In Vivo Is Directly Proportional to Period in Human Fibroblasts. *Plos One,* 5**,** e13376.

ROCK, P., GOODWIN, G., HARMER, C. & WULFF, K. 2014. Daily rest-activity patterns in the bipolar phenotype: A controlled actigraphy study. *Chronobiology International,* 31**,** 290-296.

ROENNEBERG, T., WIRZ-JUSTICE, A. & MERROW, M. 2003. Life between clocks: Daily temporal patterns of human chronotypes. *Journal of Biological Rhythms,* 18**,** 80-90.

SACK, R. L., LEWY, A. J., BLOOD, M. L., KEITH, L. D. & NAKAGAWA, H. 1992. Circadian-rhythm abnormalities in totally blind people - incidence and clinical-significance. *Journal of Clinical Endocrinology & Metabolism,* 75**,** 127-134.

SANDU, C., DUMAS, M., MALAN, A., SAMBAKHE, D., MARTEAU, C., NIZARD, C., SCHNEBERT, S., PERRIER, E., CHALLET, E., PEVET, P. & FELDER-SCHMITTBUHL, M. P. 2012. Human skin keratinocytes, melanocytes, and fibroblasts contain distinct circadian clock machineries. *Cellular and Molecular Life Sciences,* 69**,** 3329-3339.

SCHNEIDER, E. L. & MITSUI, Y. 1976. Relationship between in vitro cellular aging and in vivo human age. *Proceedings of the National Academy of Sciences of the United States of America,* 73**,** 3584-3588.

TRACY, L. E., MINASIAN, R. A. & CATERSON, E. J. 2016. Extracellular Matrix and Dermal Fibroblast Function in the Healing Wound. *Advances in Wound Care,* 5**,** 119-136.

VITATERNA, M. H., KO, C. H., CHANG, A. M., BUHR, E. D., FRUECHTE, E. M., SCHOOK, A., ANTOCH, M. P., TUREK, F. W. & TAKAHASHI, J. S. 2006. The mouse Clock mutation reduces circadian pacemaker amplitude and enhances efficacy of resetting stimuli and phase-response curve amplitude. *Proceedings of the National Academy of Sciences of the United States of America,* 103**,** 9327-9332.

WEAVER, D. R. 1998. The suprachiasmatic nucleus: A 25-year retrospective. *Journal of Biological Rhythms,* 13**,** 100-112.

WELSH, D. K., TAKAHASHI, J. S. & KAY, S. A. 2010. Suprachiasmatic Nucleus: Cell Autonomy and Network Properties. *Annual Review of Physiology,* 72**,** 551-577.

WOOD, J., BIRMAHER, B., AXELSON, D., EHMANN, M., KALAS, C., MONK, K., TURKIN, S., KUPFER, D. J., BRENT, D., MONK, T. H. & NIMGAINKAR, V. L. 2009. Replicable differences in preferred circadian phase between bipolar disorder patients and control individuals. *Psychiatry Research,* 166**,** 201-209.

WORLD HEALTH ORGANISATION 2014. *ICD-10 classification of mental and behavioural disorders: clinical descriptions and diagnostic guidelines; 10th Revision,* Geneva.

YAGITA, K., TAMANINI, F., VAN DER HORST, G. T. J. & OKAMURA, H. 2001. Molecular mechanisms of the biological clock in cultured fibroblasts. *Science,* 292**,** 278-281.

YANG, S., VAN DONGEN, H. P. A., WANG, K., BERRETTINI, W. & BUCAN, M. 2009. Assessment of circadian function in fibroblasts of patients with bipolar disorder. *Molecular Psychiatry,* 14**,** 143-155.

YOO, S. H., YAMAZAKI, S., LOWREY, P. L., SHIMOMURA, K., KO, C. H., BUHR, E. D., SIEPKA, S. M., HONG, H. K., OH, W. J., YOO, O. J., MENAKER, M. & TAKAHASHI, J. S. 2004. PERIOD2 :: LUCIFERASE real-time reporting of circadian dynamics reveals persistent circadian oscillations in mouse peripheral tissues. *Proceedings of the National Academy of Sciences of the United States of America,* 101**,** 5339-5346.

ZHU, F. F., GAMBOA, M., FARRUGGIO, A. P., HIPPENMEYER, S., TASIC, B., SCHULE, B., CHEN-TSAI, Y. & CALOS, M. P. 2014. DICE, an efficient system for iterative genomic editing in human pluripotent stem cells. *Nucleic Acids Research,* 42**,** e34.

Chapter 4: Pharmacological Modulation of Circadian Rhythms May Influence Mood-Related Behaviours

4.1 Introduction

The SCN plays an essential role in controlling circadian rhythmicity but as we (Chapter 3) and others have shown, it is not unique in its capacity to display 24h rhythms (Yoo et al., 2004, Brown et al., 2005). Fibroblasts, like many cells in the body contain the molecular clockwork composed of TTFLs which are essential for driving physiology, affect, and behaviour (summarised in Chapter 1, *Figure 1.2*) (Takahashi, 2017). The universal synchronicity of these individual clocks is vital for maintaining health and ensuring survival, therefore it is understandable that disturbances to these rhythms may have significant physiological consequences (Preussner and Heyd, 2016).

4.1.1 Sleep and circadian rhythm disruption in bipolar disorder

The transient effects of malaise, fatigue, and irritability after travelling across multiple time zones are due to the misalignment between the external environments and our internal timekeepers. Following jet lag, the presence of a functional circadian clock will ensure full re-entrainment, requiring ~1 day for every time zone crossed (Davidson et al., 2009). However, in individuals where the circadian clock is dysfunctional, there is an additional level of complexity and severity observed. A study assessing psychiatric hospital admissions in foreign tourists prone to mental illness found that the more time zones crossed the greater the chance of the patients relapsing, emphasising the importance of a functional clock in maintaining mood stability (Katz et al., 2002).

There is now a wealth of evidence highlighting the contributions of circadian dysfunction in neuropsychiatric pathophysiology including major

depression, seasonal affective disorder, schizophrenia, and BPD (Jagannath et al., 2013). Whilst the underlying neurobiology of BPD is multifaceted and complex, sleep and circadian rhythm disruptions are so prominent that they are included in the diagnostic criteria of the DSM-V and ICD-10 (American Psychiatric Association, 2013, World Health Organisation, 2014). On a mechanistic level, through the analysis of BPD patient-derived fibroblast rhythms, we and others have shown that patients present gross disturbances in their molecular clock genes, including low amplitude rhythms, period lengthening, and variability (Yang et al., 2009, McCarthy et al., 2013). Furthermore, animal models with mutations in the core clock or accessory clock genes (*ClockΔ19* and *Afh* mutants) have proven to be effective models of mania-like behaviour and display the aforementioned changes to their behavioural and molecular circadian rhythms (Roybal et al., 2007, Vitaterna et al., 2006, Keers et al., 2012, Godinho et al., 2007). Such data suggests that patients and the animal models of mania-like behaviour may be more susceptible to perturbations by external influences relative to their healthy or control counterparts. Photic information is regarded as the dominant *zeitgeber*, where transmeridian travel has been shown to precipitate mania or depression depending on the direction of travel in susceptible individuals (Inder et al., 2016). Moreover, both the *ClockΔ19* and *Afh* mutants display abnormal phase shifting in response to a light pulse, shifting 3-9h more than their control counterparts (Vitaterna et al., 2006, Guilding et al., 2013). Therefore, although there is uncertainty regarding whether circadian disruptions are a cause or consequence of the condition, internal desynchrony appears to be strongly implicated in BPD pathophysiology and could therefore require chronobiotic pharmacological interventions.

4.1.2 Pharmacologically targeting circadian genes

BPD affects 1-2% of the population, yet investment by pharmaceutical companies towards the development of mechanistically novel therapeutics is declining, potentially due to the lack of suitable targets (Merikangas et al., 2011, Fibiger, 2012). Based on our understanding of circadian abnormalities in BPD, an appealing novel route to normalising mood instability may be to target the circadian genes. By targeting these genes we could potentially rectify the cycling of 43% of the protein coding transcriptome, highlighting the pleiotropic benefits of chronomodulatory pharmaceuticals, and there is accumulating evidence to support this theory (Zhang et al., 2014).

Firstly, stabilising sleep in patients with psychotic symptoms has proven to be effective at normalising their persecutory delusions, which suggests that sleep alone could improve mental well-being (Myers et al., 2011). Indeed, imposing a 10:14h LD schedule in medicated BPD patients was effective at rapidly reducing symptoms of mania by 50% in 3 days when the mood episode was shorter than 2 weeks. Further, dark therapy was associated with reductions in haloperidol dosage by 31% and the early release of patients from hospitals by 9 days (Barbini et al., 2005). This signifies the importance of investigating the effects of circadian rhythm manipulation on mood, as imposing regular sleep schedules are not associated with typical drug-induced side effects, and may also help combat covert non-compliance.

The mechanistically novel compound agomelatine, is a chronotherapeutic that functions synergistically as a selective melatonergic agonist, thereby promoting sleep, and a 5-HT2C antagonist which stimulates downstream

dopamine signalling (Racagni et al., 2011). It was found to be successful at normalising a spectrum of depressive symptoms including anxiety in 50% of patients. It appeared efficacious at 25mg, though some initial non-responders were successfully treated with 50mg with side effect profiles matching placebo controls (Loo et al., 2002, Kennedy and Emsley, 2006). Agomelatine not only reduced feeling of low mood, but also improved sleep quality, as early and mid-night insomnia were significantly reduced, with patterns of reduced late night insomnia emerging (Olie and Kasper, 2007). Whilst melatonin is an output of the molecular clock, this suggests that targeting the clock itself may help reduce abnormal fluctuations in mood as a new therapeutic avenue.

Indeed, 56 out of 100 top selling medicines within the USA targeted genes with circadian expression profiles. This included the atypical antipsychotic agents aripiprazole ranked number 1 and quetiapine ranked number 44, both of which are used to manage BPD. Both targeted neurotransmitter systems regulating mood including the 5-HT1B, 2A, and 2C serotonin receptors, the muscarinic acetylcholine receptor M2, the dopamine D4 receptor, and the α- 1A, 1B, and 2B adrenoreceptors (Zhang et al., 2014). Therefore, targeting these oscillatory genes encoding neurotransmitter receptors can impact multiple aspects of mood and general physiology, as each receptor can trigger down stream signalling cascades. Thus, there is a solid foundation to explore whether drugs that modulate circadian rhythms can impact mood-related behaviours.

4.1.3 Lithium

Lithium is the mainstay pharmacotherapy for BPD, and is a *bona fide* mood-stabilising agent, preventing relapse in 60% of patients (Geddes et al.,

2004). Lithium is also an established chronomodulator that increases the amplitude and lengthens the period of behavioural and molecular rhythms (Li et al., 2012). Recent studies assessing rhythmicity in *Per2::Luc* transduced fibroblasts found that 1mM lithium significantly increased amplitude by 36% in cells from control patients, with a non-significant 12% increase in cells from BPD patients (McCarthy et al., 2013). The authors also found that 10mM lithium induced period lengthening by 1h in healthy human fibroblasts and by 30min in patient cells, where no effect was observed at 1mM concentrations (McCarthy et al., 2013). Whilst McCarthy and colleagues did not analyse the prospects of lithium sensitivity, this could account for the period differences observed between patients and controls. Indeed, differences in clock gene expression are becoming apparent between these two sub-groups. Following 2 days of lithium treatment, lithium sensitive patient-derived lymphoblasts displayed greater increases in *RORα*, *BMAL1, PER1*, *CRY2*, *DEC1/2,* and *CSNK1δ* (Geoffroy et al., 2017). Based on the idea that treatment responsive patients may display greater changes to circadian parameters, this could mean that lithium sensitivity is partly associated with a circadian system that is more responsive to therapeutic interventions.

4.1.4 Nobiletin and CGS-15943

Using the results from an in-house repurposed drug screen, 2 chronomodulatory compounds of interest emerged and were further explored: nobiletin and CGS-15943. Nobiletin is a polymethoxylated flavone that is present in citrus peels. This natural flavonoid has been shown to have multiple potential health benefiting properties including: anticancer, antiviral, anti-inflammatory,

antioxidation, anti-insulin resistance, anti-osteoclastogenesis, cardioprotection, and neuroprotection (Huang et al., 2016). CGS-15943 on the other hand is a potent non-specific adenosine receptor antagonist. Whilst the A_1 and A_3 receptors are G_i coupled and inhibit downstream signalling, the A_{2A} and A_{2B} receptors are G_s coupled, therefore receptor distribution would be paramount in dictating the action of this compound (Fredholm et al., 2000). Thus, these structurally distinct molecules were of interest in exploring whether pharmacological modulation of circadian rhythms impacts rodent behaviours.

4.1.5 Aims

Whilst it is recognised that sleep and circadian rhythm disruptions are intimately involved with the pathophysiology of BPD, the theory of chronomodulation as a means of a therapy remains untested. Therefore, a hypothesis worth exploring is that targeting circadian disruptions with pharmacological compounds could alleviate psychiatric behavioural abnormalities. Instead of boosting the circadian profiles of individual genes with oscillatory transcripts, we should assess the effects of targeting the source of these oscillations, the molecular clock itself. This could impact hundreds to thousands of genes and may normalise behavioural abnormalities. This was a hypothesis we explored using various chronomodulators with lithium as a comparator. Use of such compounds on our patient-derived cell lines could also help address a 3R's issue and validate whether this model could replace the use of animals at the initial stages of the drug discovery process by acting as an alternative means for high throughput screening.

4.2 Results

A total of 8 control subject-derived fibroblasts and 16 BPD patient-derived fibroblasts were used in this study, which strived to understand whether fibroblasts could accurately model drug-induced changes to circadian rhythmicity observed *in viv*o. BPD fibroblasts were selected from the predefined categories of short (23.49h or less), medium (23.50-24.99h), or long (25.00h or more) as outlined in Chapter 3.2.5.

4.2.1 Lithium alters circadian rhythmicity in vitro

Prior to assessing the effects of novel compounds on circadian rhythmicity, we sought to follow on from previous studies and gain a deeper understanding into the *in vitro* effects of the well documented chronomodulator and mood-stabilising agent LiCl. To determine such changes, cells were treated with 1-30mM concentrations of LiCl and alterations to period and amplitude were analysed. As seen in *Figure 4.1A*, overall LiCl induced period lengthening in both control and patient cells, where significance was determined by comparing effects to vehicle treatment. After treatment with 20mM LiCl, control cells displayed period lengthening by 2.7h, where patient cells displayed lengthening by 1.9h. This may be because whilst the period induced by 20mM LiCl remained constant at 26.3-26.6h, thereby establishing an upper ceiling, the patient cells displayed trends for a longer baseline period pre-treatment by 33min. Similarly, 30mM LiCl induced period lengthening by 2.9h and 3h in controls and patient cells respectively (control→ vehicle: 23.83±0.21, 20mM: 26.55±0.54, 30mM:

26.77±0.50; bipolar→ vehicle: 24.38±0.42, 20mM: 26.32±0.28, 30mM: 27.36±0.33 h).

Due to the real-time nature of these experiments, we further assessed the consequences of LiCl on circadian amplitude (*Figure 4.1B*). Much like period lengthening, significant amplitude enhancement was also observed at 20mM and 30mM concentrations. Interestingly, the trends observed suggest the presence of greater amplitude changes in our BPD patient cells. This was because, whilst 20mM LiCl increased amplitude by 1.52±0.14 fold in control cells, there was a 1.85±0.15 fold increase observed with patient cells. Similarly, 30mM LiCl increased amplitude by 2.10±0.19 fold in control cells and by 2.49±0.21 fold in BPD cells.

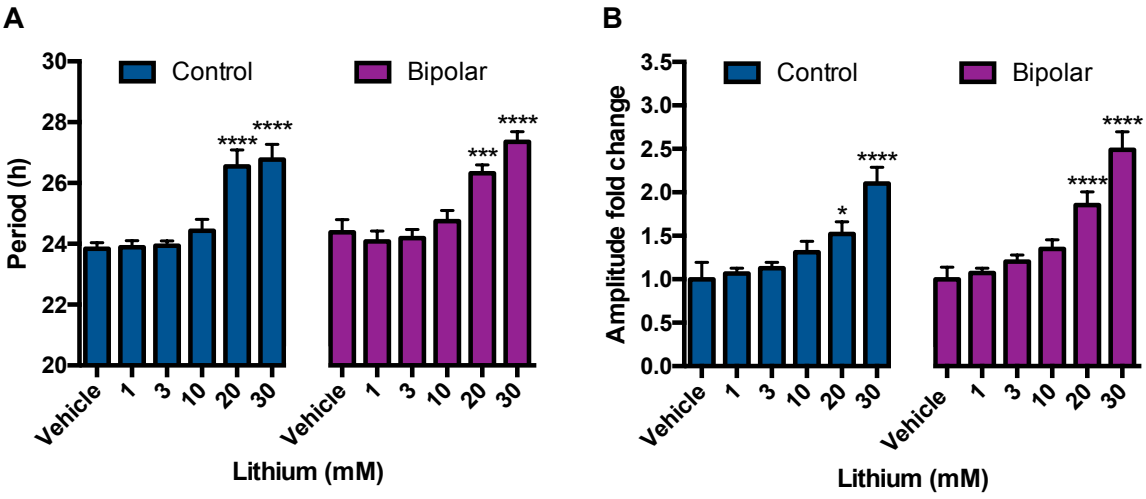

Figure 4.1. **LiCl induces period lengthening and amplitude increases in bipolar patient cell lines.** The period **(A)** and amplitude **(B)** effects induced by 1-30mM LiCl in control (n=8) and BPD patient (n=16) fibroblasts.

4.2.2 Lithium does not lengthen period in patients with longer period lengths

As patients could be divided into categories based on basal period length, we decided to perform exploratory data analysis to assess whether these characteristics could influence drug-induced responses to circadian rhythmicity. When analysing the effects of LiCl on circadian period, interesting and significant discrepancies emerged. As outlined in *Figures 4.2A-B*, patients within the short category displayed significant period lengthening at 20 and 30mM concentrations by 3.3h and 5h respectively (vehicle: 22.70±0.36, 20mM: 26.00±0.43, 30mM: 27.74±0.49 h). Similarly, patients with medium period lengths displayed 2.4h and 3.4h period lengthening after 20mM and 30mM LiCl treatment respectively (vehicle: 24.21±0.19, 20mM: 26.65±0.45, 30mM: 27.56±0.71 h). On the other hand, patients within the long category displayed more subtle and non-significant patterns of lengthening, increasing period by 1h at 30mM concentrations (vehicle: 25.76±0.24, 30mM: 26.73±0.41 h). To illustrate, the raw luminescence traces and diagrams following baseline subtraction and smoothing are displayed for exemplar fibroblast lines from the control, short, medium, and long groups (*Figures 4.2C-J*). Thus, LiCl appears to preferentially induce period lengthening in fibroblasts with period lengths of 24.99h or under.

4.2.3 Lithium increases amplitude in bipolar patient fibroblasts

Next, we assessed whether differences in period phenotype also resulted in differences in amplitude induction following LiCl treatment. As seen in *Figures 4.3A-B*, patients within the short category displayed trends for amplitude increases at 20mM by 2.03±0.35 fold, where 30mM LiCl significantly increased amplitude by 2.76±0.49 fold. Similarly, significant amplitude induction was observed from fibroblasts within the medium category such that 20mM and 30mM LiCl induced amplitude by 1.77±0.16 fold and 2.24±0.29 fold respectively. Fibroblasts from patients within the long group also followed these trends. Whilst 20mM LiCl presented trends for amplitude induction by 1.78±0.32 fold, 30mM LiCl significantly increased amplitude by 2.52±0.33 fold.

Individual exemplar traces highlight these observations (shown in *Figure 4.2*). In the representative control cell line, trends for amplitude enhancement appeared from 10mM, where 30mM LiCl led to a 3.19±0.07 fold increase (*Figure 4.3C*). Within the short, medium, and long categories, amplitude enhancement was observed at 10, 20, and 30mM concentrations, where maximal increases were by 4.13±0.16 fold, 2.87±0.12 fold, and 3.70±0.29 fold respectively (*Figures 4.3D-F*). Therefore, 30mM LiCl was able to increase amplitude to a similar degree in our fibroblast lines.

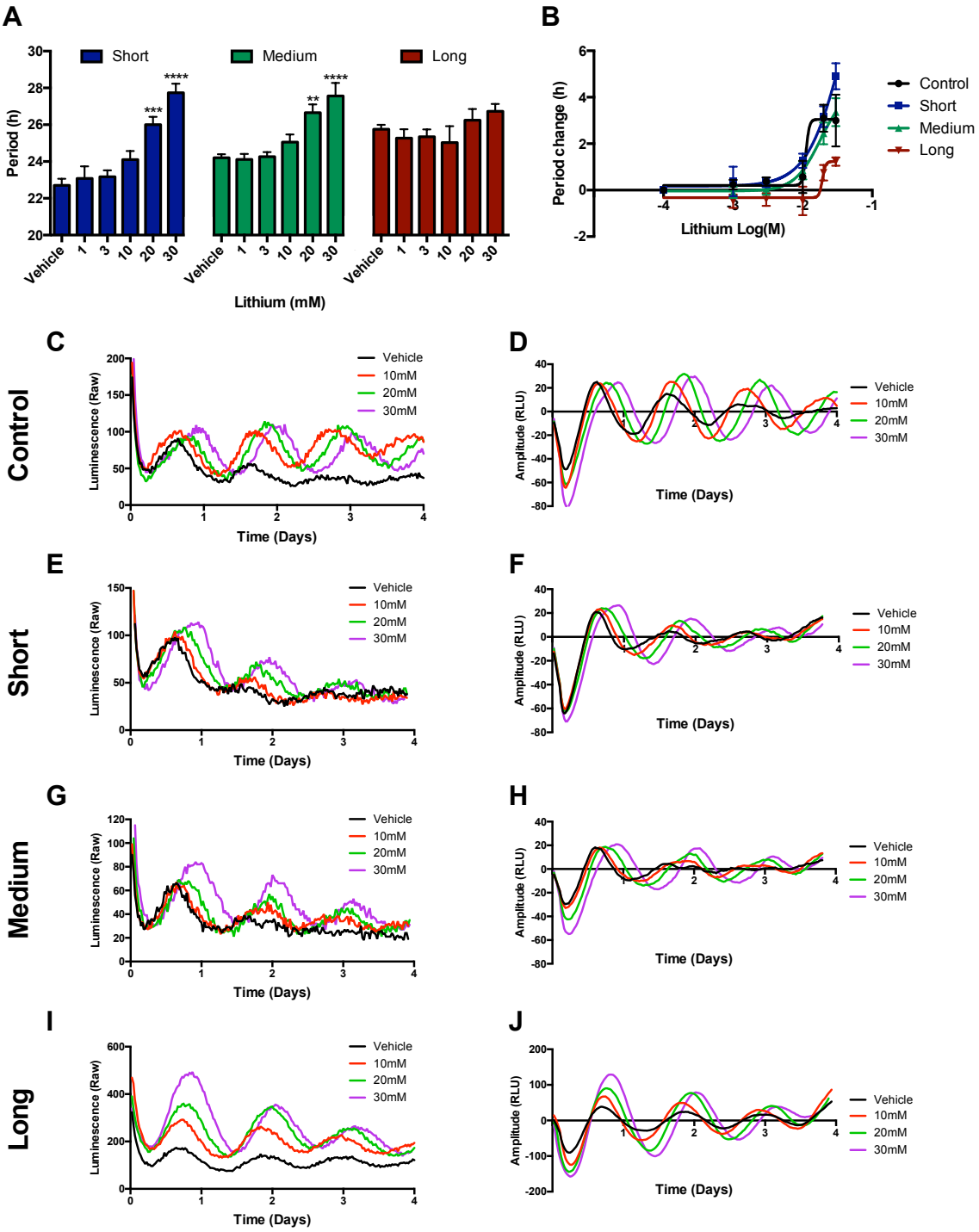

Figure 4.2. **LiCl preferentially lengthens period in control subjects or bipolar patients with short or medium period lengths. A-B)** The period changes induced by LiCl in fibroblasts derived from patients with short (n=5), medium (n=6), or long (n=5) period lengths. Raw luminescence diagrams and normalised traces for example cell lines within the control subjects **(C-D)**, as well as short **(E-F)**, medium **(G-H)**, and long **(I-J)** phenotyped BPD patients.

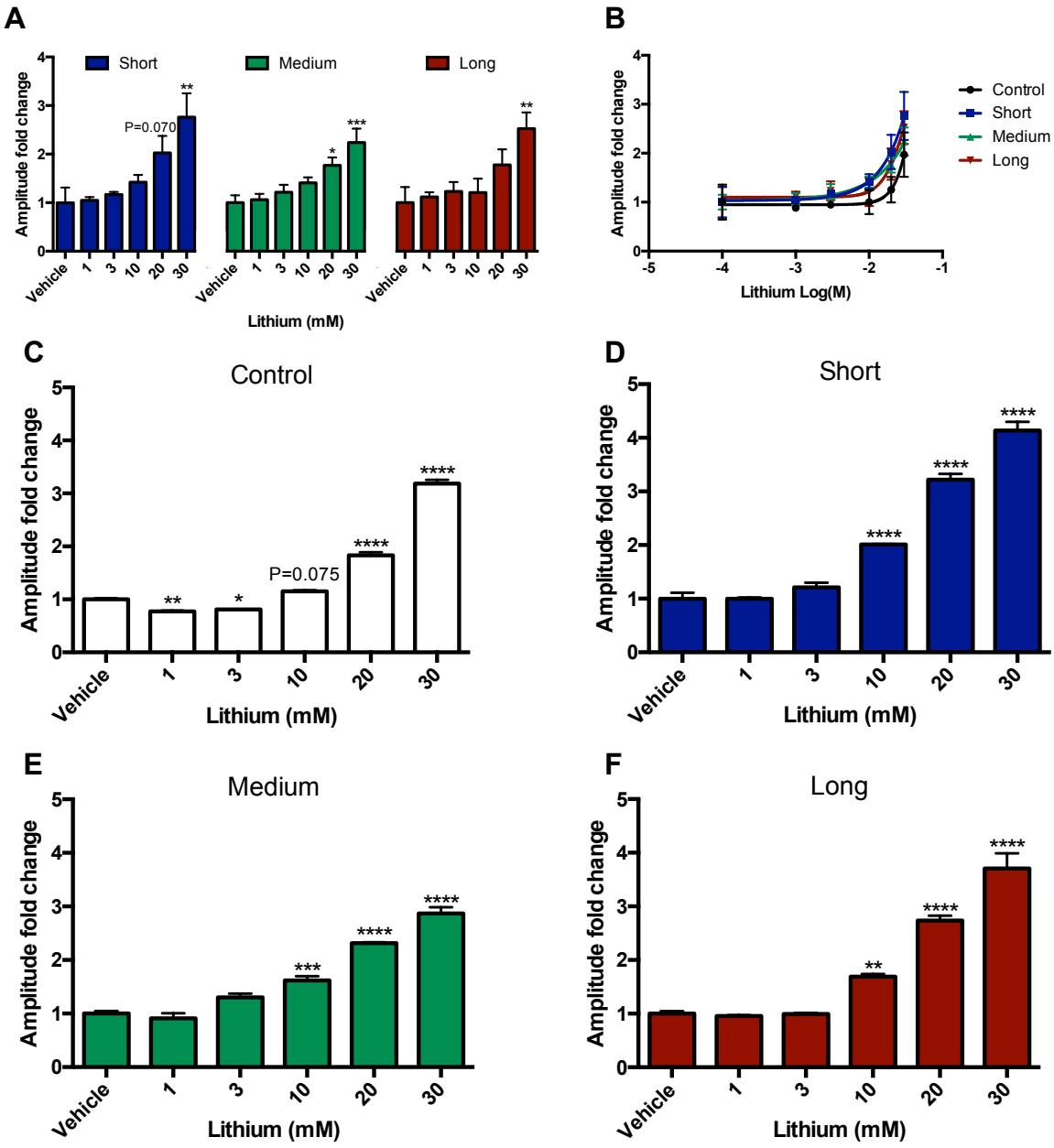

Figure 4.3. **LiCl increases amplitude in all patient-derived cell lines. A-B)** The amplitude changes induced by LiCl in fibroblasts derived from patients within the short (n=5), medium (n=6), or long (n=5) groupings. Examples of amplitude changes induced by LiCl in control (n=3) **(C),** as well as short (n=3) **(D)**, medium (n=3) **(E)**, and long (n=3) **(F)** categorised BPD patients. Accompanying bioluminescence traces can be found in *Figure 4.2*.

4.2.4 Fibroblasts' lithium response fail to discriminate between lithium-treated and non-treated patients

As lithium induced greater period lengthening in patient-derived fibroblasts belonging to the short and medium categories, we decided to investigate whether this could account for lithium sensitivity, a phenotype we associated with patients treated with lithium. To our surprise, overall LiCl failed to discriminate between the Li-T and Li-NT patients. As seen in *Figure 4.4A*, both Li-T and Li-NT patients displayed similar trends in period change after LiCl treatment, as 20mM lengthened period by 1.91±0.41h and 2.53±0.63h, and 30mM by 3.18±0.60h and 3.17±0.80h respectively. Similarly, Li-T patients displayed significant amplitude enhancement with 20mM and 30mM LiCl by 1.94±0.22 fold and 2.50±0.28 fold respectively, as highlighted in *Figure 4.4B*. The Li-NT patients also presented similar effects following LiCl treatment, as a 1.71±0.19 fold and 2.48±0.33 fold induction with 20mM and 30mM concentrations was observed. Interestingly, inspection of the lower concentrations of LiCl revealed that 10mM concentrations presented trends such that the Li-T patients displayed 22% greater amplitude enhancement relative to the Li-NT subgroup. The responses to LiCl treatment within the Li-T and Li-NT groups are further underlined in *Figures 4.4C-E*, which display the example bioluminescence traces from patient cell lines.

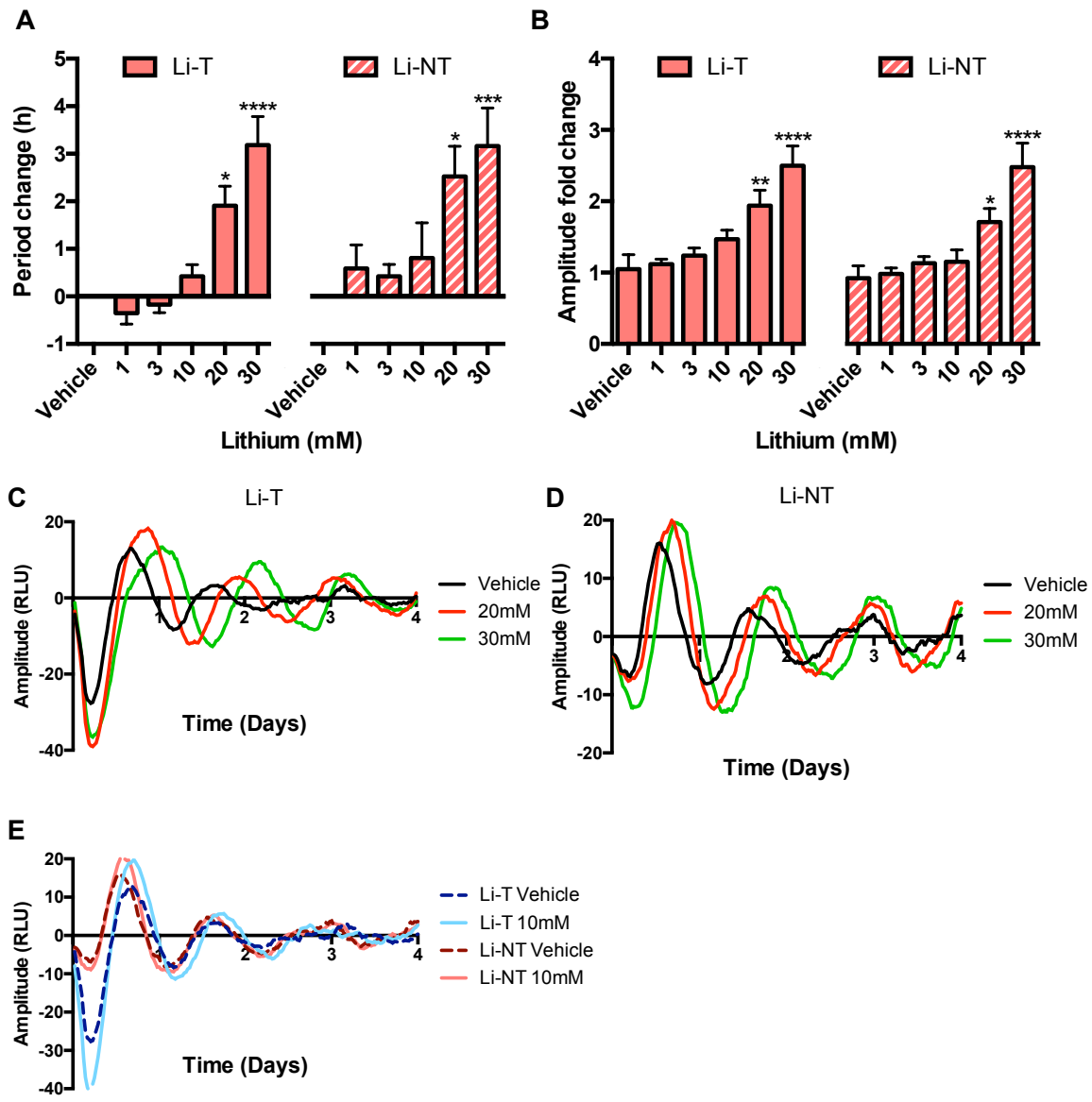

Figure 4.4. **Patient fibroblasts cannot discriminate between Li-T and Li-NT patients following treatment with LiCl. A)** The period changes induced after treatment with 1-30mM LiCl in fibroblasts from Li-T (n=10) and Li-NT patients (n=6). **B)** The resulting amplitude changes following treatment with 1-30mM LiCl in Li-T (n=10) and Li-NT patients (n=6). Representative traces highlighting drug-induced changes to circadian parameters following LiCl treatment in Li-T **(C)** and Li-NT **(D)** patients. **E)** Example traces displaying differences in amplitude enhancement following 10mM LiCl treatment in the Li-T and Li-NT fibroblasts.

4.2.5 Nobiletin alters circadian rhythmicity in vitro

To further validate our BPD cellular model and assess the hypothesis that drugs which regulate circadian rhythms may impact mood, we tested the effects of nobiletin on our patient-derived fibroblasts. As seen in *Figure 4.5A*, nobiletin appeared to have no effect on circadian period in overall patient cell lines. Interestingly, in line with previous findings, nobiletin induced greater changes to circadian amplitude (*Figure 4.5B*) (He et al., 2016). The cells from BPD patients presented stronger indications of amplitude enhancement as trends were identified with lower concentrations of 3μM by 1.52±0.09 fold. Indeed, 10, 20, and 30μM nobiletin significantly induced amplitude by 1.98±0.16 fold, 2.34±0.20 fold, and 2.50±0.22 fold respectively.

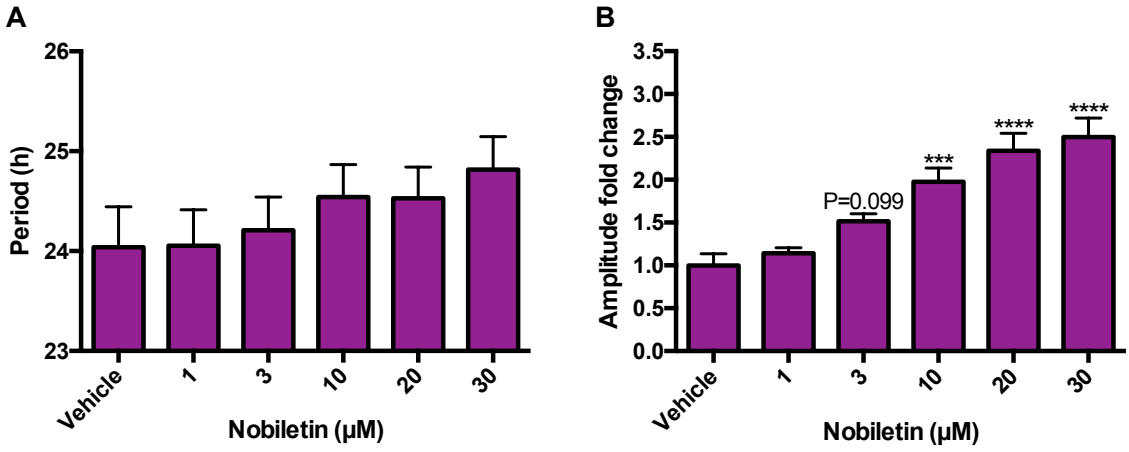

Figure 4.5. **Nobiletin induces amplitude increases in bipolar patient cell lines.** The period **(A)** and amplitude **(B)** effects induced by 1-30μM nobiletin in BPD patient cells (n=16).

4.2.6 Nobiletin lengthens period in patients with shorter period lengths

Due to the differences in period which emerged following LiCl treatment in short, medium, or long phenotyped cells, we decided to explore whether variations would also occur with alternative compounds. Nobiletin, a drug which has previously been shown to exhibit chronomodulatory effects, preferentially lengthened period of fibroblasts in the short phenotyped class (*Figures 4.6A-B*). In the short fibroblasts, trends for lengthening were observed by 1.1h at 10 and 20μM nobiletin, where 30μM significantly lengthened period by 1.5h (vehicle: 22.39±0.16, 10μM: 23.49±0.41, 20μM: 23.47±0.37, 30μM: 23.90±0.36 h). The bioluminescence traces from individual cell lines within these categories highlight these observations (*Figures 4.6C-H*). Thus, nobiletin appeared to preferentially induce period lengthening in fibroblasts with period lengths of ~23.49h or under.

4.2.7 Nobiletin increases amplitude in bipolar patient fibroblasts

Thereafter, we assessed whether categorising patients by period phenotype revealed any amplitude specific affects following nobiletin treatment. As highlighted in *Figures 4.7A-B*, cells within all categories presented patterns for amplitude enhancement. Specifically, fibroblasts within the short grouping displayed significant enhancement in amplitude at 10, 20, and 30μM concentration by 2.09±0.21 fold, 2.49±0.36 fold, and 2.70±0.43 fold respectively. Similar amplitude induction was also observed from fibroblasts within the medium group, as 10, 20, and 30μM nobiletin increased amplitude by 2.01±0.18 fold, 2.50±0.29 fold, and 2.64±0.29 fold respectively. Whilst the pattern observed suggested that nobiletin also increased amplitude within the long category, no

significant differences were found. Nonetheless, 30μM nobiletin showed trends for amplitude induction by 2.12±0.48 fold.

Representative cell lines from these defined categories further highlight these patterns, where the accompanying luminescence diagrams can be found in *Figure 4.6*. Cells from the short and medium categories presented very similar patterns, showing signs of amplitude enhancement from 3-30μM concentrations, where maximal amplitude increases were by 2.96±0.30 fold and 3.04±0.15 fold respectively (*Figures 4.7C-D*). Indeed, more subtle amplitude effects were observed from cells within the long category. In the example cell line displayed, nobiletin induced amplitude enhancement at all concentrations tested but to a lesser degree. Higher concentrations of 30μM nobiletin resulted in amplitude induction by 2.40±0.08 fold (*Figure 4.7E*). Therefore, nobiletin increased amplitude in the majority of our subject-derived fibroblasts.

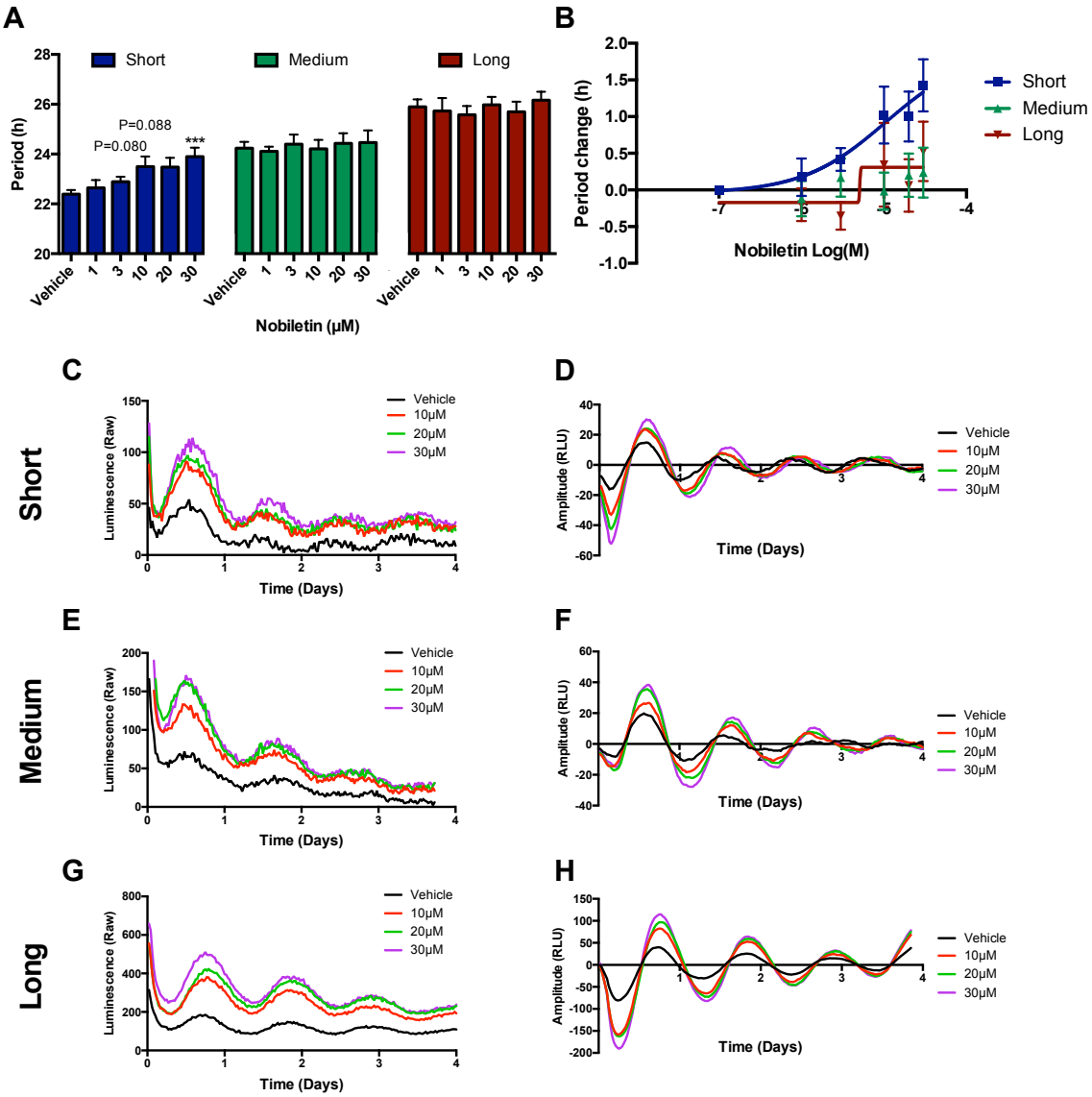

Figure 4.6. **Nobiletin preferentially lengthens period in bipolar patients with short period lengths. A-B)** The period changes induced by nobiletin in cells from patients with short (n=5), medium (n=6), or long (n=5) period lengths. Raw luminescence diagrams and normalised traces for example fibroblast lines within the short **(C-D)**, medium **(E-F)**, and long **(G-H)** phenotyped BPD patients.

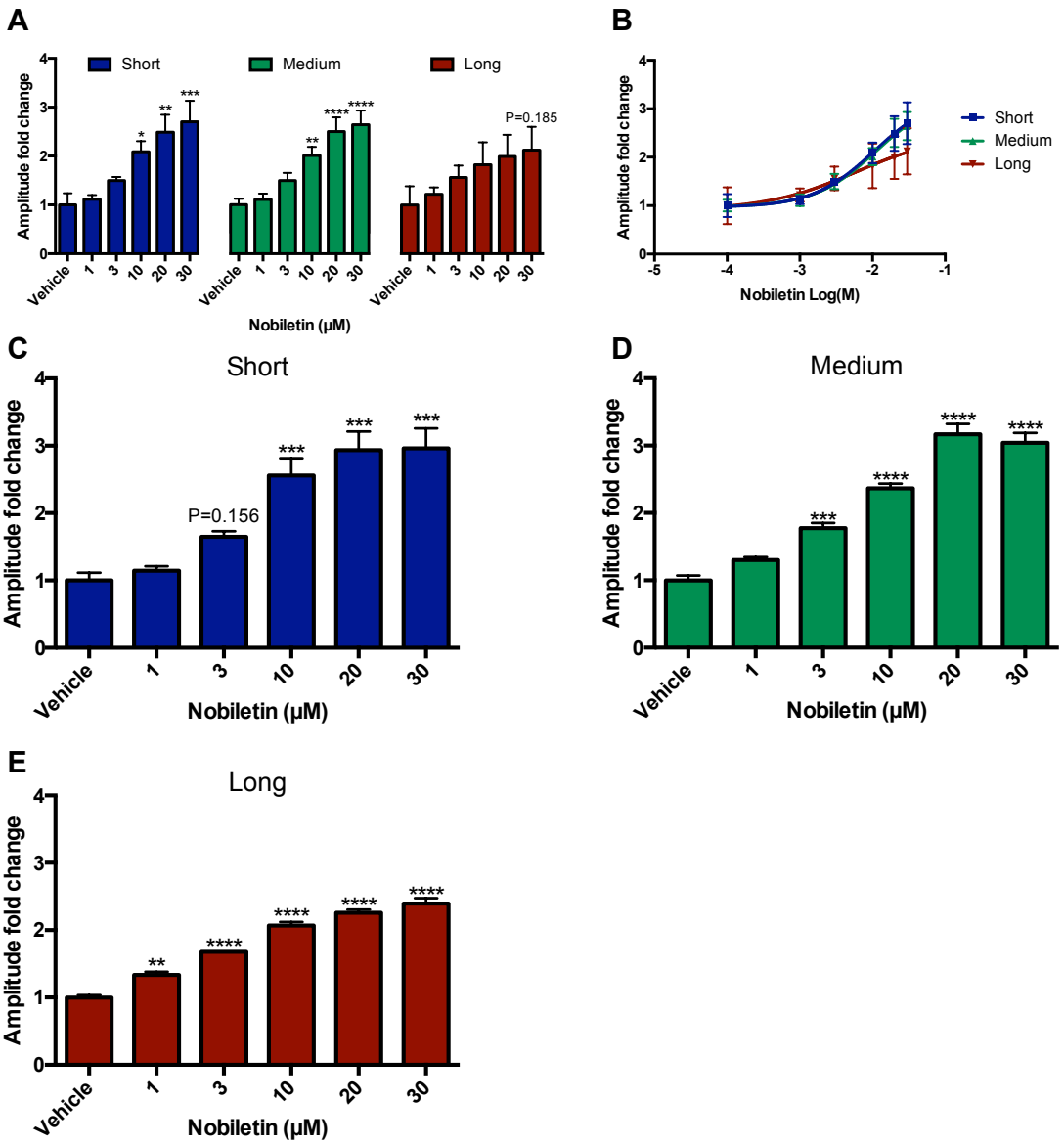

Figure 4.7. **Nobiletin increases amplitude in patient-derived cell lines. A-B)** The amplitude changes induced by nobiletin in fibroblasts derived from patients within the short (n=5), medium (n=6), or long (n=5) groupings. Examples of amplitude changes induced by nobiletin in short (n=3) **(C)**, medium (n=3) **(D),** and long (n=3) **(E)** categorised BPD patients. Accompanying bioluminescence traces can be found in *Figure 4.6*.

4.2.8 CGS-15943 altered circadian rhythmicity in vitro

We then sought to characterise the effects of CGS-15943 on patient cellular circadian parameters. CGS-15943 is a drug which has also been shown to possess chronomodulatory actions but is structurally distinct from nobiletin. As displayed in *Figure 4.8*, CGS-15943 had the most prominent overall period and amplitude effects when compared to LiCl and nobiletin. When applied to the patient fibroblasts significant lengthening was observed at all concentrations tested. Treatment with 1 and 3μM CGS-15943 lengthened period by 3.3h and 5h respectively, where 10, 20, and 30μM concentrations lengthened period by 8.7h, 10.5h, and 11.3h respectively (vehicle: 23.98±0.37, 1μM: 27.24±0.45, 3μM: 29.02±0.43, 10μM: 32.70±0.79, 20μM: 34.46±0.95, 30μM: 35.28±1.21 h) (*Figure 4.8A*). This suggests that 30μM CGS-15943 treatment should induce anti-phasic rhythmic activity relative to vehicle treatment. Moreover, enhancement of circadian amplitude was also observed, where 3μM CGS-15943 augmented amplitude by 2.11±0.17 fold, and 10, 20, and 30μM CGS-15943 concentrations by 2.72±0.26-2.96±0.28 fold (*Figure 4.8B*).

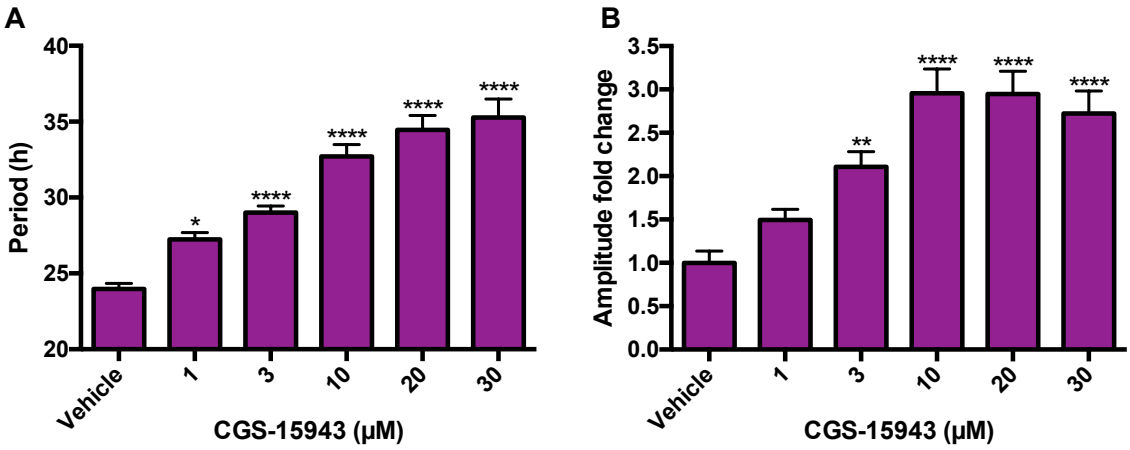

***Figure 4.8.* CGS-15943 lengthens period and increases amplitude in bipolar patient cell lines.** The period **(A)** and amplitude **(B)** effects induced by 1-30μM CGS-15943 in BPD patient fibroblasts (n=16).

4.2.9 CGS-15943 lengthens period independently of phenotypic period length

When assessing whether any differences emerged regarding the ability of CGS-15943 to induce period lengthening based on fibroblast period length, unlike LiCl and nobiletin, CGS-15943 induced lengthening uniformly across all cell lines. Firstly, as seen in *Figures 4.9A-B,* within the short category, fibroblasts displayed significant lengthening at 3, 10, 20, and 30μM concentrations by 6.5h, 10.6h, 12.6h, and 11.1h respectively (vehicle: 22.23±0.26, 3μM: 28.71±0.72, 10μM: 32.85±1.60, 20μM: 34.81±2.05, 30μM: 33.32±1.27 h). Similarly, cells classified as medium displayed lengthening by 5h, 8.5h, 10.3h, and 11.3h at 3, 10, 20, and 30μM concentrations of CGS-15943 (vehicle: 24.08±0.25, 3μM: 29.09±0.80, 10μM: 32.56±1.15, 20μM: 34.38±1.40, 30μM: 35.36±1.72 h). Whilst significant lengthening was not observed at 3μM CGS-15943 within the long category, 10, 20, and 30μM concentrations lengthened period by 7.3h, 8.8h, and 10.9h respectively (vehicle: 25.45±0.32, 10μM: 32.73±1.70, 20μM: 34.20±1.90, 30μM: 36.36±2.74h). Presenting the effects of CGS-15943 on exemplar cell lines from each category highlighted these observations (*Figures 4.9C-H*). Therefore, CGS-15943 appears to lengthen period independently of the baseline period length.

4.2.10 CGS-15943 increases amplitude in bipolar fibroblasts

We then assessed the effects of phenotypic period on circadian amplitude following treatment with CGS-15943. As displayed in *Figures 4.10A-B*, fibroblasts within the short grouping showed trends for amplitude enhancement at 3μM concentrations by 2.40±0.36 fold. Higher concentrations of 10 and 20μM presented amplitude induction by 3.47±0.70 fold and 3.44±0.59 fold respectively, where 30μM concentrations presented trends for enhancement by 2.93±0.66 fold. Similarly, significant augmentation of amplitude was found with cells within the medium category as a 2.16±0.24 fold induction was observed following treatment with 3μM CGS-15943. Treatment 10, 20, and 30μM concentrations however induced significant enhancement by 3.09±0.28-3.14±0.25 fold. Whilst the trend developing implied that CGS-15943 also increased amplitude within the long sub-group, no significant differences were found. However, when comparing the averages, the pattern identified suggested amplitude induction by 2.09±0.48 fold following treatment with 30μM CGS-15943.

Individual cellular examples highlight these observations (traces shown in *Figure 4.10*). When observing the effects of CGS-15943, all concentrations increased amplitude regardless of basal period length. However, whilst the cell line from the short and medium categories increased amplitude maximally by 2.70±0.10 fold and 3.94±0.06 fold at 20μM concentrations, cells from the long group presented enhancement by 1.75±0.09 fold (*Figures 4.10C-E*). Therefore, whilst amplitude enhancement is generally observed with CGS-15943, the effects appear subtler with the long phenotyped cell lines.

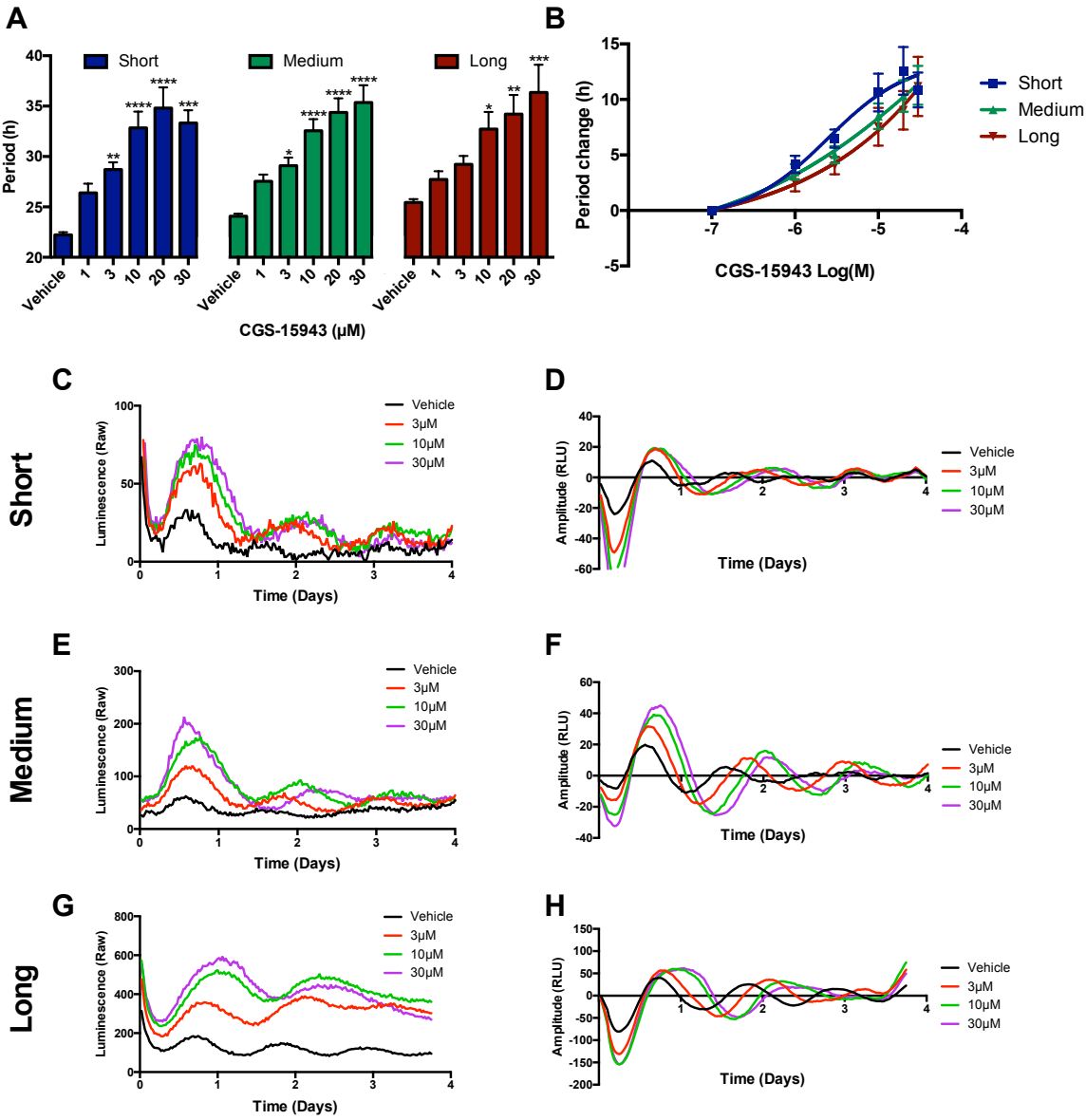

Figure 4.9. **CGS-15943 lengthens period in bipolar patients cell lines. A-B)** The period changes induced by CGS-15943 in fibroblasts derived from patients with short (n=5), medium (n=6), or long (n=5) period lengths. Raw luminescence diagrams and normalised traces for example cell lines within the short **(C-D)**, medium **(E-F)**, and long **(G-H)** phenotyped BPD patients.

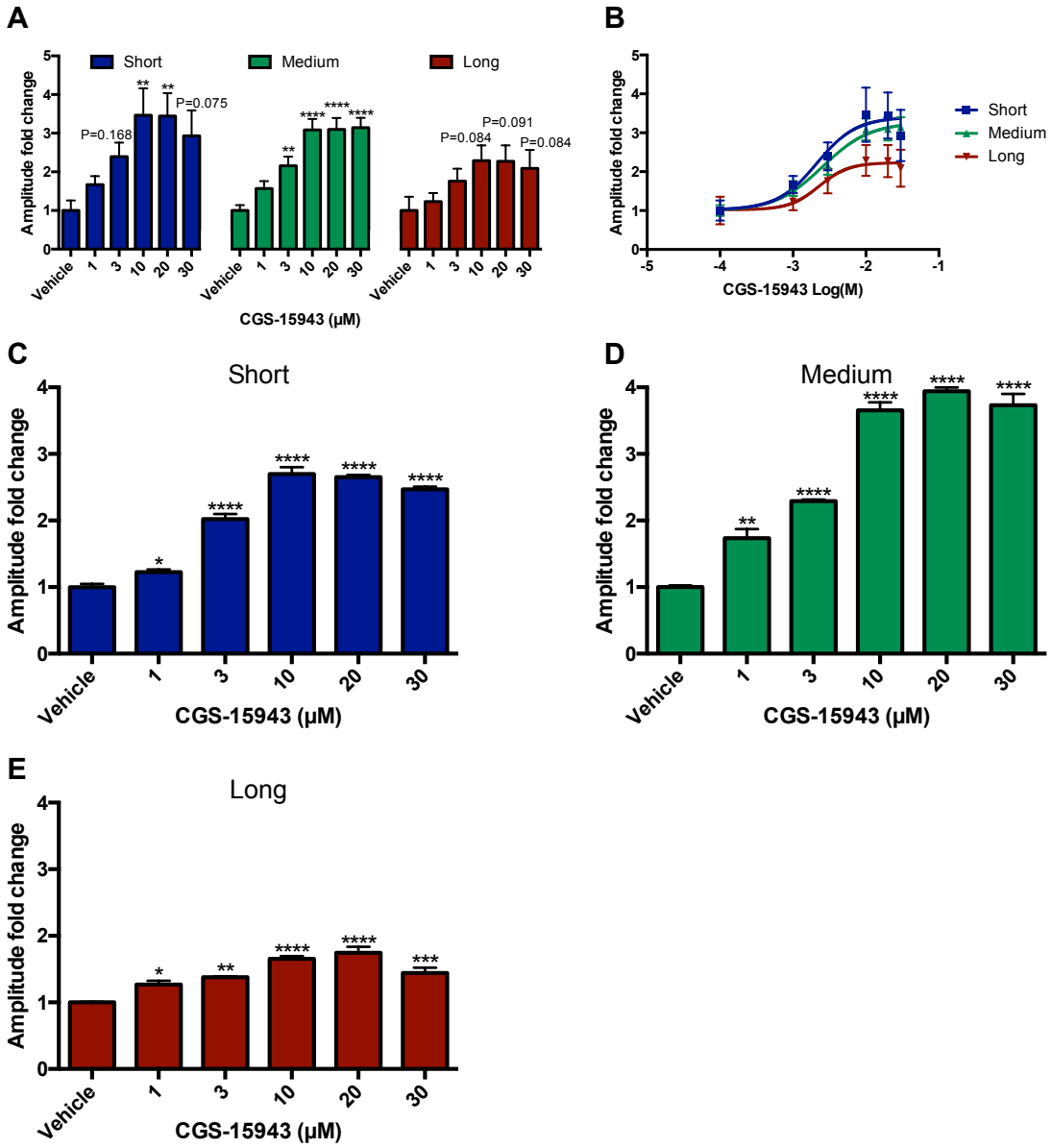

Figure 4.10. **CGS-15943 increases amplitude in patient-derived cell lines. A-B)** The amplitude changes induced by CGS-15943 in fibroblasts derived from patients within the short (n=5), medium (n=6), or long (n=5) groupings. Examples of amplitude changes induced by CGS-15943 in short (n=3) **(C)**, medium (n=3) **(D)**, and long (n=3) **(E)** categorised BPD patients. Accompanying bioluminescence traces can be found in *Figure 4.9*.

4.2.11 Changes to circadian rhythmicity are independent of lithium treatment

Despite our fibroblasts being unable to differentiate between Li-T and Li-NT patients following the application of LiCl to cells, as differences were emergent when observing amplitude, we were curious to evaluate the effects of alternative chronomodulatory drugs. As depicted in *Figure 4.11A*, when dividing the patient fibroblasts by lithium treatment, no significant period effects were observed following treatment with nobiletin. However, both groups displayed significant amplitude enhancement, where the Li-T cohort presented stronger patterns at lower concentrations (*Figures 4.11B-C*). Indeed, 3μM nobiletin showed trends of enhancement by 1.59±0.10 fold, where 10, 20, and 30μM nobiletin significantly augmented amplitude by 2.15±0.18 fold, 2.51±0.23 fold, and 2.66±0.26 fold respectively. The Li-NT group presented amplitude enhancement at the higher concentrations of 20 and 30μM by 2.06±0.39 fold and 2.23±0.42 fold respectively. Therefore, 10, 20, and 30μM nobiletin presented trends for greater amplitude increases by 22%, 18%, and 16% respectively in the Li-T subgroup.

Similar analysis was performed on the cells treated with CGS-15943, a drug capable of inducing great period lengthening in Li-T and Li-NT cell lines (*Figure 4.11D*). 3μM CGS-15943 was able to induce period lengthening by 4.88±0.73h, where 10, 20, and 30μM concentrations lengthened period by 8.54±1.32-10.43±1.62h. With the Li-NT patients, period lengthening was observed at 1 and 3μM concentrations by 4.41±0.70h and 5.66±0.54h respectively, where greater lengthening by 9.39±0.85-12.61±1.40h were found with 10, 20, and 30μM CGS-15943. Indeed, much like treatment with LiCl and

nobiletin, the trends identified suggested more muted amplitude enhancement with CGS-15943 in the Li-NT fibroblasts (*Figures 4.11E-F*). This was because in the Li-T fibroblasts, 1μM CGS-15943 presented trends for amplitude enhancement by 1.73±0.12 fold, where no such differences were found within the Li-NT group. Likewise, 3μM CGS-15943 presented patterns for greater amplitude induction in the Li-T group (2.34±0.21 fold increase), relative to the Li-NT group (1.73±0.24 fold increase). Therefore, 1 and 3μM concentrations augmented amplitude in the Li-T fibroblasts by 36% and 26% respectively. The higher concentrations appeared to show less variability when assessing lithium sensitivity as 10, 20, and 30μM concentrations of CGS-15943 augmented amplitude by 2.73±0.35-3.08±0.35 fold in the Li-T sub-group and by 2.65±0.36-2.73±0.42 fold in the Li-NT group. Thus, this evidence suggests that the Li-NT group may present more subtle amplitude enhancing effects following treatment with CGS-15943.

4.2.12 Lithium chloride, nobiletin, and CGS-15943 modulate rhythms in vivo

Following on from the cellular investigations into the effects of LiCl, nobiletin, and CGS-15943, these compounds were assessed *in vivo*. This would help determine whether fibroblasts can model circadian rhythmicity in animals, and thus provide a means of reducing the use of animals at the initial stages of the drug discovery process. Wild-type mice were administered i.p. injections of 200mg/kg LiCl, 50mg/kg nobiletin, or 5mg/kg CGS-15943 every other day for 2 weeks at CT6 or CT16 and wheel-running behaviour was assessed. As we were not administering compounds chronically, we selected a high drug dose

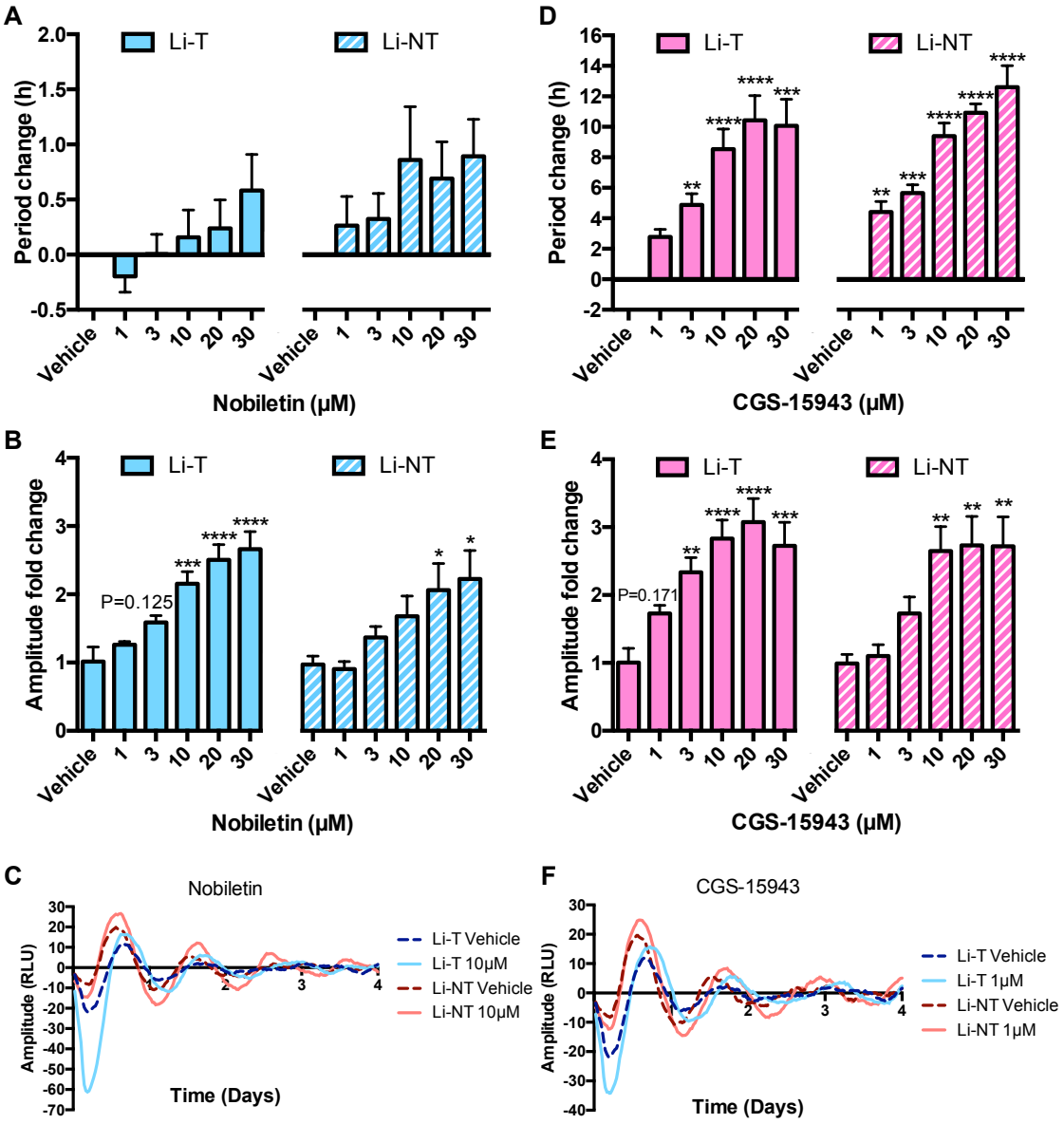

Figure 4.11. **Patient-derived fibroblasts show preliminary trends for discriminating between Li-T and Li-NT patients following treatment with nobiletin or CGS-15943.** The period **(A)** and amplitude **(B)** changes induced after treatment with 1-30μM nobiletin in fibroblasts from Li-T (n=10) and Li-NT patients (n=6). **C)** Representative traces highlighting the differences in amplitude enhancement following 10μM nobiletin treatment in the Li-T and Li-NT fibroblasts. The period **(D)** and amplitude **(E)** changes induced after treatment with 1-30μM CGS-15943 in fibroblasts from Li-T (n=10) and Li-NT patients (n=6). **F)** Representative traces highlighting the differences in amplitude enhancement following 1μM CGS-15943 treatment in the Li-T and Li-NT fibroblasts.

administered to C57BL/6 mice via an i.p. route in previous investigations (Gould et al., 2007, Yabuki et al., 2014, Jagannath et al., *manuscript in preparation*).

Firstly, as highlighted in *Figures 4.12A-B*, CT6 injections of nobiletin and CGS-15943 along with LiCl our positive control, resulted in behavioural period lengthening by ~10min, where no differences were observed on amplitude (vehicle: 23.49± 0.04, LiCl: 23.62±0.03, nobiletin: 23.61±0.02, CGS-15943: 23.60±0.03 h). These effects are highlighted by the example actograms (*Figures 4.12C-F*). Next, due to the potential conflict between phase advancing and period lengthening, we were curious to assess whether greater lengthening may be observed if the compounds were administered at CT16. As seen in *Figure 4.13A*, this was not the case, as LiCl administered at CT16 induced period lengthening by 0.23h, where nobiletin and CGS-15943 presented trends towards increasing period by 0.15-0.19h (vehicle: 23.37± 0.03, LiCl: 23.60±0.05, nobiletin: 23.56±0.05, CGS-15943: 23.52±0.09 h). Similarly to the injections at CT6, no effects on circadian amplitude were observed (*Figure 4.13B*). The behavioural consequences of these compounds are further highlighted by the representative actograms (*Figures 4.13C-F*). Therefore, LiCl, nobiletin, and CGS-15943 induced chronomodulatory period changes at CT6 and CT16.

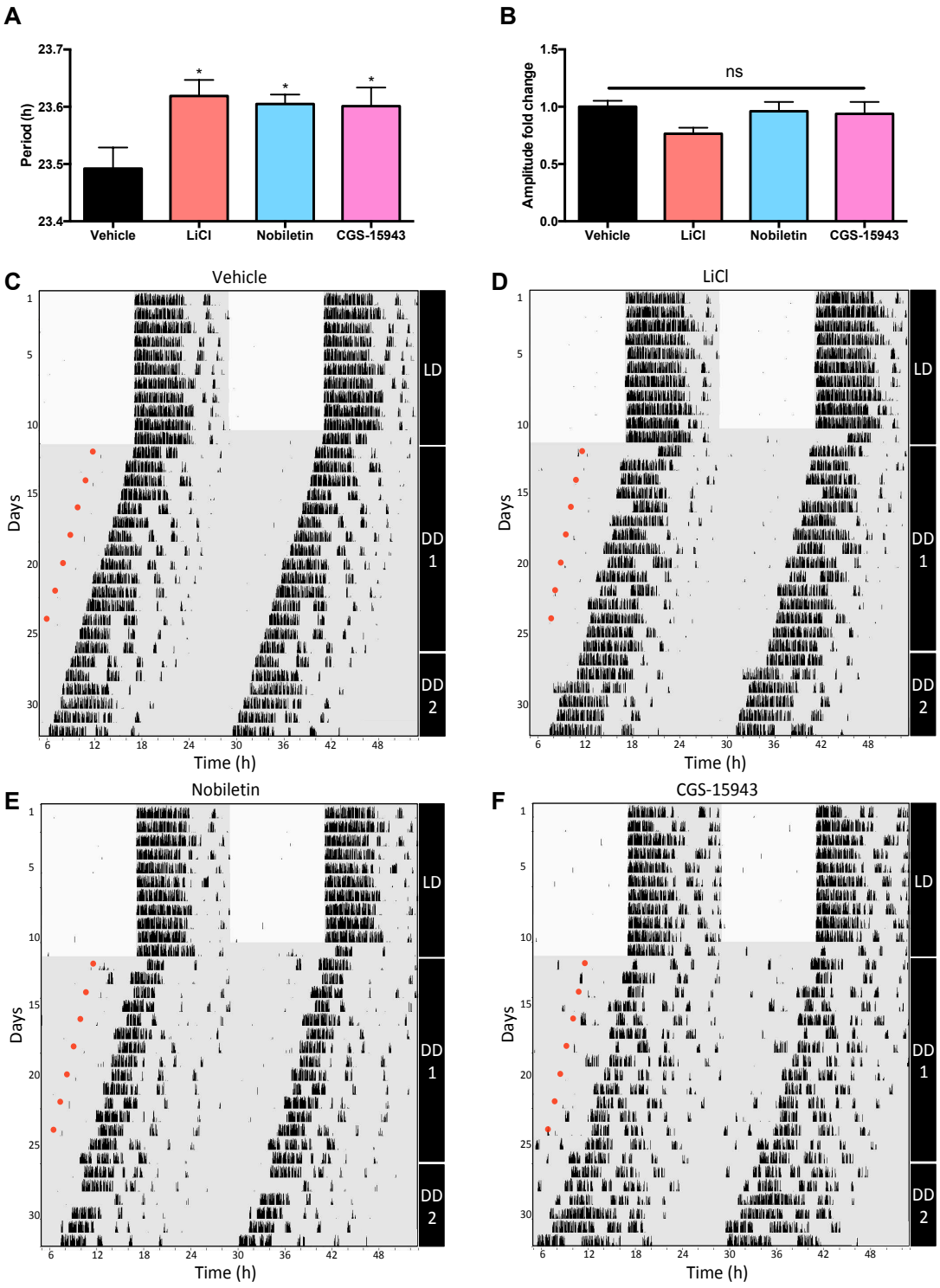

Figure 4.12. **Administering lithium chloride, nobiletin, or CGS-15943 at CT6 induces period lengthening *in vivo*.** Wild-type C57BL/6J mice were injected every other day for 2 weeks at CT6 with potential chronomodulatory compounds and wheel-running behaviour was monitored. The effects of vehicle (n=10), 200mg/kg LiCl (n=9), 50mg/kg nobiletin (n=10), or 5mg/kg CGS-15943 (n=9) on behavioural period **(A)** and amplitude **(B)**. Representative behavioural rhythms following an i.p. injection of vehicle **(C)**, LiCl **(D)**, nobiletin **(E)**, or CGS-15943 **(F)**. White: light phase, grey: dark phase, LD: light-dark cycle phase, DD1: drug administration phase, DD2: drug free phase, •: i.p. drug administration.

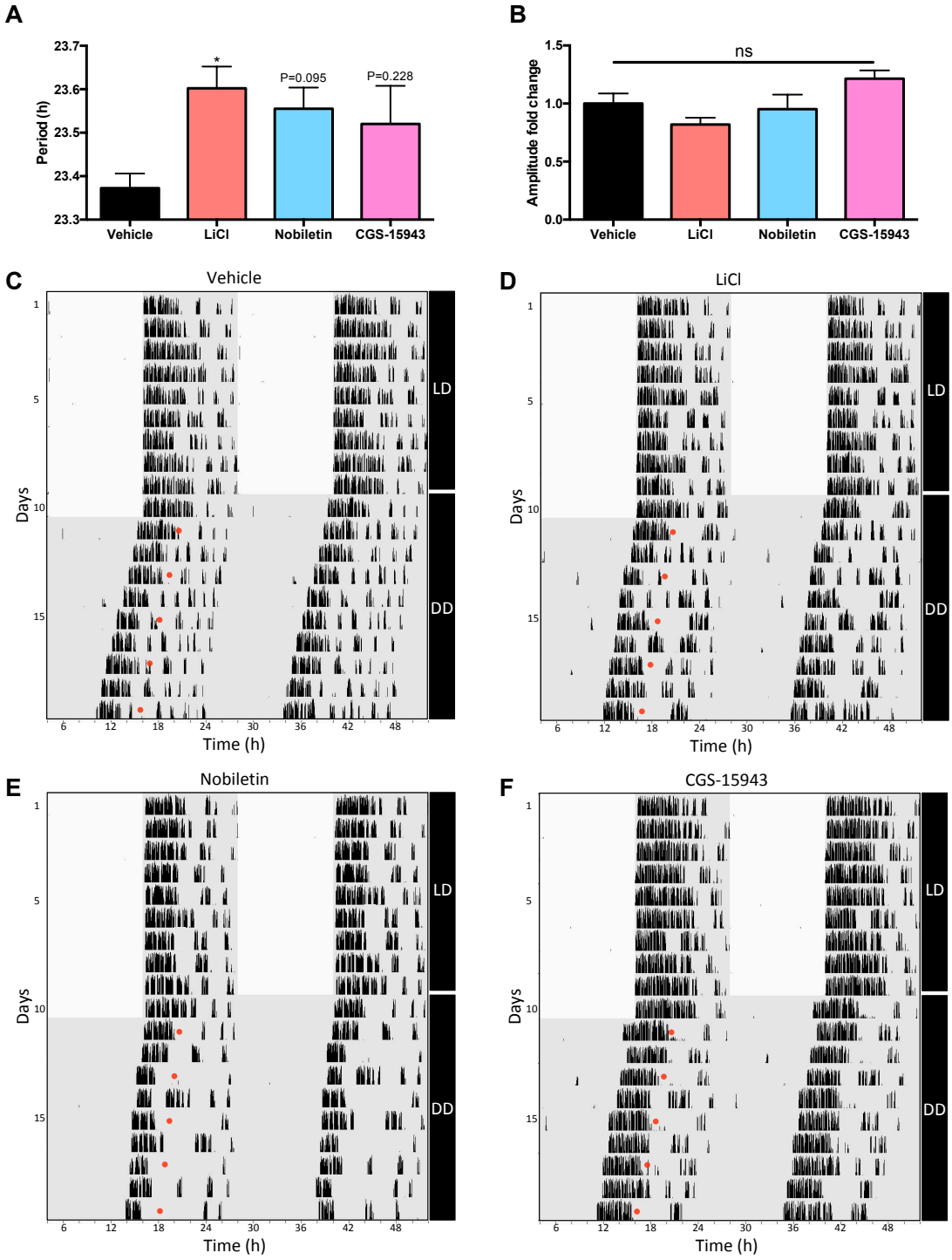

Figure 4.13. **Administering lithium chloride, nobiletin, or CGS-15943 at CT16 induces period lengthening *in vivo*.** Wild-type C57BL/6J mice were injected every other day for 2 weeks at CT16 with potential chronomodulatory compounds and wheel-running behaviour was monitored. The effects of vehicle (n=8), 200mg/kg LiCl (n=9), 50mg/kg nobiletin (n=10), or 5mg/kg CGS-15943 (n=9) on behavioural period **(A)** and amplitude **(B)**. Representative behavioural rhythms following an i.p. injection of vehicle **(D)**, LiCl **(E)**, nobiletin **(F)**, or CGS-15943 **(G)**. White: light phase, grey: dark phase, LD: light-dark cycle phase, DD: drug administration phase, •: i.p. drug administration.

4.2.13 Lithium chloride, nobiletin, and CGS-15943 reduce rearing behaviour

Knowing that the compounds of interest acted as chronomodulators both *in vitro* and *in vivo*, we went on to assess whether nobiletin and CGS-15943 could induce lithium-like behavioural changes. The OFT is a frequently used behavioural platform used to assess locomotor-related behaviours. Mice were injected at CT14-16 with the relevant compounds of interest and behaviour was assessed after 3h. As seen in *Figures 4.14A-B*, these compounds had no effect on the overall activity. The vehicle treated mice were active for 93.06±0.88% of the time, where mice treated with LiCl, nobiletin, and CGS-15943 were active for 81.06±6.30%, 82.16±6.45%, and 92.36±1.44% respectively.

Lithium is well characterised to reduce rearing, an action indicative of exploration and impulsivity. Indeed, when assessed via the OFT, we found that LiCl reduced the time spent rearing by 55% when compared to vehicle treated mice. Similarly, nobiletin reduced the time spent rearing by 65%, where trends were found which suggested that CGS-15943 also reduced rearing to a lesser degree of 27% (vehicle: 40.39±3.79, LiCl: 18.08±3.29, nobiletin: 14.09±3.91, CGS-15943: 29.48±2.90 %) (*Figures 4.14C-D*). In line with this evidence, it was also found that mice treated with these compounds spent significantly less time rearing in the centre on the OFT (*Figures 4.14E-F*). Mice treated with LiCl or nobiletin significantly reduced the number of rearing episodes by 75% and 63% respectively, where strong similar trends were identified following CGS-15943 treatment by 42% (vehicle: 1.00±0.18, LiCl: 0.25±0.05, nobiletin: 0.37±0.15, CGS-15943: 0.58±0.07 normalised rearing). Therefore, it was found that nobiletin and CGS-15943 showed strong indications of lithium-like behaviours.

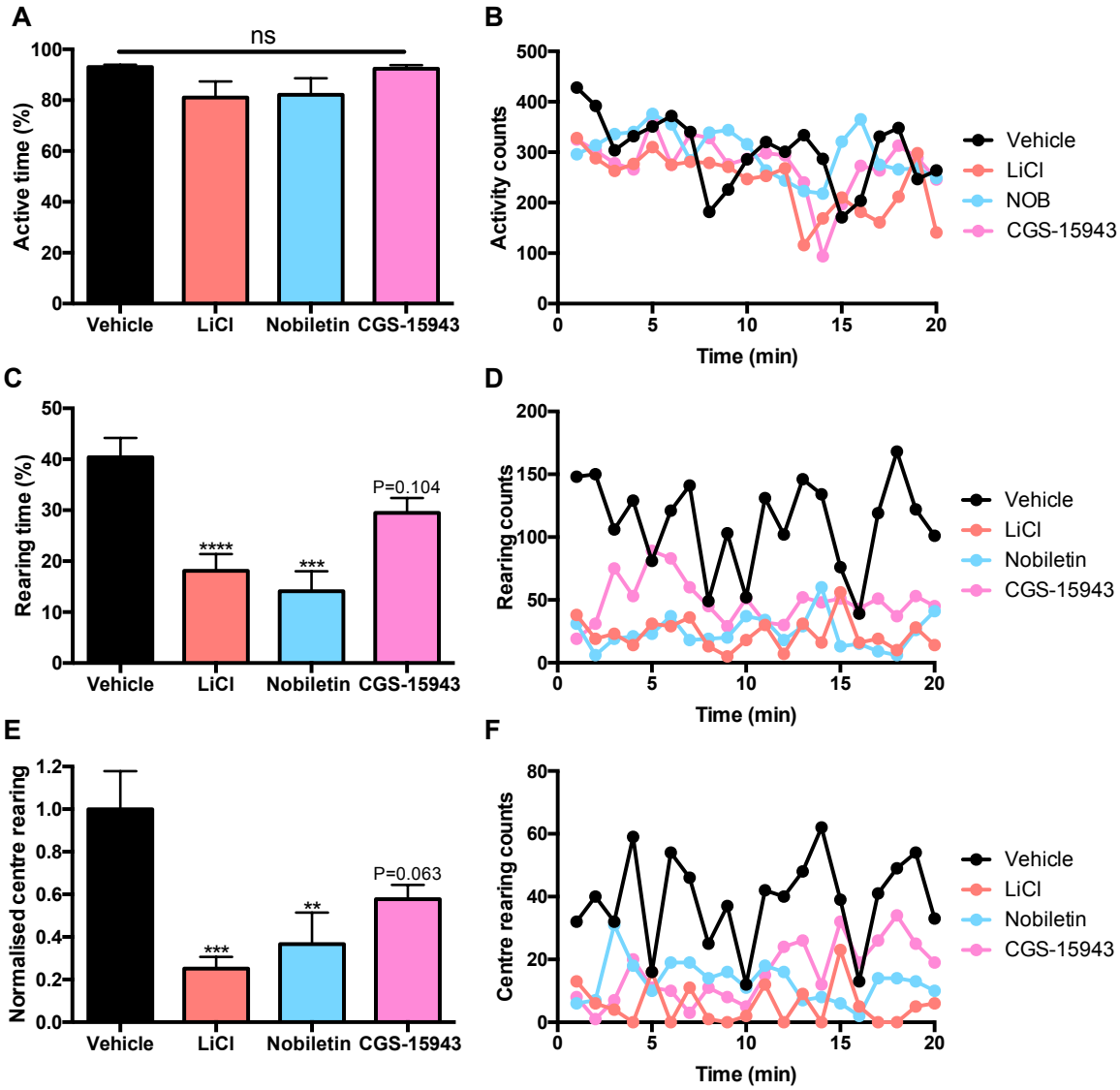

Figure 4.14. **Lithium chloride and nobiletin reduce rearing behaviour, with strong trends emerging for CGS-15943 in the open field test.** Animals were administered vehicle, (n=8), 200mg/kg LiCl (n=9), 50mg/kg nobiletin (n=9), or 5mg/kg CGS-15943 (n=8) at CT14-16 and tested after 3h under dim red light conditions. **A-B)** The effects of these compounds on the time spent active with example traces of activity counts. **C-D**) The time spent rearing with illustrative traces of rearing counts. **E-F)** The normalised number of centre rears with representative traces highlighting these findings.

4.2.14 Lithium chloride, nobiletin, and CGS-15943 reduce anxiety-related behaviour

As lithium is also known to impact anxiety-related behaviours, the final behavioural paradigm assessed was the EPM. Much like our findings with the OFT, the compounds of interest did not affect the overall distance travelled as vehicle treated mice travelled 10.13±0.71m and mice treated with LiCl, nobiletin, or CGS-15943 travelled between 7.56±1.89-12.51±1.17m (*Figure 4.15A*). Likewise, no differences were observed in the amount of time spent active, where mice were active for 52.75±11.52-78.76±3.21% of the time (*Figure 4.15B*).

Interestingly, differences were identified when assessing the number of entries into the open arm of the elevated plus maze. As depicted in *Figure 4.15C,* mice treated with LiCl were 2.7 times more likely to enter the open arm relative to vehicle treated mice. Additionally, treatment with either nobiletin or CGS-15943 also increased the number of open arm entries by 2.5 and 2.7 fold respectively, indicating that these compounds may possess anxiolytic effects (vehicle: 6.43±1.56, LiCl: 17.60±3.14, nobiletin: 16.29±3.12, CGS-15943: 17.57±3.30 entries). Furthermore, treatment with these compounds also impacted the amount of time spent in the open arm of the EPM (*Figures 4.15D-E*). Mice treated with LiCl spent 4.5 fold more time within the open arms relative to vehicle treated mice. Similarly, administering nobiletin or CGS-15943 increased the time spent in the open arms by 3.7 fold and 3.9 fold respectively (vehicle: 3.27±1.22, LiCl: 14.74±4.03, nobiletin: 12.04±2.49, CGS-15943: 12.61±2.46 %). Thus, as exemplified in the tracking plots LiCl, nobiletin, and CGS-15943 modulated anxiety-related behaviours (*Figure 4.15E*).

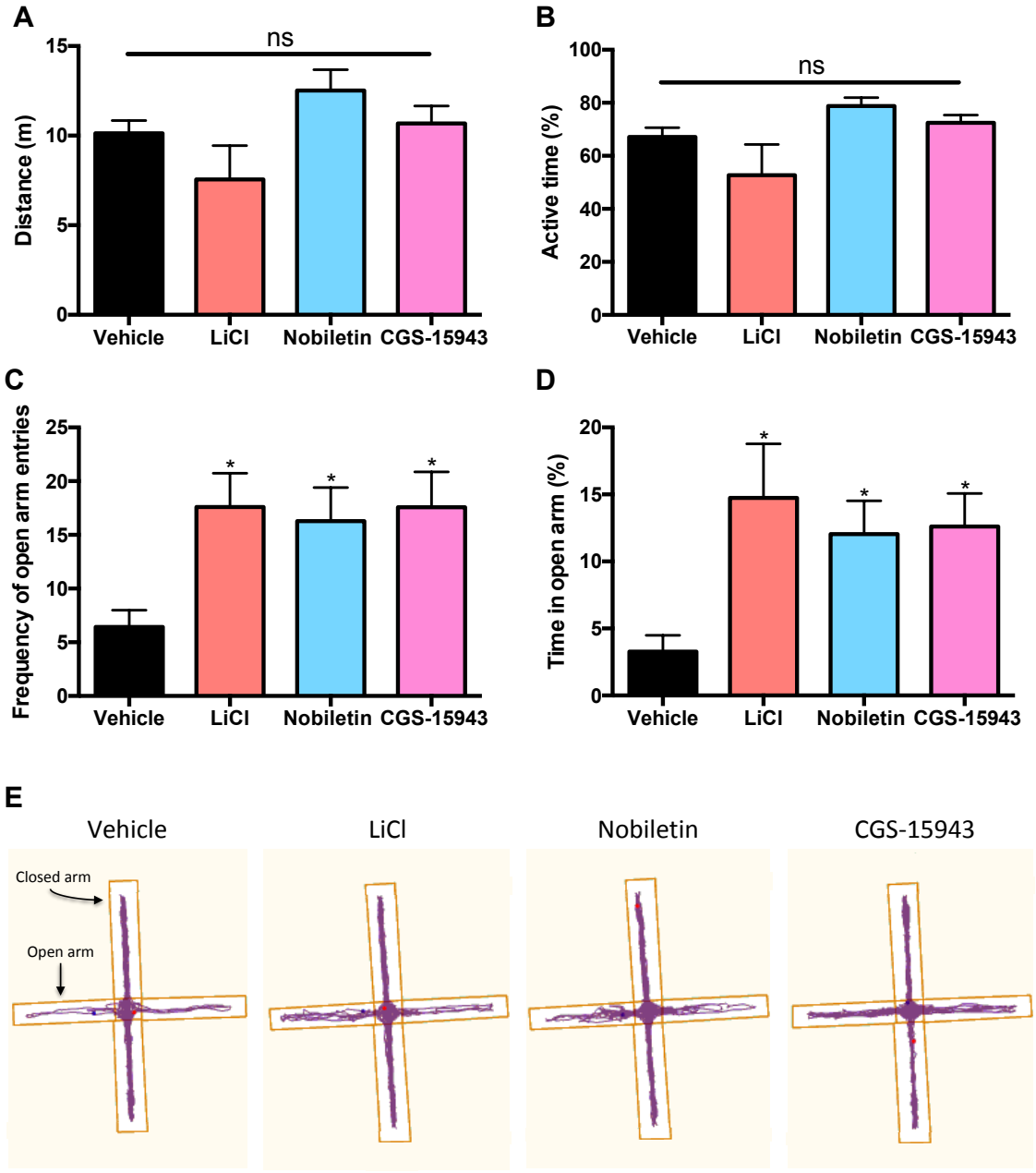

Figure 4.15. **Lithium chloride, nobiletin, and CGS-15943 reduce anxiety-like behaviour in the elevated plus maze.** Animals were administered i.p. injections of vehicle, (n=7), 200mg/kg LiCl (n=5), 50mg/kg nobiletin (n=7) or 5mg/kg CGS-15943 (n=7) and tested 1.5-2h after the OFT. The effects of these compounds on distance travelled **(A)**, the amount of time spent active **(B)**, the number of entries into the open arm **(C)**, and the amount of time spent in the open arm of the EPM **(D)**. **E)** Representative tracking plots for mice administered vehicle, LiCl, nobiletin, or CGS-15943. The blue and red dots signify the position of the animal when analysis began and ended respectively.

4.2.15 Period length is correlated with behaviour

Finally, by evaluating the emergent trends within the overall *in vivo* data, we can identify whether any correlations exist between circadian rhythmicity and rodent behaviours. Circadian period was our primary focus as *in vivo* period lengthening was observed and because fibroblast period length was enhanced following treatment with LiCl, nobiletin, and CGS-15943. We compared period change induced by these compounds at CT6 with the respective amount of time spent rearing in the OFT or in the open arms of the EPM. As seen in by the regression analysis depicted in *Figure 4.16A*, no significant correlation was apparent between period and the amount of time spent rearing (R^2= 0.226). However, a weak positive correlation was observed when assessing anxiety-like behaviour, as the longer the circadian period length, the more time spent in the open arms of the EPM (R^2= 0.397) (*Figure 4.16B*). Therefore, it was found that nobiletin and CGS-15943 could induce chronomodulation as well as inducing lithium-like behavioural changes.

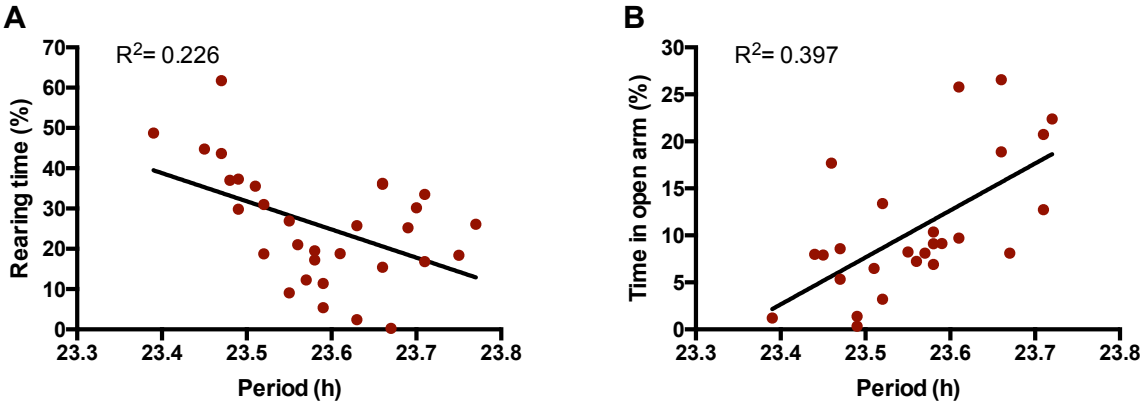

Figure 4.16. **A longer circadian period is moderately correlated with anxiety-related behaviour.** Regression analysis was performed comparing the overall drug-induced (vehicle, LiCl, nobiletin, and CGS-15943) circadian period of mice at CT6 and the amount of time spent rearing in the OFT (n=31) **(A)** or the amount of time spent in the open arms of the EPM (n=26) **(B)**.

4.3 Discussion

BPD is associated with significant sleep and circadian rhythm disruptions, where lithium, a drug known to exhibit significant chronomodulatory effects, remains a gold standard therapy. By examining the effects of LiCl on our patient-derived fibroblasts, we found that these cells model the known *in vivo* effects of LiCl, namely period lengthening and amplitude enhancement. We further went on to show that amplitude enhancement occurred independently of phenotypic period length, where LiCl preferentially lengthened period in fibroblasts with short and medium period lengths. However, whether the patients were consuming and therefore responsive to lithium could not account for this discrepancy, as our cellular model did not show significant *in vitro* differences in when comparing Li-T and Li-NT patients. We then went on to characterise the circadian consequences of two structurally distinct molecules, nobiletin and CGS-15943. Such compounds induced significant chronomodulatory changes both *in vitro* and *in vivo*. The trends observed suggested that Li-NT patients displayed lower amplitude changes following treatment with LiCl, nobiletin, or CGS-15943. Furthermore, nobiletin and CGS-15943 also induced lithium-like behaviours. Thus, our preliminary study found correlations between drugs that modulate circadian rhythms and their impact on overt behaviours.

4.3.1 Lithium-induced changes in fibroblast rhythms show the same direction of effect as behavioural changes

The primary treatment objective for BPD is to induce euthymia and to prevent recurrent mood episodes, where lithium remains a key treatment option

despite its numerous side effects. Our study confirmed that the BPD fibroblast model may provide a solid indication of drug-induced behavioural changes to circadian rhythmicity by: 1) assessing the effects of the known chronomodulator LiCl, and 2) the re-purposed compounds nobiletin and CGS-15943.

Firstly, we confirmed previous findings in showing that LiCl induced behavioural period lengthening and went on to find dose-dependent period lengthening in our BPD fibroblasts, specifically those with a basal period shorter that 24.99h. Much like our investigation, McCarthy and colleagues did not find period lengthening with 1mM LiCl in fibroblasts transduced with *Per2::Luc*. However, they did find that 10mM lithium lengthened period by 30min in patient cells, where we observed lengthening by 22min (McCarthy et al., 2013). Whilst they did not assess higher drug concentrations, this suggests that our findings, with a larger cohort of BPD fibroblasts, accurately reflect previous findings and extend them further. The mechanistic pathways responsible for this period effect remain elusive and are investigated in Chapter 5.

Relative to behavioural period lengthening by ~10min in mice, the cellular model displayed lengthening by up to 3h. Therefore, the fibroblasts displayed more extreme changes following drug-induced perturbations. Brown and colleagues also found this to be the case, as assessing fibroblast rhythms from circadian mutants with long or short behavioural periods resulted in cellular period changes that were up to 4 times more exaggerated, yet represented the correct patterns (Brown et al., 2005). This suggests that drug-induced fibroblast period is not entirely the same as behavioural period, but provides a strong indication of the potential physiological consequences. Indeed,

fundamental differences exist when simplifying from a whole animal model to a cultured cellular model, such as cellular drug concentration, drug clearance, and BBB permeability. It also suggests that when screening for novel compounds, only molecules with extreme changes to circadian parameters should be considered, as it is likely that the magnitude of change *in vivo* will be diminished relative to *in vitro*.

Consistent with our findings, McCarthy and colleagues showed that 1mM LiCl on *Per2::Luc* BPD fibroblasts did not induce any amplitude enhancement, and in contrast to previous findings, 10mM lithium decreased amplitude by 27% and 37% in control and BPD patient fibroblasts respectively (McCarthy et al., 2013). Indeed, our patient-derived fibroblast model was more indicative of predicted responses with 10mM LiCl, as trends of a 35% increase in amplitude were found. The lack of amplitude enhancement found by McCarthy et al., is surprising as lithium at 20mM concentrations in murine PER2::LUC lung fibroblasts showed significant amplitude enhancement by 2.5 fold and period lengthening by 1h (Li et al., 2012). Therefore, the reason for dampening is not due to poor cell health or the circadian gene of interest, and mechanistically, amplitude increases may be due to GSK3β inhibition, through the augmentation of *Per2* gene transcription (Li et al., 2012).

Furthermore, whilst the BPD fibroblasts show amplitude enhancement following LiCl treatment, no such effects were found in our behavioural study using wild-type mice. This may be because effects are typically observed following chronic lithium treatment. Additionally, previous studies have found that BPD patient fibroblasts displayed dampened *BMAL* and *REV-EVBα* rhythms,

thus it is plausible that greater amplitude effects would be observed in these cell lines relative to control cell lines, a pattern we also observed in the current investigation (Yang et al., 2009). By extension, greater physiological amplitude changes may be observed in animal models of mania-like behaviour, such as the *Clock*Δ19 or *Myshkin* mutants. Whilst studies have found that LiCl can normalise locomotor and anxiety-related behavioural abnormalities, the effects of lithium on mutant wheel-running activity remain elusive (Roybal et al., 2007, Kirshenbaum et al., 2011). Thus, our fibroblast model portrayed period and amplitude changes that were associated with lithium administration *in vivo*.

4.3.2 Fibroblasts can indicate novel drug-induced changes to behavioural rhythms

Our study also found that the polymethoxylated flavone nobiletin induced period lengthening in the short phenotyped fibroblasts (with a period of 23.49h or under), as well as physiological lengthening *in vivo* to a similar degree as LiCl. This appeared sensible as mice too have an average basal period of 23.5h, thus period lengthening accurately modeled responses within a subset of our fibroblasts. Moreover, 5-50μM nobiletin has previously been found to dose-dependently increase amplitude by ~2-3.5 fold, as well as period in *Per2::Luc* fibroblasts derived from heterozygous *Clock*Δ*19* mice, suggesting that nobiletin can lengthen period in multiple models of circadian disruption (He et al., 2016). Whilst previous studies found no wheel-running period effects following 200mg/kg nobiletin administered via oral gavage, this would equate to less than 50mg/kg nobiletin administered via an i.p. injection (He et al., 2016). Therefore, period differences may have been observed as we administered higher doses. Interestingly, the authors found that the effects of nobiletin on the molecular

clock were due to activation of RORα, thereby increasing *Bmal* transcription and protein accumulation. Thus, a direct link between nobiletin and the molecular clock has been established (He et al., 2016). This adds a further layer of evidence suggesting that our cellular model depicts period alterations *in vivo.*

In a similar fashion to nobiletin, the adenosine receptor antagonist CGS-15943 was found to induce significant period lengthening *in vitro* in all cell lines as well as *in vivo* to a similar extent as LiCl. Previous assessments using U2OS cells found that 5mM caffeine lengthened period by ~3h (Burke et al., 2015). Further investigations revealed that 10μM CGS-15943 also induced period lengthening by ~5h, effects which are believed to be through cyclic adenosine monophosphate (cAMP)-dependent mechanisms (Burke et al., 2015, O'Neill et al., 2008). This is an interesting finding as it establishes the route by which the adenosine pathway may be altering the clock. Indeed, cAMP is considered an extension of the molecular clock, controlling the TTFL and therefore acting as an input signal but also oscillating with a 24h rhythm as an output signal, thus impacting the molecular clock (Burke et al., 2015, O'Neill et al., 2008). Therefore, CGS-15943 can also modulate the molecular clock, adding to the evidence suggesting that fibroblasts are a valid tool for drug discovery.

Whilst LiCl, nobiletin, and CGS-15943 displayed *in vitro* amplitude enhancing effects, these effects were not replicated *in vivo*. This could indicate that the fibroblasts are a more accurate tool for investigating drug-induced period changes. However, no differences may have been observed as our compounds were administered acutely, injecting mice every other day. This would provide sufficient time for greater drug clearance thereby taking

significantly longer to reach the required cellular concentrations. Indeed, in our circadian assays the fibroblasts are continuously bathed in a supply of the molecule of interest and lithium is administered chronically for the treatment of BPD. Therefore, should we have formulated chow or fluid containing the relevant compounds or have implanted mini infusion pumps, all of which allow the continuous dosing of unrestrained animals, amplitude changes may have been more apparent. Indeed, the period changes we observed with lithium treatment were 2 times lower than previous findings, where lithium chow for 1 month induced period lengthening by 20min (Li et al., 2012). Therefore, as well as the possibility of amplitude changes becoming more apparent when using animal models with dampened circadian rhythms, it would also be interesting to assess whether chronic drug administration induces greater chronomodulatory effects.

Overall, we found that LiCl, nobiletin, and CGS-15943, all induced physiological period lengthening, as predicted by our patient-derived fibroblasts. Further, these compounds impact the molecular clock via alternative dominant targets and therefore the effects observed are not due to actions associated with a particular target, but show how this model can portray drug-induced changes involving multiple signaling pathways. As heterogeneity was observed based on the fibroblast basal period, this could imply the use of multiple cell lines to understand the dominant effects of a drug and to aid in identifying the target patient group.

4.3.3 Fibroblasts trends associated with lithium sensitivity

LiCl failed to induce the same degree of period lengthening in fibroblasts with a longer basal period. However, this does not appear to be due to the

'ceiling effect' of the cells capacity to induce period lengthening, as one of the novel drugs tested, CGS-15943, was able to induce period lengthening in these cell lines by 10.61h at 30μM concentrations. However, it does show that lithium has a ceiling effect for circadian period, further suggesting that period lengthening and amplitude enhancement are induced via different molecular targets.

We hypothesised that discrepancies in circadian period may be associated with responsiveness to lithium treatment. However, to our surprise, no significant differences in circadian period or amplitude were apparent between the Li-T and Li-NT groups. This could be due to difficulty in characterisation of patient sensitivity to lithium. We characterised patients as Li-T if they were consuming lithium at the time of the biopsy. This was because the average consistent time of lithium consumption was high at 10.19 years, suggesting that lithium was impacting these patients enough to warrant being encompassed into their long-term treatment plans. However, lithium may not have been extremely effective at normalising mood instability, as overall effectiveness averaged 6.00±0.49 on a scale from 1 to 10, and lithium did not undoubtedly stabilise mood in 20% of our Li-T cohort (Chapter 3, *Table 3.3*). Therefore, should more extreme responders vs. non-responders be tested in the future, differences in LiCl-induced rhythmicity may become apparent. Typically responders to treatment are classified as presenting a 50% reduction in mood-based questionnaires such as the Hamilton Rating Scale for Depression or the Young Mania Rating Scale following treatment onset (McCall, 2015, Earley et al., 2018). Whilst this information was not available at the time of this study, future

investigations may benefit by distinguishing patients at the more extreme ends, for example in patients experiencing >75% improvement in mood vs. <25% improvements.

It is prudent to acknowledge that lithium may induce changes in both Li-T and Li-NT patients albeit to different degrees. An increasing weight of evidence suggests that Li-T patient cell lines display heightened amplitude effects in *RORα*, *BMAL1, PER1*, *CRY2*, *DEC1/2,* and *CSNK1δ* after 2 days of lithium treatment (Geoffroy et al., 2017). Indeed, further inspection of our data identified similar trends in *Bmal* rhythmicity, as 10mM LiCl, 10μM nobiletin, as well as 1 and 3μM CGS-15943, resulted in 22%, 22%, 36%, and 26% greater amplitude induction in the Li-T fibroblasts respectively. Thus, the pattern emerging suggests that greater amplitude changes may be observed in the Li-T over the Li-NT patients, and more accurate characterisation of lithium sensitivity may unmask these circadian discrepancies.

4.3.4 Circadian rhythms as a future biomarker for chronomodulation sensitivity

Patients in the short, medium, and long categories displayed different chronomodulatory responses to pharmacological compounds. Generally, the long phenotyped patients appeared less sensitive to our compounds, suggesting that this cohort of patients may be harder to treat. If this were true, one would hypothesise that such a cohort may be consuming more drugs overall. Although a small sample size, the trends observed appear to suggest this may be the case. As seen in *Table 4.1*, the mean, mode, and median for the long fibroblast cohort is greater than that observed with the short and medium groups. Furthermore, as displayed in the correlogram in Chapter 3.2.9, a long circadian period was

correlated with the consumption of more medications. Therefore, if future larger scale studies confirm this finding, use of patient-derived fibroblasts could act as a biomarker for lithium sensitivity. All that would be required is a non-invasive skin biopsy, the cells could be cultured and basal circadian rhythmicity assessed. Such experimental studies could drastically reduce the time required to find effective treatments for BPD patients.

Table 4.1. The mean, mode, and median highlighting the total number of drugs consumed by patients in the short, medium, or long categories.

Category	n	Mean±SEM	Mode	Median
Short	13	2.23±0.30	1	2
Medium	17	2.18±0.32	2	2
Long	9	2.89±0.51	5	3

4.3.5 Nobiletin and CGS-I5943 modulate rearing behaviours

In addition to validating fibroblasts as a model for BPD, we were also curious to understand whether pharmacological modulation of circadian rhythms could impact rodent behaviours. Firstly, we found that nobiletin and CGS-15943, much like LiCl reduced or showed strong indications for reducing rearing behaviours in the OFT. Rearing can be indicative of exploratory and impulsive behaviours, where actions are performed without full prior forethought, a key symptom associated with mania (O'Donnell and Gould, 2007). By extension, impulsivity is also associated with suicidality, where rates of attempted suicide in BPD patients double those found with unipolar depressives (Chen and Dilsaver, 1996). Therefore, in line with the knowledge that lithium is the only mood-stabiliser currently known to reduce suicidal tendencies, the ability of this compound to reduce rearing behaviours is paramount in indicating its mood-regulating and anti-manic properties (Song et al., 2017). Indeed, when

assessing 22 different behavioural traits for lithium-specific qualities, the most consistent behaviours included lengthened circadian period and reduced rearing, along with reduced aggression, increased conditioned taste aversion and increased pilocarpine seizures (O'Donnell and Gould, 2007). Moreover, in the search for future lithium mimetics rearing was the trait of interest, further emphasising its importance (Singh et al., 2013).

Previous assessments of nobiletin on wild-type mice showed no differences in overall locomotor activity or rearing behaviour in the OFT. However, behaviour was only scored for 3min, after administering a single acute dose of 25-100mg/kg nobiletin via oral gavage 1h before the test (Yi et al., 2011). Therefore, the experiment was not performed for long enough to surpass the initial environmental habituation time, lower doses were administered, and did not account for the additional time required for first pass metabolism and accumulation in the brain. Indeed, in animal models for Alzheimer's disease, 10mg/kg nobiletin (i.p.) presented trends for further reducing rearing behaviours, in line with our investigation. Interestingly, these effects were thought to be exerted through modulation of cAMP-PKA signaling, as nobiletin increased P-extracellular signal-related kinase (ERK) levels in the brain by ~100% (Onozuka et al., 2008). Rats modeling post-traumatic stress disorder through exposure to chronic stress also did not display any differences in activity or rearing behaviour following the administration of tangeritin, another citrus peel polymethoxylated flavone (Lee et al., 2018). However, the authors did find that 100mg/kg of tangeritin induced elevations in dopamine and 5-HT to a similar extent as fluoxetine in the medial prefrontal cortex, striatum, hippocampus, and amygdala (Lee et al., 2018). This suggests that such flavones

can regulate rodent behaviours, as they can accumulate in key limbic and reward-regulating brain regions and target affect modulating neurotransmitter systems.

Similarly, whilst it could be hypothesised that CGS-15943, a psychostimulant would increase locomotor behaviour, this was not found to true when assessing the amount of time spent active in the OFT. The animals did however present strong indications for reducing impulsivity-related rearing behaviours. Indeed, similar trends were apparent after administering mice 3-100mg/kg (i.p.) caffeine on the first day of testing (Angelucci et al., 1999). Interestingly, with the higher dose of 100mg/kg of caffeine, a reduction in rearing was observed 1h after administration (Svenningsson et al., 1995). Both studies found that habituation was affected by caffeine consumption, as vehicle treated animals displayed a rapid reduction in rearing with increased time, an effect which took significantly longer after caffeine consumption. Thus, when assessing the effects of caffeine after multiple days of testing, or after multiple hours in the apparatus, rearing is significantly higher in the caffeine treated animals. As we tested mice in a novel environment on a single occasion, we observed reductions in rearing, where the adenosine receptor antagonists theophylline (50mg/kg) and CPA (1mg/kg) also reduced rearing behaviours (El Yacoubi et al., 2000a, Bishnoi et al., 2007). Indeed, chronic consumptions of caffeine has been found to increase 5-HT_1 and 5-HT_2 receptor densities in the mouse cortex by up to 30%, and brainstem 5-HT levels can rise by 40%, suggesting caffeine can modulate serotonergic tone as a potential mechanism via which mood changes may occur (Shi et al., 1993, Berkowitz and Spector, 1971).

4.3.6 Nobiletin and CGS-I5943 modulate anxiety-related behaviours

Nobiletin also displayed anxiolytic behaviour in the EPM. In animal models of Alzheimer's disease, 50mg/kg (i.p.) nobiletin increased the time spent in the open arms of the EPM by ~3 fold with trends for a 3 fold increase found for the number of entries into the open arm, suggesting the induction of anxiolytic behaviour (Nakajima et al., 2013). Similarly, we observed reductions in anxiety following CGS-15943 administration exemplified by an increase in the number of entries and time spent in the open arms of the EPM. Indeed, caffeine, a non-specific drug, possesses potent anxiogenic properties, noted through reductions in the frequency of open arm entries and the time spent there (El Yacoubi et al., 2000b, Bhattacharya et al., 1997). However, treatment with more specific adenosine receptor antagonists found that the A_{2A} receptor antagonist SCH58261 significantly increased the number of transitions into the light chamber of the light dark box by ~60%. Additionally, similar trends were found after co-administering mice with A_1 and A_{2A} receptor antagonists (DPCPX, SCH58261), where at the highest concentrations, mice spent 57% more time in the open arms of the EPM, and entered the open arms 44% more (El Yacoubi et al., 2000b). Therefore, it would be a mistake to presume that all adenosine receptor antagonists exhibit anxiogenic properties.

Whilst reductions in rearing are considered a *bona fide* characteristic of lithium, the deductions regarding anxiety-related behaviour are mixed (O'Donnell and Gould, 2007). Interestingly, the *Clock*Δ19 mutants are a model of mania and thus display increased risk-taking behaviours as they spend more time in the centre of the OFT and enter the open arm of the EPM more

frequently. In such animals, chronic lithium treatment was able to normalise behaviours to near wild-type levels (Roybal et al., 2007). Similarly, lithium reduced the time spent in the open arms of the EPM in the *Myshkin* model of mania (Kirshenbaum et al., 2011). Therefore, lithium may act to stabilise anxiety-related behaviours, and thus the effects of our compounds should be assessed on similar models to see whether lithium-like effects are observed, or whether these molecules would exacerbate mania-like phenotypes by further reducing anxiety. However, our aims were to assess whether any changes in behaviour were apparent, and not to identify a lithium mimetic at this stage, a question for future studies to address.

4.3.7 Conclusion

This study had two predominant aims, evaluating a 3R's question as well as a scientific query. We addressed the 3Rs issue by validating that BPD patient-derived fibroblasts contain a molecular clock which models drug-induced changes to circadian parameters *in vivo*. As we have created stable circadian reporter transduced cell lines with known basal circadian properties, certain cell lines can be cherry-picked such that this model will hopefully be implemented in future drug discovery processes. This will replace the use of animals at the initial stages of drug discovery and therefore reduce the overall numbers of animals utilised. Further, it will provide investigators with a high-throughput model with greater human relevance and may overcome issues with poor predictivity associated with animal models, ultimately aiding the identification of more efficacious therapeutics.

The scientific hypothesis we were testing provided a solid foundation suggesting that pharmacological modulation of circadian rhythms may regulate overt behaviours. Circadian disturbances are well established in BPD, yet despite these needs, there are no molecular clock targeted chronomodulatory drugs on the market. Our BPD fibroblast model could be used for preliminary future drug screening processes as we have provided initial evidence suggesting that modulation of the molecular clock could regulate features of behaviour.

However, we acknowledge that there were some limitations which future investigations could address. Whilst within our BPD cohort, we did not observe any sex or age related differences in circadian rhythmicity, gender and aged-matched controls may provide greater information when observing drug-induced changes for future screening purposes. Moreover, in order to further validate whether the pharmacological overlap between the circadian and mood regulatory system is true: 1) more chronomodulatory compounds should be validated against our fibroblast model, and 2) these compounds should be assessed in animal models with similar circadian and behavioural abnormalities exhibited by BPD patients.

Overall, we have provided evidence for the first time to show that human fibroblasts display dose-dependent changes in period and amplitude after pharmacological perturbation. These effects display changes typically observed through wheel-running analysis and provide a means of high throughput drug screening. Whilst the stabilisation of mood may not exclusively be associated with the regulation of circadian functions, clock genes are an attractive novel target which present great pharmacological potential.

4.4 References

AMERICAN PSYCHIATRIC ASSOCIATION 2013. *Diagnostics and Statisitcal Manual of Mental Disorders (DSM) 5th edition,* Washington.

ANGELUCCI, M. E. M., VITAL, M., CESARIO, C., ZADUSKY, C. R., ROSALEN, P. L. & DA CUNHA, C. 1999. The effect of caffeine in animal models of learning and memory. *European Journal of Pharmacology,* 373**,** 135-140.

BARBINI, B., BENEDETTI, F., COLOMBO, C., DOTOLI, D., BERNASCONI, A., CIGALA-FULGOSI, M., FLORITA, M. & SMERALDI, E. 2005. Dark therapy for mania: a pilot study. *Bipolar Disorders,* 7**,** 98-101.

BERKOWITZ, B. A. & SPECTOR, S. 1971. Effect of caffeine and theophylline on disposition of brain serotonin in rat. *European Journal of Pharmacology,* 16**,** 322-+.

BHATTACHARYA, S. K., SATYAN, K. S. & CHAKRABARTI, A. 1997. Anxiogenic action of caffeine: an experimental study in rats. *Journal of Psychopharmacology,* 11**,** 219-224.

BISHNOI, M., CHOPRA, K. & KULKARNI, S. K. 2007. Theophylline, adenosine receptor antagonist prevents behavioral, biochemical and neurochemical changes associated with an animal model of tardive dyskinesia. *Pharmacological Reports,* 59**,** 181-191.

BROWN, S. A., FLEURY-OLELA, F., NAGOSHI, E., HAUSER, C., JUGE, C., MEIER, C. A., CHICHEPORTICHE, R., DAYER, J. M., ALBRECHT, U. & SCHIBLER, U. 2005. The period length of fibroblast circadian gene expression varies widely among human individuals. *Plos Biology,* 3**,** 1813-1818.

BURKE, T. M., MARKWALD, R. R., MCHILL, A. W., CHINOY, E. D., SNIDER, J. A., BESSMAN, S. C., JUNG, C. M., O'NEILL, J. S. & WRIGHT, K. P. 2015. Effects of caffeine on the human circadian clock in vivo and in vitro. *Science Translational Medicine,* 7**,** 305ra146.

CHEN, Y. W. & DILSAVER, S. C. 1996. Lifetime rates of suicide attempts among subjects with bipolar and unipolar disorders relative to subjects with other axis I disorders. *Biological Psychiatry,* 39**,** 896-899.

DAVIDSON, A. J., CASTANON-CERVANTES, O., LEISE, T. L., MOLYNEUX, P. C. & HARRINGTON, M. E. 2009. Visualizing jet lag in the mouse suprachiasmatic nucleus and peripheral circadian timing system. *European Journal of Neuroscience,* 29**,** 171-180.

EARLEY, W., DURGAM, S., LU, K. F., RUTH, A., NEMETH, G., LASZLOVSZKY, I. & YATHAM, L. N. 2018. Clinically relevant response and remission outcomes in cariprazine-treated patients with bipolar I disorder. *Journal of Affective Disorders,* 226**,** 239-244.

EL YACOUBI, M., LEDENT, C., MENARD, J. F., PARMENTIER, M., COSTENTIN, J. & VAUGEOIS, J. M. 2000a. The stimulant effects of caffeine on locomotor behaviour in mice are mediated through its blockade of adenosine A(2A) receptors. *British Journal of Pharmacology,* 129**,** 1465-1473.

EL YACOUBI, M., LEDENT, C., PARMENTIER, M., COSTENTIN, J. & VAUGEOIS, J. M. 2000b. The anxiogenic-like effect of caffeine in two experimental procedures measuring anxiety in the mouse is not shared by selective A(2A) adenosine receptor antagonists. *Psychopharmacology,* 148**,** 153-163.

FIBIGER, H. C. 2012. Psychiatry, The Pharmaceutical Industry, and The Road to Better Therapeutics. *Schizophrenia Bulletin,* 38**,** 649-650.

FREDHOLM, B. B., ARSLAN, G., HALLDNER, L., KULL, B., SCHULTE, G. & WASSERMAN, W. 2000. Structure and function of adenosine receptors and their genes. *Naunyn-Schmiedebergs Archives of Pharmacology,* 362**,** 364-374.

GEDDES, J. R., BURGESS, S., HAWTON, K., JAMISON, K. & GOODWIN, G. M. 2004. Long-term lithium therapy for bipolar disorder: Systematic review and meta-analysis of randomized controlled trialls. *American Journal of Psychiatry,* 161**,** 217-222.

GEOFFROY, P. A., CURIS, E., COURTIN, C., MOREIRA, J., MORVILLERS, T., ETAIN, B., LAPLANCHE, J. L., BELLIVIER, F. & MARIE-CLAIRE, C. 2017. Lithium response in bipolar disorders and core clock genes expression.: *The World Journal of Biological Psychiatry*, 18, 1–14.

GODINHO, S. I. H., MAYWOOD, E. S., SHAW, L., TUCCI, V., BARNARD, A. R., BUSINO, L., PAGANO, M., KENDALL, R., QUWAILID, M. M., ROMERO, M. R., O'NEILL, J., CHESHAM, J. E., BROOKER, D., LALANNE, Z., HASTINGS, M. H. & NOLAN, P. M. 2007. The after-hours mutant reveals a role for Fbxl3 in determining mammalian circadian period. *Science,* 316**,** 897-900.

GOULD, T. D., O'DONNELL, K. C., PICCHINI, A. M. & MANJI, H. K. 2007. Strain differences in lithium attenuation of d-amphetamine-induced hyperlocomotion: A mouse model for the genetics of clinical response to lithium. *Neuropsychopharmacology,* 32**,** 1321-1333.

GUILDING, C., SCOTT, F., BECHTOLD, D. A., BROWN, T. M., WEGNER, S. & PIGGINS, H. D. 2013. Suppressed cellular oscillations in after-hours mutant mice are associated with enhanced circadian phase-resetting. *Journal of Physiology-London,* 591**,** 1063-1080.

HE, B. K., NOHARA, K., PARK, N., PARK, Y. S., GUILLORY, B., ZHAO, Z. Y., GARCIA, J. M., KOIKE, N., LEE, C. C., TAKAHASHI, J. S., YOO, S. H. & CHEN, Z. 2016. The Small Molecule Nobiletin Targets the Molecular Oscillator to Enhance Circadian Rhythms and Protect against Metabolic Syndrome. *Cell Metabolism,* 23**,** 610-621.

HUANG, H., LI, L. F., SHI, W. M., LIU, H., YANG, J. Q., YUAN, X. L. & WU, L. H. 2016. The Multifunctional Effects of Nobiletin and Its Metabolites In Vivo and In Vitro. *Evidence-Based Complementary and Alternative Medicine,* 2016.

INDER, M. L., CROWE, M. T. & PORTER, R. 2016. Effect of transmeridian travel and jetlag on mood disorders: Evidence and implications. *Australian and New Zealand Journal of Psychiatry,* 50**,** 220-227.

JAGANNATH, A., PEIRSON, S. N. & FOSTER, R. G. 2013. Sleep and circadian rhythm disruption in neuropsychiatric illness. *Current opinion in neurobiology,* 23**,** 888-94.

KATZ, G., KNOBLER, H. Y., LAIBEL, Z., STRAUSS, Z. & DURST, R. 2002. Time zone change and major psychiatric morbidity: The results of a 6-year study in Jerusalem. *Comprehensive Psychiatry,* 43**,** 37-40.

KEERS, R., PEDROSO, I., BREEN, G., AITCHISON, K. J., NOLAN, P. M., CICHON, S., NOETHEN, M. M., RIETSCHEL, M., SCHALKWYK, L. C. & FERNANDES, C. 2012. Reduced Anxiety and Depression-Like Behaviours in the Circadian Period Mutant Mouse Afterhours. *Plos One,* 7**,** e38263.

KENNEDY, S. H. & EMSLEY, R. 2006. Placebo-controlled trial of agomelatine in the treatment of major depressive disorder. *European Neuropsychopharmacology,* 16**,** 93-100.

KIRSHENBAUM, G. S., CLAPCOTE, S. J., DUFFY, S., BURGESS, C. R., PETERSEN, J., JAROWEK, K. J., YUECEL, Y. H., CORTEZ, M. A., SNEAD, O. C., III, VILSEN, B., PEEVER, J. H., RALPH, M. R. & RODER, J. C. 2011. Mania-like behavior induced by genetic dysfunction of the neuron-specific Na+,K+-ATPase alpha 3 sodium pump. *Proceedings of the National Academy of Sciences of the United States of America,* 108**,** 18144-18149.

LEE, B., SHIM, I., LEE, H. & HAHM, D. H. 2018. The polymethoxylated flavone, Tangeretin improves cognitive memory in rats experiencing a single episode of prolonged post-traumatic stress. *Animal Cells and Systems,* 22**,** 54-62.

LI, J., LU, W.-Q., BEESLEY, S., LOUDON, A. S. I. & MENG, Q.-J. 2012. Lithium Impacts on the Amplitude and Period of the Molecular Circadian Clockwork. *Plos One,* 7**,** e33292.

LOO, H., HALE, A. & D'HAENEN, H. 2002. Determination of the dose of agomelatine, a melatoninergic agonist and selective 5-HT2C antagonist, in the treatment of major depressive disorder: a placebo-controlled dose range study. *International Clinical Psychopharmacology,* 17**,** 239-247.

MCCALL, W. V. 2015. A rest-activity biomarker to predict response to SSRIs in major depressive disorder. *Journal of Psychiatric Research,* 64**,** 19-22.

MCCARTHY, M. J., WEI, H., MARNOY, Z., DARVISH, R. M., MCPHIE, D. L., COHEN, B. M. & WELSH, D. K. 2013. Genetic and clinical factors predict lithium's effects on PER2 gene expression rhythms in cells from bipolar disorder patients. *Translational Psychiatry,* 3**,** e318.

MERIKANGAS, K. R., JIN, R., HE, J. P., KESSLER, R. C., LEE, S., SAMPSON, N. A., VIANA, M. C., ANDRADE, L. H., HU, C. Y., KARAM, E. G., LADEA, M., MEDINA-MORA, M. E., ONO, Y., POSADA-VILLA, J., SAGAR, R., WELLS, J. E. & ZARKOV, Z. 2011. Prevalence and Correlates of Bipolar Spectrum Disorder in the World Mental Health Survey Initiative. *Archives of General Psychiatry,* 68**,** 241-251.

MYERS, E., STARTUP, H. & FREEMAN, D. 2011. Cognitive behavioural treatment of insomnia in individuals with persistent persecutory delusions: A pilot trial. *Journal of Behavior Therapy and Experimental Psychiatry,* 42**,** 330-336.

NAKAJIMA, A., AOYAMA, Y., NGUYEN, T. T. L., SHIN, E. J., KIM, H. C., YAMADA, S., NAKAI, T., NAGAI, T., YOKOSUKA, A., MIMAKIC, Y., OHIZUMI, Y. & YAMADA, K. 2013. Nobiletin, a citrus flavonoid, ameliorates cognitive impairment, oxidative burden, and hyperphosphorylation of tau in senescence-accelerated mouse. *Behavioural Brain Research,* 250**,** 351-360.

O'DONNELL, K. C. & GOULD, T. D. 2007. The behavioral actions of lithium in rodent models: Leads to develop novel therapeutics. *Neuroscience and Biobehavioral Reviews,* 31**,** 932-962.

O'NEILL, J. S., MAYWOOD, E. S., CHESHAM, J. E., TAKAHASHI, J. S. & HASTINGS, M. H. 2008. cAMP-dependent signaling as a core component of the mammalian circadian pacemaker. *Science,* 320**,** 949-953.

OLIE, J. P. & KASPER, S. 2007. Efficacy of agomelatine, a MT1/MT2 receptor agonist with 5-HT2C antagonistic properties, in major depressive disorder. *International Journal of Neuropsychopharmacology,* 10**,** 661-673.

ONOZUKA, H., NAKAJIMA, A., MATSUZAKI, K., SHIN, R. W., OGINO, K., SAIGUSA, D., TETSU, N., YOKOSUKA, A., SASHIDA, Y., MIMAKI, Y., YAMAKUNI, T. & OHIZUMI, Y. 2008. Nobiletin, a citrus flavonoid, improves memory impairment and A beta pathology in a transgenic mouse model of Alzheimer's Disease. *Journal of Pharmacology and Experimental Therapeutics,* 326**,** 739-744.

PREUSSNER, M. & HEYD, F. 2016. Post-transcriptional control of the mammalian circadian clock: implications for health and disease. *Pflugers Archiv-European Journal of Physiology,* 468**,** 983-991.

RACAGNI, G., RIVA, M. A., MOLTENI, R., MUSAZZI, L., CALABRESE, F., POPOLI, M. & TARDITO, D. 2011. Mode of action of agomelatine: Synergy between melatonergic and 5-HT2C receptors. *World Journal of Biological Psychiatry,* 12**,** 574-587.

ROYBAL, K., THEOBOLD, D., GRAHAM, A., DINIERI, J. A., RUSSO, S. J., KRISHNAN, V., CHAKRAVARTY, S., PEEVEY, J., OEHRLEIN, N., BIRNBAUM, S., VITATERNA, M. H., ORSULAK, P., TAKAHASHI, J. S., NESTLER, E. J., CARLEZON, W. A., JR. & MCCLUNG, C. A. 2007. Mania-like behavior induced by disruption of CLOCK. *Proceedings of the National Academy of Sciences of the United States of America,* 104**,** 6406-6411.

SHI, D., NIKODIJEVIC, O., JACOBSON, K. A. & DALY, J. W. 1993. Chronic caffeine alters the density of adenosine, adrenergic, cholinergic, GABA, and serotonin receptors and calcium channels in mouse-brain. *Cellular and Molecular Neurobiology,* 13**,** 247-261.

SINGH, N., HALLIDAY, A. C., THOMAS, J. M., KUZNETSOVA, O. V., BALDWIN, R., WOON, E. C. Y., ALEY, P. K., ANTONIADOU, I., SHARP, T., VASUDEVAN, S. R. & CHURCHILL, G. C. 2013. A safe lithium mimetic for bipolar disorder. *Nature Communications,* 4**,** 1332.

SONG, J., SJOLANDER, A., JOAS, E., BERGEN, S. E., RUNESON, B., LARSSON, H., LANDEN, M. & LICHTENSTEIN, P. 2017. Suicidal Behavior During Lithium and Valproate Treatment: A Within-Individual 8-Year Prospective Study of 50,000 Patients With Bipolar Disorder. *American Journal of Psychiatry,* 174**,** 795-802.

SVENNINGSSON, P., NOMIKOS, G. G. & FREDHOLM, B. B. 1995. Biphasic changes in locomotor behavior and in expression of messenger-RNA for NGFI-A and NGFI-B in rat striatum following acute caffeine administration. *Journal of Neuroscience,* 15**,** 7612-7624.

TAKAHASHI, J. S. 2017. Transcriptional architecture of the mammalian circadian clock. *Nature Reviews Genetics,* 18**,** 164-179.

VITATERNA, M. H., KO, C. H., CHANG, A. M., BUHR, E. D., FRUECHTE, E. M., SCHOOK, A., ANTOCH, M. P., TUREK, F. W. & TAKAHASHI, J. S. 2006. The mouse Clock mutation reduces circadian pacemaker amplitude and enhances efficacy of resetting stimuli and phase-response curve amplitude. *Proceedings of the National Academy of Sciences of the United States of America,* 103**,** 9327-9332.

WORLD HEALTH ORGANISATION 2014. *ICD-10 classification of mental and behavioural disorders: clinical descriptions and diagnostic guidelines; 10th Revision,* Geneva.

YABUKI, Y., OHIZUMI, Y., YOKOSUKA, A., MIMAKI, Y. & FUKUNAGA, K. 2014. Nobiletin treatment improves motor and cognitive deficits seen in MPTP-induced parkinson model mice. *Neuroscience,* 259**,** 126-141.

YANG, S., VAN DONGEN, H. P. A., WANG, K., BERRETTINI, W. & BUCAN, M. 2009. Assessment of circadian function in fibroblasts of patients with bipolar disorder. *Molecular Psychiatry,* 14**,** 143-155.

YI, L. T., XU, H. L., FENG, J., ZHAN, X., ZHOU, L. P. & CUI, C. C. 2011. Involvement of monoaminergic systems in the antidepressant-like effect of nobiletin. *Physiology & Behavior,* 102**,** 1-6.

YOO, S. H., YAMAZAKI, S., LOWREY, P. L., SHIMOMURA, K., KO, C. H., BUHR, E. D., SIEPKA, S. M., HONG, H. K., OH, W. J., YOO, O. J., MENAKER, M. & TAKAHASHI, J. S. 2004. PERIOD2 :: LUCIFERASE real-time reporting of circadian dynamics reveals persistent circadian oscillations in mouse peripheral tissues. *Proceedings of the National Academy of Sciences of the United States of America,* 101**,** 5339-5346.

ZHANG, R., LAHENS, N. F., BALLANCE, H. I., HUGHES, M. E. & HOGENESCH, J. B. 2014. A circadian gene expression atlas in mammals: Implications for biology and medicine. *Proceedings of the National Academy of Sciences of the United States of America,* 111**,** 16219-16224.

Chapter 5: Lithium-Induced Perturbations of the Phosphoinositide Cycle Alter Molecular Circadian Rhythms

5.1 Introduction

Sleep and circadian rhythm disruptions are a core feature of BPD. Patients have been found to exhibit gross sleep disruptions including reduced sleep needs and fragmented sleep patterns (Harvey, 2008). This is in combination with reduced amplitude behavioural and molecular rhythms, where we (in Chapters 3 and 4) and others have shown tendencies for a lengthened molecular clock period (Rock et al., 2014, Yang et al., 2009, McCarthy et al., 2013, Bamne et al., 2013). Briefly, such clocks are composed of multiple interlocking TTFLs, which regulate aspects of physiological, mental, and behavioural well-being (summarised in Chapter 1, *Figure 1.2*) (Takahashi, 2017).

5.1.1 The known circadian consequences of lithium treatment

The mood-stabiliser lithium continues to be a first line therapy for BPD. Despite being almost 70 years since its serendipitous discovery, there is still great uncertainty as to how lithium exhibits its therapeutic effects (Cade, 1949). With blood plasma levels being maintained at 0.6-1.5mM, one hypothesis is that lithium normalises circadian disruptions. Lithium has consistently shown period lengthening and amplitude enhancing effects in a multitude of species including rodents and humans (Kripke and Wyborney, 1980, Johnsson et al., 1979, Li et al., 2012, Geoffroy et al., 2017). Whilst the amplitude effects are believed to be due to glycogen synthase kinase 3β (GSK3β) inhibition through increases in *Per2* gene transcription, specific GSK3β inhibition induces period shortening (Li et al., 2012). This suggests that the period lengthening effects occur through independent and as yet elusive mechanisms.

5.1.2 Lithium-induced inhibition of inositol monophosphatase

As a polypharmacological agent, lithium has numerous molecular targets including four magnesium-dependent phosphomonoesterases: inositol monophosphatase (IMPase) and inositol polyphosphate 1-phosphatase (IPPase) of the phosphoinositide (PI) pathway, fructose 1,6-bisphosphatase involved in gluconeogenesis, and bisphosphate 3' nucleotidases, which regulates AMP production (York et al., 1995). Specifically, the role of the phosphoinositide (PI) pathway has received much attention due to the early discovery that lithium is a potent inhibitor of IMPase (Berridge et al., 1982).

As seen in *Figure 5.1*, this G-protein coupled receptor (GCPR) pathway is initiated with the binding of an extracellular ligand to the G_q-coupled receptor at the cell surface. Ligand binding activates phospholipase C (PLC) which hydrolyses phosphatidylinositol 4,5-bisphosphate (PIP2) into the important second messengers inositol 1,4,5-trisphosphate (IP3) and diacylglycerol (DAG), which then initiate their own signal transduction cascades. DAG induces a conformational change within protein kinase C (PKC), stimulating it to phosphorylate subsequent downstream targets (Berridge, 1984). IP3 on the other hand, as well as inducing intracellular calcium mobilisation, is successively dephosphorylated to phosphatidylinositol 4,5-bisphosphate (IP2), where IPPase then aids the conversion to inositol monophosphate (IP). The key enzyme IMPase then catalyses the conversion of IP to myo-inositol, the most abundant inositol stereoisomer. Myo-inositol is then used to regenerate PIP2 and the cycle continues (Berridge et al., 1989). Furthermore, D-glucose 6-phosphate is converted to IP via the enzyme inositol-3-phosphate synthase 1 (ISYNA1),

establishing a *de novo* source of myo-inositol biosynthesis (Eisenberg Jr and Parthasarathy, 1987). The sodium myo-inositol co-transporters (SMIT) also increase intracellular myo-inositol levels by extruding sodium ions against their concentration gradient (van Calker and Belmaker, 2000). The multitude of molecules implicated in this pathway shows the intricacies of such a system and highlights the significant impact pharmacological perturbations may have.

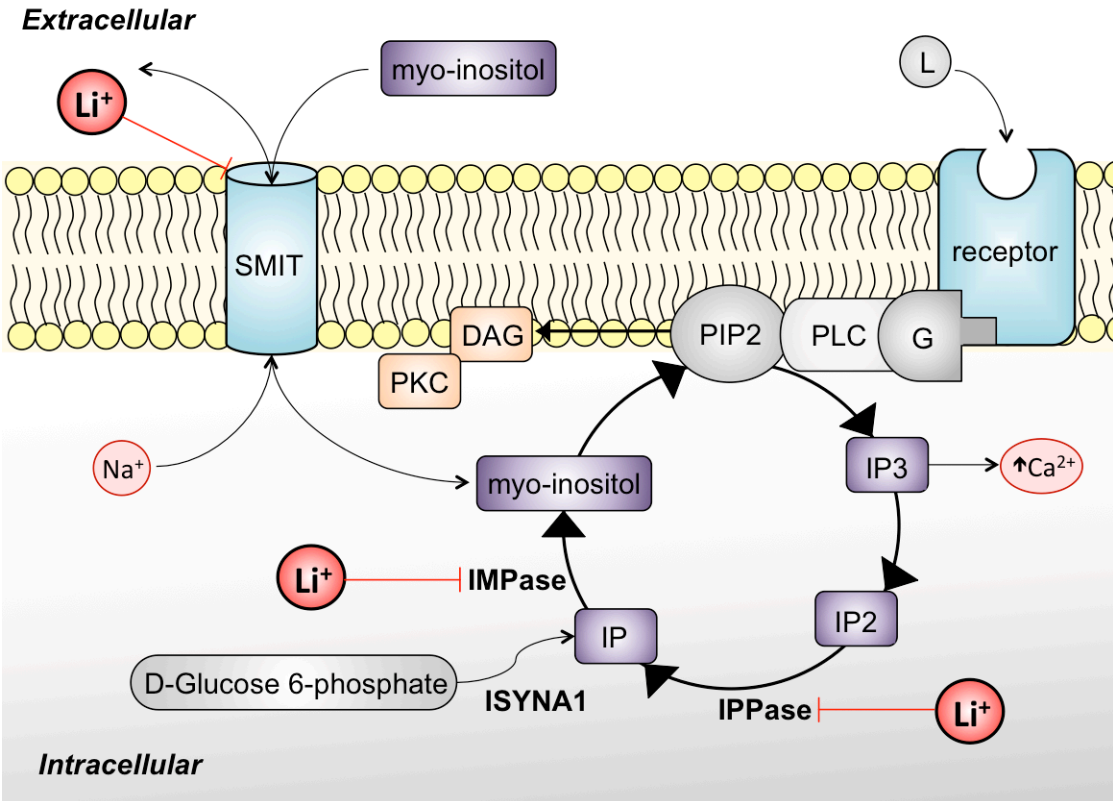

Figure 5.1. **Schematic representation of the phosphoinositide pathway.** Lithium inhibits multiple components of the PI pathway including the SMITs, preventing extracellular myo-inositol entry, IPP, preventing IP generation, and IMPase reducing myo-inositol recycling and *de novo* biosynthesis. Reduced myo-inositol results in less PIP2 regeneration and perturbs the actions of the second messengers IP3 and DAG, which influence multiple components of this signalling pathway. L: ligand, G: G-protein, Na^+: sodium ions, Li^+: lithium ions, Ca^{2+}: calcium ions, other abbreviations can be found in the text.

5.1.3 The inositol depletion hypothesis

By displacing magnesium ions, lithium uncompetitively inhibits IMPase, causing an accumulation of IP, with depleted myo-inositol levels. This idea formed the foundation of Michael Berridge's inositol depletion hypothesis, which stated that IMPase antagonism and myo-inositol depletion may be responsible for lithium's therapeutic effects (Berridge et al., 1982). As myo-inositol cannot then regenerate PIP2, there is an overall reduction in second messenger signalling and so lithium may act to dampen overstimulated neural networks.

Initial studies performed on rodent models have confirmed lithium-induced IMPase inhibition, as LiCl decreased cortical myo-inositol levels by 30%, where levels remained reduced for up to 48h (Allison and Stewart, 1971). Similarly, IP levels were elevated with an associative 2.5 fold increase in the cortex, which suggested that indeed IMPase was being inhibited (Allison et al., 1976). Additionally, it was found that 0.8mM lithium was required to reduce the maximal enzymatic activity by 50%, where inhibition was observed from 0.3mM upwards (Naccarato et al., 1974).

Myo-inositol has poor BBB (3% efficiency) and cell permeability, where regional concentrations vary depending on cellular synthesis, conservation, and flux mechanisms (Patishi et al., 1996, Lubrich et al., 2000, Fisher et al., 2002). A major influx route is via the SMITs, which are abundant within the neurones and glial cells (Spector and Lorenzo, 1975, Inoue et al., 1996). Further, intracerebroventricular injections of myo-inositol can normalise IMPase inhibitor-induced behaviours, suggesting that higher concentrations can impact cellular myo-inositol entry (Belmaker et al., 1998, Singh et al., 2013). Lithium can

also further deplete intracellular myo-inositol via inhibition of the SMITs and reduce SMIT mRNA levels (Lubrich and van Calker, 1999). Interestingly, additional mood-stabilisers such as valproic acid and carbamazepine also function via similar mechanisms, further suggesting that inositol depletion may be implicated in inducing euthymia (Williams et al., 2002, Lubrich et al., 2000).

Curiously, simply generating *Impa1*$^{-/-}$ or *Impa2*$^{-/-}$ mice is insufficient to fully replicate lithium's effects, suggesting a more complex entanglement in the PI pathway (Cryns et al., 2007, Cryns et al., 2008). Also, BPD patients with abnormalities in their PI signalling pathway have been noted through reduced levels of IMPase enzyme activity, as well as *Impa1* and *Impa2* expression in lymphoblasts and lymphocytes (Shamir et al., 1998, Nemanov et al., 1999, Yoon et al., 2001). As lower enzyme levels have also been observed in post-mortem brain samples, how this is implicated in BPD pathophysiology is still ambiguous, as this should indicate lower cellular myo-inositol levels (Belmaker et al., 1998). However, as follow up studies have failed to replicate such data, there could be great inter-individual variability or it is plausible that elevated IMPase is cell-type and region specific, and therefore undetected when coarsely dividing the brain into frontal, occipital, and cerebellar regions (Shapiro et al., 2000).

Pharmacological tools have proven to be effective at investigating the PI pathway. A drug 500-1000 times more effective at inhibiting IMPase is the polar bisphosphonate L690,330. The compound was created through targeted modification of IP, but was found to have low BBB and cell permeability (Atack et al., 1993). This led to the development of the esterified pro-drug L690,488, which becomes hydrolysed to L690,330 within the cell. This intracellular

neutralisation of the charged molecules enabled the drug to become more cell permeant (lithium: IC50-0.8mM, L690,330: IC50-0.3μM) (Atack et al., 1994, Atack et al., 1993). Moreover, recent findings demonstrate that a re-purposed drug, labelled a lithium mimetic, also functions via IMPase inhibition (ebselen: IC50-1.5μM). Ebselen reduced IMPase activity, was clinically safe, and reduced amphetamine-induced hyperactivity in mice (Singh et al., 2013). As such compounds function via IMPase inhibition, the inositol depletion hypothesis provides a solid foundation warranting further investigation.

5.1.4 Inositol recycling within the circadian system

Interestingly, the effects of lithium on inositol recycling have been noted in the master clock, the SCN, where lithium elevated IP3, IP2, and IP levels (Nadakavukaren et al., 1990). Subsequently, Mason and Biello found that the application of lithium dose-dependently reduced the spontaneous firing rate of SCN neurones. These effects were normalised with myo-inositol, where similar isomers showed no such effects (Mason and Biello, 1992). This suggests that the cells of the SCN contain a functioning and lithium responsive PI system.

5.1.5 Aims

Thus, we know that lithium-induced circadian period lengthening and amplitude increasing effects occur via independent pathways, that IMPase is inhibited at therapeutic concentrations, and that the master clock contains a lithium-sensitive PI pathway. With this in mind, we sought to determine whether targeting IMPase within the PI pathway was responsible for lithium-induced period lengthening.

5.2 Results

5.2.1 Cells exhibited differential responses to LiCl treatment

To identify an appropriate *in vitro* model that mimics lithium's *in vivo* period lengthening and amplitude enhancing effects, three distinct cell lines were screened. LiCl between 0.3-30mM was assessed as circadian effects have previously been reported and cell viability was maintained (*Figures 5.2J-L*).

The *Bmal::Luc* MMHD3 murine pre-hepatocytes presented with the largest period effects with significant amplitude enhancement (*Figures 5.2A-C*). Circadian period lengthening was observed with 20mM and 30mM LiCl, which induced 2.5h and 3.4h increases respectively (vehicle: 23.98±0.08, 20mM: 26.48±0.49, 30mM: 27.39±0.41 h). 10mM LiCl presented a non-significant trend of 41min lengthening (24.67±0.16 h). Moreover, amplitude was enhanced by 18% at 10mM, 26% at 20mM, and 31% at 30mM LiCl (vehicle: 515.10±1.92, 10mM: 606.30±6.08, 20mM: 650.70±17.10, 30mM: 672.30±37.95 RLU). Subsequently, a *Bmal::Luc* human fibroblast line was assessed (*Figures 5.2D-F*). Cells showed period lengthening at 20mM and 30mM by 50min to 1.8h (vehicle: 24.54±0.17, 20mM: 25.47±0.10, 30mM: 26.38±0.10 h). Additionally, amplitude enhancement was observed from 10mM to 30mM by 15-38% (vehicle: 3.53±0.05, 10mM: 4.12±0.13, 20mM: 4.05±0.14, 30mM: 4.87±0.07 RLU).

In stark contrast, the human osteosarcoma *Bmal::Luc* U2OS cells presented with no period change at concentrations up to 30mM. Moreover, dose-dependent amplitude dampening was observed from 3mM-30mM ranging between 20-36% (vehicle: 4574±153.80, 3mM: 3650±174.50, 10mM:

3457±346.20, 30mM: 2907±521.80 RLU) (*Figures 5.2G-I*). Surprisingly cell-type dependent effects of lithium on circadian rhythms have never been reported in the literature. However, as period was the parameter of primary interest and the MMHD3 cells appeared most sensitive to LiCl-induced lengthening, these cells were used for the majority of subsequent experiments.

5.2.2 Inositol-less media potentiated period lengthening

In order to investigate whether the PI pathway is implicated in inducing period changes, the effects of inositol depletion were first assessed. As seen in *Figure 5.1*, there are multiple sources of inositol, a key source being the interstitial fluid or media. Therefore, the effects of control media containing standard concentrations of 40μM myo-inositol were compared against custom-made inositol-less media. Cell-type specific responses were observed as seen in *Figures 5.3A-C*. The inositol-less media alone potentiated circadian period by 1h in the MMHD3 cells (control: 23.66±0.06, inositol-less: 24.72±0.09 h), where again no significant effect was observed in the U2OS cells (control: 23.98±0.16, inositol-less: 24.30±0.07 h). By extension, the expression of IMPA1 protein (30kDa) in the different cell lines was examined through western blot analysis. As seen in *Figures 5.3D-E*, the U2OS cells showed 40% lower expression levels when normalised to β-actin (42kDa), suggesting there may be fundamental differences on the cellular reliance of IMPase activity between these cell lines (MMHD3: 12.36±0.24, U2OS: 8.82±0.25 relative expression).

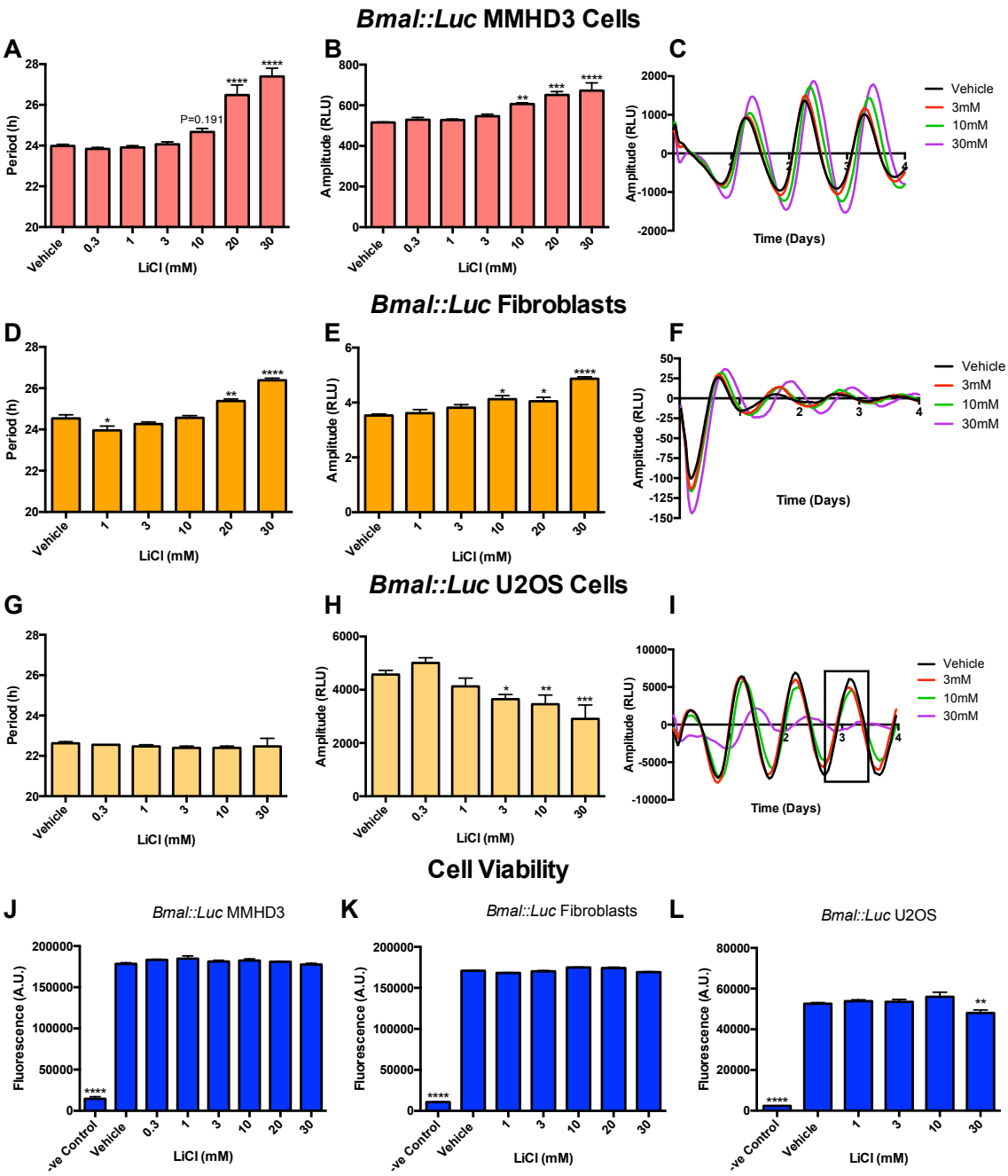

Figure 5.2. **Lithium lengthens period and increases amplitude of circadian rhythms in a cell-specific manner.** The dose-dependent period and amplitude effects of LiCl with representative bioluminescent traces, for *Bmal::Luc* MMHD3 cells (n=4) **(A-C)**, *Bmal::Luc* fibroblasts (n=3) **(D-E)**, and *Bmal::Luc* U2OS cells (n=4) **(G-I)**. Cell viability assay **(J-L)**.

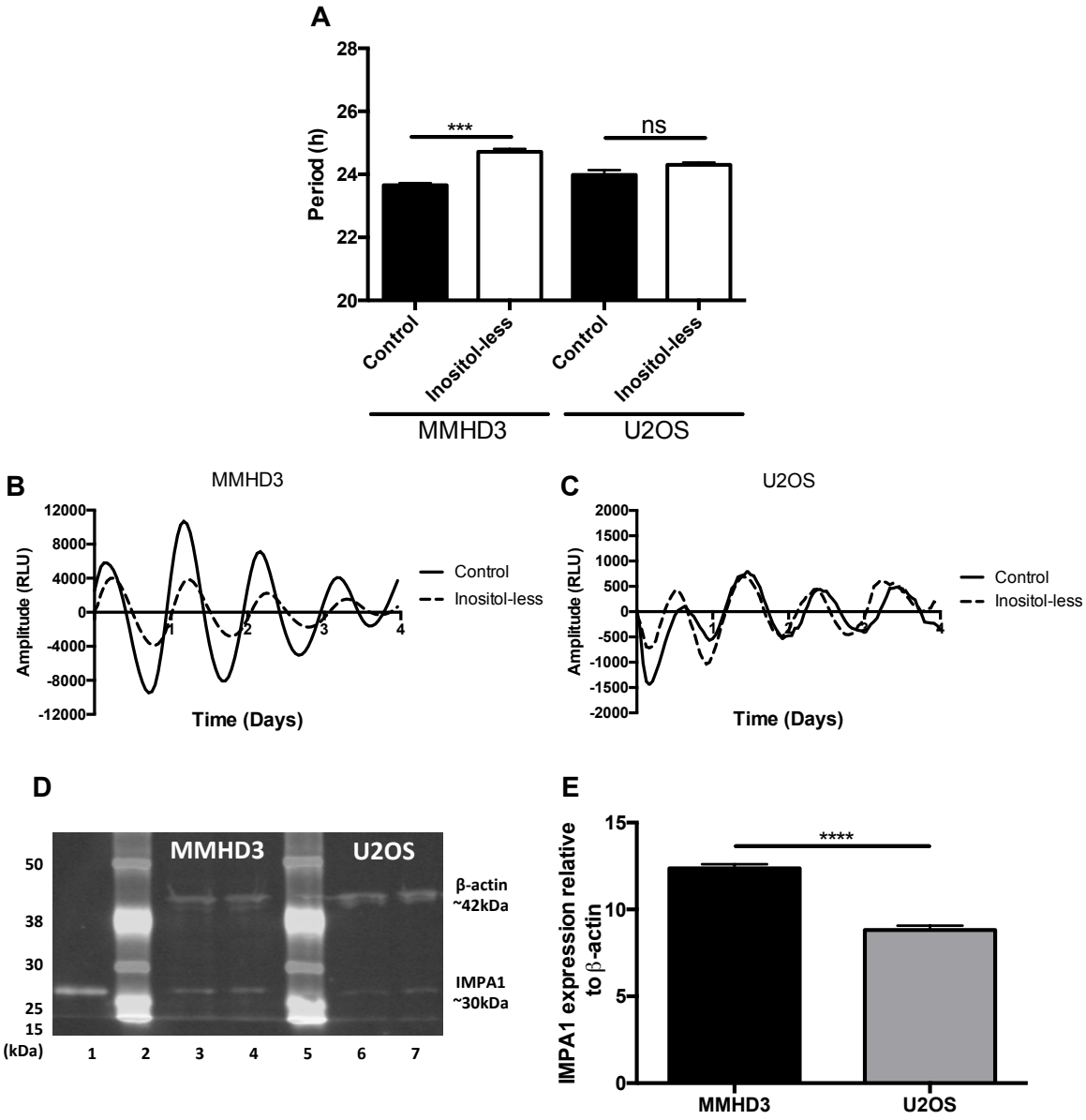

Figure 5.3. **Inositol-less media potentiates period lengthening in the MMHD3 cells. A)** Cells were treated with control media containing 40μM myo-inositol or custom-made inositol-less media and circadian period was examined. **C-D)** Representative luminescence traces for the MMHD3 and U2OS cells. **D-E)** Western blot analysis revealed differential expression of IMPA1 protein in the U2OS cells (wells 6-7; n=5) when compared to the MMHD3 cells (wells 3-4; n=5). 20μg of protein were loaded per well and optical density was assessed. IMPA1 (30kDa) expression was normalised to β-actin (42kDa), where well 1 contained 100ng pure human IMPA1, and wells 2 and 5 contain the chameleon-duo pre-stained protein ladder (markings present on the y-axis).

5.2.3 Inositol-depletion potentiated LiCl-induced period change

As removing extracellular inositol was sufficient to induce period changes in the MMHD3 cells, the effects of targeting both intracellular inositol with LiCl, and extracellular inositol with inositol-less media was assessed. As seen in *Figure 5.4A*, 10mM and 30mM LiCl in standard media conditions induced 49min and 4.2h period lengthening respectively, akin to our aforementioned findings. Again, when comparing media effects alone through comparison of vehicle treated cells, a 1h period lengthening effect was observed. Moreover, cells treated with either 10mM or 30mM LiCl in inositol-less media also lengthened period by 55min and 4.5h respectively (vehicle: 24.77±0.10, 10mM: 25.68±0.10, 30mM: 29.31±0.10 h). Through analysis of dose-response curves, it becomes apparent that inositol-less media potentiated LiCl-induced period lengthening at every concentration. When comparing like concentrations in different medias, period lengthening ranging between 55min-1.3h was observed, as seen in *Figures 5.4B-C*.

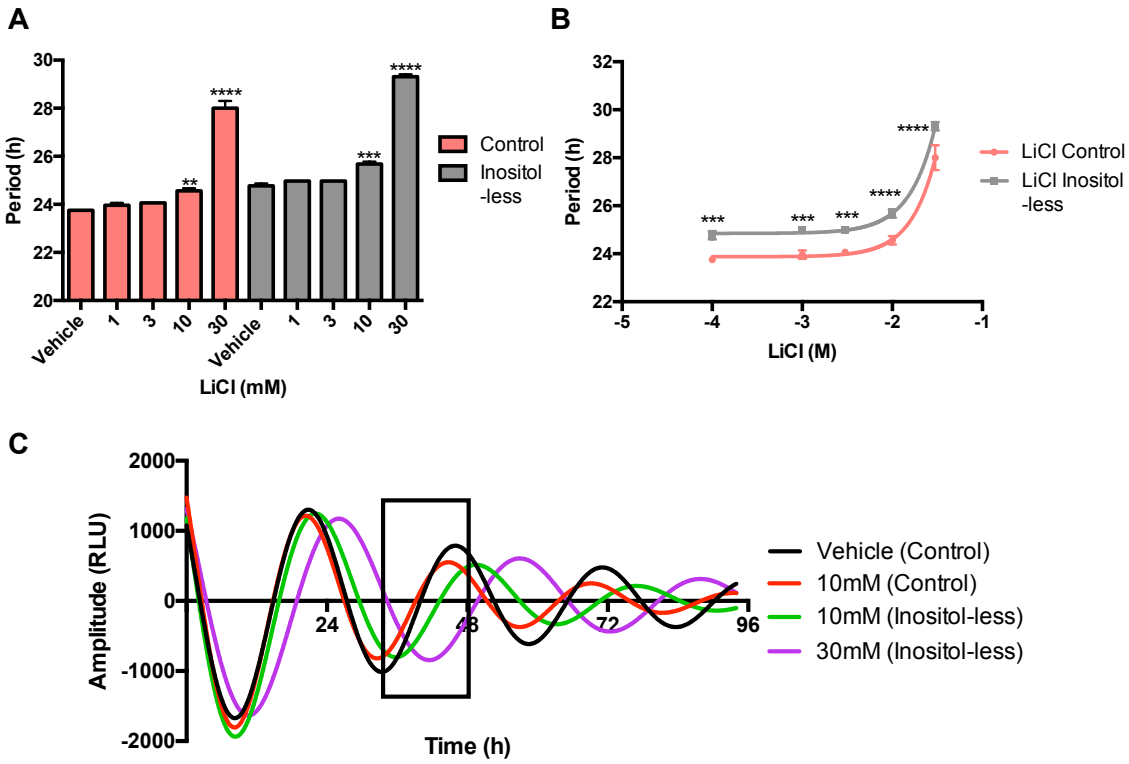

Figure 5.4. **Inositol-less media potentiates LiCl-induced period lengthening in the MMHD3 cells. A)** The period effects observed when treating cells with LiCl in the presence of control inositol-containing or inositol-less media (n=3). **B)** Dose-response curve showing the effects of inositol depletion with LiCl treatment (n=3). **C)** Example traces, highlighting the combined LiCl and media effects on circadian period.

5.2.4 Myo-inositol did not rescue LiCl-induced period effects in vitro

Given that lithium inhibits IMPase and lengthens the period of the molecular clock in the MMHD3 cells, the effects of co-administering myo-inositol was tested under control media conditions (*Figures 5.5A-B*). We hypothesised that exogenous myo-inositol would normalise the depleted intracellular concentrations and thereby revert the circadian period phenotype observed. As neither 40μM nor 1mM myo-inositol affected osmolality, measured using an osmometer, both concentrations were tested in the presence of LiCl. 30mM LiCl induced significant period lengthening by 3.2h. Despite showing a trend, treatment with either 40μM or 1mM myo-inositol failed to significantly reverse the period lengthening effect of lithium (vehicle: 22.81±0.31, 30mM LiCl: 25.98±0.29, +40μM myo-inositol: 26.06±0.60, +1mM myo-inositol: 25.20±0.34 h). As no significant difference was observed when compared to lithium treatment alone, myo-inositol did not appear to normalise LiCl-induced period lengthening.

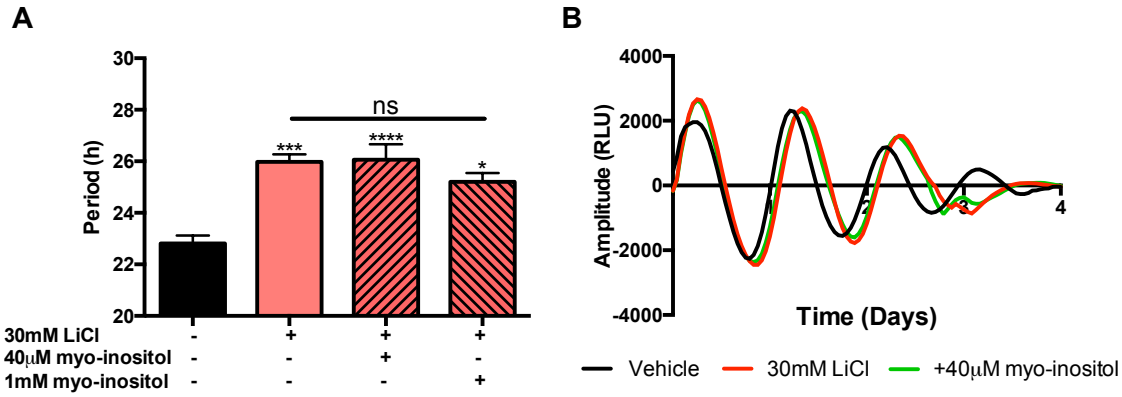

Figure 5.5. **Myo-inositol does not reverse LiCl-induced period effects in the MMHD3 cells. A)** The effects of treating MMHD3 cells with 30mM LiCl in the presence of either 40μM or 1mM myo-inositol (n=6). **B)** Representative bioluminescence traces highlighting the effects described in the bar graph.

5.2.5 LiCl reduced cellular myo-inositol entry

As lithium has previously been shown to reduce SMIT expression (Lubrich and van Calker, 1999), to determine whether exogenous myo-inositol was entering the intracellular environment, [^{3}H] myo-inositol content was examined in the MMHD3 cells (*Figures 5.6A-B*). Approximate baseline myo-inositol levels, denoted by normalised counts per minute after 1min, showed that LiCl reduced intracellular myo-inositol by 2.4 fold (1min → vehicle: 163.30±24.06, LiCl: 68.88±9.30 counts per minute/µg/mL). Moreover, it was found that 30mM LiCl, showed reduced intracellular myo-inositol levels at 1, 3, and 10min by 58%, 59%, and 36% respectively (3min→ vehicle: 224.50±4.52, LiCl: 92.60±5.48; 10min → vehicle: 261.40±27.02, LiCl: 167.80±16.07 counts per minute/µg/mL). The area under the curve analysis found that LiCl reduced [^{3}H] myo-inositol content by 1.6 times (*Figure 5.6C*).

As radioactivity assays were performed after 48h of LiCl treatment, sufficient time had elapsed for the cells to accommodate drug-induced gene expression changes. The mRNA levels of *Slc5a3*, encoding SMIT1 were assessed after 24h and 48h of 30mM LiCl or NaCl treatment in the MMHD3 cells (*Figure 5.6D*). Gene expression was normalised to the housekeeping gene *Gapdh*, for which baseline expression showed with no significant effects. After 24h and 48h of LiCl treatment *Slc5a3* expression was reduced by 29% and 48% respectively, when compared to NaCl (NaCl → 0h: 0.83±0.06, 24h: 0.58±0.03, 48h: 0.64±0.06; LiCl → 0h: 0.68±0.08, 24h: 0.41±0.07, 48h: 0.33±0.09 relative expression).

In contrast to LiCl, the potent IMPase inhibitor L690,488 showed high specificity for the IMPase enzyme, with no reported effects on the SMITs (Atack

et al., 1994). It was hypothesised that a drug which reduces intracellular myo-inositol should enhance SMIT expression to aid myo-inositol homeostasis. Indeed, 24h and 48h of 3μM L690,488 treatment elevated *Slc5a3* expression by 2.3 and 2.1 fold respectively, when compared to vehicle treated cells (*Figure 5.6E)* (vehicle → 0h: 0.75±0.03, 24h: 0.52±0.05, 48h: 0.54±0.05; L690,488 → 0h: 0.84±0.05, 24h: 1.22±0.06, 48h: 1.13±0.13 relative expression).

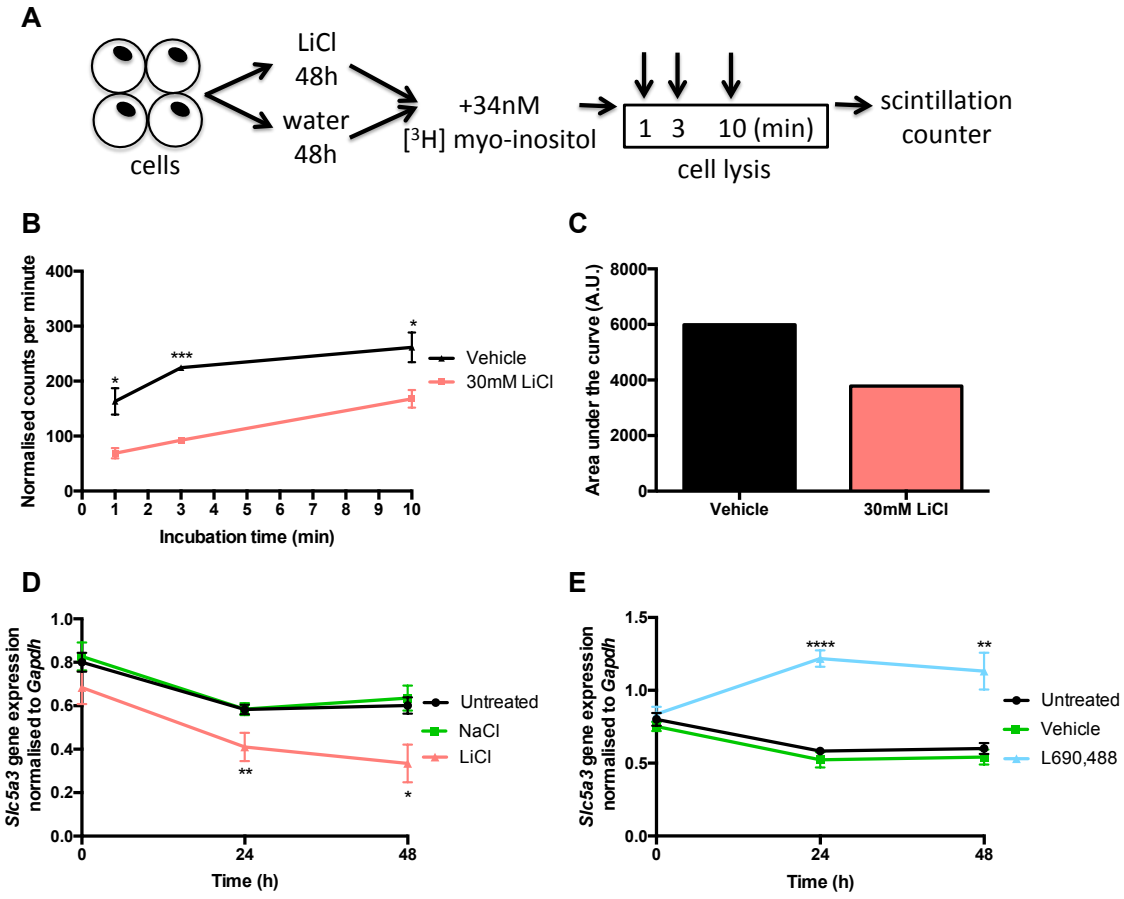

Figure 5.6. **LiCl reduces intracellular entry of myo-inositol in the MMHD3 cells. A)** Schematic representation of the protocol implemented to assess intracellular [3H] myo-inositol content. Cells were treated with 30mM LiCl or vehicle for 48h after which 34nM [3H] myo-inositol was added and intracellular myo-inositol content was examined. **B)** The consequences of incubating cells with 30mM LiCl on cellular myo-inositol concentrations (n=3). **C)** Area under the curve analysis showing the overall [3H] myo-inositol counts per minute following LiCl or vehicle treatment. *Slc5a3* gene expression after 24h and 48h of treatment with LiCl (n=4) **(D)** or 3μM L690,488 (n=4) **(E)**. Relative gene expression data is presented after normalisation to *Gapdh*.

5.2.6 Small molecule IMPase inhibitors partially mimicked the effects of LiCl

To further clarify whether IMPase antagonism could be responsible for LiCl-induced period lengthening, two small molecule IMPase inhibitors were tested on the MMHD3 cells- L690,488 and ebselen at concentrations where cell viability was moderately reduced (*Figures 5.7C-D*). It was hypothesised that both drugs would lengthen period, with potentiated effects under inositol-less conditions.

The IMPase inhibitor L690,488 was found to induce significant period lengthening at 1 and 3μM concentrations under inositol-containing conditions by 3.4 and 9.3h respectively, where 0.3μM showed a non-significant trend of 2.4h lengthening (vehicle: 22.90±0.22, 0.3μM: 25.33±1.50, 1μM: 26.25±0.72, 3μM: 32.15±0.03 h). It was then found that under inositol-less conditions, 1μM L690,488 lengthened period by 4.3h, thereby displaying trends for potentiation by 54min (vehicle: 24.10±0.40, 0.3μM: 25.80±1.65, 1μM: 28.43±0.19, 3μM: 28.55±0.68 h) (*Figures 5.7A*, E).

Ebselen showed similar but more subtle effects as seen in *Figures 5.7B, E*. Period lengthening by 2.9h was observed at 30μM concentrations under control media conditions (vehicle: 23.00±0.20, 30μM: 25.90±0.40 h). Similarly, under inositol-less conditions, a 2.6h period lengthening effect was observed with 30μM ebselen (vehicle: 23.50±0.25, 30μM: 26.07±0.82 h). A trend for greater lengthening was observed with 10μM ebselen, as inositol-less conditions further lengthened period by 33min (10μM → control: 23.35±0.20, inositol-less: 23.90±0.55 h).

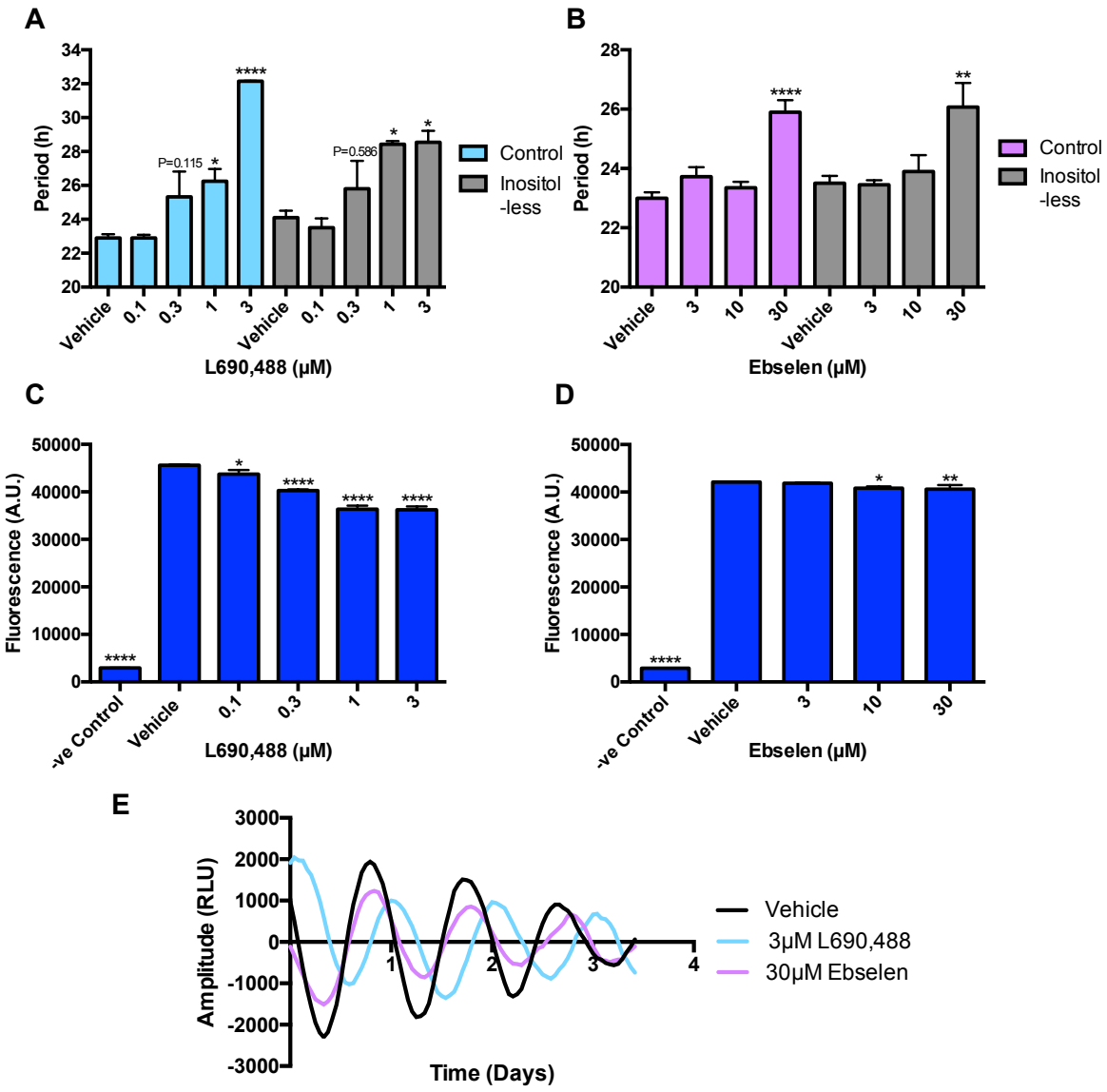

Figure 5.7. **Small molecule inhibitors of IMPase lengthen circadian period in the MMHD3 cells. A)** The period changes observed with L690,488 treatment under control or inositol-less conditions (n=4). **B)** The effects of ebselen on circadian period under control or inositol-less medias (n=4). **C-D)** Cell viability assay. **E)** Example traces of period lengthening induced by small molecule inhibitors under control media conditions.

5.2.7 Myo-inositol rescued small molecule induced period lengthening

In accordance with assessing the reversibility of LiCl-induced period lengthening with myo-inositol, the idea that myo-inositol should normalise small inhibitor induced period lengthening was also tested, as there is currently no evidence suggesting that these molecules inhibit the SMITs (*Figures 5.8A-B*). By using the MMHD3 cells, it was found that co-administering 3μM L690,488 with an additional 40μM myo-inositol under inositol-containing media conditions grossly reduced period lengthening by 4.1h (vehicle: 22.25±0.31, L690,488: 27.35±0.30, +40μM myo-inositol: 23.25±0.13 h). Similarly, 30μM ebselen alone also induced 5.2h period lengthening, an effect which was reversed by 4.8h after myo-inositol supplementation (ebselen: 27.47±0.52, +40μM myo-inositol: 22.67±0.67 h). Thus, myo-inositol reversed small molecule IMPase inhibitor induced period lengthening.

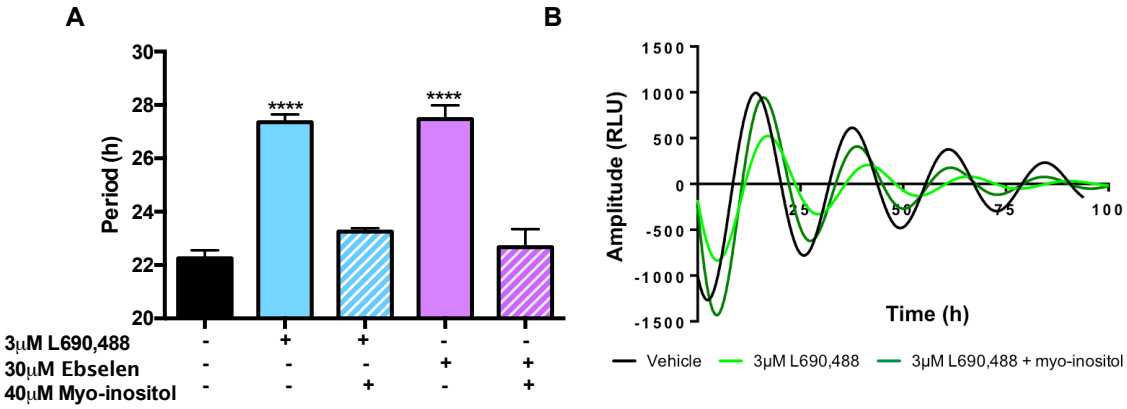

Figure 5.8. **Myo-inositol co-administration with small molecule IMPase inhibitors normalises drug induced period lengthening in the MMHD3 cells.** **A)** The consequences of treating MMHD3 cells with 3μM L690,488 and 30μM ebselen with 40μM myo-inositol (n=4). **B)** Representative bioluminescence diagram highlighting the effects of L690,488 and myo-inositol co-administration.

5.2.8 L690,488 mimics lithium-induced changes in circadian gene expression

Lithium has previously been shown to impact the molecular clock by affecting core and accessory clock gene expression (Osland et al., 2011). Therefore, as well as validating these findings in the MMHD3 cells, it was hypothesised that L690,488 should also impact the molecular clock in a similar manner. Cells were treated for 48h after dexamethasone-induced cell synchronisation and transcript levels were assessed. As seen in *Figures 5.9A-B*, LiCl elevated *Per2* gene transcription by 69% when compared to NaCl, where L690,488 elevated *Per2* by 38% (NaCl: 0.35±0.05, LiCl: 0.59±0.04, vehicle: 0.32±0.03, L690,488: 0.44±0.02 relative expression).

Similarly, as depicted in *Figures 5.9C-D*, LiCl also enhanced *Bmal* gene expression by 94%, where L690,488 induced a 93% increase (NaCl: 0.17±0.01, LiCl: 0.33±0.05, vehicle: 0.14±0.02, L690,488: 0.27±0.03 relative expression). Neither drug induced significant changes to *Per1* transcript levels in the MMHD3 cells (*Figures 5.9E-F*). This may be due to low expression levels, as basal *Per2* and *Bmal* were expressed at 32 and 15 times *Per1* levels respectively when analysing the untreated cell values (*Per1*: 0.01±0.00, *Per2*: 0.33±0.02, *Bmal*: 0.15±0.01 relative expression). It should be acknowledged that as only a single time point was examined, analysis of gene expression changes between compounds should be treated with caution. This is because it is plausible that as well as inducing amplitude changes, the drugs may be inducing phase change, and so future studies should use multiple time points to account for these effects.

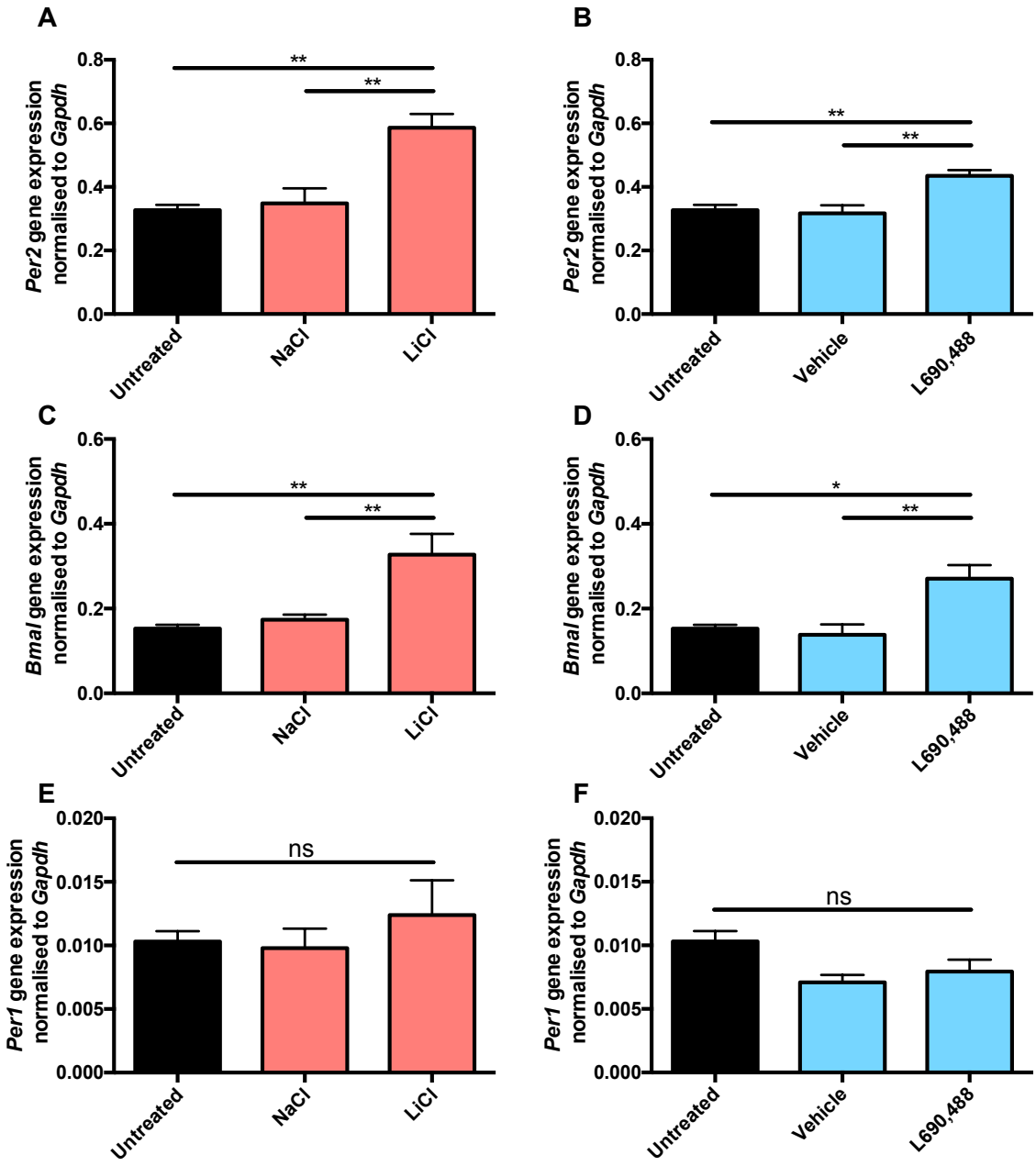

Figure 5.9. **LiCl and L690,488 elevate *Per2* and *Bmal* gene expression in the MMHD3 cells.** The effects of 48h of 30mM LiCl, 30mM NaCl, 3μM L690,488 or vehicle treatment on circadian gene expression. The effect of LiCl on *Per2* **(A)**, *Bmal* **(C)** and *Per1* transcript expression **(E)**. The effects of the IMPase inhibitor L690,488 on *Per2* **(B)**, *Bmal* **(D)**, and *Per1* gene expression **(F).** All transcripts were normalised to *Gapdh* (n=4 each).

5.2.9 Impa1 siRNA induced modest period changes in vitro

In addition to pharmacological modulation, genetic perturbation of the PI pathway represents an alternative experimental method worthy of exploration. It was hypothesised that specifically targeting IMPase via siRNA-mediated knockdown of *Impa1* in the MMHD3 cells should also reduce intracellular myo-inositol levels and therefore induce period lengthening. Cells were treated with siRNA for 24h followed by dexamethasone treatment and luminescence recording. Data shown are for concentrations that did not appreciably alter cell viability; 50nM, 25nM, and 12.5nM siRNA were also tested but grossly reduced viability (*Figure 5.10D*). siControl, was used as the non-targeting control, where dose-dependent circadian effects were not observed and therefore combined values were presented. As seen in *Figure 5.10A,* the positive control, 50nM *Csnk1δ* siRNA, induced 2.5h period lengthening, where 3.13nM and 6.25nM *Impa1* siRNA induced significant lengthening, although by 25min and 34min respectively (*siControl*: 23.42±0.04, *Csnk1δ:* 25.88±0.00, 3.13nM *Impa1*: 23.83±0.08, 6.26nM *Impa1*: 23.98±0.08 h).

As changes in *Bmal* gene expression were prominent with L690,488, the effects of *Impa1* specific knockdown on the molecular clock were assessed. It was found that 3.13nM *Impa1* siRNA presented with trends of increased *Bmal* expression when normalised to *Gapdh* by 39%, where 6.25nM significantly increased expression by 156% (*siControl*: 0.85±0.06, 3.13nM: 1.18±0.05, 6.25nM: 2.18±0.34 relative expression) (*Figure 5.10B*). Finally, to confirm that the aforementioned effects were due to gene knockdown, transcript levels in siControl treated vs. siRNA treated wells were compared (*Figure 5.10C*). *Csnk1δ*

expression was reduced by 95%, where 3.13nM and 6.25nM *Impa1* siRNA both reduced transcript levels by 76% (*Csnk1δ* knockdown*:* 4.65±0.38, 3.13nM *Impa1* knockdown: 24.11±3.46, 6.25nM *Impa1* knockdown: 23.51±4.86 %).

5.2.10 Isyna1 siRNA induced modest period changes in vitro

As *Isyna1* encodes the enzyme required for *de novo* myo-inositol biosynthesis from D-glucose 6-phosphate, it was hypothesised that knocking down in this enzyme would reduce intracellular myo-inositol and induce period lengthening. The positive control was identical to that used with *Impa1* knockdown and it was found that 3.13nM *Isyna1* induced no changes in circadian period, where 6.25nM significantly lengthened period but only by 25min (3.13nM *Isyna1*: 23.23±0.08, 6.25nM *Isyna1*: 23.83±0.15 h) (*Figure 5.11A*). When assessing the impact of *Isyna1* on the molecular clock, it was found to have no effect of *Bmal* gene transcription (*Figure 5.11B*). To confirm that these effects were due to *Isyna1* reductions, gene knockdown was assessed (*Figure 5.11C*). Both 3.13nM and 6.25nM *Isyna1* siRNA resulted in 98% reductions to *Isyna1,* where cell viability was maintained (3.13nM *Isyna1* knockdown: 2.36± 0.01, 6.25nM *Isyna1* knockdown: 2.50± 0.01 %) (*Figure 5.11D*).

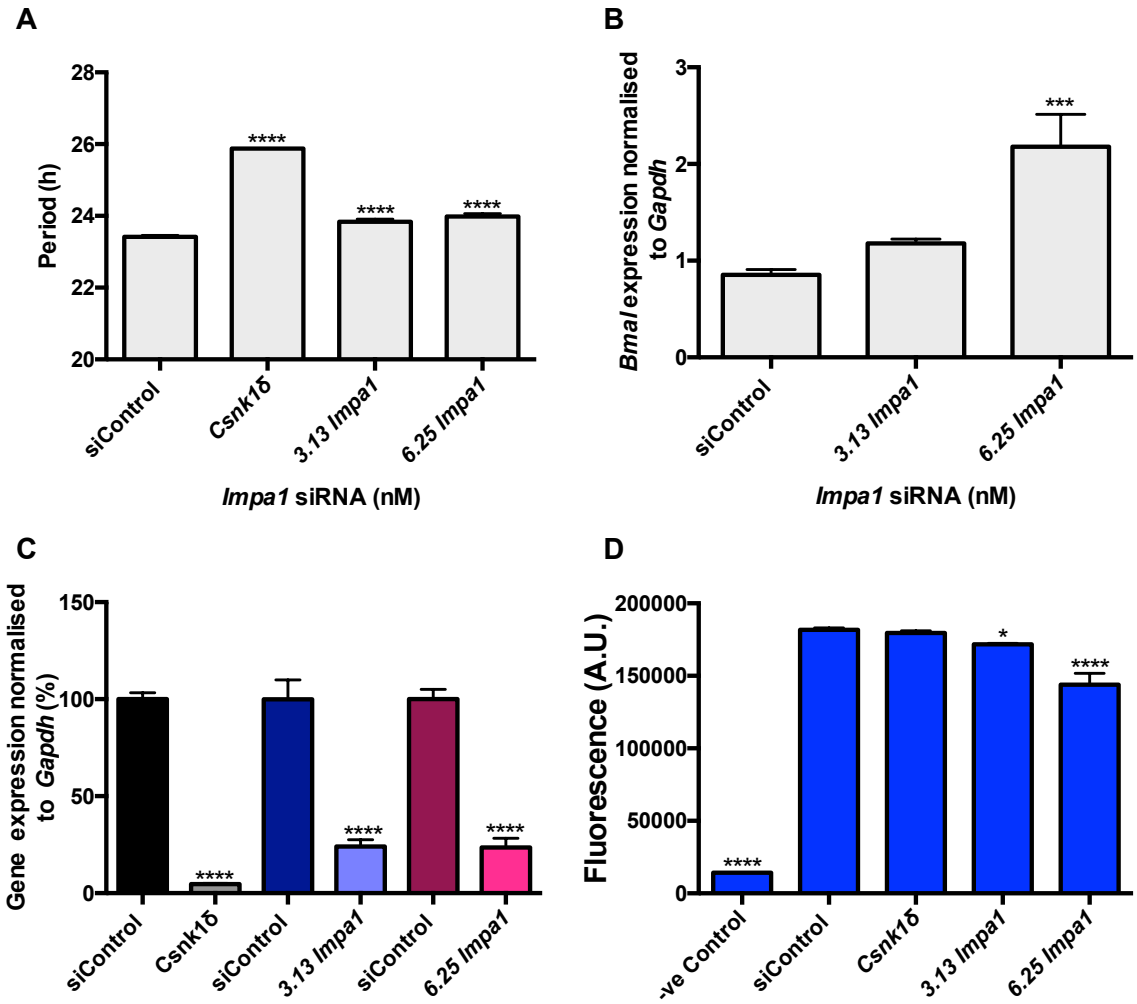

***Figure 5.10. Impa1* siRNA induced subtle changes to circadian parameters in the MMHD3 cells.** The effects of 50nM *Csnk1δ,* 3.23nM, or 6.25nM *Impa1* siRNA on circadian period (n=4) **(A).** As siControl showed no circadian effect, values from both doses were collated (n=8). **B)** The effects of *Impa1* knockdown on the molecular clock were assessed through changes in *Bmal* gene expression (n=4). **C)** Validation of transcript knockdown normalised to *Gapdh* (n=4). **D)** Cell viability assay.

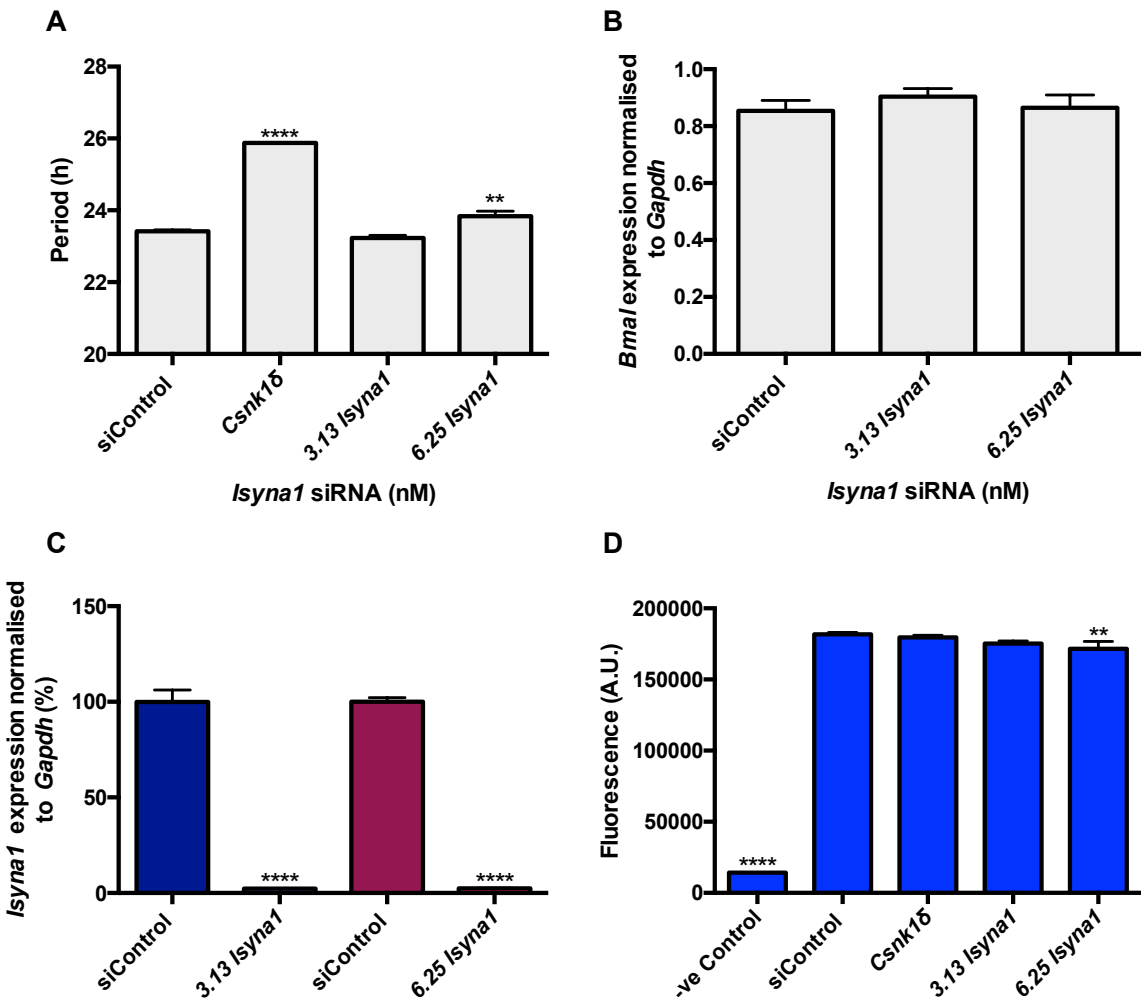

***Figure 5.11. Isyna1* siRNA induced subtle changes to circadian parameters in the MMHD3 cells.** The effects of 50nM *Csnk1δ,* 3.23nM, or 6.25nM *Isyna1* siRNA on circadian period (n=4) **(A)**. As siControl showed no circadian effect, values from both doses were collated (n=8). **B)** The effects of *Isyna1* knockdown *Bmal* gene expression (n=4). **C)** Validation of transcript knockdown normalised to *Gapdh* (n=4). **D)** Cell viability assay.

5.2.11 Understanding the downstream consequences of IMPase inhibition

Lithium modulates multiple signalling pathways involving numerous transcription factors (Malhi et al., 2013). To ascertain which transcription factors are affected by IMPase inhibition, both 30mM LiCl and 3μM L690,488 were tested on the Cignal 45 reporter assay. Interestingly, treatment with either compound induced the activity of the same 6 transcription factors (*Figure 5.12A*). These included ATF2/3/4 of the amino acid deprivation pathway, the transcription factor **C/EBP** (*Figure 5.12B*), **AP1** of the mitogen activated protein kinase (MAPK) pathway (*Figure 5.12C*), NFκB of the inflammatory pathway, and SP1 (as seen in *Table 5.1*). Despite the preliminary nature of some experiments (n=2), specific targets warranting further investigation were identified.

Table 5.1. Summary of the changes in luminescence detected after treatment with 30mM LiCl or 3μM L690,488 in the Cignal 45 reporter assay.

Transcription factor	LiCl (%)	L690,488 (%)
ATF2/3/4	57.32±17.75	137.50±10.87
C/EBP	79.85± 9.09	145.20± 11.57
AP1	48.13±10.58	51.17±2.73
NFκB	62.17±14.46	157.40±35.91
SP1	35.38±8.83	51.99± 18.06

When assessing the effects of vehicle alone, the only transcription factor which displayed increased activity was CBF/NF-Y/YY1, a protein involved with the endoplasmic reticulum stress pathway (*Figure 5.12D*). No other transcription factor displayed changes in activity. Water increased the activity of CBF/NF-Y/YY1 to the same extent as luminescence levels displayed by the positive control and therefore subsequent changes in activity of this transcription factor were disregarded following treatment with LiCl or L690,488.

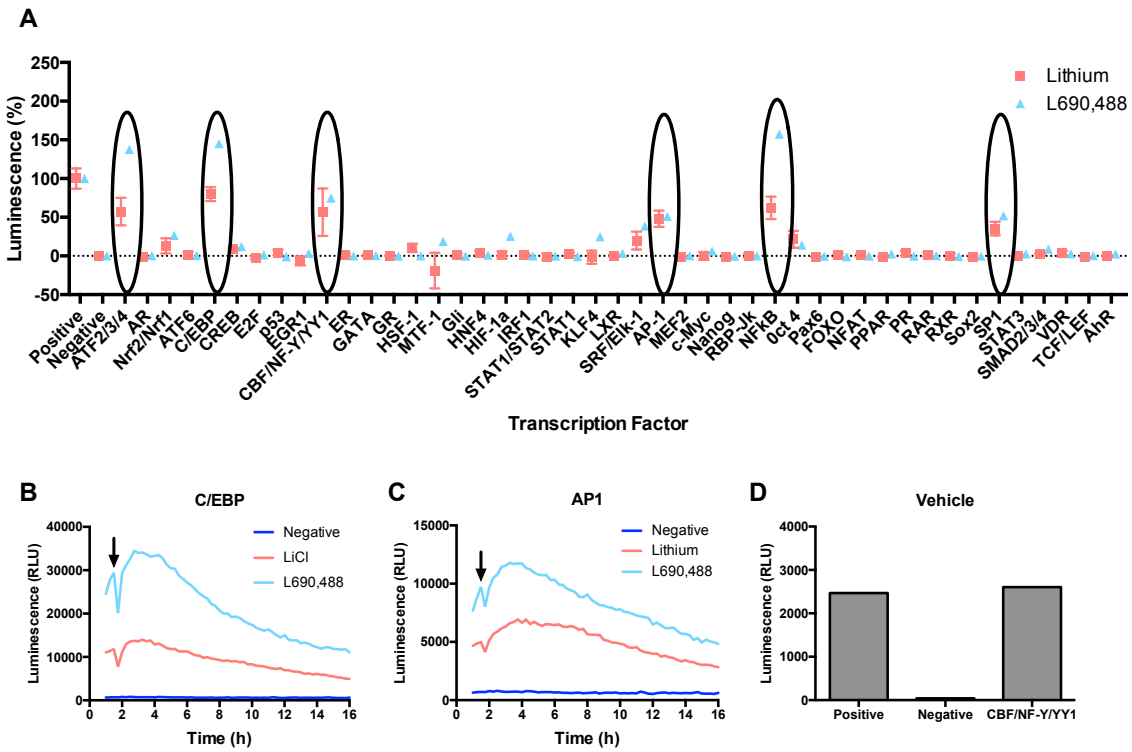

Figure 5.12. **LiCl and L690,488 treatment activate the same transcription factors in the MMHD3 cells. A)** Use of the Cignal 45 reporter assay allowed the detection of drug-induced changes in transcription factor activation. Both 30mM LiCl (n=6) and 3µM L690,488 (n=2) increased activation of the same transcription factors: ATF2/3/4, C/EBP, CBF/NF-Y/YY1, AP1, NFκB, and SP1. **B-C)** Example luminescence traces showing the increased expression of C/EBP or AP1 after LiCl or L690,488 treatment. **D)** Vehicle increased expression of CBF/NF-Y/YY1 alone (n=2). Arrow indicates time of drug addition.

5.2.12 Reducing P-ERK does not normalise period lengthening

Of the 5 transcriptional pathways activated, two were explored in further detail. As AP1 forms part of the MAPK pathway, the role of P-ERK was further examined. It was predicted that: 1) drugs that inhibited IMPase should increase P-ERK levels and 2) that inhibiting P-ERK should normalise LiCl-induced period lengthening. Firstly, an ERK ELISA was performed in order to assess the impact of IMPase inhibiting drugs on P-ERK (*Figure 5.13A*). 30mM NaCl did not show differences in P-ERK levels, whereas 500nM of the ERK inhibitor SCH772984 reduced P-ERK levels by 2.50±0.09 fold (NaCl: 1.07±0.08, SCH772984: 0.40±0.09 normalised P-ERK expression). It was then established that both LiCl and L690,488 raised P-ERK by 1.84±0.09 fold and 1.86±0.21 fold respectively.

Subsequently, after confirming that co-administering 500nM SCH772984 with LiCl did not impact cell viability (*Figure 5.13B*), the hypothesis that SCH772984 could normalise LiCl-induced period lengthening was assessed. As seen in *Figure 5.13C,* SCH772984 alone had no significant effect on period (vehicle: 24.26±0.20, SCH772984: 24.57±0.10 h). Whilst 10-30mM LiCl alone resulted in period lengthening, potentiation with SCH772984 co-administration was observed (LiCl → 10mM: 24.67±0.00, 20mM: 25.07±0.10, 30mM: 25.68±0.10 h). This was because 10mM, 20mM, and 30mM LiCl in the presence of SCH772984 induced period lengthening by 55min, 1.7h, and 2.2h respectively (LiCl+SCH772984 → 10mM: 25.17±0.10, 20mM: 25.98±0.10, 30mM: 26.48±0.00 h). Furthermore, when assessing amplitude (*Figures 5.13D, E*), SCH772984 alone or in combination with LiCl induced significant amplitude dampening, where higher concentrations of lithium started to display amplitude enhancement.

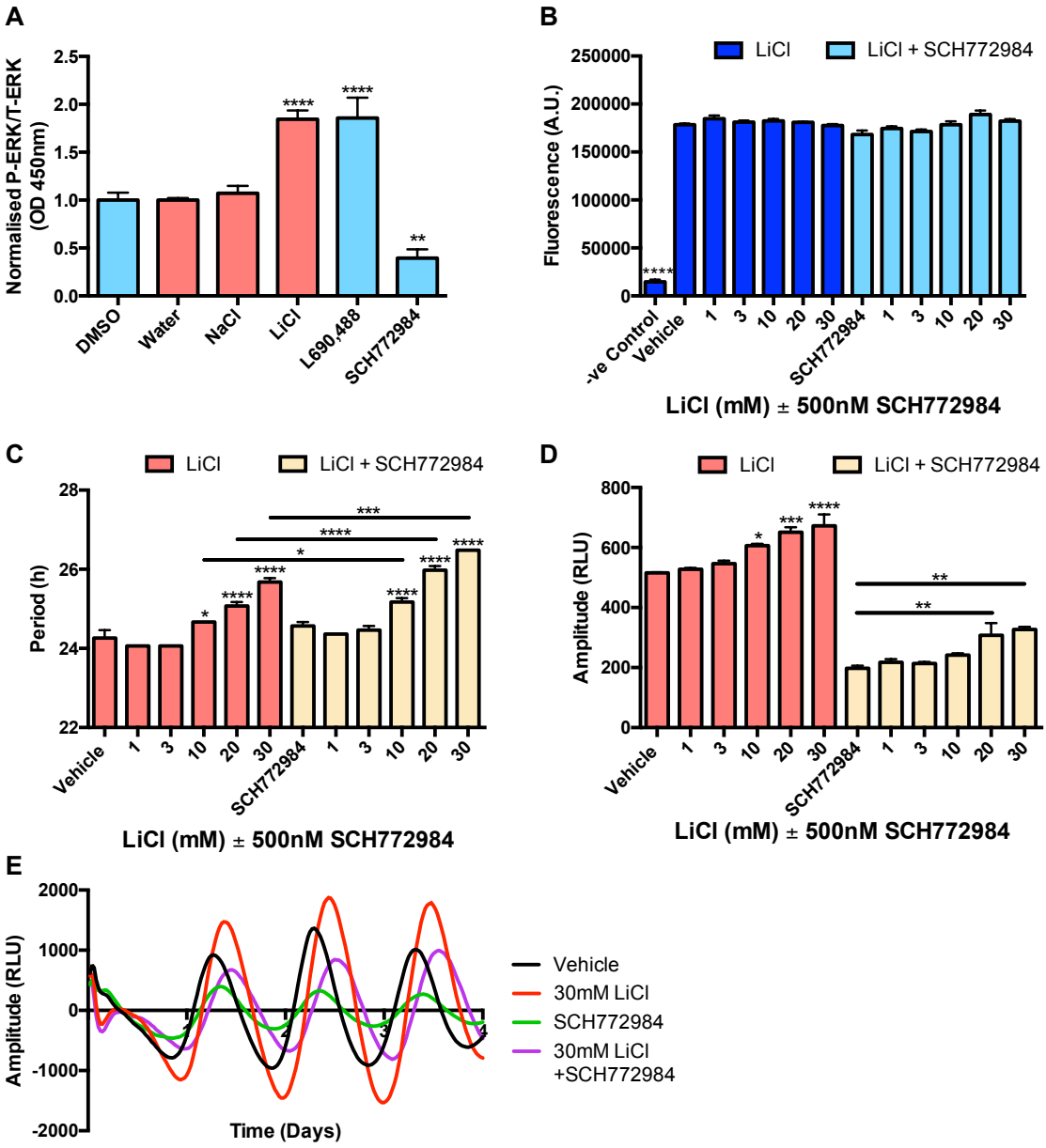

Figure 5.13. **Inhibition of P-ERK is not responsible for LiCl-induced period lengthening in the MMHD3 cells. A)** Performance of an ERK ELISA to assess drug-induced alterations to P-ERK, 30mM NaCl, 30mM LiCl, 3µM L690,488, and 500nM SCH772984 (n=3-7). **B)** Cell viability assay (n=3). The effects of 500nM SCH772984 co-administration with LiCl on circadian period (n=3) **(C)** and amplitude (n=3) **(D)**. SCH772984 did not normalise drug induced period lengthening. **E)** Representative luminescence traces highlighting the effects of SCH772984 on the molecular clock.

5.2.13 C/EBP may play a role in inducing period lengthening

The role of the transcription factor CCAAT/enhancer-binding protein (C/EBP), with specific focus on the α isoform was also explored. It was predicted that: 1) IMPase inhibiting drugs would elevate C/EBPα transcript levels and 2) that knocking down C/EBPα expression would normalise LiCl-induced period lengthening. Following pharmacological treatment, C/EBPα expression was analysed to assess the effects observed with the Cignal 45 reporter assay. LiCl, increased C/EBPα expression by 1.9 and 2.3 fold after 24 and 48h respectively (NaCl → 0h: 0.23±0.02, 24h: 0.14±0.01, 48h: 0.18±0.01; LiCl → 0h: 0.18±0.02, 24h: 0.26±0.02, 48h: 0.42±0.04 relative expression) (*Figure 5.14A*). Similarly, L690,488 also increased C/EBPα transcript levels by 25% and 50% after 24h and 48h respectively (vehicle → 0h: 0.19±0.01, 24h: 0.16±0.02, 48h: 0.18±0.02; L690,488 → 0h: 0.20±0.01, 24h: 0.20±0.01, 48h: 0.27±0.02 relative expression) (*Figure 5.14B*).

Further analysis of the role of C/EBPα was assessed using siRNA-mediated gene knockdown. Remarkably, the Tukey post-hoc test revealed that knocking down C/EBPα in the presence of 15mM lithium reduced both LiCl-induced period lengthening and amplitude enhancement, as displayed in *Figures 5.14C-F*. Specifically, period lengthening was reduced by 29min when comparing the effects of lithium treatment with 50nM control or C/EBPα siRNA (*siControl*: 23.45±0.00, *Csnk1δ:* 23.91±0.09, C/EBPα*:* 23.53±0.08, *siControl* + 15mM LiCl: 23.76±0.00, C/EBPα + 15mM LiCl: 23.27±0.07 h). Similarly, in the presence of C/EBPα siRNA, lithium-induced amplitude enhancement was reduced by 41%

(*siControl*: 200.00±9.66, *Csnk1δ:* 405.20±13.64, C/EBPα*:* 131.80±8.40, *siControl* + 15mM LiCl: 318.20±12.16, C/EBPα + 15mM LiCl: 186.20±7.68 RLU).

These effects were clarified using a higher concentration of LiCl. Indeed, similar trends were emergent, as following knockdown of C/EBPα, 30mM LiCl reduced period lengthening by 32min (*siControl*: 24.67±0.12, C/EBPα*:* 24.21±0.09, *siControl* + 30mM LiCl: 25.39±0.07, C/EBPα + 30mM LiCl: 24.85±0.07 h) (*Figures 5.14G, I*). Furthermore, as seen in *Figure 5.14H* lithium-induced amplitude enhancement was reduced by 21%, *(siControl*: 91.16±1.29, C/EBPα*:* 81.64±3.00, *siControl* + 30mM LiCl: 147.70±9.19, C/EBPα + 30mM LiCl: 116.40±3.41 RLU). Finally, to confirm that the effects being observed were due to knockdown of the gene of interest, qPCR analysis found that use of the siRNA knocked down C/EBPα by 95% (*siControl*: 100±10.81, C/EBPα*:* 4.69±1.42 %) (*Figure 5.14J*). Therefore, our data suggests that lithium may induce chronomodulatory changes via the modulation of C/EBPα.

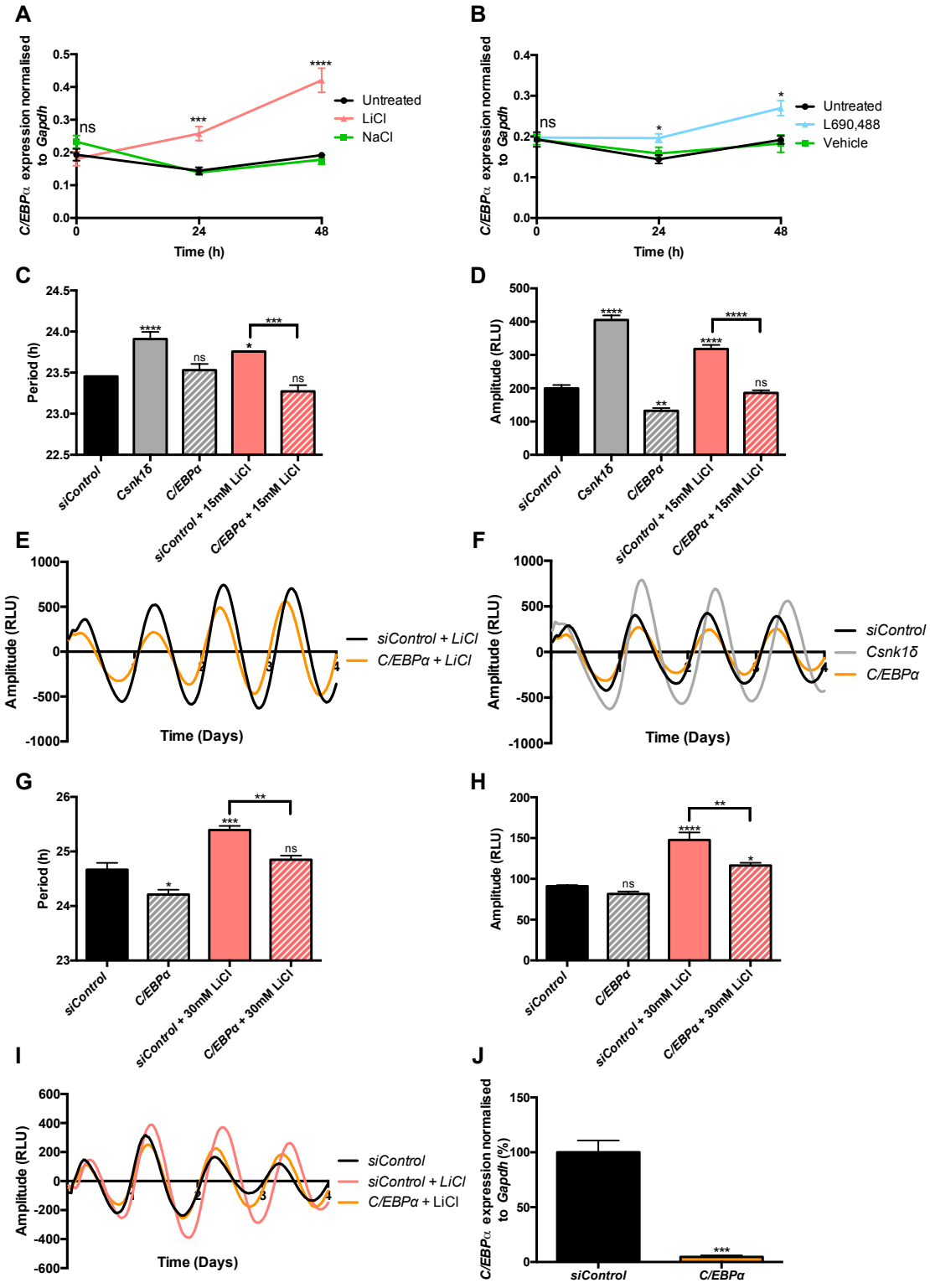

Figure 5.14. **C/EBPα siRNA normalises LiCl-induced period lengthening and amplitude enhancement.** C/EBPα expression after 24h and 48h of treatment with 30mM LiCl (n=4) **(A)** or 3μM L690,488 (n=4) **(B).** The effects of 50nM siControl, *Csnk1δ,* or C/EBPα and 15mM LiCl on circadian period (n=4) **(C)** or amplitude (n=4) **(D)** with representative traces **(E-F)**. Similar experiments were performed using 30mM LiCl, assessing period (n=4) **(G)** and amplitude (n=4) **(H)**, with exemplar traces highlighting these effects **(I)**. **J)** Validation of transcript knockdown (n=4). Gene expression was normalised to *Gapdh*.

5.2.14 Myo-inositol reduced LiCl-induced period change in SCN slice cultures

In order to identify whether the observations found *in vitro* possessed any biological validity, the effects of LiCl were assessed on organotypic SCN sections using PER2::LUC knockin mice. It was hypothesised that: 1) LiCl would lengthen the period of the SCN, as previously described (Li et al., 2012) and 2) the period effects would be reverted with myo-inositol treatment. As seen in *Figures 5.15A, C*, it was found that LiCl induced dose-dependent PER2 period changes within the SCN as 4mM and 8mM LiCl lengthened period by 2.26±0.14h and 2.42±0.88h respectively (vehicle: 0.41±0.32h). Interestingly, a trend for period lengthening was emerging with 2mM LiCl, which induced lengthening by 27min (0.86±0.20h). Despite previous reports of lithium increasing amplitude (Li et al., 2012), no significant changes were observed, as both vehicle and 2-8mM LiCl showed trends of amplitude dampening (vehicle: -1867±742.60, 2mM: -2413±668.30, 4mM: 22±18.12, 8mM: -1895±565.00 (*Figure 5.15B*).

The co-administration of LiCl and myo-inositol was then tested to see whether exogenous myo-inositol could replenish depleted stores and normalise period (*Figures 5.15D-E*). Interestingly, the data suggests that the addition of 1mM myo-inositol was able to reduce circadian period by 1.4h (vehicle: 0.10±0.30, 4mM LiCl: 2.26±0.14, +1mM myo-inositol: 0.91±0.26 h). There were also a lack of drug-induced amplitude effects found upon co-administration with myo-inositol (*Figure 5.15F*). Whilst previous unpublished studies performed by myself, not included in this thesis, found that myo-inositol did not appear to impact SCN rhythms, these findings are preliminary, and do suggest that myo-inositol supplementation may indeed normalise period in cultured tissues.

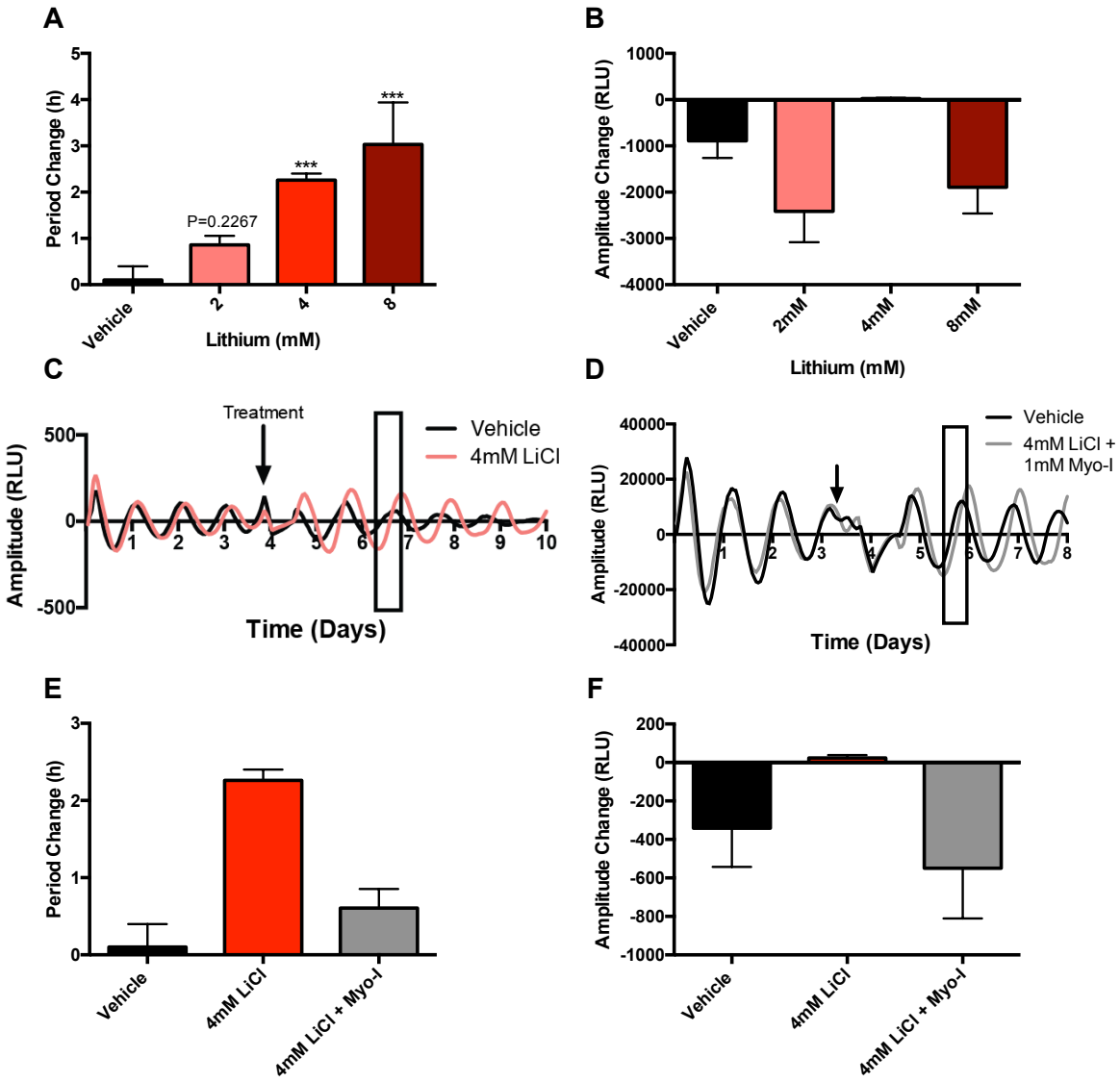

Figure 5.15. **Myo-inositol partially rescued LiCl-induced period lengthening in SCN slice culture.** The period change **(A)** or amplitude change **(B)** incurred after treatment with vehicle (n=11), 2mM (n=6), 4mM (n=5), and 8mM (n=4) LiCl. **C-D)** Representative traces showing the effects of adding 4mM LiCl alone or in combination with 1mM myo-inositol. SCN sections were cultured for 4 days after which drugs were added (indicated by the arrow), and left for a further 4 days. The period change **(E)** or amplitude change **(F)** incurred after treatment with vehicle (n=9), 4mM LiCl (n=5), or 4mM LiCl with 1mM myo-inositol (n=7).

5.2.15 IMPase is enriched in the master clock

To be a viable circadian target capable of influencing the behaviour of an organism, it would be beneficial for a molecule to target the SCN directly. Therefore, the question of whether IMPase is expressed in the mammalian master clock was assessed through immunohistochemistry. Firstly, western blotting of mouse brain homogenates validated the anti-IMPA1 antibody. Strong detection of IMPA1 was found with 1-4µg of proteins (30kDa) (*Figure 5.16A*). Next, the primary antibody was used on 50µm coronal brain sections containing the SCN. The IRDye far-red fluorescent antibody allowed imaging with the LI-COR Odyssey Infrared Imaging System. The mid-SCN region, located just above the optic chiasm, was clearly demarcated after staining and appeared as two almond shape nuclei (*Figure 5.16B)*, thus confirming the presence of IMPA1 within the SCN.

Further analysis of IMPA1 expression through use of the Alexa Fluor 488 green fluorescent secondary antibody allowed higher resolution images to be acquired. Brain slices were co-stained with the nuclear stain DAPI, as seen in *Figure 5.16C*. The use of an Olympus FV1000 laser-scanning microscope confirmed that IMPA1 is expressed within cells of the SCN. Higher objective images found that IMPA1 (green) was located predominantly in the cytoplasm, unlike the nuclear stain DAPI. To confirm this was not due to the secondary antibody artefacts, control mid-SCN sections were stained with the secondary antibody alone (*Figure 5.16D*). Overlapping IMPA1 and nuclear staining images showed that whilst there was some residual staining, the overall levels were not substantial.

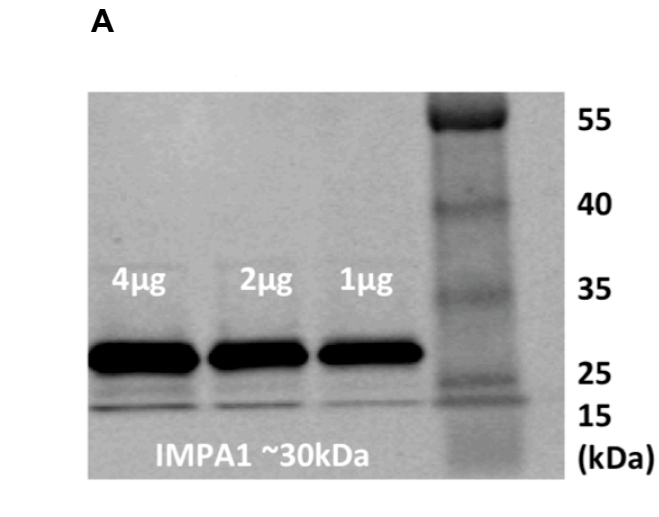
A
4µg
2µg
1µg
IMPA1 ~30kDa
55
40
35
25
15
(kDa)
B
SCN
C
IMPA1
DAPI
IMPA1 + DAPI
10x
60x
60x
magnified

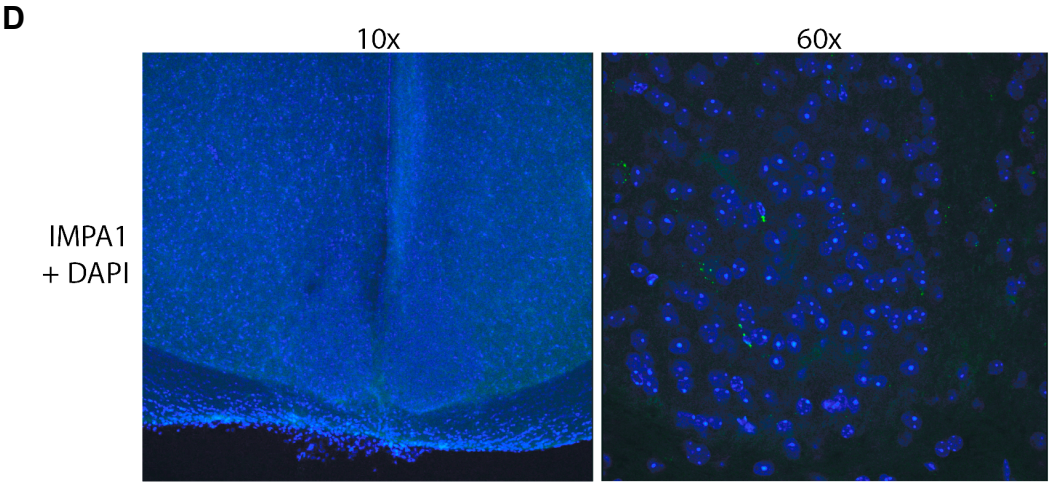

Figure 5.16. **Immunohistochemistry reveals enrichment of IMPA1 in the SCN. A)** Western blot stain loaded with 1, 2, and 4µg of mouse brain homogenate to validate the IMPA1 antibody (30kDa). **B)** 50µM brain sections containing the mid-SCN were stained with the IRDye far-red fluorescent secondary antibody and imaged using the LI-COR Odyssey Infrared Imaging System, where the SCN is demarcated above the optic chiasm. **C)** Higher resolution images were acquired with the Alexa Fluor 488 secondary antibody (green) with the nuclear stain DAPI (blue) on the Olympus FV1000 laser-scanning microscope. Objectives on the y-axis. **D)** Control sections were incubated with the secondary antibody alone.

5.3 Discussion

It is recognised that lithium's effects on the molecular clock may be important, however the mechanism surrounding period lengthening remains unknown. This investigation aimed to elucidate whether IMPase of the PI pathway was responsible for such effects as both IMPase and GSK3β are claimed to be the dominant targets for mediating lithium's therapeutic effects (Phiel and Klein, 2001). Whilst the amplitude enhancing effects have previously been shown to occur via specific GSK3β inhibition, a target which induces period shortening, IMPase could be a plausible alternative target especially as it elongates circadian period (Li et al., 2012). Here we show for the first time that lithium-induced period lengthening may occur via inositol depletion, which through currently undetermined mechanisms results in the activation of the transcription factor C/EBP (summarised in *Figure 5.18*), a finding which may help further understand the mechanistic consequences of IMPase inhibition.

5.3.1 Understanding the cell-type specific responses

LiCl induced significant period lengthening in 2 of 3 cell lines investigated, where the drug had no effect on the U2OS cells. U2OS cells are immortal cells that harbour many chromosomal alterations, however, as they still contain the molecular clockwork required to produce robust 24h rhythms, they are routinely used in circadian research. Recent evidence suggests that of the thousands of circadian transcription factor binding sites, only ~2% showed rhythmic oscillations and many of these oscillations were low in amplitude (Hoffmann et al., 2014). The MMHD3 cells however, are murine cells used in

their hepatoblast form and also express rhythmic clock genes (Ramanathan et al., 2014). The murine liver was found to contain one the highest number of rhythmic transcripts of the 12 organs analysed as 16% showed significant rhythmic patterns (Zhang et al., 2014). As the numbers of rhythmic transcripts are higher in the mouse liver relative to the U2OS cells, this suggests that the U2OS molecular clock has weaker control of downstream clock controlled genes. Interestingly, cell-type specific changes in the molecular clockwork are becoming more apparent as knocking down core clock genes (*Clock, Npas2*, *Bmal*, *Per, Cry)* or the accessory genes (*Rev-erbα/β* and *Fbxl3*) resulted in differential effects on circadian rhythmicity, factors which may culminate in cell specific altered drug responses (Ramanathan et al., 2014).

It has previously been shown that lithium can accumulate differentially in a cell-type specific manner. In two wild-type strains of yeast, extracellular treatment with 100mM lithium resulted in 2.5mM and 10mM cytoplasmic concentrations (Vaden et al., 2001). Therefore, it could be suggested that the observed differences may be due to lithium simply not accumulating in the U2OS cells. However, lithium has been shown to accumulate in bone tissues to a similar degree as the hypothalamus, a value 3 times the lithium concentration in the liver (Ebadi et al., 1974). This suggests that lithium accumulation may not have been an issue in the U2OS cells. By employing a technique called 'inductively coupled plasma mass spectrometry' (ICP-MS), which enables the detection of total cellular metal concentrations, we confirmed that lithium was accumulating in the U2OS cells 2.1, 1.7, and 2.0 times more at 1, 10, and 30mM concentrations when compared to the MMHD3 cells (*Figure 5.17*). Therefore, whilst lithium may

accumulate in the U2OS cells, this model is not suitable for understanding the consequential effects of IMPase inhibition. Our investigation showed that the U2OS cells contained 40% lower IMPA1 protein levels, a finding which was coupled with no period effects under inositol-less media conditions, suggesting that the PI system may be less responsive in this cellular model. As the liver is known to be one of the strongest peripheral oscillators, the MMHD3 cell showed high amplitude basal oscillations for 4-5 days after dexamethasone-induced synchronisation, they showed the predicted amplitude enhancing and period lengthening effects of LiCl, and contained high expression levels of the target of interest, it was the cell line selected for the majority of our *in vitro* experiments.

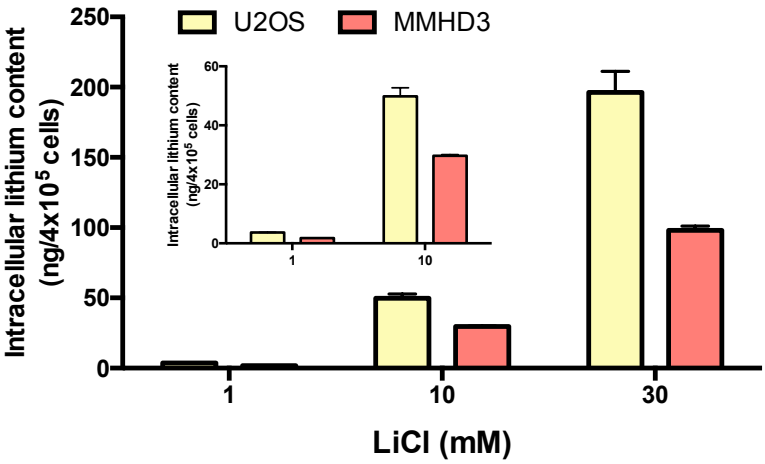

Figure 5.17. **Lithium accumulated within the U2OS and MMHD3 cells.** By assessing intracellular lithium content using ICP-MS, lithium was accumulating to a greater degree in the U2OS cells when compared to the MMHD3 cells (n=3).

5.3.2 Inositol-less media exacerbated period lengthening

It was found that inositol-less media alone lengthened the circadian period by 1h in MMHD3 cells and potentiated LiCl-induced period lengthening at every subsequent concentration tested. Moreover, similar trends were identified for the small molecule IMPase inhibitors: the reversible inhibitor L690,488 and the irreversible inhibitor ebselen (Atack, 1997, Singh et al., 2013). This may be

due to dual targeting of inositol stores; intracellular myo-inositol levels are reduced through IMPase inhibition and extracellular inositol is removed from the culture medium, resulting in less myo-inositol entry via the SMITs. The effects of LiCl may have been more pronounced than the alternative IMPase inhibitors tested, as LiCl has additional inhibitory effects on both IPPase and the SMITs, effects not reported with L690,488 or ebselen (Azad and Tomar, 2014, Atack et al., 1994). Lithium inhibits IPPase, thereby reducing conversion of IP2 to IP, resulting in less substrate availability for IMPase and ultimately reduced myo-inositol regeneration (Berridge et al., 1989). Correspondingly, LiCl also reduces *Slc5a3* expression in the cerebellum and cortex, an effect corroborated with the MMHD3 cells, thereby reducing myo-inositol entry from the extracellular environment, and aiding the depletion of intracellular stores (Lubrich et al., 2000). This provides an additional means of reducing myo-inositol as it suggests the presence of reduced transporter numbers on the cell surface.

The high degree of selectivity of L690,488 for IMPase made it an invaluable tool for assessing the specific consequences of IMPase inhibition throughout this study (Atack et al., 1994). Interestingly, it was found that 48h of L690,488 treatment elevated *Slc5a3* expression. This may be to aid myo-inositol homeostasis by providing a means for more myo-inositol entry. Therefore, using L690,488 in future studies may help to understand whether lithium induces therapeutic benefits primarily because of general inositol depletion, or targeted IMPase inhibition, as L690,488 does not impact the SMITs. Indeed, under inositol-less conditions, there is no extracellular myo-inositol available to enter the cells, which may be why trends for potentiation at 1μM were observed.

Nonetheless, the effects of removing or inhibiting *Impa1* specifically on *Slc5a3* expression *in vitro* or *in vivo* are yet to be clarified.

5.3.3 The effects of IMPase inhibition on the molecular clock

LiCl has previously been shown to impact multiple molecular clock gene expression patterns in immortalised cells as well as healthy human and BPD patients cell lines (Osland et al., 2011, Yin et al., 2006, McCarthy et al., 2013, Geoffroy et al., 2017). Our analysis confirmed previous findings by showing that lithium elevated *Per2* and *Bmal* transcription. Analysis was performed after 48h, as previous evidence suggests lithium-like effects on the molecular clock occur between 16-72h of treatment (Yin et al., 2006). As predicted, selective inhibition of IMPase via L690,488 also increased *Per2* and *Bmal* transcripts, where both drugs elevated *Bmal* levels to a greater degree than *Per2*. As *Bmal* levels were increased to a similar degree, this suggests that IMPase inhibition may be responsible for LiCl-induced elevated *Bmal* transcription. However, L690,488 induced *Per2* levels by approximately half the degree observed with LiCl. This suggests that additional targets may be responsible for elevations in *Per2* levels. Indeed, GSK3β inhibition has been shown to elevate *Per2* and may therefore account for a degree of the additional increase (Li et al., 2012).

Of particular note were the effects of siRNA-mediated *Impa1* knockdown. *Impa1* knockdown at concentration where 34min period lengthening was observed induced significant *Bmal* expression. Moreover, these effects were specific to IMPase, as *Isyna1* knockdown had no impact on *Bmal* gene expression. This added to the body of evidence suggesting that IMPase inhibition contributes to the significant alterations lithium has on the molecular clock.

5.3.4 Moderate lithium-like effects observed with Impa1 knockdown

It could be hypothesised that removing the *Impa1* gene should mimic the effects of LiCl-induced IMPase inhibition, as it would prevent IP conversion to myo-inositol. Similarly, removal of the *Slc5a3* or *Isyna1* gene should prevent myo-inositol cell entry, or myo-inositol synthesis from D-glucose 6-phosphate respectively, removing further means of inositol availability. Our results showed moderate period effects with either *Impa1* or *Isyna1* siRNA-mediated knockdown. Where *Isyna1* knockdown resulted in only ~4% of transcripts remaining, *Impa1* siRNA left 24% persisting, and higher concentrations of *Impa1* siRNA appeared toxic for the cells. This could be sufficient transcript level in the MMHD3 cells to maintain a functional PI pathway without enough myo-inositol depletion to induce greater period lengthening.

It should be noted that rodent models, wherein key components of the PI pathway are mutated or removed, also do not show typical lithium-like responses. Whilst both *Impa1* inactivated mutants and *Slc5a3*$^{-/-}$ mice display increased sensitivity to pilocarpine-induced seizures and increase mobility in the forced swim test, in accordance with lithium treatment, other key behavioural phenotypes are not mimicked (Cryns et al., 2008, Bersudsky et al., 2008).

Unlike lithium treated wild-type mice, in the open field test, *Impa1* mutant animals displayed hyperambulatory activity with increased rearing behaviours (Cryns et al., 2008). As lithium was initially found to be beneficial in BPD due to its calming effects on patients, increased motor activity is surprising (Cade, 1949). Moreover, rearing is correlated with behavioural impulsivity, a phenotype which could be associated with suicidal tendencies in BPD (O'Donnell and Gould,

2007). As we showed in Chapter 4, one of lithium's key behavioural effects *in vivo* is a reduction in rearing, where ebselen was also able to reduce rearing in amphetamine-induced mouse models of mania. These effects were believed to be due to IMPase inhibition, as the phenotype was rescued by exogenous inositol administration (Singh et al., 2013). Interestingly, Ohnishi and colleagues found that *Impa1* mutants, in which enzymatic activity was eliminated, showed elevated daytime activity. Moreover, such mice displayed a lengthened behavioural period under LD conditions, an effect that was not normalised with inositol supplementation. However, much like our findings with *Impa1* siRNA in the MMHD3 cells, the effects were moderate causing lengthening by ~10min (Ohnishi et al., 2014). This suggests that whilst inositol depletion may be implicated in inducing period lengthening, these actions are more complex, potentially due to the multiple sources of inositol availability and the numerous components of the PI pathway. However, compensation is not currently thought to occur with IMPA2 (Cryns et al., 2008). Indeed, according to 'The Human Protein Atlas' IMPA2 protein levels appear undetectable in hepatocyctes, where IMPA1 was more prominent (Uhlén et al., 2015). Similarly, the 'European Bioinformatics Institute Gene Expression Atlas' revealed low expression levels of murine liver *Impa2*, with much higher expression of *Impa1* (Kapushesky et al., 2009). Our data found that *Isyna1* induces more subtle period effects without modulating *Bmal* expression. *Isyna1* could arguably have less of a role in modulating period under standard media conditions as there is sufficient inositol availability. However, the effects may be potentiated under inositol-less conditions, due to the increased drive for myo-inositol requirement.

Additionally, it is plausible that currently unknown compensatory mechanisms may be counteracting these effects.

5.3.5 The role of ERK in modulating rhythms

Two pathways from the Cignal 45 assay were explored in further detail to identify whether they may be implicated in the downstream effects of IMPase inhibition and circadian period lengthening. The first pathway that was explored was the role of the evolutionary conserved MAPK pathway, as AP1 activity was significantly elevated and SRF/Elk1 presented with similar trends.

Of the multiple currently identified MAPK pathways, we decided to focus on ERK1/2, as there is a wealth of evidence implicating ERK in circadian rhythm modulation. As well as knowing that photic induction of P-ERK is gated in the rodent SCN, P-ERK is key in pineal melatonin synthesis as it regulates n-acetyltransferase production, the rate-limiting enzyme (Hughes et al., 2004, Ho et al., 2003). Therefore, being a highly conserved ubiquitous pathway implicated in rhythm modulation through modification of light-induced responses, it was thought that ERK may be the transcription factor implicated in modulating circadian genes as a downstream consequence of IMPase inhibition.

The compound SCH772984 has been shown to be potent and highly selective for ERK1/2 inhibition and was therefore used in this investigation (Morris et al., 2013). Whilst our study confirmed that SCH772984 was reducing P-ERK levels in the MMHD3 cells, the drug did not normalise the effects of LiCl-induced period lengthening, demonstrating that ERK may not be the ultimate target responsible for the effects of lithium on decelerating the molecular clock.

ERK is a known target of lithium and previous studies have shown opposing effects in neurones and astrocytes (Pardo et al., 2003). This study also found that the effects on ERK were not due to GSK3β or inositol depletion, as pharmacological tools or inositol supplementation had minimal impact (Pardo et al., 2003). Thus, it could be concluded that in our MMHD3 cellular model, IMPase inhibition was inducing P-ERK, but this induction was not responsible for modulating circadian gene transcription, which may then promote period lengthening.

5.3.6 The role of C/EBP in modulating rhythms

The second target of interest was the basic leucine zipper transcription factor C/EBP, which binds to CCAAT motifs present in promoter region of genes, where the isoforms C/EBPα and C/EBPβ both have enriched liver expression patterns (Hayashi et al., 1999, Flodby et al., 1995). Our investigation found that C/EBP levels were significantly elevated after both lithium and L690,488 treatment suggesting transcription factor induction as a consequence of IMPase inhibition. Studies have shown that in human hepatoma cells, C/EBPα had 2.8 times greater expression levels when compared to the mRNA expression of C/EBPβ (Masaki et al., 2006). C/EBPα was therefore the isoform used to assess LiCl and L690,488-induced changes in mRNA expression. Indeed, in accordance with the drug-induced changes in *Per2* and *Bmal* expression, both drugs increased expression of C/EBPα after 24 and 48h of treatment. The similar time course with which such changes occur suggests that this transcription factor may be mediating clock gene expression. Furthermore, region specific enrichment of C/EBPα has been found in the hypothalamus (Draper et al., 2010). Therefore,

whilst the SCN was not examined, this data suggests that C/EBPα can be expressed in neurones and that it is also expressed in the hypothalamus, alluding to the idea that C/EBPs may play a role in regulating rhythmicity.

Indeed, there is evidence showing that C/EBPs can modulate circadian gene expression. Use of NIH-3T3 cells found that amongst the 158 C/EBP target genes were *Per2*, *Rev-erbα,* and *Dbp,* highlighting the relationship between C/EBP and the molecular clock for the first time. Further analysis of the NIH-3T3 cells along with fresh murine bone marrow cells and human hematopoietic cancer cells established that *Per2* specifically was regulated by C/EBPα and ε binding to their elements on the *Per2* promoter. Interestingly, *Rev-erbα* was downregulated by C/EBPα and ε (Gery et al., 2005, Thoennissen et al., 2012). As we failed to detect any C/EBPε in the MMHD3 cells, this suggests that C/EBPα plays the dominant role in regulating clock gene expression. Therefore, much like lithium and L690,488, C/EBPα can elevate *Per2* gene transcription, as well as *Bmal* transcription via the suppression of its negative regulator *Rev-erbα*.

Lithium is a known modulator of C/EBPs, where elevated levels of C/EBPα have previously been reported in response to lithium. GSK3β can phosphorylate and inactivate C/EBPα, an effect which is reversed by lithium treatment (Ross et al., 1999). It was found that whilst lithium stabilises C/EBPα, GSK3β inhibition did not affect C/EBPα mRNA expression. The authors were also unable to find an effect with L690,330 in their cell line and therefore suggest that the effects were not due to IMPase inhibition (Shim and Smart, 2003). However, as our data with L690,488 suggests, when looking at both the Cignal 45 assay and the real-time PCR data, the lack of any significance may be due to the low

permeable nature of L690,330. Additionally, as L690,488 induced C/EBPα by 50%, where LiCl induced levels by 133%, this suggests that other IMPase and GSK3β-independent targets may also be implicated in modulating responses. Interestingly, our preliminary findings with both 15mM and 30mM LiCl suggest that lithium-induced period lengthening is normalised by knocking down C/EBP expression. Such findings provide a foundation to prompt further exploration of the role of C/EBPs in chronomodulation.

Inhibition of a signalling pathway such as that associated with lithium-induced IMPase inhibition, could lead to altered gene expression through direct or indirect disinhibition of the transcription factor of interest. For example, it could be that a factor implicated in reducing the expression or activity of C/EBP is inhibited, thereby causing disinhibition and increased activity of this transcription factor, where C/EBP can then modulate gene expression. Alternatively, inhibition of a signalling pathway could lead to the activation of factors such as protein kinases, which can then phosphorylate and activate C/EBPs. Thus, as outlined in *Figure 5.18,* our data suggests that activation of C/EBPα may induce period lengthening through a molecular pathway directly linking IMPase inhibition with the circadian clock.

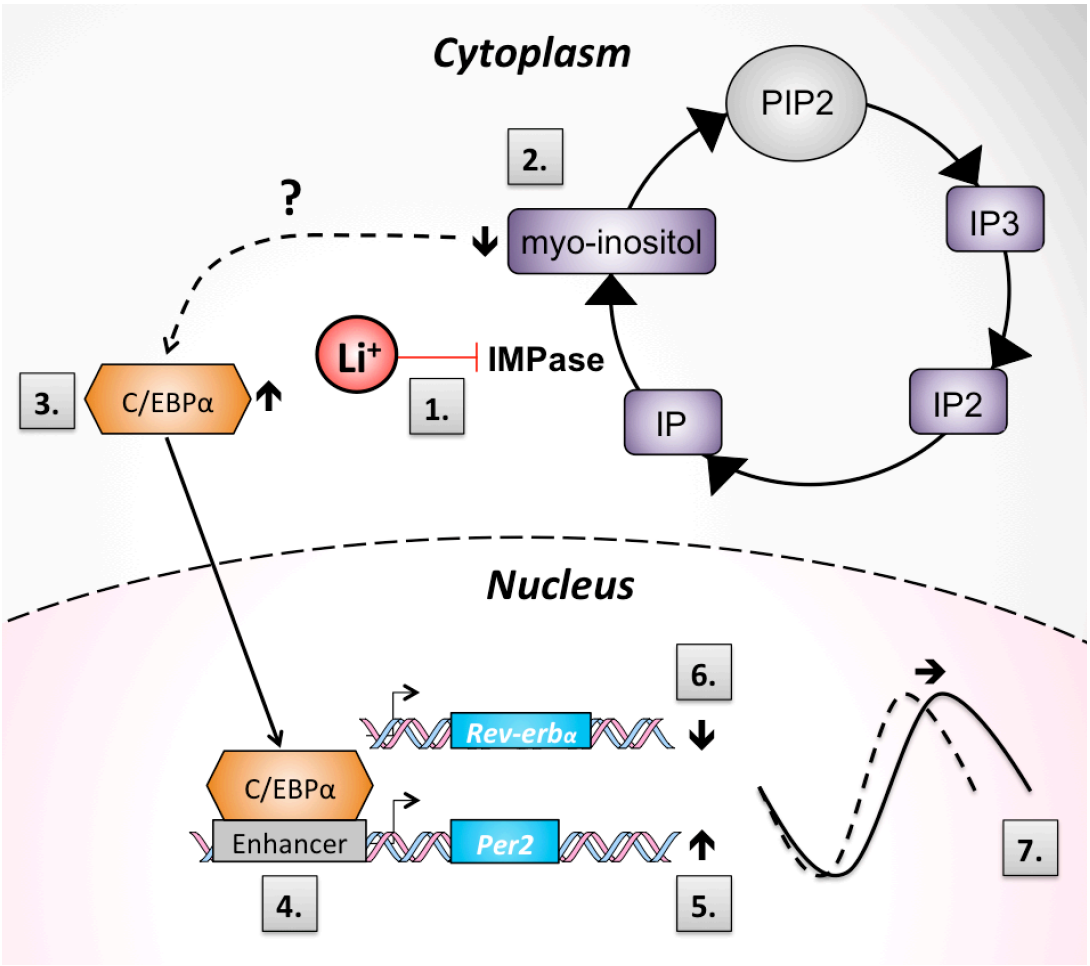

Figure 5.18. **Schematic diagram of the potential mechanism via which period lengthening may be occurring in the MMHD3 cells. 1.** Lithium inhibits IMPase, a fundamental enzyme of the PI pathway. **2.** This results in less intracellular myo-inositol concentrations, which reduce the regeneration of PIP2, ultimately perturbing this cycle. **3.** Through currently unknown mechanisms, this results in the increased activation of the transcription factor C/EBPα. **4.** C/EBPα can bind to CCAAT motifs in the promoter region of *Per2* and *Rev-erbα*. **5.** This results in increased gene transcription of *Per2*. **6.** Concomitantly, there is a reduction in *Rev-erbα* expression, providing an indirect means for elevating *Bmal* gene transcription. **7.** This increase in clock gene transcript levels could result in period lengthening.

5.3.7 Myo-inositol rescue in vitro and ex vivo

LiCl reduced intracellular [^{3}H] myo-inositol content and reduced *Slc5a3* levels in the MMHD3 cells, in line with previous findings (Lubrich and van Calker, 1999). As myo-inositol has poor cell permeability, entry predominantly occurs via the SMITs. This provided a plausible explanation as to why myo-inositol was unable to rescue LiCl-induced period lengthening, as it suggested that LiCl was inhibiting the SMITs and reducing receptor expression. As mentioned previously, reductions in the number of SMITs will only potentiate the effects of inositol depletion. Moreover, it suggests that lithium can lower SMIT activity in our cell line, thereby reducing the amount of inositol able to enter the intracellular environment, an additional property of LiCl (Lubrich and van Calker, 1999).

Our investigation confirmed previous findings in showing that LiCl was able to modulate the period of the master clock. Additionally, we found that 1mM myo-inositol was able to significantly rescue period lengthening induced by 4mM LiCl in organotypic SCN sections. Whilst the cerebrospinal fluid contains very low levels (400-600μM) of myo-inositol, regions of the brain can contain up to 11mM myo-inositol (van Calker and Belmaker, 2000, Kaiser et al., 2005, Fisher et al., 2002). Specifically, analysis of the rodent hypothalamic content has shown relatively high myo-inositol from 3.7-6.6mM (Fisher et al., 2002); a K_m of 25-50μM suggests that the transporters are constantly functioning at maximal velocity (van Calker and Belmaker, 2000). Our results show that the hypothalamus was more receptive to period normalisation upon administration of exogenous myo-inositol. Moreover, myo-inositol content appears to accumulate to the greatest degree in the hypothalamus, where relative to cortical

content, baseline hypothalamic levels were 70% higher and 50% higher 2h after inositol administration (Patishi et al., 1996). This suggests that the SCN may have greater means of allowing myo-inositol to enter the cell, for example through higher SMIT expression. This also suggests that the hypothalamus is more susceptible to the effects of inositol depletion as basal myo-inositol concentration is so high. In concert with this idea, chronic lithium-induced reductions in myo-inositol are not found unanimously but occur predominantly in the hypothalamus. Serum concentrations of 0.8mM lithium resulted in a 21% reduction hypothalamic myo-inositol, however no differences were observed in the cortex, cerebellum, caudate, or hippocampus (Lubrich et al., 1997, Belmaker et al., 1998). Therefore, the experiments on cultured SCN slices suggest that the observations made with the MMHD3 cells are translatable. This claim is supported by the immunohistochemical detection of IMPA1 enrichment within the SCN, reported for the first time. As IMPA1 is highly expressed in the region where it can modulate circadian rhythms, it is a viable period lengthening target.

5.3.8 Conclusions

Returning to the original hypothesis, this investigation set out to determine whether IMPase and by extension the inositol depletion hypothesis, is the molecular mechanism behind lithium's period lengthening effects. The MMHD3 cells proved to be an excellent *in vitro* model of lithium's effects on circadian rhythms. Use of these cells revealed a pathway via which period lengthening could be occurring. Our data trail suggests that lithium inhibits IMPase leading to intracellular inositol depletion; that less myo-inositol is available to regenerate PIP2; and that multiple downstream targets are

impacted. We show that C/EBPα is upregulated in response to lithium treatment and directly increases the transcription of *Per2* and indirectly elevates *Bmal* expression. This augmentation of gene transcription can then affect the rising and/or falling phase of oscillations by modifying the time taken to build-up transcripts or protein degradation, which then ultimately results in period lengthening. Preliminary evidence substantiates these claims as IMPA1 was enriched specifically in the SCN and LiCl lengthened the SCN period, an effect which was normalised with myo-inositol co-administration.

Future studies could build upon these foundations by assessing the basal C/EBP mRNA and protein levels within the SCN, to assess whether these cells express this transcription factor and if so to what extent. Further, it would be interesting to determine whether C/EBP expression is altered in the SCN following IMPase inhibition, as this would confirm that the gene expression changes found *in vitro* are translatable.

Overall, these results demonstrate that inositol depletion via IMPase inhibition could be responsible for LiCl-induced period lengthening. These results are of importance as lithium has a very narrow therapeutic window and is associated with numerous undesirable side effects, making patient compliance an issue. Whilst the mechanisms via which lithium induces therapeutic benefits remains largely unknown, should it function via normalisation of circadian disruptions, these results may provide a solid foundation in identifying novel therapeutics associated with fewer side effects. Further, if validated, a screening program for C/EBP activators could be initiated with promise of identifying a novel sub-class of mood-stabilising agents.

5.4 References

ALLISON, J. H., BLISNER, M. E., HOLLAND, W. H., HIPPS, P. P. & SHERMAN, W. R. 1976. Increased brain myoinositol 1-phosphate in lithium-treated rats. *Biochemical and Biophysical Research Communications,* 71**,** 664-670.

ALLISON, J. H. & STEWART, M. A. 1971. Reduced brain inositol in lithium-treated rats. *Nature-New Biology,* 233**,** 267-&.

ATACK, J. R. 1997. Inositol monophosphatase inhibitors - Lithium mimetics? *Medicinal Research Reviews,* 17**,** 215-224.

ATACK, J. R., COOK, S. M., WATT, A. P., FLETCHER, S. R. & RAGAN, C. I. 1993. In vitro and in vivo inhibition of inositol monophosphatase by the bisphosphonate L-690,330. *Journal of Neurochemistry,* 60**,** 652-658.

ATACK, J. R., PRIOR, A. M., FLETCHER, S. R., QUIRK, K., MCKERNAN, R. & RAGAN, C. I. 1994. Effects of L-690,488, a prodrug of the bisphosphonate inositol monophosphatase inhibitor L-690,330, on phosphatidylinositol cycle markers. *Journal of Pharmacology and Experimental Therapeutics,* 270**,** 70-76.

AZAD, G. K. & TOMAR, R. S. 2014. Ebselen, a promising antioxidant drug: mechanisms of action and targets of biological pathways. *Molecular Biology Reports,* 41**,** 4865-4879.

BAMNE, M. N., PONDER, C. A., WOOD, J. A., MANSOUR, H., FRANK, E., KUPFER, D. J., YOUNG, M. W. & NIMGAONKAR, V. L. 2013. Application of an ex vivo cellular model of circadian variation for bipolar disorder research: a proof of concept study. *Bipolar Disorders,* 15**,** 694-700.

BELMAKER, R. H., AGAM, G., VAN CALKER, D., RICHARDS, M. H. & KOFMAN, O. 1998. Behavioral reversal of lithium effects by four inositol isomers correlates perfectly with biochemical effects on the PI cycle: Depletion by chronic lithium of brain inositol is specific to hypothalamus, and inositol levels may be abnormal in postmortem brain from bipolar patients. *Neuropsychopharmacology,* 19**,** 220-232.

BERRIDGE, M. J. 1984. Inositol trisphosphate and diacylglycerol as 2nd messengers. *Biochemical Journal,* 220**,** 345-360.

BERRIDGE, M. J., DOWNES, C. P. & HANLEY, M. R. 1982. Lithium amplifies agonist-dependent phosphatidylinositol responses in brain and salivary-glands. *Biochemical Journal,* 206**,** 587-595.

BERRIDGE, M. J., DOWNES, C. P. & HANLEY, M. R. 1989. Neural and developmental actions of lithium - a unifying hypothesis. *Cell,* 59**,** 411-419.

BERSUDSKY, Y., SHALDUBINA, A., AGAM, G., BERRY, G. T. & BELMAKER, R. H. 2008. Homozygote inositol transporter knockout mice show a lithium-like phenotype. *Bipolar Disorders,* 10**,** 453-459.

CADE, J. F. J. 1949. Lithium salts in the treatment of psychotic excitement. *Medical Journal of Australia,* 2**,** 349-352.

CRYNS, K., SHAMIR, A., SHAPIRO, J., DANEELS, G., GORIS, I., VAN CRAENENDONCK, H., STRAETEMANS, R., BELMAKER, R. H., AGAM, G., MOECHARS, D. & STECKLER, T. 2007. Lack of lithium-like behavioral and molecular effects in IMPA2 knockout mice. *Neuropsychopharmacology,* 32**,** 881-891.

CRYNS, K., SHAMIR, A., VAN ACKER, N., LEVI, I., DANEELS, G., GORIS, I., BOUWKNECHT, J. A., ANDRIES, L., KASS, S., AGAM, G., BELMAKER, H., BERSUDSKY, Y., STECKLER, T. & MOECHARS, D. 2008. IMPA1 is essential for embryonic development and lithium-like pilocarpine sensitivity. *Neuropsychopharmacology,* 33**,** 674-684.

DRAPER, S., KIRIGITI, M., GLAVAS, M., GRAYSON, B., CHONG, C. N. A., JIANG, B., SMITH, M. S., ZELTSER, L. M. & GROVE, K. L. 2010. Differential gene expression between neuropeptide Y expressing neurons of the dorsomedial nucleus of the Hypothalamus and the Arcuate Nucleus: Microarray Analysis Study. *Brain Research,* 1350**,** 139-150.

EBADI, M. S., SIMMONS, V. J., HENDRICKSON, M. J. & LACY, P. S. 1974. Pharmacokinetics of lithium and its regional distribution in rat-brain. *European Journal of Pharmacology,* 27**,** 324-329.

EISENBERG JR, F. & PARTHASARATHY, R. 1987. Measurement of biosynthesis of myo-inositol from glucose 6-phosphate. *Methods in enzymology*, 141,127-143.

FISHER, S. K., NOVAK, J. E. & AGRANOFF, B. W. 2002. Inositol and higher inositol phosphates in neural tissues: homeostasis, metabolism and functional significance. *Journal of Neurochemistry,* 82**,** 736-754.

FLODBY, P., LIAO, D. Z., BLANCK, A., XANTHOPOULOS, K. G. H. & HALLSTROM, P. 1995. Expression of the liver-enriched transcription factors C/EBP-alpha, C/EBP-beta, HNF-1, and HNF-4 in preneoplastic nodules and hepatocellular-carcinoma in rat-liver. *Molecular Carcinogenesis,* 12**,** 103-109.

GEOFFROY, P. A., CURIS, E., COURTIN, C., MOREIRA, J., MORVILLERS, T., ETAIN, B., LAPLANCHE, J. L., BELLIVIER, F. & MARIE-CLAIRE, C. 2017. Lithium response in bipolar disorders and core clock genes expression.: *The World Journal of Biological Psychiatry*, 18, 1–14.

GERY, S., GOMBART, A. F., YI, W. S., KOEFFLER, C., HOFMANN, W. K. & KOEFFLER, H. P. 2005. Transcription profiling of C/EBP targets identifies Per2 as a gene implicated in myeloid leukemia. *Blood,* 106**,** 2827-2836.

HARVEY, A. G. 2008. Sleep and circadian rhythms in bipolar disorder: Seeking synchrony, harmony, and regulation. *American Journal of Psychiatry,* 165**,** 820-829.

HAYASHI, Y., WANG, W., NINOMIYA, T., NAGANO, H., OHTA, K. & OTOH, H. 1999. Liver enriched transcription factors and differentiation of hepatocellular carcinoma. *Journal of Clinical Pathology-Molecular Pathology,* 52**,** 19-24.

HO, A. K., MACKOVA, M., PRICE, L. & CHIK, C. L. 2003. Diurnal variation in p42/44 mitogen-activated protein kinase in the rat pineal gland. *Molecular and Cellular Endocrinology,* 208**,** 23-30.

HOFFMANN, J., SYMUL, L., SHOSTAK, A., FISCHER, T., NAEF, F. & BRUNNER, M. 2014. Non-Circadian Expression Masking Clock-Driven Weak Transcription Rhythms in U2OS Cells. *Plos One,* 9**,** e102238.

HUGHES, A. T., FAHEY, B., CUTLER, D. J., COOGAN, A. N. & PIGGINS, H. D. 2004. Aberrant gating of photic input to the suprachiasmatic circadian pacemaker of mice lacking the VPAC(2) receptor. *Journal of Neuroscience,* 24**,** 3522-3526.

INOUE, K., SHIMADA, S., MINAMI, Y., MORIMURA, H., MIYAI, A., YAMAUCHI, A. & TOHYAMA, M. 1996. Cellular localization of Na+/MYO-inositol cotransporter mRNA in the rat brain. *Neuroreport,* 7**,** 1195-1198.

JOHNSSON, A., PFLUG, B., ENGELMANN, W. & KLEMKE, W. 1979. Effect of lithium-carbonate on circadian periodicity in humans. *Pharmakopsychiatrie Neuro-Psychopharmakologie,* 12**,** 423-425.

KAISER, L. G., SCHUFF, N., CASHDOLLAR, N. & WEINER, M. W. 2005. Scyllo-inositol in normal aging human brain: H-1 magnetic resonance spectroscopy study at 4 Tesla. *Nmr in Biomedicine,* 18**,** 51-55.

KAPUSHESKY, M., EMAM, I., HOLLOWAY, E., KURNOSOV, P., ZORIN, A., MALONE, J., RUSTICI, G., WILLIAMS, E., PARKINSON, H. & BRAZMA, A., 2009. Gene expression atlas at the European bioinformatics institute. *Nucleic acids research*, 38, D690-D698.

KRIPKE, D. F. & WYBORNEY, V. G. 1980. Lithium slows rat circadian activity rhythms. *Life Sciences,* 26**,** 1319-1321.

LI, J., LU, W.-Q., BEESLEY, S., LOUDON, A. S. I. & MENG, Q.-J. 2012. Lithium Impacts on the Amplitude and Period of the Molecular Circadian Clockwork. *Plos One,* 7**,** e33292.

LUBRICH, B., PATISHI, Y., KOFMAN, O., AGAM, G., BERGER, M., BELMAKER, R. H. & VANCALKER, D. 1997. Lithium-induced inositol depletion in rat brain after chronic treatment is restricted to the hypothalamus. *Molecular Psychiatry,* 2**,** 407-412.

LUBRICH, B., SPLEISS, O., GEBICKE-HAERTER, P. J. & VAN CALKER, D. 2000. Differential expression, activity and regulation of the sodium/myo-inositol cotransporter in astrocyte cultures from different regions of the rat brain. *Neuropharmacology,* 39**,** 680-690.

LUBRICH, B. & VAN CALKER, D. 1999. Inhibition of the high affinity myo-inositol transport system: A common mechanism of action of antibipolar drugs? *Neuropsychopharmacology,* 21**,** 519-529.

MALHI, G. S., TANIOUS, M., DAS, P., COULSTON, C. M. & BERK, M. 2013. Potential Mechanisms of Action of Lithium in Bipolar Disorder Current Understanding. *Cns Drugs,* 27**,** 135-153.

MASAKI, T., MATSUURA, T., OHKAWA, K., MIYAMURA, T., OKAZAKI, I., WATANABE, T. & SUZUKI, T. 2006. All-trans retinoic acid down-regulates human albumin gene expression through the induction of C/EBP beta-LIP. *Biochemical Journal,* 397**,** 345-353.

MASON, R. & BIELLO, S. M. 1992. A neurophysiological study of a lithium-sensitive phosphoinositide system in the hamster suprachiasmatic (SCN) biological clock in vitro. *Neuroscience Letters,* 144**,** 135-138.

MCCARTHY, M. J., WEI, H., MARNOY, Z., DARVISH, R. M., MCPHIE, D. L., COHEN, B. M. & WELSH, D. K. 2013. Genetic and clinical factors predict lithium's effects on PER2 gene expression rhythms in cells from bipolar disorder patients. *Translational Psychiatry,* 3**,** e318.

MORRIS, E. J., JHA, S., RESTAINO, C. R., DAYANANTH, P., ZHU, H., COOPER, A., CARR, D., DENG, Y. G., JIN, W. H., BLACK, S., LONG, B., LIU, J., DINUNZIO, E., WINDSOR, W., ZHANG, R. M., ZHAO, S. X., ANGAGAW, M. H., PINHEIRO, E. M., DESAI, J., XIAO, L., SHIPPS, G., HRUZA, A., WANG, J., KELLY, J., PALIWAL, S., GAO, X. L., BABU, B. S., ZHU, L., DAUBLAIN, P., ZHANG, L., LUTTERBACH, B. A., PELLETIER, M. R., PHILIPPAR, U., SILIPHAIVANH, P., WITTER, D., KIRSCHMEIER, P., BISHOP, W. R., HICKLIN, D., GILLILAND, D. G., JAYARAMAN, L., ZAWEL, L., FAWELL, S. & SAMATAR, A. A. 2013. Discovery of a Novel ERK Inhibitor with Activity in Models of Acquired Resistance to BRAF and MEK Inhibitors. *Cancer Discovery,* 3**,** 742-750.

NACCARATO, W. F., RAY, R. E. & WELLS, W. W. 1974. Biosynthesis of myo-inositol in rat mammary gland. Isolation and properties of the enzymes.: *Archives of biochemistry and biophysics*, 164, 194-201.

NADAKAVUKAREN, J. J., WELSH, D. K. & REPPERT, S. M. 1990. Aluminum fluoride reveals a phosphoinositide system within the suprachiasmatic region of rat hypothalamus. *Brain Research,* 507**,** 181-188.

NEMANOV, L., EBSTEIN, R. P., BELMAKER, R. H., OSHER, Y. & AGAM, G. 1999. Effect of bipolar disorder on lymphocyte inositol monophosphatase mRNA levels. *International Journal of Neuropsychopharmacology,* 2**,** 25-29.

O'DONNELL, K. C. & GOULD, T. D. 2007. The behavioral actions of lithium in rodent models: Leads to develop novel therapeutics. *Neuroscience and Biobehavioral Reviews,* 31**,** 932-962.

OHNISHI, T., MURATA, T., WATANABE, A., HIDA, A., OHBA, H., IWAYAMA, Y., MISHIMA, K., GONDO, Y. & YOSHIKAWA, T. 2014. Defective Craniofacial Development and

Brain Function in a Mouse Model for Depletion of Intracellular Inositol Synthesis. *Journal of Biological Chemistry,* 289**,** 10785-10796.

OSLAND, T. M., FERNO, J., HAVIK, B., HEUCH, I., RUOFF, P., LAERUM, O. D. & STEEN, V. M. 2011. Lithium differentially affects clock gene expression in serum-shocked NIH-3T3 cells. *Journal of Psychopharmacology,* 25**,** 924-933.

PARDO, R., ANDREOLOTTI, A. G., RAMOS, B., PICATOSTE, F. & CLARO, E. 2003. Opposed effects of lithium on the MEK-ERK pathway in neural cells: inhibition in astrocytes and stimulation in neurons by GSK3 independent mechanisms. *Journal of Neurochemistry,* 87**,** 417-426.

PATISHI, Y., LUBRICH, B., BERGER, M., KOFMAN, O., VANCALKER, D. & BELMAKER, R. H. 1996. Differential uptake of myo-inositol in vivo into rat brain areas. *European Neuropsychopharmacology,* 6**,** 73-75.

PHIEL, C. J. & KLEIN, P. S. 2001. Molecular targets of lithium action. *Annual Review of Pharmacology and Toxicology,* 41**,** 789-813.

RAMANATHAN, C., XU, H. Y., KHAN, S. K., SHEN, Y., GITIS, P. J., WELSH, D. K., HOGENESCH, J. B. & LIU, A. C. 2014. Cell Type-Specific Functions of Period Genes Revealed by Novel Adipocyte and Hepatocyte Circadian Clock Models. *Plos Genetics,* 10**,** e1004244.

ROCK, P., GOODWIN, G., HARMER, C. & WULFF, K. 2014. Daily rest-activity patterns in the bipolar phenotype: A controlled actigraphy study. *Chronobiology International,* 31**,** 290-296.

ROSS, S. E., ERICKSON, R. L., HEMATI, N. & MACDOUGALD, O. A. 1999. Glycogen synthase kinase 3 is an insulin-regulated C/EBP alpha kinase. *Molecular and Cellular Biology,* 19**,** 8433-8441.

SHAMIR, A., EBSTEIN, R. P., NEMANOV, L., ZOHAR, A., BELMAKER, R. H. & AGAM, G. 1998. Inositol monophosphatase in immortalized lymphoblastoid cell lines indicates susceptibility to bipolar disorder and response to lithium therapy. *Molecular Psychiatry,* 3**,** 481-482.

SHAPIRO, J., BELMAKER, R. H., BIEGON, A., SEKER, A. & AGAM, G. 2000. Scyllo-inositol in post-mortem brain of bipolar, unipolar and schizophrenic patients. *Journal of Neural Transmission,* 107**,** 603-607.

SHIM, M. & SMART, R. C. 2003. Lithium stabilizes the CCAAT/enhancer-binding protein alpha (C/EBP alpha) through a glycogen synthase kinase 3 (GSK3)-independent pathway involving direct inhibition of proteasomal activity. *Journal of Biological Chemistry,* 278**,** 19674-19681.

SINGH, N., HALLIDAY, A. C., THOMAS, J. M., KUZNETSOVA, O. V., BALDWIN, R., WOON, E. C. Y., ALEY, P. K., ANTONIADOU, I., SHARP, T., VASUDEVAN, S. R. & CHURCHILL, G. C. 2013. A safe lithium mimetic for bipolar disorder. *Nature Communications,* 4**,** 1332.

SPECTOR, R. & LORENZO, A. V. 1975. Myo-inositol transport in the central nervous system. *American Journal of Physiology-Legacy Content*, 228, 1510-1518.

TAKAHASHI, J. S. 2017. Transcriptional architecture of the mammalian circadian clock. *Nature Reviews Genetics,* 18**,** 164-179.

THOENNISSEN, N. H., THOENNISSEN, G. B., ABBASSI, S., NABAVI-NOUIS, S., SAUER, T., DOAN, N. B., GERY, S., MULLER-TIDOW, C., SAID, J. W. & KOEFFLER, H. P. 2012. Transcription factor CCAAT/enhancer-binding protein alpha and critical circadian clock downstream target gene PER2 are highly deregulated in diffuse large B-cell lymphoma. *Leukemia & Lymphoma,* 53**,** 1577-1585.

UHLÉN, M., FAGERBERG, L., HALLSTRÖM, B.M., LINDSKOG, C., OKSVOLD, P., MARDINOGLU, A., SIVERTSSON, Å., KAMPF, C., SJÖSTEDT, E., ASPLUND, A. & OLSSON, I., 2015. Tissue-based map of the human proteome. *Science*, 347, 1260419.

VADEN, D. L., DING, D., PETERSON, B. & GREENBERG, M. L. 2001. Lithium and valproate decrease inositol mass and increase expression of the yeast INO1 and INO2 genes for inositol biosynthesis. *Journal of Biological Chemistry,* 276**,** 15466-15471.

VAN CALKER, D. & BELMAKER, R. H. 2000. The high affinity inositol transport system implications for the pathophysiology and treatment of bipolar disorder. *Bipolar Disorders,* 2**,** 102-107.

WILLIAMS, R. S. B., CHENG, L. L., MUDGE, A. W. & HARWOOD, A. J. 2002. A common mechanism of action for three mood-stabilizing drugs. *Nature,* 417**,** 292-295.

YANG, S., VAN DONGEN, H. P. A., WANG, K., BERRETTINI, W. & BUCAN, M. 2009. Assessment of circadian function in fibroblasts of patients with bipolar disorder. *Molecular Psychiatry,* 14**,** 143-155.

YIN, L., WANG, J., KLEIN, P. S. & LAZAR, M. A. 2006. Nuclear receptor Rev-erba is a critical lithium-sensitive component of the circadian clock. *Science,* 311**,** 1002-1005.

YOON, I. S., LI, P. P., SIU, K. P., KENNEDY, J. L., COOKE, R. G., PARIKH, S. V. & WARSH, J. J. 2001. Altered IMPA2 gene expression and calcium homeostasis in bipolar disorder. *Molecular Psychiatry,* 6**,** 678-683.

YORK, J. D., PONDER, J. W. & MAJERUS, P. W. 1995. Definition of a metal-dependent Li+-inhibited phosphomonoesterase protein family based upon a conserved 3-dimensional core structure. *Proceedings of the National Academy of Sciences of the United States of America,* 92**,** 5149-5153.

ZHANG, R., LAHENS, N. F., BALLANCE, H. I., HUGHES, M. E. & HOGENESCH, J. B. 2014. A circadian gene expression atlas in mammals: Implications for biology and medicine. *Proceedings of the National Academy of Sciences of the United States of America,* 111**,** 16219-16224.

Chapter 6: *In Vitro* Modulation of the Adenylate Cyclase Pathway Influences Molecular Circadian Rhythmicity

6.1 Introduction

It is widely acknowledged that sleep and circadian rhythm disruptions form a core component of many neuropsychiatric disorders, including BPD (Jagannath et al., 2013). Therefore, a novel route to treating such disorders may be to target these disruptions. Lithium is a principal mood-stabilising agent used in the treatment of BPD. This ion also induces significant chronomodulatory effects, increasing both period and amplitude. We previously found that lithium-induced inhibition of IMPase causes circadian period lengthening (Chapter 5). Additionally, post-translational modifications including the actions of cAMP and various kinases play an important role in providing input signals to the molecular clock. Therefore, as adenylate cyclase (AC) is an additional well characterised target of lithium, we set out to understand the chronomodulatory consequences of AC inhibition.

6.1.1 The adenylate cyclase pathway

The AC signalling cascade (*Figure 6.1*) is a major GPCR pathway that may affect both mood and circadian regulation. Investigations of the AC-cAMP-protein kinase A (PKA) signalling pathway began over 60 years ago, initiated by the discovery of the pivotal second messenger molecule known as cAMP by Earl Sutherland, for which he later won the Nobel Prize in Physiology or Medicine (Rall and Sutherland, 1958, Sutherland and Rall, 1958). Whilst these initial discoveries showed the presence of cAMP in the liver, heart, muscle, and brain, it is now known to have ubiquitous expression patterns (Pierre et al., 2009). As a ubiquitous and conserved second messenger molecule, cAMP is involved in many

diverse physiological functions, from learning and memory to olfaction, and nociception to name a few (Wong et al., 1999, Wong et al., 2000, Collier and Roy, 1974).

There are currently 10 known isoforms of AC encoded by different genes, whereby 9 are membrane bound (AC1-AC9) and exhibit high levels of sequence conservation and one exists as a soluble form (AC10) (Hanoune and Defer, 2001). The membrane bound isoforms can be broadly divided into four categories as summarised in *Table 6.1*. They are composed of 12 membrane-spanning regions divided into 2 clusters with 2 large cytoplasmic domains named C1 and C2 (~40kDa each) located between the 6th and 7th transmembrane regions and after the 12th membrane region. Heterodimerisation of the cytoplasmic domains is critical for the catalytic activity of AC, catalysing the conversion of ATP to cAMP, which acts as the fundamental second messenger molecule utilised by the AC pathway (Hurley, 1999).

Table 6.1. Classification of the membrane bound adenylate cyclase isoforms (adapted from Sadana and Dessauer, 2009).

Class	Isoforms	Activity
Group I	AC1 AC3 AC8	• Moderate activation of PKC • Calcium sensitive • Calcium-calmodulin sensitive
Group II	AC2 AC4 AC7	• PKC sensitive • Calcium insensitive
Group III	AC5 AC6	• PKA sensitive • PKC sensitive
Group IV	AC9	• PKC sensitive • Calcineurin sensitive • Forskolin insensitive

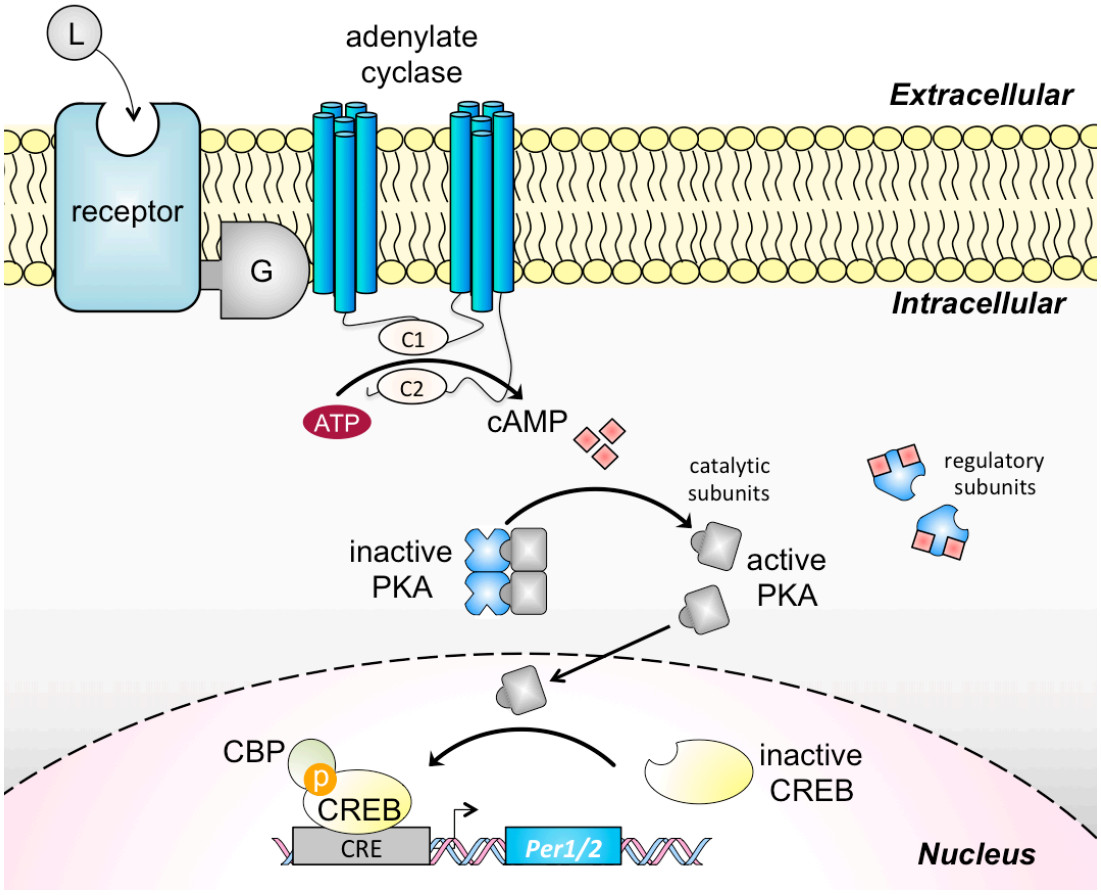

Figure 6.1. **Schematic diagram of the adenylate cyclase pathway.** This major GPCR pathway can be initiated by ligands such as neurotransmitters binding to their appropriate receptors. Depending on whether the receptor is G_s or G_i coupled, this induces activation or inhibition of AC respectively. Activated AC can then catalyse the conversion of ATP to cAMP. The elevation in cAMP levels enables four molecules to bind to the regulatory subunits of the PKA enzyme reducing their affinity towards the catalytic subunits. The catalytic subunits then enter the nucleus where they are able to phosphorylate many proteins including CREB, allowing the co-factor CBP to attach. This induces in the transcription of genes with CRE elements in their promoter regions, such as the core clock genes *Per1/2*. L: ligand, G: G-protein, P: phosphorylation, other abbreviations are found in the text.

After ligand binding to GPCRs (e.g. serotonin or adrenaline), AC can be activated or inhibited via the G-proteins G_s and G_i respectively, which will then determine changes in cAMP levels and subsequently effect the activation of hyperpolarization-activated cyclic nucleotide-gated channels (HCN) (mediating spontaneous rhythmic activity in the heart and brain), Epac (modulating GTP protein binding to Rap1), and PKA (Bos, 2003, Lewis and Chetkovich, 2011).

PKA is structurally comprised of 2 regulatory and 2 catalytic subunits present under basal conditions as an inactive holoenzyme (Johnson et al., 2001). The regulatory proteins serve to prevent excessive phosphorylation of serine/threonine residues of downstream targets and to anchor the catalytic subunits to specific cellular locations via A kinase anchoring proteins (Wong and Scott, 2004). The co-operative binding of 2 cAMP molecules to the regulatory subunit induces a conformational change allowing a further 2 cAMP molecules to bind. This results in dissociation of the regulatory and catalytic subunits, freeing the catalytic subunits to phosphorylate and regulate various cytoplasmic and nuclear proteins (Su et al., 1995).

An important target, and the first transcription factor shown to be controlled by phosphorylation, is the nuclear cAMP response element (CRE) binding protein (CREB) that is subject to phosphorylation by PKA at serine 133 (Gonzalez and Montminy, 1989). Following phosphorylation, binding of CREB to the CRE TGACGTCA recognition sequence results in conformational changes that facilitate binding of the transcriptional co-activator CREB-binding protein (CBP) which subsequently promotes gene transcription (Chrivia et al., 1993).

6.1.2 The role of adenylate cyclase signalling in regulating circadian rhythms

The AC signalling pathway is pivotal to many regulatory aspects of the SCN. cAMP is considered essential in the modulation of the molecular clock and generation of mammalian circadian rhythms. Current evidence suggests that pharmacological manipulation of this pathway modulates period, amplitude, and phase responses (O'Neill et al., 2008). It was found that light induced CREB phosphorylation, an action that was gated by the circadian clock. Phosphorylation only occurred during the dark phase, a time where light-induce phase shifting also occurred (Ginty et al., 1993). Subsequently, the SCN was found to contain 24h expression patters in CRE-mediated gene transcription, an effect that was potentiated with a 1h light pulse (Obrietan et al., 1999). The *Per1* and *Per2* genes both contain functional CRE elements upstream of the E-box elements and were found to be the two light-inducible core clock components. Whilst *Per2* values peaked ~2h following light exposure, *Per1* levels peak immediately (Albrecht et al., 1997, Shearman et al., 1997, Travnickova-Bendova et al., 2002). It should be noted that CREB phosphorylation can also occur via alternative means such as the MAPK pathway, where both the cAMP and MAPK pathways induce CRE-mediated *Per1* gene transcription and synergistic actions may be responsible for its rapid rate of induction (Travnickova-Bendova et al., 2002). This suggests that CREB-mediated core clock gene transcription is vital in allowing organisms to adapt to external environments by enabling clock re-setting.

Additionally, light activates ipRGCs, which then directly innervate the ventrolateral SCN neurones via the RHT (Reppert and Weaver, 2002). Along with

synaptic glutamate, the neuropeptide PACAP is also released. Functional studies have found that PACAP alone, or in concert with glutamate facilitate light signalling to the clock (Harrington et al., 1999, Chen et al., 1999). This neuropeptide binds to GPCRs and activates the MAPK and AC signalling pathways, both of which impact CREB-mediated gene transcription (Eiden et al., 2008). Furthermore, PACAP knockout mice exhibited highly attenuated light-induced phase advances (Kawaguchi et al., 2003). Moreover, the ventrolateral neurones contain an abundance of the neuropeptide VIP. After biding to its cognate VPAC2 receptor, VIP activates AC-cAMP-PKA-CREB signalling (Langer, 2012). Indeed, VIP or VPAC2 knockout mice show altered light responses, including behavioural arrhythmicity or period variability, dampened SCN firing rate rhythms and abnormalities in gating photic responses (Harmar et al., 2002, Aton et al., 2005, Cutler et al., 2003, Hughes et al., 2004).

6.1.3 The role of adenylate cyclase signalling in bipolar disorder

Being such a core signalling pathway mediating many aspects of physiological functions, it is plausible that AC signalling may be defective in patients with BPD. A recent genome wide association study including over 9,000 patients and 14,000 controls found polymorphisms in the gene encoding AC2 (Muhleisen et al., 2014). Moreover, initial studies found that when assessing [^{3}H] cAMP content from deceased BPD patients, there were reductions is cytosolic binding within the frontal, temporal, parietal, and occipital cortices, as well as the cerebellum and thalamus (Rahman et al., 1997). Whilst this may suggest reduced PKA activity, subsequent studies found that basal and cAMP-stimulated PKA activity was higher in the temporal cortex of BPD subjects (Fields et al.,

1999). This may be because Epac and HCN are also targets of cAMP and so alterations to the ratio of these targets in the brain may account for the observed discrepancy. Moreover, elevated expression of the PKA catalytic subunit was detected in the frontal and temporal cortices, suggesting increased kinase activity (Chang et al., 2003). Further studies substantiated these claims as BPD lymphoblasts showed reduced [^{3}H] cAMP binding to PKA and elevated PKA activity (Karege et al., 2004).

This upregulation of PKA signalling could then suggest an increase in CREB-mediated gene transcription. Indeed, basal phosphorylated CREB levels were elevated by ~40% in BPD lymphoblasts. Interestingly, basal levels were also found to be significantly elevated in both affected and unaffected relatives of BPD patients responsive to lithium treatment, suggesting that signalling dysfunction may have an inherent genetic role in BPD pathophysiology (Alda et al., 2013). Moreover, when comparing responses in patient-derived fibroblasts to healthy controls, forskolin stimulation augmented CREB induction by 3.3 fold (Gaspar et al., 2014). However, large inter-individual variations in transcriptional activity were observed, which may account for the mixed literature on the associations between CREB and BPD, as Alda et al. did not find any significant elevations in forskolin-stimulated CREB (Gaspar et al., 2014, Alda et al., 2013). Also, reductions in CREB have been identified in post-mortem pre-frontal cortex and cingulate gyrus samples. Whilst areas such as the temporal cortex were not analysed, this could indicate region specific variability, all of which could contribute to BPD pathophysiology (Ren et al., 2014).

Interestingly, of the pharmacological actions of lithium, inhibition of AC occurs via competitive displacement of magnesium from the magnesium-binding site (Mork and Geisler, 1987). The first publication assessing lithium's effects on AC found inhibition of noradrenaline-induced and histamine-induced cAMP in rat and rabbit cortical slices respectively, from 2mM concentrations (Forn and Valdecasas, 1971). Subsequently, human-based studies have shown that near therapeutic lithium concentrations were able to inhibit β2-adrenergic-induced (via salbutamol) AC activity, noradrenaline-induced AC activity, and forskolin-induced AC activity (Belmaker, 1981, Newman et al., 1983, Ebstein et al., 1987). The latter study also highlighted the variable response of lithium on AC activity, which may be implicated in altered patient drug responses. Therefore, it is plausible that lithium may function via moderating overstimulated AC signaling.

6.1.4 Aims

Thus, we know that circadian rhythm disruptions are core to BPD, a condition also associated with disrupted AC signalling pathways, and that these pathways mediate many vital aspects of a functioning circadian system. The available literature suggests that inhibition of this pathway induces period lengthening and amplitude dampening. Given that lithium also lengthens period but increases amplitude, we set out to further explore whether the manipulation of the AC pathway could modulate circadian periodicity. Given that cAMP can be generated by various AC isoforms and in turn act via numerous targets to alter gene transcription, we explored the effects of pharmacologically targeting proteins involved in this signal transduction cascade, to evaluate whether AC could be a viable period modulating target for future drug discovery.

6.2 Results

The murine MMHD3 cells and human U2OS cells were used to assess the effects of pharmacologically targeting AC, PKA, and CBP on circadian period in order to address the hypothesis that inhibiting any pivotal component of this pathway would induce period lengthening.

6.2.1 LiCl reduces cAMP and CREB activity in the MMHD3 cells

AC is believed to be amongst the numerous targets of lithium. We have previously shown in Chapter 5.2.1 that LiCl induced period lengthening in the MMHD3 cells by 2.5h and 3.4h at 20 and 30mM concentrations respectively, with no effect in U2OS cells. Therefore, to elucidate whether LiCl modulates AC in the MMHD3 cell model, the effects of LiCl on cAMP and CREB activity were assessed. As the *cAMP::GloSensor* assay, for reasons unknown, failed to detect any changes in cAMP concentration in this cell line, a cAMP ELISA was used as an alternative method of investigation. It was found that LiCl dose-dependently reduced cAMP concentrations by 36% and 46% at 20 and 30mM concentrations respectively (vehicle: 0.17±0.01, 20mM: 0.12±0.00, 30mM: 0.09±0.01 pmol/3x10^4 cells) (*Figures 6.2A-B*). Concurrently, both 20 and 30mM LiCl significantly reduced forskolin-induced CREB activity by 65% and 70% respectively 20mM: 35.46±11.50, 30mM: 30.02±7.13 % change) (*Figures 6.2C-D).* Therefore, LiCl was also able to reduce cAMP and CREB activity in the MMHD3 cells at concentrations where we observe period lengthening. Based on these findings, we decided to further explore the AC pathway.

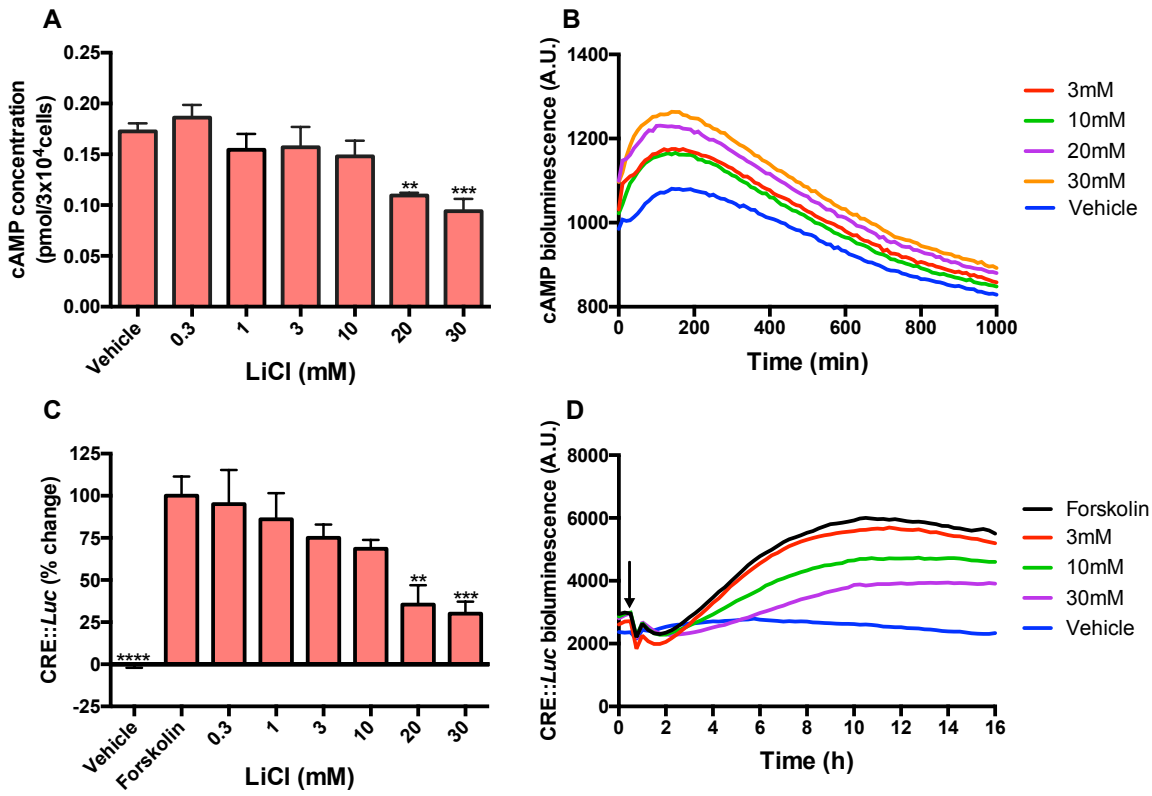

Figure 6.2. **LiCl reduces cAMP and CREB activity in the MMHD3 cells. A-B)** The effects of LiCl on cAMP in the cAMP ELISA assay (n=4), with example bioluminescence traces. **C-D)** The effects of LiCl on CREB induction using a CRE::*Luc* assay (n=6), and characteristic trace diagrams. Arrow indicates time of forskolin treatment.

6.2.2 Vidarabine lengthens period in the U2OS cells

In order to investigate the relationship between AC inhibition and circadian period, we first assessed the synthetic anti-viral drug vidarabine that possesses an IC50 from 2.2μM (AC5) to 250μM (AC2) (Brand et al., 2013). As seen in *Figures 6.3A-B*, forskolin-induced CREB activity was reduced from 100μM concentrations by 51%, where 300μM and 1mM concentrations reduced activity by 85% and 94% respectively (100μM: 48.97±3.96, 300μM: 15.25±1.21, 1mM: 6.46±0.18 % change). As displayed in *Figures 6.3C-E*, vidarabine also induced dose-dependent period lengthening in the U20S cells, where concentrations of 30μM, 100μM, 300μM, and 1mM vidarabine lengthened circadian period by 2h, 3.7h, 5.5h, and 7.7h respectively (vehicle: 23.16±0.06, 30μM: 25.20±0.14, 100μM: 26.85±0.12, 300μM: 28.68±1.32, 1mM: 30.85±1.28 h). Further, vidarabine showed significant amplitude dampening (39%-66%) at all concentrations tested within U2OS cells. In all instances cells were tested at concentrations that did not compromise cell viability (*Figure 6.3F*) and, as such, the reduction in amplitude was not due to cell death. Therefore, cAMP may either be important for amplitude maintenance, vidarabine could increase cellular desynchrony, or a non-specific effect of vidarabine may be occurring. Consequently, vidarabine reduced cAMP and CREB in the U2OS cells and lengthened circadian period.

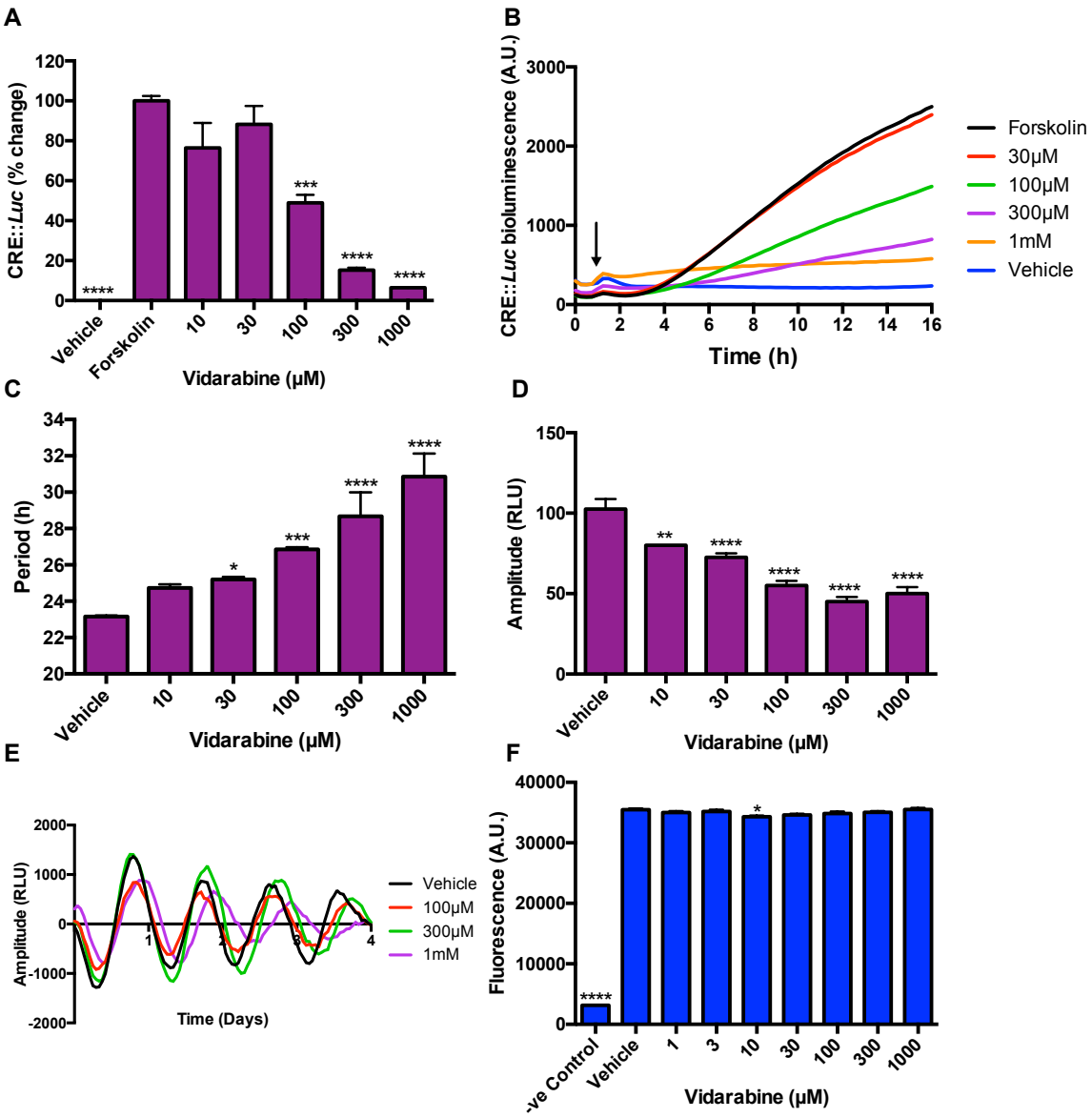

Figure 6.3. **Vidarabine reduces cAMP, CREB, and lengthens period in the U2OS cells. A-B)** The effects of vidarabine on CREB activity using a CRE::*Luc* assay (n=3) and characteristic trace diagrams. The period **(C)** and amplitude **(D)** effects of vidarabine on *Bmal::Luc* U2OS cells (n=4), with representative luminescence traces **(E)**. **F)** Cell viability assay (n=4). Arrow indicates time of forskolin treatment.

6.2.3 Vidarabine lengthens period in the MMHD3 cells

To confirm the effects observed in the U2OS cells, vidarabine was also tested on the MMHD3 cells. As *Figures 6.4A-B* show, concentrations of vidarabine of 3μM or greater reduced cellular cAMP. Specifically, 3μM, 10μM, 30μM, 100μM, 300μM, and 1mM reduced cAMP levels by 30%, 52%, 66%, 60%, 78%, and 80% respectively (vehicle: 0.22±0.01, 3μM: 0.16±0.02, 10μM: 0.12±0.01, 30μM: 0.07±0.00, 100μM: 0.09±0.01, 300μM: 0.05±0.00, 1mM: 0.05±0.01 pmol/3x10^4 cells).

Thereafter, a linear relationship was observed between forskolin-stimulated cAMP and CREB induction. Dose-dependent decreases in CREB activity were observed from 10μM, which reduced activity by 28%, where 30μM, 100μM, 300μM, and 1mM reduced activity by 38%, 59%, 75%, and 87% respectively (10μM: 72.06±7.25, 30μM: 62.06±13.97, 100μM: 40.88±4.33, 300μM: 25.25±7.65, 1mM: 12.94±2.99 % change) (*Figures 6.4C-D*). Vidarabine also lengthened circadian period (*Figures 6.4E, G*). Whilst trends for lengthening were emergent at 10μM concentrations by 3.3h, 30μM, 100μM, and 1mM vidarabine lengthened period by 4.6h, 4h, and 7.8h respectively (vehicle: 24.20±0.12, 10μM: 27.53±0.28, 30μM: 28.80±0.15, 100μM: 28.17±2.19, 1mM: 31.97±0.56 h). Moreover, at concentrations where lengthening was observed (10μM-1mM), amplitude dampening was found in the range of 28%-50% (*Figure 6.4F*). Finally, cell viability was largely maintained at all concentrations tested (*Figure 6.4H*). Thus, vidarabine also reduced cAMP and CREB in the MMHD3 cells and lengthened circadian period.

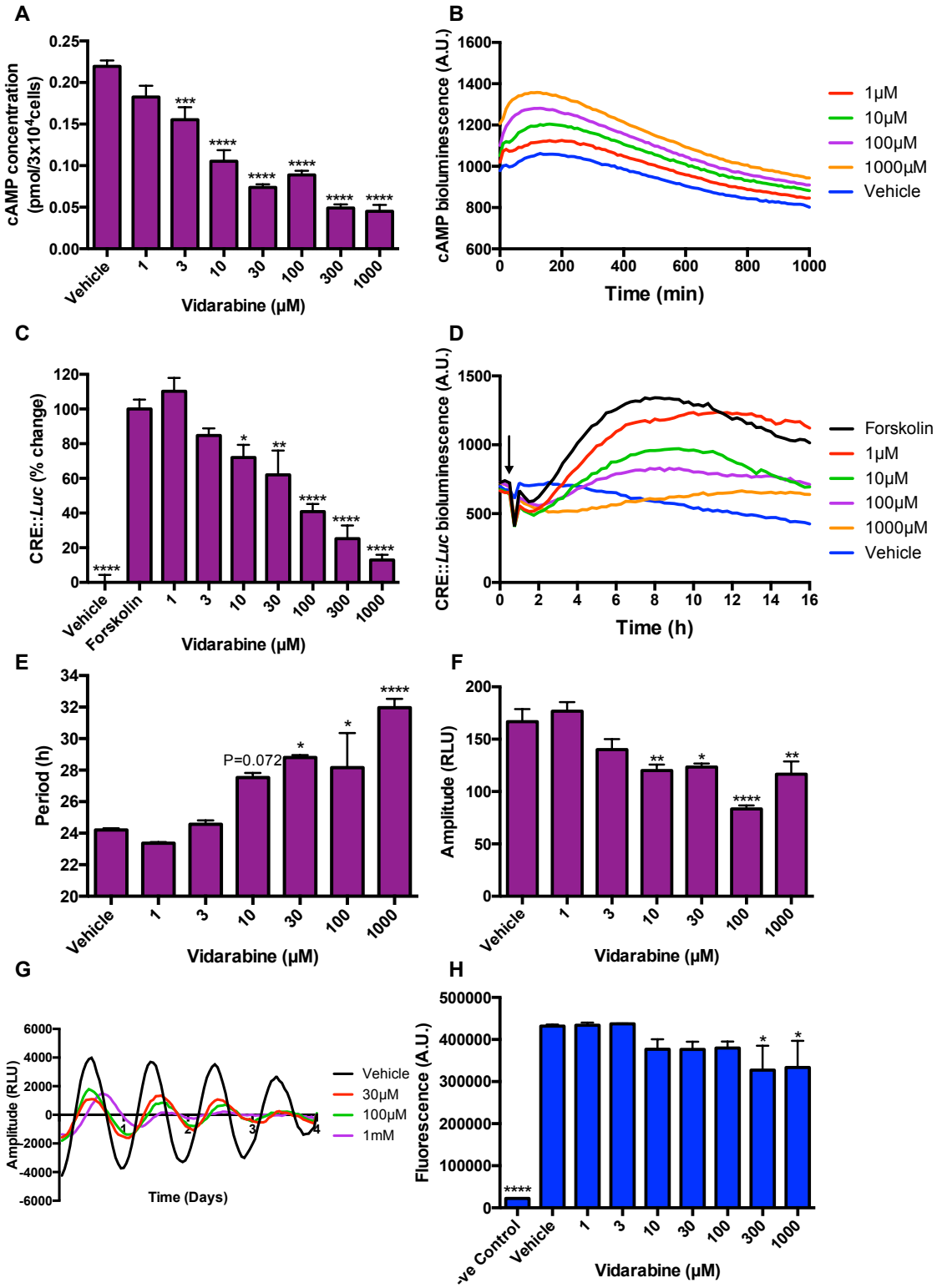

Figure 6.4. **Vidarabine reduces cAMP, CREB, and lengthens period in the MMHD3 cells. A-B)** The effects of vidarabine on cAMP in the cAMP ELISA assay (n=4), with example bioluminescence traces. **C-D)** The effects of vidarabine on CREB induction using a CRE::*Luc* assay (n=3) and characteristic trace diagrams. The period **(E)** and amplitude **(F)** effects of vidarabine on *Bmal::Luc* MMHD3 cells (n=3), with representative luminescence traces **(E)**. **H)** Cell viability assay (n=3). Arrow indicates time of forskolin treatment.

6.2.4 2'5'-dideoxyadenosine lengthens period in the U2OS cells

A second AC inhibitor, 2'5'-dideoxyadenosine (IC50=2.7μM) was assessed on the U2OS cells to confirm that AC inhibition could induce period lengthening (Desaubry et al., 1996a). Using the *cAMP::GloSensor* assay, reductions in forskolin-induced cAMP levels were observed from 100μM concentrations and above, where 100μM, 300μM, and 1mM 2'5'-didioxyadenosine resulted in 28%, 52%, and 62% cAMP inhibition (100μM: 72.47±11.24, 300μM: 47.71±4.86, 1mM: 37.85±5.10 % change) (*Figures 6.5A-B*). Concurrently, the CRE::*Luc* assay revealed that 2'5'-didioxyadenosine reduced forskolin-stimulated CREB induction at 100μM, 300μM, and 1mM concentrations by 38%, 62%, and 89% respectively (100μM: 62.42±2.82, 300μM: 38.23±0.88, 1mM: 10.82±12.46 % change) (*Figures 6.5C-D*). We proceeded to test the hypothesis that 2'5'-didioxyadenosine would also induce period lengthening. As seen in *Figures 6.5E, G*, 300μM and 1mM 2'5'-didioxyadenosine lengthened period by 59min and 2h respectively (vehicle: 23.21±0.16, 300μM: 24.19±0.24, 1mM: 25.16±0.05 h). Additionally, amplitude dampening was observed between 10μM to 300μM concentrations by 8%-19%, where 1mM was no longer significantly different to vehicle treated cells (*Figure 6.5F*). Similarly to previous experiments, cells were tested at concentrations where viability was maintained (*Figure 6.5H*). In summary, 2'5'-didioxyadenosine reduced cAMP and CREB in the U2OS cells and lengthened circadian period.

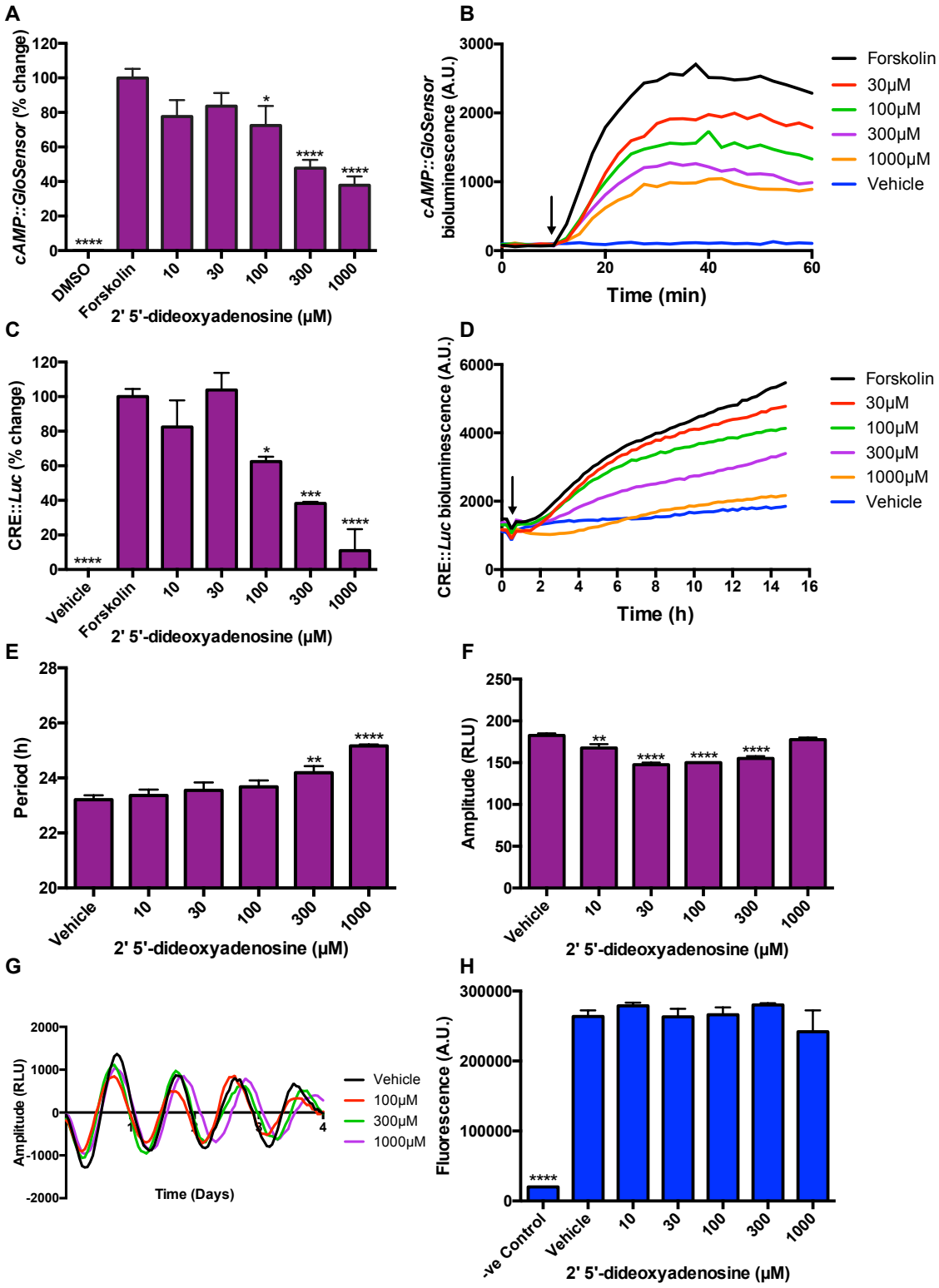

Figure 6.5. **2'5'-dideoxyadenosine reduces cAMP, CREB, and lengthens period in the U2OS cells. A-B)** The effects of 2'5'-didioxyadenosine on cAMP in the *cAMP::GloSensor* assay (n=6), with example traces. **C-D)** The effects of 2'5'-didioxyadenosine on the CRE::*Luc* assay (n=3), and characteristic trace diagrams. The period **(E)** and amplitude **(F)** effects of 2'5'-didioxyadenosine on *Bmal::Luc* U2OS cells (n=4), with representative luminescence traces **(E)**. **H)** Cell viability assay (n=4). Arrow indicates time of forskolin treatment.

6.2.5 2'5'-dideoxyadenosine lengthens period in the MMHD3 cells

To confirm that the effects observed were not a phenomena specific to the U2OS cells, 2'5'-didioxyadenosine was also tested on the MMHD3 cells. The cAMP ELISA highlighted that 2'5'-didioxyadenosine reduced cAMP levels at all concentrations tested. A dose-dependent effect was observed as 10μM reduced cAMP levels by 29%, 30μM and 100μM by 43%, 300μM by 56%, and 1mM by 52%, as seen in *Figures 6.6A-B* (vehicle: 0.22±0.01, 10μM:0.16±0.02, 30μM: 0.13±0.00, 100μM:0.13±0.01, 300μM: 0.10±0.01, 1mM:0.11±0.00 pmol/3x10^4 cells). The basal MMHD3 cellular cAMP concentration was 0.22pmol/3x10^4 cells, a concentration lower than previous assessments with HepG2 liver cells, where 0.23pmol/μg protein was detected (Abcam ab65355 manual).

In concert with the reductions in cAMP, reductions in forskolin-induced CREB activity were observed at all concentrations assessed. Indeed, 10μM reduced CREB induction by 55%, 30μM by 60%, 100μM by 67%, 300μM by 86%, and 1mM by 81% (*Figures 6.6C-D)* (10μM: 45.33±5.99, 30μM: 40.10±2.81, 100μM: 32.99±1.17, 300μM: 14.38±2.30, 1mM: 18.98±2.51 % change). When assessing the circadian effects of 2'5'-didioxyadenosine, no amplitude changes were found, but all concentrations tested lengthened circadian period, as seen in *Figures 6.6E-G*. Concentrations between 10μM and 300μM lengthened period by 1.3-1.7h, where 1mM 2'5'-didioxyadenosine lengthened period by 2.9h (vehicle: 24.06±0.11, 10μM: 25.35±0.15, 30μM: 25.68±0.27, 100μM: 25.37±0.10, 300μM: 25.80±0.19, 1mM: 26.94±0.29 h). Therefore, 2'5'-didioxyadenosine, at concentrations where cell viability was largely maintained (*Figure 6.6H*), reduced cAMP and CREB in the MMHD3 cells and lengthened circadian period.

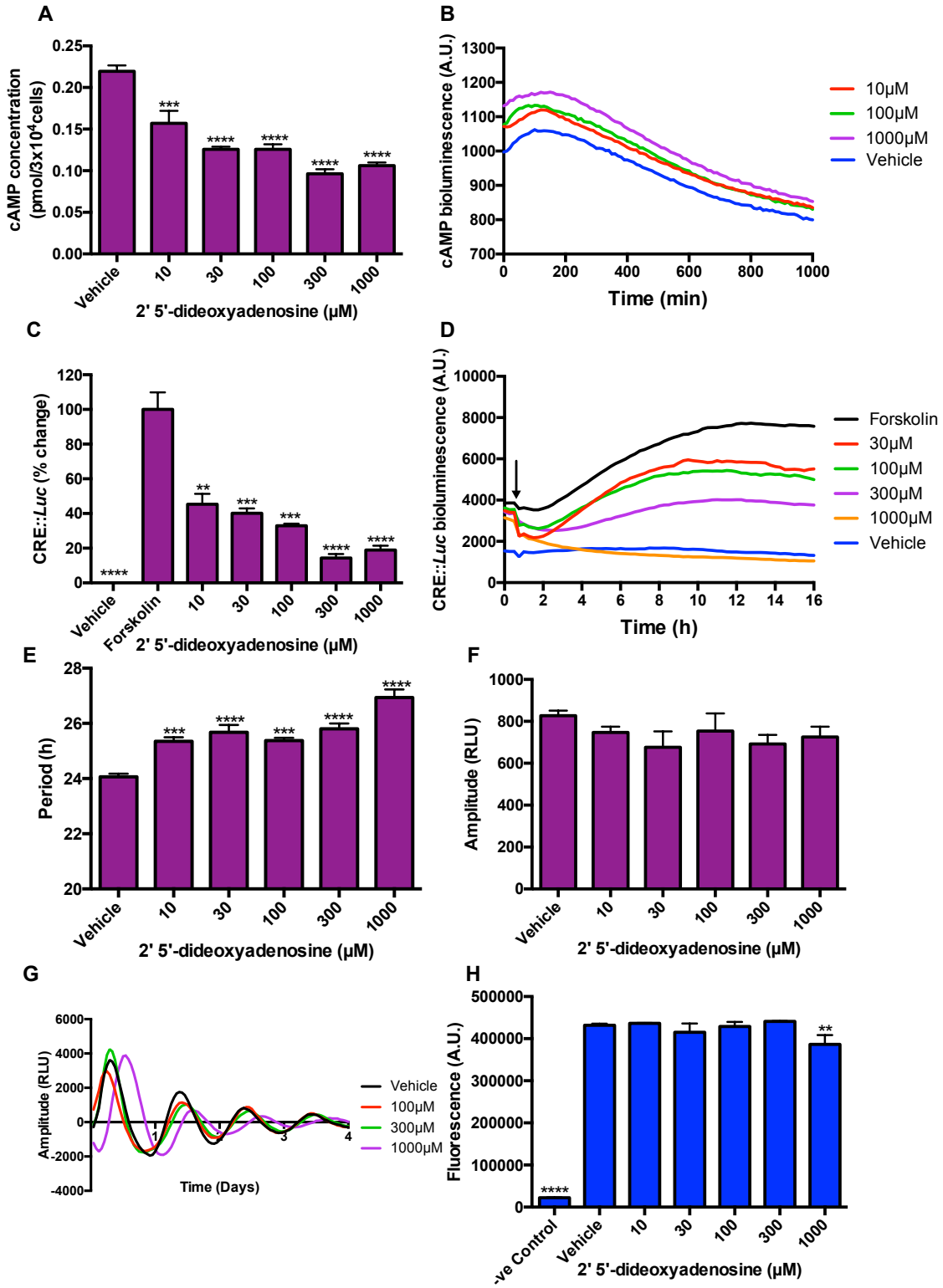

Figure 6.6. **2'5'-dideoxyadenosine reduces cAMP, CREB, and lengthens period in the MMHD3 cells. A-B)** The effects of 2'5'-didioxyadenosine on cAMP in the cAMP ELISA assay (n=4), with example traces. **C-D)** The effects of 2'5'-didioxyadenosine on a CRE::*Luc* assay (n=3), and characteristic trace diagrams. The period **(E)** and amplitude **(F)** effects of 2'5'-didioxyadenosine on *Bmal::Luc* MMHD3 cells (n=4), with representative luminescence traces **(E)**. **H)** Cell viability assay (n=4). Arrow indicates time of forskolin treatment.

6.2.6 Adenylate cyclase 6 is responsible for period lengthening in the MMHD3 cells

As there are currently 10 known isoforms of AC, we decided to explore which isoform or isoforms could be responsible for period lengthening using an siRNA-mediated gene knockdown approach. First, expression levels of each AC isoform were assessed in the MMHD3 cells. There was no AC3, 4, 5, 8, or 10 expressed in this cell line, where cells were regarded as not expressing AC if values were <0.0001 or undetectable. Further, AC1, 2, and 7 were expressed at very low levels as seen in *Figure 6.7A*, where values after being normalised to *Gapdh* were 0.056, 0.001, and 0.006 A.U. respectively. On the other hand, AC6 and AC9 showed high expression levels of 2.318 A.U. and 1.433 A.U. respectively.

Expression data suggested that the AC6 and AC9 isoforms may be predominantly responsible for mediating the period lengthening effects observed with AC inhibition. When assessing the effects of siRNA knockdown of these isoforms an interesting discrepancy emerged between AC6 and AC9, without grossly affecting cell viability (*Figure 6.7B)*. The positive control *Csnk1δ* induced period lengthening by 3.2h, AC6 knockdown lengthened period by 2.3h, and no period effect was observed with AC9 (*siControl*: 21.73±0.06, *Csnk1δ*: 24.95±0.09 AC6: 24.00± 0.24, AC9: 22.35±0.31 h) (*Figures 6.7C, E*). Moreover, whilst *Csnk1δ* and AC6 increased amplitude by 111% and 28% respectively, AC9 induced amplitude dampening by 37% (*Figure 6.7D*). Finally, to confirm that these effects were due to gene knockdown, qPCR analysis confirmed that cellular *Csnk1δ* expression was reduced by 73%, AC6 levels by 89%, and AC9 was partially knocked down by 51.8%, as seen in *Figure 6.7F* (*Csnk1δ* knockdown*:* 27.17±1.26, AC6 knockdown: 11.45±0.72, AC9 knockdown: 28.18±1.80 %).

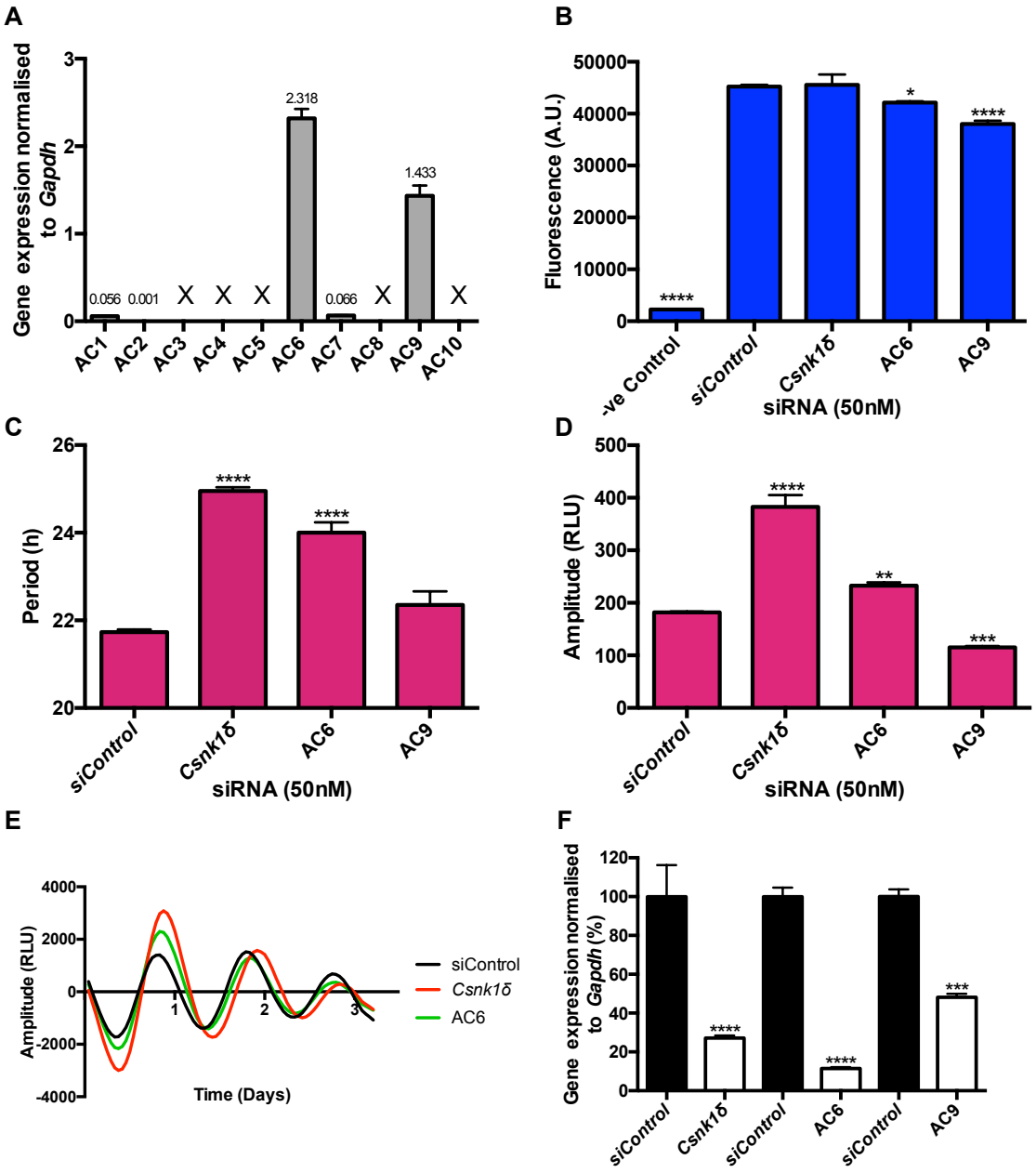

Figure 6.7. **siRNA targeting AC6 lengthens circadian period in the MMHD3 cells. A)** AC isoform expression normalised to *Gapdh* in the MMHD3 cells (n=4). **B)** Cell viability assay (n=4). The period **(C)** or amplitude **(D)** effects after knocking down *Csnk1δ,* AC6, or AC9 (n=4). **E)** Representative traces highlighting the circadian effects of siRNA-induced transcript knockdown. **F)** Validation of transcript knockdown normalised to *Gapdh* (n=4).

6.2.7 H89 lengthens period in the U2OS cells

As AC inhibition lengthened circadian period in line with the proposed hypothesis, inhibition of PKA was subsequently tested using H89, a compound marketed as a potent selective inhibitor of PKA (IC50: 135nM) (Davies et al., 2000). When assessing changes in forskolin-induced CREB activity, H89 showed curious effects in the U2OS cells, as potentiation of CREB activity was observed at 0.3μM and 1μM, by 60% and 25% respectively (0.3μM: 159.60±8.03, 1μM: 125.10±3.04 % change) (*Figures 6.8A-B*). As seen in *Figures 6.8G-H*, we validated these effects using a second PKA inhibitor, KT5720 (IC50: 3.3μM), where similar effects were observed, as 0.3-3μM concentrations were potentiating forskolin-stimulated CREB activity (KT5720 → 0.3μM: 128.50±4.24, 1μM: 140.60±6.56, 3μM: 123.60±8.21 % change) (Davies et al., 2000). However, as concentrations increased, dose-dependent reductions in CREB activity were observed, such that 3μM H89 reduced activity by 28%, 10μM by 100%, and 30μM by 151% (3μM: 71.84±4.33, 10μM: -0.43±1.53, 30μM: -50.66±2.04 % change). This shows that 10μM concentrations reduced intracellular CREB activity to basal levels pre-forskolin stimulation, where 30μM was able to reduce the basal physiological activity of PKA. Indeed, at these concentrations, significant period effects were also observed as 10μM lengthened period by 1.5h, and 30μM lengthened period by 5.1h (vehicle: 23.26±0.07, 10μM: 24.73±0.17, 30μM: 28.40±0.65 h) (*Figures 6.8C, E*). Moreover, 30μM H89 also significantly reduced rhythm amplitude by 51% (*Figure 6.8D*). Finally all drugs were tested at concentrations that did not negatively impact cell viability (*Figure 6.8F*). Thus, at concentrations where H89 reduced CREB activity in the U2OS cells, period lengthening was observed.

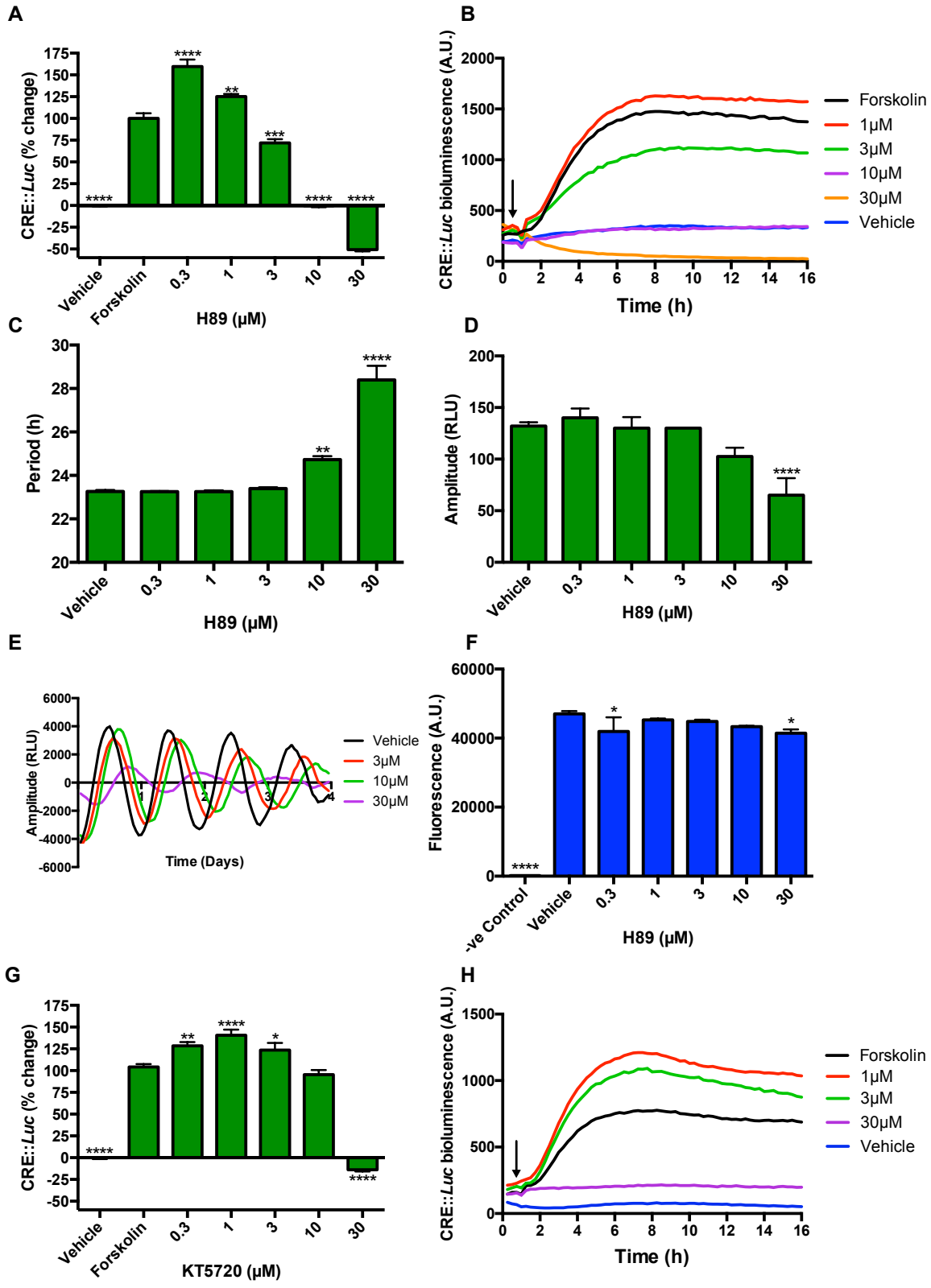

Figure 6.8. **H89 reduces CREB activity and lengthens period in the U2OS cells. A-B)** The effects of H89 on CREB activity using a CRE::*Luc* assay (n=6) and characteristic trace diagrams. The period **(C)** and amplitude **(D)** effects of H89 on *Bmal::Luc* U2OS cells (n=4), with representative luminescence traces **(E)**. **F)** Cell viability assay (n=4). **G-H)** The effects of KT5720 on CREB activity (n=6), and representative traces. Arrow indicates time of forskolin treatment.

6.2.8 H89 lengthens period in the MMHD3 cells

To verify the period lengthening effects found with H89 in the U2OS cells, this compound was also tested in the MMHD3 cell line. As seen in *Figures 6.9A-B*, no potentiation of forskolin-stimulated CREB induction was observed at lower concentrations. On the contrary, all concentrations dose-dependently reduced CREB activity. Whilst 1 and 3μM H89 reduced CREB activity by 62% and 92% respectively, both 10μM and 30μM concentrations resulted in 118% and 120% reductions respectively (1μM: 38.35±10.11, 3μM: 7.97±8.03, 10μM: -17.63±7.40, 30μM: -20.11±17.63 % change). Therefore, much like the U2OS cells, higher concentrations of H89 appeared to reduce basal PKA cellular activity.

Furthermore, when assessing circadian rhythm parameters as seen in *Figures 6.9C-E*, both 10μM and 30μM concentrations presented with period lengthening effects by 5.3h and 8.4h and amplitude dampening by 48% and 31% respectively (vehicle: 23.00±0.00, 10μM: 28.33±1.21, 30μM: 31.40±0.15 h). In summary, when the MMHD3 cells were tested at concentrations where cell viability was maintained (*Figure 6.9F)*, H89 reduced CREB activity and induced significant period lengthening.

6.2.9 CBP112 induced period lengthening in the U2OS cells

With the knowledge that both AC and PKA inhibitors were able to induce period lengthening in the U2OS and MMHD3 cells, CREB was the final component of this pathway to be assessed. As CREB activity requires the co-factor CBP to mediate gene transcription, the effects of CBP inhibitors on circadian period were investigated. CBP112, a CBP inhibitor with an IC50 of 0.17μM dose-

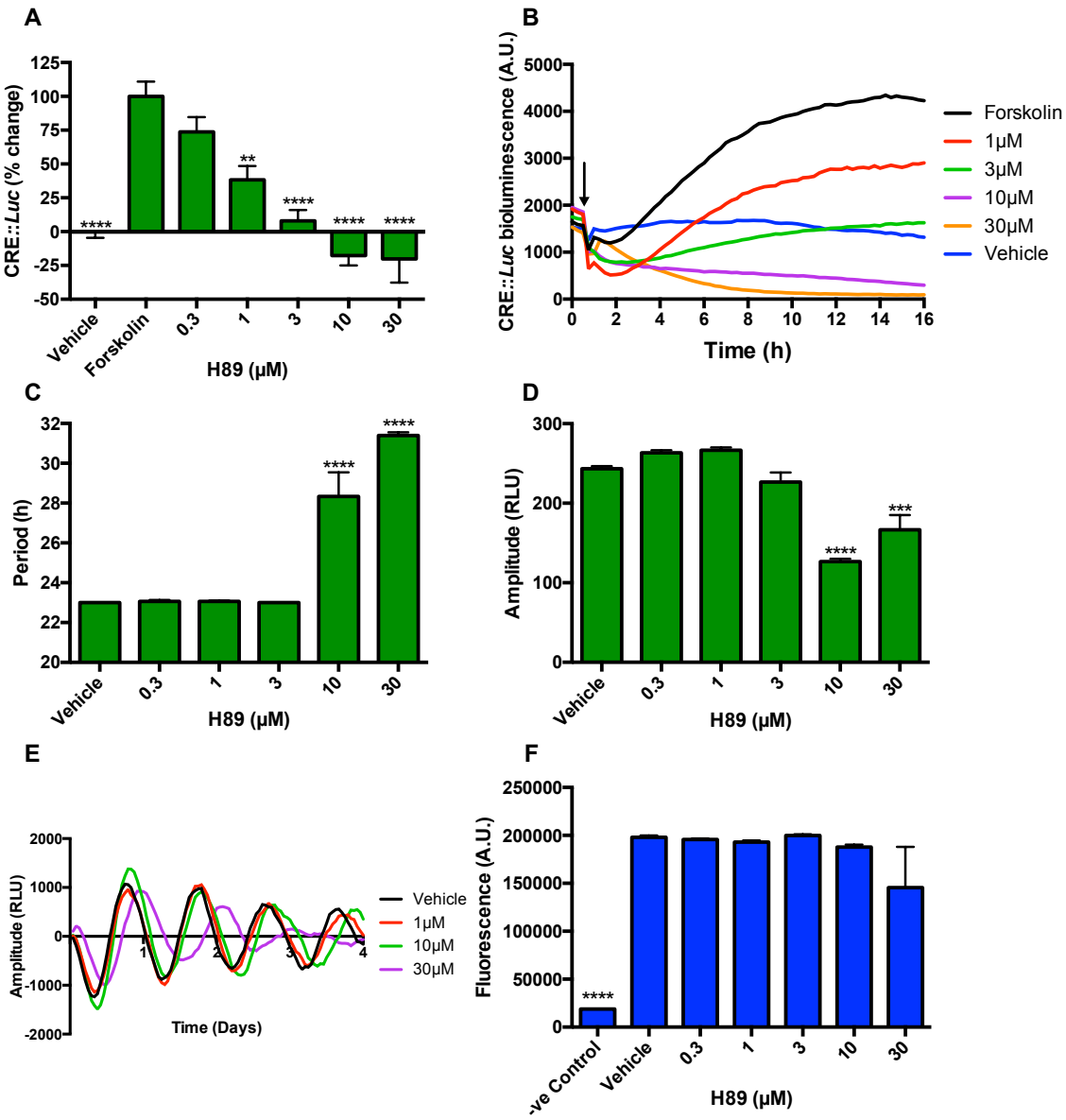

Figure 6.9. **H89 reduces CREB activity and lengthens period in the MMHD3 cells. A-B)** The effects of H89 on CREB induction using a CRE::*Luc* assay (n=6), and characteristic trace diagrams. The period **(C)** and amplitude **(D)** effects of H89 on *Bmal::Luc* MMHD3 cells (n=3), with representative luminescence traces **(E)**. **F)** Cell viability assay (n=3). Arrow indicates time of forskolin treatment.

dependently reduced CREB activity, where 30μM concentrations presented trends for reductions by 34% (Picaud et al., 2015). 100μM concentrations on the other hand significantly reduced activity by 53%, as seen in *Figures 6.10A-B* (30μM: 65.53±4.53, 100μM: 46.87±8.22 % change). The effect of this compound on circadian parameters was then assessed (*Figures 6.10C-E*). Period lengthening by 30min and 1.2h was observed at 30μM and 100μM respectively, with no significant effect on circadian amplitude (vehicle: 23.83±0.04, 30μM: 24.33±0.05, 100μM: 24.98±0.11 h). Thus, at concentrations where cell viability was maintained (*Figure 6.10F*), CBP112 reduced CREB and induced period lengthening.

6.2.10 CBP112 induced period lengthening in the MMHD3 cells

The effects of CBP112 were then tested on the MMHD3 cells. Much like the U2OS cells, trends for dose-dependent reductions were observed, as seen in *Figures 6.11A-B*. CBP112 showed patterns of decreased forskolin-stimulated CREB induction at 30μM by 31%, where 100μM induced significant reductions by 82% (30μM: 69.36±8.38, 100μM: 18.85±7.83 % change). The effects of CBP112 were then tested on rhythmic parameters (*Figures 6.11C-E*). Much like the U2OS cells, CBP112 did not appear to affect amplitude but significantly lengthened period by 1.1h and 1.5h at 30μM and 100μM concentrations respectively (vehicle: 23.83±0.18, 30μM: 24.90±0.20, 100μM: 25.37±0.47 h). Therefore, when assessing the effects of CBP inhibition with CBP112, at concentrations where cell viability was maintained (*Figure 6.11F*), CREB was reduced and period lengthening was observed.

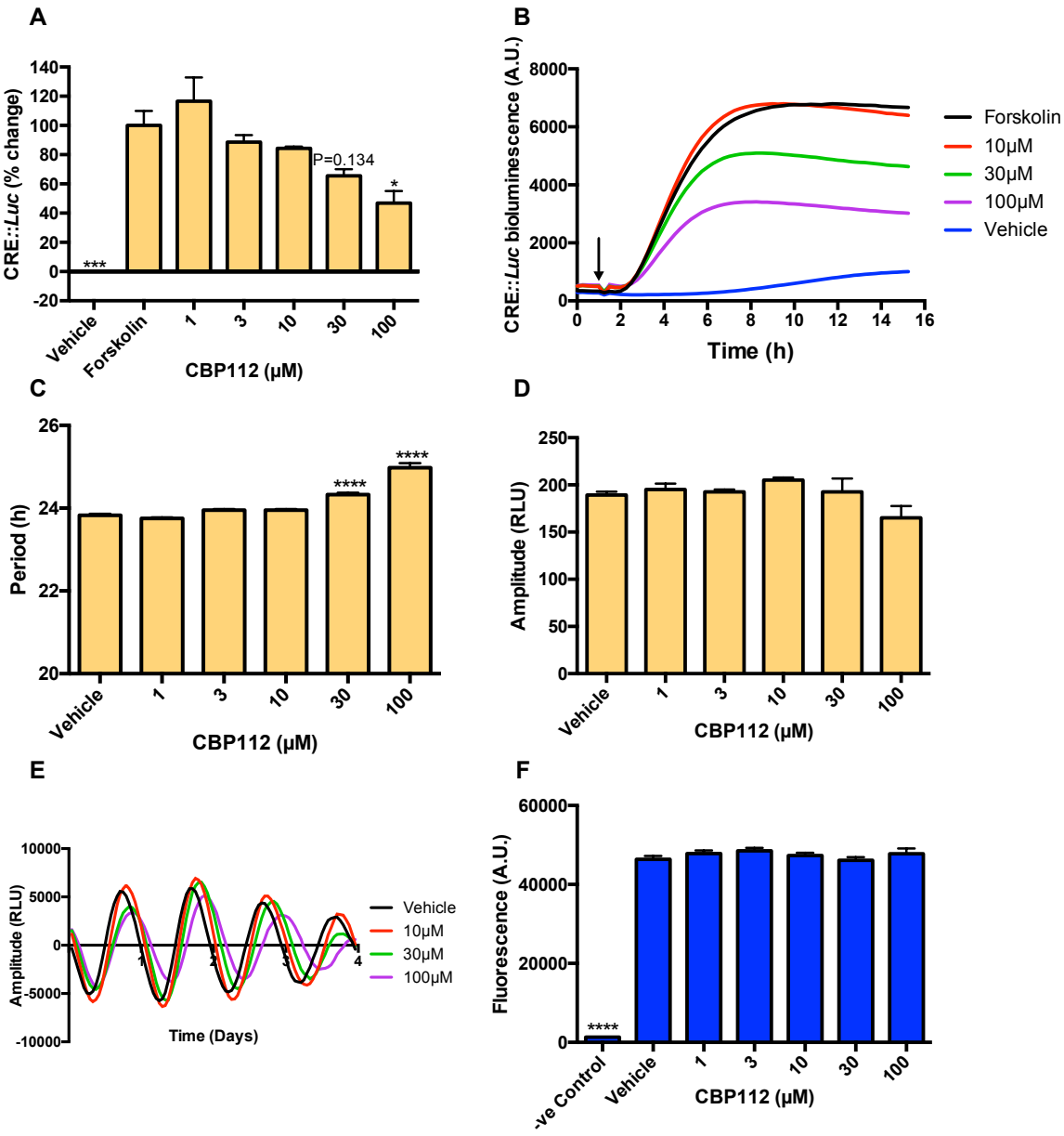

Figure 6.10. **CBP112 reduces CREB activity and lengthens period in the U2OS cells. A-B)** The effects of CBP112 on CREB activity using a CRE::*Luc* assay (n=3), and characteristic trace diagrams. The period **(C)** and amplitude **(D)** effects of CBP112 on *Bmal::Luc* U2OS cells (n=4), with representative luminescence traces **(E)**. **F)** Cell viability assay (n=4). Arrow indicates time of forskolin treatment.

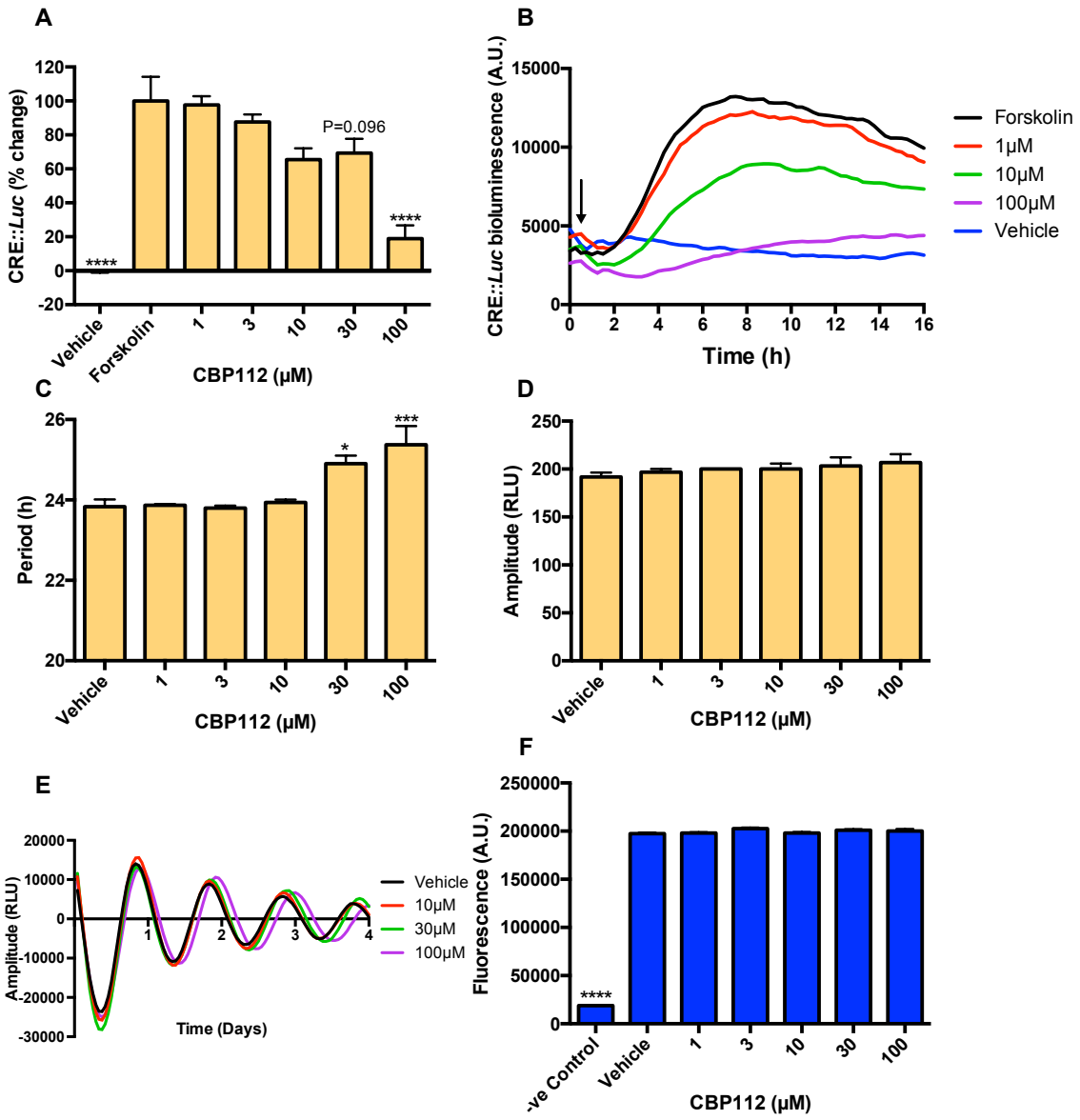

Figure 6.11. **CBP112 reduces CREB activity and lengthens period in the MMHD3 cells. A-B)** The effects of CBP112 on CREB activity using a CRE::*Luc* assay (n=3), and characteristic trace diagrams. The period **(C)** and amplitude **(D)** effects of CBP112 on *Bmal::Luc* MMHD3 cells (n=3), with representative luminescence traces **(E)**. **F)** Cell viability assay (n=3). Arrow indicates time of forskolin treatment.

6.2.11 CBP30 induced period lengthening in the U2OS cells

A second CBP inhibitor, CBP30 (IC50= 0.12μM) was tested to further assess the consequences of CREB modulation in the U2OS cells (Conery et al., 2016). As seen in *Figures 6.12A-B*, CBP30 induced dose-dependent reductions in forskolin-stimulated CREB activity, where 10 and 30μM concentrations reduced CREB induction by 32% and 58% respectively (10μM: 68.41±2.78, 30μM: 41.90±0.42 % change). In concert with this, CBP30 lengthened period by 39min at 10μM and 30μM induced lengthening by 2.5h (vehicle: 23.83±0.04, 10μM: 24.48±0.03, 30μM: 26.35±0.20 h) (*Figures 6.12C, E*). At 30μM, CBP30 also induced amplitude dampening by 30% and cell viability was maintained at all concentrations tested (*Figures 6.12D, F*). Thus, CBP30 was able to reduce CREB activity and induce greater period lengthening than CBP112 in the U2OS cells.

6.2.12 CBP30 induced period lengthening in the MMHD3 cells

Much like the U2OS cells, CBP30 was more potent than CBP112 at reducing CREB activity in the MMHD3 cells. As seen in *Figures 6.13A-B*, CBP30 reduced forskolin-induced CREB activity by 44%, 63%, and 98% at 3, 10, and 30μM concentrations respectively (3μM: 56.39±4.10, 10μM: 36.94±4.88, 30μM: 2.30±6.24 % change). Changes to circadian parameters were also observed, as 3μM lengthened period by 1h and reduced amplitude by 17%, 10μM enhanced period by 2h and decreased amplitude by 32%, and 30μM lengthened period by 1.6h and reduced amplitude by 34% (vehicle: 23.83±0.18, 3μM: 24.87±0.15, 10μM: 25.80±0.40, 30μM: 25.47±0.03 h) (*Figures 6.13C-E*). Therefore, at concentrations where cell viability was unaffected (*Figure 6.13F*), CBP30 reduced CREB activity in the MMHD3 cells and lengthened circadian period.

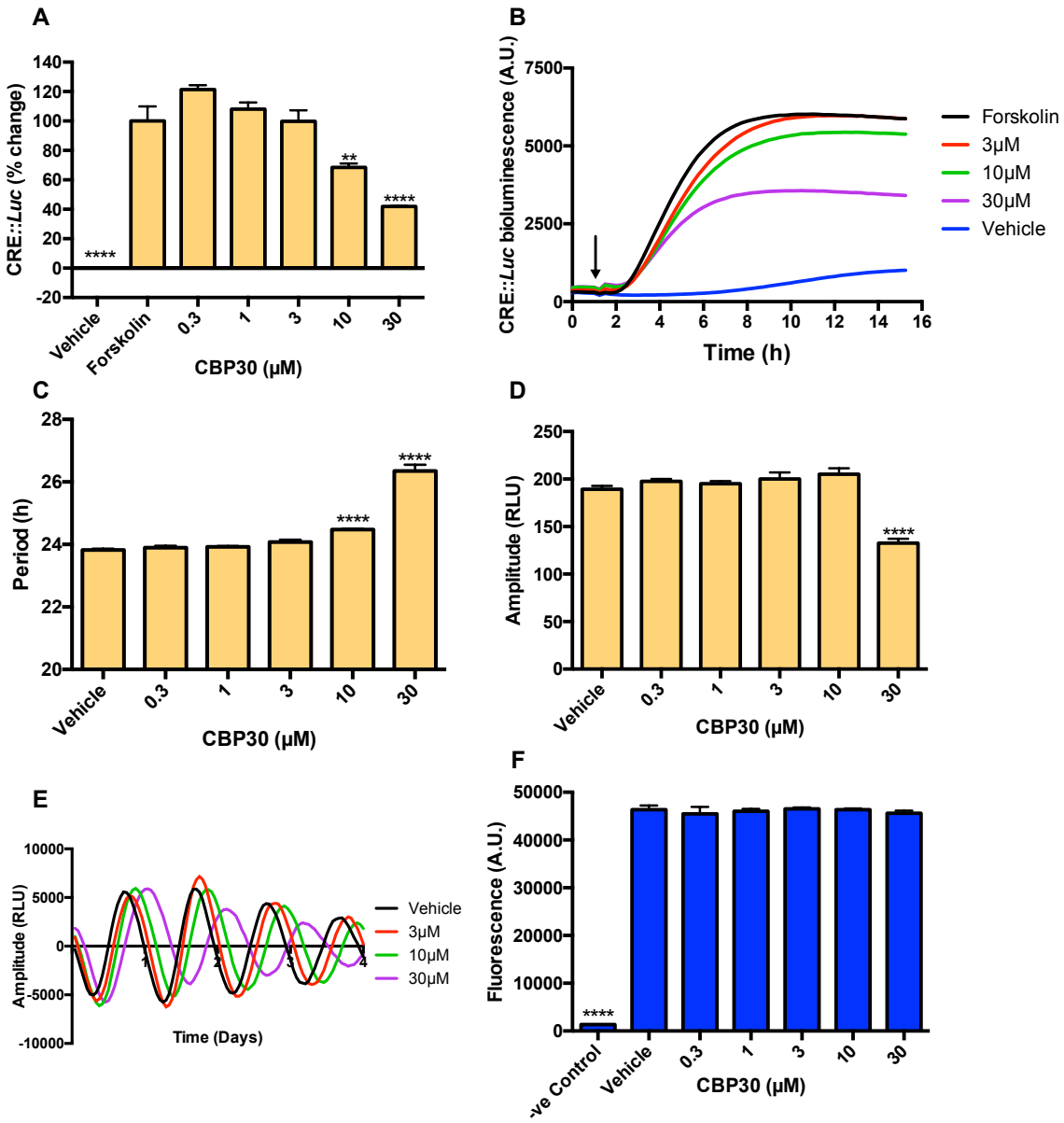

Figure 6.12. **CBP30 reduces CREB activity and lengthens period in the U2OS cells. A-B)** The effects of CBP30 on CREB induction using a CRE::*Luc* assay (n=3), and characteristic trace diagrams. The period **(C)** and amplitude **(D)** effects of CBP30 on *Bmal::Luc* U2OS cells (n=4), with representative luminescence traces **(E)**. **F)** Cell viability assay (n=4). Arrow indicates time of forskolin treatment.

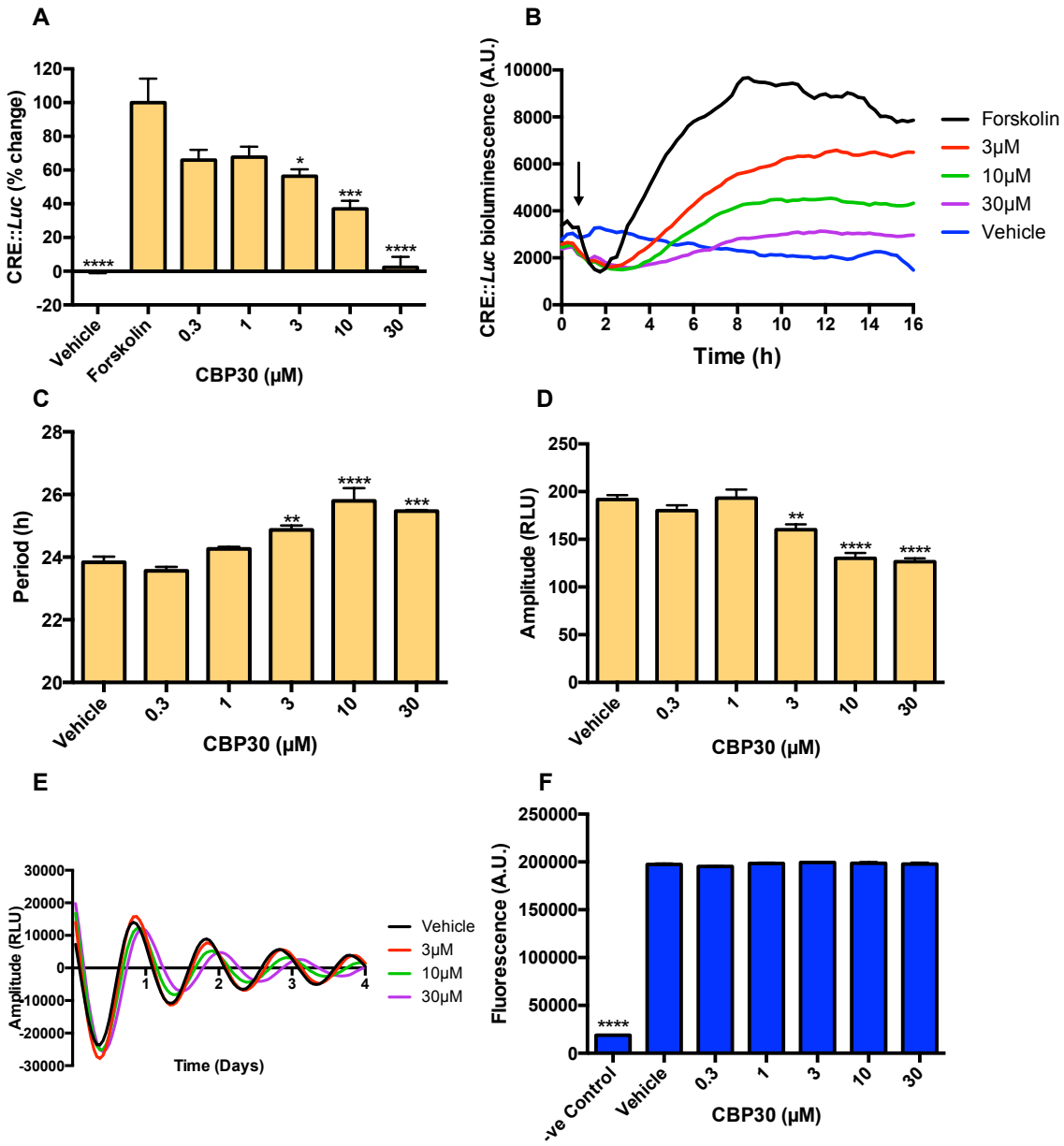

Figure 6.13. **CBP30 reduces CREB activity and lengthens period in the MMHD3 cells. A-B)** The effects of CBP30 on CREB activity using a CRE::*Luc* assay (n=3), and characteristic trace diagrams. The period **(C)** and amplitude **(D)** effects of CBP30 on *Bmal::Luc* MMHD3 cells (n=3), with representative luminescence traces **(E)**. **F)** Cell viability assay (n=3). Arrow indicates time of forskolin treatment.

6.2.13 Increased CREB suppression increases period lengthening

Finally, assessment of the overall trends observed from the data obtained would allow identification of any correlations when examining the relationship between CREB inhibition and circadian period. *Table 6.2* summarises the extent of forskolin-stimulated reductions in CREB activity, and their associative period phenotypes following treatment with pharmacological tools perturbing this pathway. The pattern identified is such that the greater the suppression of CREB activity, the greater the period lengthening phenotype in both the U2OS and MMHD3 cell lines.

Table 6.2. Summary of the reductions in CREB activity observed with significant period lengthening in the MMHD3 and U2OS cells.

Treatment		U2OS cells		MMHD3 cells	
Drug	**(μM)**	**CREB ↓ (%)**	**Period change (h)**	**CREB ↓ (%)**	**Period change (h)**
Vidarabine	30	12	2	38	4.6
	100	51	3.7	59	4
	300	85	5.5		
	1,000	94	7.7	87	7.8
2'5'-	10			55	1.3
didioxyadenosine	30			60	1.6
	100			67	1.3
	300	62	1.0	86	1.7
	1,000	89	2.0	81	2.9
H89	10	28	1.5	118	5.3
	30	100	5.1	120	8.4
CBP112	30	34	0.5	31	1.1
	100	53	1.2	81	1.5
CBP30	3			44	1
	10	32	0.7	63	2
	30	58	2.5	98	1.6
LiCl	20,000			65	2.5
	30,000			70	3.4

6.2.14 Period lengthening is independent of P-ERK activity

As the MAPK pathway can phosphorylate CREB and as aspects of lithium's therapeutic actions are attributed to ERK activation, we decided to investigate the contributory effects of ERK on circadian period lengthening. Firstly, in order to assess whether AC inhibiting drugs impacted P-ERK levels, an ERK ELISA was performed (*Figure 6.14A*). It was found that both 1mM vidarabine and 30μM H89 significantly elevated P-ERK levels by 2.0 and 2.9 fold respectively (vehicle: 1.00±0.08, vidarabine: 1.98±0.58, H89: 2.91±0.18 normalised expression). Moreover, 1μM phorbol 12-myristate 13-acetate (PMA), a compound which induces P-ERK via the activation of PKC, elevated expression by 2.5 fold (PMA: 2.48±0.04 normalised expression).

Subsequently, the circadian effects of the ERK activator PMA were assessed. In spite of ERK activation, at any given concentration where cell viability was maintained, PMA did not exhibit any period lengthening effects (*Figures 6.14B-C*). The only effect observed was at 25nM, where a period shortening phenotype of 1.3h was seen (vehicle: 23.30±0.26, 25nM: 22.02±0.49h) (*Figures 6.14C, E).* This is interesting, as we have previously shown in Chapter 5, *Figure 5.13* that the ERK inhibitor SCH772984 potentiated LiCl-induced period lengthening. Moreover, PMA around its EC50 of 14nM significantly dampened amplitude by 37% followed by higher concentrations increased amplitude by 46% (*Figure 6.14D*) (Hollingsworth et al., 1986). Therefore, ERK may play less of a direct role in inducing period lengthening than CREB.

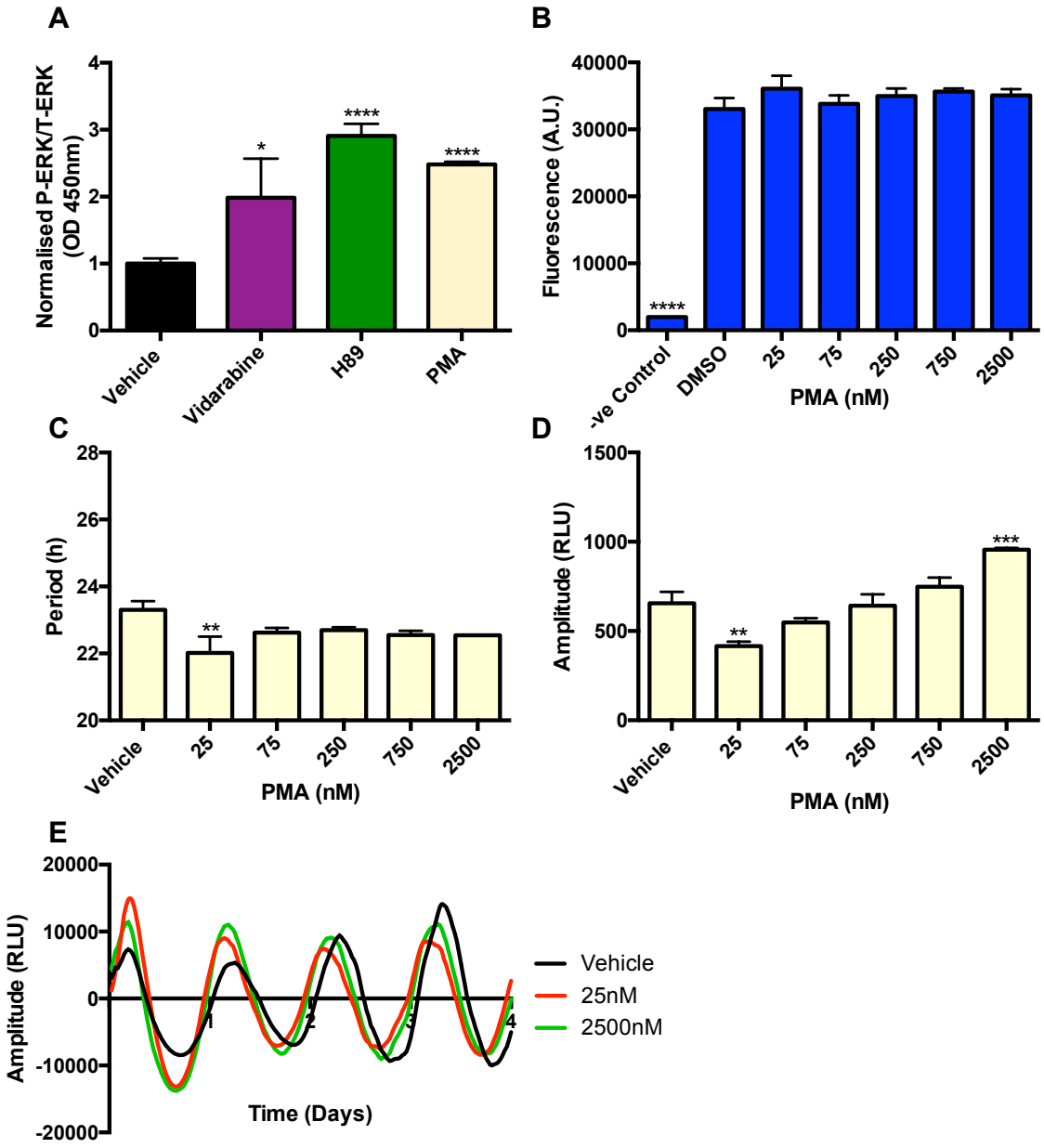

Figure 6.14. **Activation of ERK is not responsible for period lengthening induced by inhibition of the AC pathway in the MMHD3 cells. A)** Performance of an ERK ELISA to assess drug-induced alterations to P-ERK, using 1mM vidarabine, 30μM H89, or 1μM PMA (n=4-7). **B)** Cell viability assay (n=4). The effects of the ERK activator PMA on circadian period **(C)** and amplitude (n=4) **(D)**. **E)** Representative luminescence traces highlighting the effects of PMA on the molecular clock.

6.3 Discussion

The original motivations for investigating the AC pathway were to explore whether lithium, a gold standard therapy for BPD, was inducing period changes via inhibition of this signalling cascade. Whilst we no longer think this is lithium's dominant method of inducing period lengthening, for reasons later discussed (Chapter 7), we did find that perturbing all vital components of this pathway using pharmacological tools resulted in period lengthening in two distinct cell lines- the human U2OS and murine MMHD3 cells. Both the AC and MAPK pathways can modulate CREB activity. However, our study demonstrates that although CREB and ERK are affected by lithium as previously described, period lengthening was independent of increased P-ERK activity. AC was targeted using vidarabine or 2'5'-didioxyadenosine, PKA was inhibited using H89 and CBP was targeted using CBP112 or CBP30, all of which reduced CREB activity and induced period lengthening as outlined in *Figure 6.15*.

6.3.1 The significance of adenylate cyclase and group III isoforms

Our investigation found that inhibition of AC induced period lengthening. Use of siRNA-mediated gene knockdown suggests that AC6 is predominantly responsible for these effects in the MMHD3 cells, as it was highly expressed and knockdown induced period lengthening by 2.3h, akin to our positive control. However, as knockdown of AC9 was incomplete, its role in period lengthening cannot be completely eliminated. Membrane bound AC isoforms are broadly divided into 4 categories, where AC5 and 6 fall into group III, as seen in *Table 6.1*. Indeed, this is the category containing the PKA sensitive isoforms, further

suggesting that the mechanism via which period lengthening could occur is via disruption of CREB-mediated gene transcription (Sadana and Dessauer, 2009).

Most AC isoforms are expressed in mammalian central nervous tissues where AC1 and 8 show high levels of expression in the murine brain, followed by AC2, 5, 6, and 9 (Visel et al., 2006, Pierre et al., 2009). Further analysis found that AC2 and 5 had the greatest expression levels in the hypothalamus, followed by moderate expression of AC1, 3, 6, 8, and 9 (Visel et al., 2006, Sanabra and Mengod, 2011). This is interesting as the hypothalamus contains the SCN, a vital element of the circadian system enabling bodily rhythmic synchrony. Therefore, whilst the dominant isoform may vary between *in vitro* studies in the MMHD3 cells and *in vivo* studies assessing periodicity within the SCN, this suggests that group III AC inhibition could modulate circadian periodicity.

When observing the role of AC in BPD, the dominant isoforms implicated were AC5 and 7. Mann et al., found that 1mM LiCl inhibited forskolin-stimulated AC5 activity, reducing cAMP accumulation by 25% in immortalised COS-7 cells. Moreover, the use of an alternative stimulant, a dopamine D1 receptor agonist found that LiCl inhibited AC5 and 7 to the greatest degree, reducing cAMP by 50% and 40% respectively. However, following pre-incubation with LiCl, none of the group I calcium sensitive isoforms showed inhibition after calcium stimulation (Mann et al., 2008). This suggests that lithium may function via the modulation of specific lithium-sensitive isoforms. Moreover, LiCl is a well established amplitude enhancer, therefore it follows that this molecule does not target AC9, as knockdown of this isoform reduced amplitude in the MMHD3 cells.

Such findings also suggest that targeting AC could be partially responsible for lithium-induced period lengthening.

Carbamazepine also reduced basal or stimulation-induced intracellular cAMP levels and CREB activity (Palmer et al., 1979, Elphick et al., 1990, Chen et al., 1996). Interestingly, carbamazepine was found to act upon AC1 and AC5, decreasing forskolin-induced cAMP levels by 40 and 50% respectively. Furthermore, much like lithium, treatment with a dopamine receptor agonist revealed that AC5 and 7 were the most sensitive isoforms (Mann et al., 2009). Therefore, lithium and carbamazepine are best responsive to a common target, AC5, suggesting that targeting PKA may play a role in inducing or maintaining euthymia.

The following question then arises: do AC5 or AC6 mutant mice exhibit lithium-like effects? Should either AC5 or 6 be truly implicated in modulating the actions of lithium, it could be hypothesised that removal of these genes, or inducing null mutations in animal models should mimic the effects of lithium. There appears to be a greater body of research focusing on AC5, potentially due to its higher expression levels within the brain. Indeed, much like lithium, AC5 homozygous knockout mice display less time being immobile in the forced swim test for depressive behaviours and spend more time in the open arm of the elevated plus maze and in the light chamber of the light dark box, thereby exhibiting anxiolytic behaviour (Mann et al., 2009, Krishnan et al., 2008). However, there are mixed findings of whether such mice display lower levels of locomotor activity, as one would predict. Initial studies by Iwamoto and colleagues found reductions in locomotion and rearing behaviours, in line with

the proposed hypothesis (Iwamoto et al., 2003). However, subsequent studies found increased activity or similar trends emerging when examining behaviour between 40min and 2h (Kim et al., 2006, Krishnan et al., 2008, Mann et al., 2009). This therefore suggests that aspects of lithium-like responses are mimicked by removal of AC5 activity. As AC5 was not expressed in the murine MMHD3 cells, the actions via which PKA modulated CREB activity were predominantly via AC6. However, it is plausible that these effects may be shared *in vivo*, as both isoforms are expressed in the central nervous system.

The reagents implemented to investigate the consequences of AC inhibition were vidarabine and 2'5'-didioxyadenosine. Vidarabine is a synthetic nucleoside analogue which inhibits AC non-competitively, thereby reducing forskolin-stimulated cAMP and CREB-mediated gene transcription (Braeunig et al., 2013, Iwatsubo et al., 2012, De Lorenzo et al., 2014). Vidarabine was previously reported to function as a selective AC5 antagonist (Vatner et al., 2013, De Lorenzo et al., 2014). However, examination of earlier studies suggested that it is selective for both AC5 and 6, as previous studies failed to acknowledge the structural similarities between the two isoforms (Seifert, 2014, Brand et al., 2013). 2'5'-didioxyadenosine is also a non-competitive AC inhibitor also previously shown to reduce intracellular cAMP (Desaubry et al., 1996a, Desaubry et al., 1996b). Indeed, alternative adenosine analogues have also shown to function mainly via actions against AC5 and 6 (Brand et al., 2013). In our investigation, the majority of AC inhibitor-induced actions were due to inhibition of AC6, further adding to the growing body of evidence implicating group III isoforms in regulating mood and circadian rhythms.

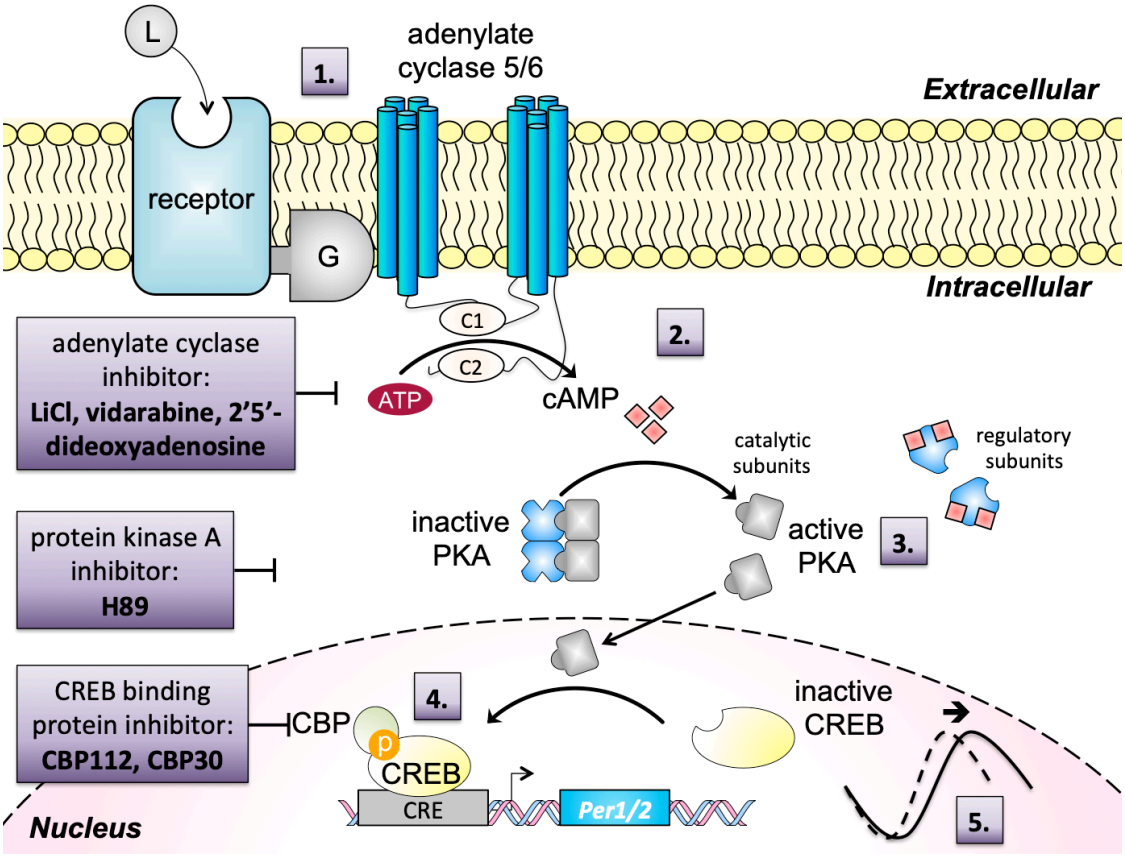

Figure 6.15. **Schematic diagram of the mechanism via which inhibition of the adenylate cyclase pathway may induce period lengthening in the MMHD3 cells. 1-2.** Inhibition of group III AC isoforms using compounds such as LiCl, vidarabine or 2'5'-didioxyadenosine result in reductions to cAMP. **3.** As a consequence, there is less cAMP available to activate PKA, effects which can also be seen by using the PKA inhibitor H89. **4.** Less active PKA results in less phosphorylation and activation of CREB, where the CBP inhibitors CBP112 and CBP30 also induce similar effects. **5.** This results in less CREB-mediated transcription of *Per1/2*, thus taking longer to accumulate sufficient transcript levels, and may result in circadian period lengthening.

6.3.2 Modulation of CREB activity

H89 was used to assess the effects of inhibiting PKA. Competitive inhibitors of protein kinases are known to lack selectivity, due to the structural similarities between the ATP binding domain of kinases (Lochner and Moolman, 2006). Whilst H89 is a more selective PKA inhibitor than many other compounds, at 10μM, as used in the current investigation, H89 inhibits an additional 8 targets by 75% or more. The targets which were inhibited to an equal extent included: ribosomal protein S6 kinase beta-1 (IC50: 80nM), mitogen and stress activated protein kinase I (IC50: 120nM), and rho-associated protein kinase II (IC50: 270nM). Yet, of the 28 compounds screened, 10μM H89 exhibited the most potent inhibition of PKA, reducing activity by 98%, with an IC50 of 135nM (Davies et al., 2000). Therefore, despite its limitations, H89 was the most favourable compound to use. As we confirmed that the compound was reducing CREB activity, in combination with the data obtained from assessing AC and CBP inhibition, this strengthens the evidence implicating CREB signalling in altering circadian period.

Use of H89 on the U2OS cells revealed that 1μM concentrations or lower potentiated CREB activity. This effect was verified with an alternative inhibitor, KT5720 (10μM), reported to reduce PKA activity by 61% (Davies et al., 2000). Whilst such concentrations did not induce any period or amplitude changes, the mechanisms for this remain elusive. One possibility could be associated with increased recruitment of transducers of regulated CREB activity (TORCs). TORCs enhance CREB activity by increasing its interaction with TFIID, a component of the RNA polymerase II holoenzyme which induces gene transcription

independently of affecting CREB-DNA binding (Conkright et al., 2003). Alternatively, such actions could be associated with off-target effects. When analysing common targets of 10μM H89 and KT5720 which reduced activity by 75% or more, MAPK-activated protein kinase 1b, AMP-activated protein kinase, and checkpoint kinase 1 appeared as potential candidates which may be implicated in mediating these effects (Davies et al., 2000).

The transcriptional co-activator CBP is essential in allowing CREB to initiate gene transcription. Therefore, the competitive CBP inhibitors CBP112 and CBP30 were used to assess their ability to modulate circadian period. Our data corroborate previous reports which show that CBP30 is more potent than CBP112 (Picaud et al., 2015, Hammitzsch et al., 2015). This was because 30μM CBP30 inhibited forskolin-stimulated CREB induction by 1.7 and 3.2 fold greater than CBP112 in the U2OS and MMHD3 cells respectively. Congruently, 30μM CBP30 induced 5 and 1.5 fold greater period lengthening effects than CBP112 in U2OS and MMHD3 cells respectively. Period lengthening may occur as by inhibiting *Per* gene transcription, it takes longer to accumulate sufficient quantities of PER protein which can then dimerise with CRY to inhibit the activity of CLOCK and BMAL, thereby decelerating the clock.

It should be acknowledged that this investigation utilised drug concentrations beyond their known IC50s. However, with the exception of CBP112 and CBP30, for which IC50s were calculated using *in vitro* assays, most IC50s were calculated using purified protein assays. Therefore, when such compounds are used in cellular assays the concentrations required to induce similar effects will be an order of magnitude greater. Whilst we confirmed that

cAMP or CREB activity was being modulated at doses where chronomodulation was observed, the use of higher concentrations does lead to the possibility that off-target effects may be partially responsible for period changes. Future investigations may overcome these issues by utilising non-pharmacological techniques, specifically by exploring the effects of dose-dependent siRNA induced gene knockdown of PKA, CBP, and CREB. Should our hypothesis hold true, gene knockdown should also result in a significant period lengthening phenotype.

It is acknowledged that both the MAPK and AC pathways can regulate *Per1* gene transcription through synergistic modulation of CREB activity (Travnickova-Bendova et al., 2002). We therefore decided to assess the contribution of P-ERK activation on modulating circadian period, as our data found that vidarabine and H89 were both able to elevate P-ERK. PMA has been shown to increase the activity of Ras, which activated Raf-1 by 80% *in vit*ro, where Raf-1 is known to activate ERK1/2 via MEK1/2 activation (Verin et al., 2000). It was used as the pharmacological agent of choice to explore the actions of ERK as our P-ERK assay also confirmed that PMA elevated P-ERK to a similar extent as the AC targeting compounds. However, PMA did not lengthen period in the MMHD3 cells and a period shortening phenotype was observed, an effect also found in other studies (Hirota et al., 2008). This suggests that AC inhibition-induced period lengthening was independent of ERK activity. *In vivo* examinations of alternations to the MAPK pathway revealed that phase shifting responses are greatly altered, with no effect on circadian period. For example removal of Raf kinase inhibitor protein, a protein which prevents Raf-induced

activation of MEK, showed no differences in circadian period or amplitude, determined by assessment of wheel-running activity (Antoun et al., 2012). Similarly, following the removal of the suprachiasmatic nucleus circadian oscillatory protein– a protein which negatively regulates Ras – did not induce any overt period changes in rodents (Shimizu et al., 2016). This suggests that the MAPK pathway does not have a dominant or essential role in controlling circadian periodicity.

A plausible explanation for the increased P-ERK observed with vidarabine and H89 may be due to an intersection between the MAPK and AC signalling cascades. Indeed, PKA has been shown to inhibit Raf-1 and as such, inhibition of AC or PKA would result in disinhibition and therefore elevations in Raf-1, P-MEK, and P-ERK activity (Yan et al., 2007). These actions have been associated with AC5 and whilst our MMHD3 cells lack detectable AC5 mRNA, the structural similarity between AC5 and 6 suggests that AC6 could be mediating these effects.

6.3.3 The effects of targeting adenylate cyclase signalling in vivo

As the current investigation examined the effects of perturbing the AC pathway *in vitro*, the translatability of these findings is questionable. Evidence suggests that's the drugs used in the current study may induce similar effects in whole animals. The use of a non-competitive AC inhibitor THFA induced significant period lengthening by 7h in *Per1::Luc* SCN explant tissues and by 7h in peripheral tissues including the liver of PER2::LUC mice. Moreover, intracerebral administration of THFA into the SCN of mice induced behavioural period lengthening by ~35min. Indeed, use of additional AC inhibitors, including 2'5'-didioxyadenosine and 9-cyclopentyl adenine induced period lengthening by

~3h in *Per1::Luc* SCN sections (O'Neill et al., 2008). Therefore, as SCN explant and behavioural period lengthening can be observed, the AC pathway may modulate circadian period *in vivo*. This suggests that administration of vidarabine or 2'5'-didioxyadenosine should also induce behavioural period lengthening, as all drugs function as P-site inhibitors. However, use of dual PKA regulatory subunit inhibitors Rp-8-CPT-cAMPS and Rp-8-Br-cAMPS did not appear to induce any significant period changes (O'Neill et al., 2008). Whilst this may be due to the lipophilic nature of the drugs, the effects of H89 *in vivo* are yet to be established.

The data from our study also illustrate that vidarabine, 2'5'-didioxyadenosine (U2OS cells only), H89, and CBP30 induced amplitude dampening effects in our cell lines. CBP112 however did not exhibit any significant dampening effects. This may be due to drug potency, as CBP30 reduced CREB activity and induced greater period lengthening overall. Moreover, this study showed for the first time that amplitude dampening effects may be due to pharmacological actions upon AC9, as siRNA-mediated knockdown showed significant amplitude dampening, where enhancement was observed with AC6 knockdown. This suggests that downstream pathways, perhaps involving PKC or calcineurin may be responsible for inducing these effects (Sadana and Dessauer, 2009). Indeed, AC9 is moderately expressed in the hypothalamus and so could also be responsible for modulating these effects *in vivo* (Visel et al., 2006). Whilst hypothalamic AC mRNA expression has been assessed, specificity within the SCN remains elusive.

It was found that MDL-12,330A, an irreversible AC inhibitor and THFA induced dose-dependent amplitude dampening effects in SCN tissues (O'Neill et al., 2008). Moreover, either increasing cAMP using forskolin or IBMX, or deceasing cAMP using MDL-12,330A or pertussis toxin on the SCN induced amplitude dampening (Aton et al., 2006, O'Neill et al., 2008). This suggests that cAMP regulation is finely tuned by the master clock to generate coherent and amplified rhythms. Such factors highlight the importance of cAMP second messenger signalling in circadian rhythm generation.

6.3.4 Rhythmicity within the adenylate cyclase pathway

Whilst the AC pathway can modulate circadian rhythmicity via the regulation of CREB, the clock also controls the AC pathway. Indeed, 24h oscillatory patterns have been observed in AC isoforms. An initial study analysing rodent AC1 expression found 24h patterns within the pineal gland (Tzavara et al., 1996). Subsequently, analysis of human retinal pigment epithelial cells revealed 24h patterns in AC5, 6, and 7 mRNA, where all MCF-7 cell isoforms showed 24h variability, though only AC3 and 6 showed significant circadian mRNA expression patterns (Pavan et al., 2006, Mohamadian et al., 2017). As the PKA sensitive isoforms exhibit circadian expression patterns, this suggests that it is important for the clock to gate the activity of this kinase.

Moreover, PKA induced excessive phosphorylation in cells from *Cry1* or *Cry2* knockout mice, effects which were abolished with H89. This led to the idea that one function of CRY is to inhibit the actions of AC, thereby reducing cAMP production, and hence showing the direct control of the circadian clock on cAMP (Narasimamurthy et al., 2012). As expected circadian expression patterns of P-

CREB are found within the SCN, peaking during the subjective night (Obrietan et al., 1999). Therefore, many CREB regulated genes are also clock controlled. For example, brain-derived neurotropic factor is a key protein in memory function and is downregulated in neuropsychiatric disorders, where lithium normalises such consequences (Cunha et al., 2006). Interestingly, this neurotropic factor is also induced by PKA-CREB signalling and drugs acting via this pathway have antidepressant effects (Xue et al., 2016). This adds to the body of evidence entangling AC signalling with circadian disruption and mood disorders.

6.3.5 Conclusions

To conclude, our investigation found that pharmacological inhibition of AC, PKA, and CBP induced period lengthening *in vitro*. Lithium treatment is effective at stabilising mood, where one hypothesis is that lithium functions via normalisation of circadian rhythms. To this effect, as lithium inhibits AC at concentrations where period lengthening occurs, it is plausible that this pathway forms part of the mechanism via which euthymia may be achieved. The group III isoforms specifically may be key in modulating period effects and previous studies have indicated lithium to target similar isoforms. Therefore, pending further investigation, this pathway may aid in identifying novel mood-modulating therapeutics in the future, with fewer associated side effects.

Whilst the highest concentrations of CBP inhibiting agents induced period lengthening by 1.2-2.5h, inhibiting PKA lengthened period by 5.1-8.4h. This suggested that whilst CREB can modulate period, alternative targets may also be implicated. Group III and IV AC isoforms are also sensitive to PKC, suggesting that it may also be a target worthy of further exploration (Sadana and Dessauer,

2009). To further validate the *in vivo* importance of the AC pathway in modulating mood and circadian rhythms, it would be important to verify whether our compounds induce similar effects on rodent wheel-running behaviour and on mice with behavioural abnormalities such as the mania-like *ClockΔ19* or *Afh* mice. This information would be important in validating that: 1) pharmacological agents that modulate circadian rhythms can also modulate mood and 2) the AC pathway is a key intersection between circadian rhythms and mood regulation.

6.4 References

ALBRECHT, U., SUN, Z. S., EICHELE, G. & LEE, C. C. 1997. A differential response of two putative mammalian circadian regulators, mper1 and mper2, to light. *Cell,* 91**,** 1055-1064.

ALDA, M., SHAO, L., WANG, J. F., DE LARA, C. L., JAITOVICH-GROISMAN, I., LEBEL, V., SUN, X. J., DUFFY, A., GROF, P., ROULEAU, G. A., TURECKI, G. & YOUNG, L. T. 2013. Alterations in phosphorylated cAMP response element-binding protein (pCREB) signaling: an endophenotype of lithium-responsive bipolar disorder? *Bipolar Disorders,* 15**,** 824-831.

ANTOUN, G., CANNON, P. B. & CHENG, H.-Y. M. 2012. Regulation of MAPK/ERK Signaling and Photic Entrainment of the Suprachiasmatic Nucleus Circadian Clock by Raf Kinase Inhibitor Protein. *Journal of Neuroscience,* 32**,** 4867-4877.

ATON, S. J., COLWELL, C. S., HARMAR, A. J., WASCHEK, J. & HERZOG, E. D. 2005. Vasoactive intestinal polypeptide mediates circadian rhythmicity and synchrony in mammalian clock neurons. *Nature Neuroscience,* 8**,** 476-483.

ATON, S. J., HUETTNER, J. E., STRAUME, M. & HERZOG, E. D. 2006. GABA and G(i/o) differentially control circadian rhythms and synchrony in clock neurons. *Proceedings of the National Academy of Sciences of the United States of America,* 103**,** 19188-19193.

BELMAKER, R. H. 1981. Receptors, adenylate-cyclase, depression and lithium. *Biological Psychiatry,* 16**,** 333-350.

BOS, J. L. 2003. Epac: a new cAMP target and new avenues in cAMP research. *Nature Reviews Molecular Cell Biology,* 4**,** 733-738.

BRAEUNIG, J. H., SCHWEDA, F., HAN, P.-L. & SEIFERT, R. 2013. Similarly Potent Inhibition of Adenylyl Cyclase by P-Site Inhibitors in Hearts from Wild Type and AC5 Knockout Mice. *Plos One,* 8**,** e68009.

BRAND, C. S., HOCKER, H. J., GORFE, A. A., CAVASOTTO, C. N. & DESSAUER, C. W. 2013. Isoform Selectivity of Adenylyl Cyclase Inhibitors: Characterization of Known and Novel Compounds. *Journal of Pharmacology and Experimental Therapeutics,* 347**,** 265-275.

CHANG, A., LI, P. P. & WARSH, J. J. 2003. Altered cAMP-dependent protein kinase subunit immunolabeling in post-mortem brain from patients with bipolar affective disorder. *Journal of Neurochemistry,* 84**,** 781-791.

CHEN, D., BUCHANAN, G. F., DING, J. M., HANNIBAL, J. & GILLETTE, M. U. 1999. Pituitary adenylyl cyclase-activating peptide: A pivotal modulator of glutamatergic regulation of the suprachiasmatic circadian clock. *Proceedings of the National Academy of Sciences of the United States of America,* 96**,** 13468-13473.

CHEN, G., PAN, B. S., HAWVER, D. B., WRIGHT, C. B., POTTER, W. Z. & MANJI, H. K. 1996. Attenuation of cyclic AMP production by carbamazepine. *Journal of Neurochemistry,* 67**,** 2079-2086.

CHRIVIA, J. C., KWOK, R. P. S., LAMB, N., HAGIWARA, M., MONTMINY, M. R. & GOODMAN, R. H. 1993. Phosphorylated CREB binds specifically to the nuclear-protein CBP. *Nature,* 365**,** 855-859.

COLLIER, H. O. J. & ROY, A. C. 1974. Morphine-like drugs inhibit stimulation by E prostaglandins of cyclic-AMP formation by rat-brain homogenate. *Nature,* 248**,** 24-27.

CONERY, A. R., CENTORE, R. C., NEISS, A., KELLER, P. J., JOSHI, S., SPILLANE, K. L., SANDY, P., HATTON, C., PARDO, E., ZAWADZKE, L., BOMMI-REDDY, A., GASCOIGNE, K. E., BRYANT, B. M., MERTZ, J. A. & SIMS, R. J. 2016. Bromodomain inhibition of the transcriptional coactivators CBP/EP300 as a therapeutic strategy to target the IRF4 network in multiple myeloma. *Elife,* 5**,** e10483.

CONKRIGHT, M. D., CANETTIERI, G., SCREATON, R., GUZMAN, E., MIRAGLIA, L., HOGENESCH, J. B. & MONTMINY, M. 2003. TORCs: Transducers of regulated CREB activity. *Molecular Cell,* 12**,** 413-423.

CUNHA, A. B. M., FREY, B. N., ANDREAZZA, A. C., GOI, J. D., ROSA, A. R., GONCALVES, C. A., SANTIN, A. & KAPCZINSKI, F. 2006. Serum brain-derived neurotrophic factor is decreased in bipolar disorder during depressive and manic episodes. *Neuroscience Letters,* 398**,** 215-219.

CUTLER, D. J., HARAURA, M., REED, H. E., SHEN, S., SHEWARD, W. J., MORRISON, C. F., MARSTON, H. M., HARMAR, A. J. & PIGGINS, H. D. 2003. The mouse VPAC(2) receptor confers suprachiasmatic nuclei cellular rhythmicity and responsiveness to vasoactive intestinal polypeptide in vitro. *European Journal of Neuroscience,* 17**,** 197-204.

DAVIES, S. P., REDDY, H., CAIVANO, M. & COHEN, P. 2000. Specificity and mechanism of action of some commonly used protein kinase inhibitors. *Biochemical Journal,* 351**,** 95-105.

DE LORENZO, M. S., CHEN, W., BALJINNYAM, E., CARLINI, M. J., LA PERLE, K., BISHOP, S. P., WAGNER, T. E., RABSON, A. B., VATNER, D. E., PURICELLI, L. I. & VATNER, S. F. 2014. 'Reduced malignancy as a mechanism for longevity in mice with adenylyl cyclase type 5 disruption'. *Aging Cell,* 13**,** 102-110.

DESAUBRY, L., SHOSHANI, I. & JOHNSON, R. A. 1996a. 2',5'-dideoxyadenosine 3'-polyphosphates are potent inhibitors of adenylyl cyclases. *Journal of Biological Chemistry,* 271**,** 2380-2382.

DESAUBRY, L., SHOSHANI, N. & JOHNSON, R. A. 1996b. Inhibition of adenylyl cyclase by a family of newly synthesized adenine nucleoside 3'-polyphosphates. *Journal of Biological Chemistry,* 271**,** 14028-14034.

EBSTEIN, R. P., MOSCOVICH, D., ZEEVI, S., AMIRI, Z. & LERER, B. 1987. Effect of lithium in vitro and after chronic treatment on human-platelet adenylate-cyclase activity - postreceptor modification of 2nd messenger signal amplification. *Psychiatry Research,* 21**,** 221-228.

EIDEN, L. E., SAMAL, B., GERDIN, M. J., MUSTAFA, T., VAUDRY, D. & STROTH, N. 2008. Discovery of Pituitary Adenylate Cyclase-Activating Polypeptide-Regulated Genes through Microarray Analyses in Cell Culture and In Vivo. *Neural Signaling: Opportunities for Novel Diagnostic Approaches and Therapies,* 1144**,** 6-20.

ELPHICK, M., TAGHAVI, Z., POWELL, T. & GODFREY, P. P. 1990. Chronic carbamazepine down-regulates adenosine-A2 receptors - studies with the putative selective adenosine antagonists PD115,199 and PD116,948. *Psychopharmacology,* 100**,** 522-529.

FIELDS, A., LI, P. P., KISH, S. J. & WARSH, J. J. 1999. Increased cyclic AMP-dependent protein kinase activity in postmortem brain from patients with bipolar affective disorder. *Journal of Neurochemistry,* 73**,** 1704-1710.

FORN, J. & VALDECASAS, F. G. 1971. Effects of lithium on brain adenyl cyclase activity. *Biochemical Pharmacology,* 20**,** 2773-+.

GASPAR, L., VAN DE WERKEN, M., JOHANSSON, A. S., MORIGGI, E., OWE-LARSSON, B., KOCKS, J. W. H., LUNDKVIST, G. B., GORDIJN, M. C. M. & BROWN, S. A. 2014. Human cellular differences in cAMP - CREB signaling correlate with light-dependent melatonin suppression and bipolar disorder. *European Journal of Neuroscience,* 40**,** 2206-2215.

GINTY, D. D., KORNHAUSER, J. M., THOMPSON, M. A., BADING, H., MAYO, K. E., TAKAHASHI, J. S. & GREENBERG, M. E. 1993. Regulation of CREB phosphorylation in the suprachiasmatic nucleus by light and a circadian clock. *Science,* 260**,** 238-241.

GONZALEZ, G. A. & MONTMINY, M. R. 1989. Cyclic-AMP stimulates somatostatin gene-transcription by phosphorylation of CREB at serine-133. *Cell,* 59**,** 675-680.

HAMMITZSCH, A., TALLANT, C., FEDOROV, O., O'MAHONY, A., BRENNAN, P. E., HAY, D. A., MARTINEZ, F. O., AL-MOSSAWI, M. H., DE WIT, J., VECELLIO, M., WELLS, C., WORDSWORTH, P., MUELLER, S., KNAPP, S. & BOWNESS, P. 2015. CBP30, a selective CBP/p300 bromodomain inhibitor, suppresses human Th17 responses. *Proceedings of the National Academy of Sciences of the United States of America,* 112**,** 10768-10773.

HANOUNE, J. & DEFER, N. 2001. Regulation and role of adenylyl cyclase isoforms. *Annual Review of Pharmacology and Toxicology,* 41**,** 145-174.

HARMAR, A. J., MARSTON, H. M., SHEN, S. B., SPRATT, C., WEST, K. M., SHEWARD, W. J., MORRISON, C. F., DORIN, J. R., PIGGINS, H. D., REUBI, J. C., KELLY, J. S., MAYWOOD, E. S. & HASTINGS, M. H. 2002. The VPAC(2) receptor is essential for circadian function in the mouse suprachiasmatic nuclei. *Cell,* 109**,** 497-508.

HARRINGTON, M. E., HOQUE, S., HALL, A., GOLOMBEK, D. & BIELLO, S. 1999. Pituitary adenylate cyclase activating peptide phase shifts circadian rhythms in a manner similar to light. *Journal of Neuroscience,* 19**,** 6637-6642.

HIROTA, T., LEWIS, W. G., LIU, A. C., LEE, J. W., SCHULTZ, P. G. & KAY, S. A. 2008. A chemical biology approach reveals period shortening of the mammalian circadian clock by specific inhibition of GSK-3 beta. *Proceedings of the National Academy of Sciences of the United States of America,* 105**,** 20746-20751.

HOLLINGSWORTH, E. B., UKENA, D. & DALY, J. W. 1986. The protein-kinase-C activator phorbol-12-myristate-13-acetate enhances cyclic-AMP accumulation in pheochromocytoma cells. *Febs Letters,* 196**,** 131-134.

HUGHES, A. T., FAHEY, B., CUTLER, D. J., COOGAN, A. N. & PIGGINS, H. D. 2004. Aberrant gating of photic input to the suprachiasmatic circadian pacemaker of mice lacking the VPAC(2) receptor. *Journal of Neuroscience,* 24**,** 3522-3526.

HURLEY, J. H. 1999. Structure, mechanism, and regulation of mammalian adenylyl cyclase. *Journal of Biological Chemistry,* 274**,** 7599-7602.

IWAMOTO, T., OKUMURA, S., IWATSUBO, K., KAWABE, J. I., OHTSU, K., SAKAI, I., HASHIMOTO, Y., IZUMITANI, A., SANGO, K., AJIKI, K., TOYA, Y., UMEMURA, S., GOSHIMA, Y., ARAI, N., VATNER, S. F. & ISHIKAWA, Y. 2003. Motor dysfunction in type 5 adenylyl cyclase-null mice. *Journal of Biological Chemistry,* 278**,** 16936-16940.

IWATSUBO, K., BRAVO, C., UECHI, M., BALJINNYAM, E., NAKAMURA, T., UMEMURA, M., LAI, L., GAO, S., YAN, L., ZHAO, X., PARK, M., QIU, H., OKUMURA, S., IWATSUBO, M., VATNER, D. E., VATNER, S. F. & ISHIKAWA, Y. 2012. Prevention of heart failure in mice by an antiviral agent that inhibits type 5 cardiac adenylyl cyclase. *American Journal of Physiology-Heart and Circulatory Physiology,* 302**,** H2622-H2628.

JAGANNATH, A., PEIRSON, S. N. & FOSTER, R. G. 2013. Sleep and circadian rhythm disruption in neuropsychiatric illness. *Current opinion in neurobiology,* 23**,** 888-94.

JOHNSON, D. A., AKAMINE, P., RADZIO-ANDZELM, E., MADHUSUDAN & TAYLOR, S. S. 2001. Dynamics of cAMP-dependent protein kinase. *Chemical Reviews,* 101**,** 2243-2270.

KAREGE, F., SCHWALD, M., PAPADIMITRIOU, P., LACHAUSSE, C. & CISSE, M. 2004. The cAMP-dependent protein kinase A and brain-derived neurotrophic factor expression in lymphoblast cells of bipolar affective disorder. *Journal of Affective Disorders,* 79**,** 187-192.

KAWAGUCHI, C., TANAKA, K., ISOJIMA, Y., SHINTANI, N., HASHIMOTO, H., BABA, A. & NAGAI, K. 2003. Changes in light-induced phase shift of circadian rhythm in mice lacking PACAP. *Biochemical and Biophysical Research Communications,* 310**,** 169-175.

KIM, K. S., LEE, K. W., IM, J. Y., YOO, J. Y., KIM, S. W., LEE, J. K., NESTLER, E. J. & HAN, P. L. 2006. Adenylyl cyclase type 5 (AC5) is an essential mediator of morphine action. *Proceedings of the National Academy of Sciences of the United States of America,* 103**,** 3908-3913.

KRISHNAN, V., GRAHAM, A., MAZEI-ROBISON, M. S., LAGACE, D. C., KIM, K.-S., BIRNBAUM, S., EISCH, A. J., HAN, P.-L., STORM, D. R., ZACHARIOU, V. & NESTLER, E. J. 2008. Calcium-sensitive adenylyl cyclases in depression and anxiety: Behavioral and biochemical consequences of isoform targeting. *Biological Psychiatry,* 64**,** 336-343.

LANGER, I. 2012. Mechanisms involved in VPAC receptors activation and regulation: lessons from pharmacological and mutagenesis studies.: *Frontiers in endocrinology*, 3, 129.

LEWIS, A. S. & CHETKOVICH, D. M. 2011. HCN channels in behavior and neurological disease: Too hyper or not active enough? *Molecular and Cellular Neuroscience,* 46**,** 357-367.

LOCHNER, A. & MOOLMAN, J. A. 2006. The many faces of H89: A review. *Cardiovascular Drug Reviews,* 24**,** 261-274.

MANN, L., HELDMAN, E., BERSUDSKY, Y., VATNER, S. F., ISHIKAWA, Y., ALMOG, O., BELMAKER, R. H. & AGAM, G. 2009. Inhibition of specific adenylyl cyclase isoforms by lithium and carbamazepine, but not valproate, may be related to their antidepressant effect. *Bipolar Disorders,* 11**,** 885-896.

MANN, L., HELDMAN, E., SHALTIEL, G., BELMAKER, R. H. & AGAM, G. 2008. Lithium preferentially inhibits adenylyl cyclase V and VII isoforms. *International Journal of Neuropsychopharmacology,* 11**,** 533-539.

MOHAMADIAN, S., GOLALIPOUR, M., YAZDANI, Y., FARAZMANDFAR, T., TABARRAEI, A. & SHAHBAZI, M. 2017. Oscillation in expression of Adenylyl Cyclase isoforms: new insight to regulation of molecular clock. *Biological Rhythm Research,* 48**,** 113-119.

MORK, A. & GEISLER, A. 1987. Effects of lithium on calmodulin-stimulated adenylate-cyclase activity in cortical membranes from rat-brain. *Pharmacology & Toxicology,* 60**,** 17-23.

MUHLEISEN, T. W., LEBER, M., SCHULZE, T. G., STROHMAIER, J., DEGENHARDT, F., TREUTLEIN, J., MATTHEISEN, M., FORSTNER, A. J., SCHUMACHER, J., BREUER, R., MEIER, S., HERMS, S., HOFFMANN, P., LACOUR, A., WITT, S. H., REIF, A., MULLER-MYHSOK, B., LUCAE, S., MAIER, W., SCHWARZ, M., VEDDER, H., KAMMERER-CIERNIOCH, J., PFENNIG, A., BAUER, M., HAUTZINGER, M., MOEBUS, S., PRIEBE, L., CZERSKI, P. M., HAUSER, J., LISSOWSKA, J., SZESZENIA-DABROWSKA, N., BRENNAN, P., MCKAY, J. D., WRIGHT, A., MITCHELL, P. B., FULLERTON, J. M., SCHOFIELD, P. R., MONTGOMERY, G. W., MEDLAND, S. E., GORDON, S. D., MARTIN, N. G., KRASNOW, V., CHUCHALIN, A., BABADJANOVA, G., PANTELEJEVA, G., ABRAMOVA, L. I., TIGANOV, A. S., POLONIKOV, A., KHUSNUTDINOVA, E., ALDA, M., GROF, P., ROULEAU, G. A., TURECKI, G., LAPRISE, C., RIVAS, F., MAYORAL, F., KOGEVINAS, M., GRIGOROIU-SERBANESCU, M., PROPPING, P., BECKER, T., RIETSCHEL, M., NOTHEN, M. M. & CICHON, S. 2014. Genome-wide association study reveals two new risk loci for bipolar disorder. *Nature Communications,* 5**,** 3339.

NARASIMAMURTHY, R., HATORI, M., NAYAK, S. K., LIU, F., PANDA, S. & VERMA, I. M. 2012. Circadian clock protein cryptochrome regulates the expression of proinflammatory cytokines. *Proceedings of the National Academy of Sciences of the United States of America,* 109**,** 12662-12667.

NEWMAN, M., KLEIN, E., BIRMAHER, B., FEINSOD, M. & BELMAKER, R. H. 1983. Lithium at therapeutic concentrations inhibits human-brain noradrenaline-sensitive cyclic-AMP accumulation. *Brain Research,* 278**,** 380-381.

O'NEILL, J. S., MAYWOOD, E. S., CHESHAM, J. E., TAKAHASHI, J. S. & HASTINGS, M. H. 2008. cAMP-dependent signaling as a core component of the mammalian circadian pacemaker. *Science,* 320**,** 949-953.

OBRIETAN, K., IMPEY, S., SMITH, D., ATHOS, J. & STORM, D. R. 1999. Circadian regulation of cAMP response element-mediated gene expression in the Suprachiasmatic nuclei. *Journal of Biological Chemistry,* 274**,** 17748-17756.

PALMER, G. C., JONES, D. J., MEDINA, M. A. & STAVINOHA, W. B. 1979. Anticonvulsant drug actions on in vitro and in vivo levels of cyclic-AMP in the mouse-brain. *Epilepsia,* 20**,** 95-104.

PAVAN, B., FRIGATO, E., POZZATI, S., PRASAD, P. D., BERTOLUCCI, C. & BIONDI, C. 2006. Circadian clocks regulate adenylyl cyclase activity rhythms in human RPE cells. *Biochemical and Biophysical Research Communications,* 350**,** 169-173.

PICAUD, S., FEDOROV, O., THANASOPOULOU, A., LEONARDS, K., JONES, K., MEIER, J., OLZSCHA, H., MONTEIRO, O., MARTIN, S., PHILPOTT, M., TUMBER, A., FILIPPAKOPOULOS, P., YAPP, C., WELLS, C., CHE, K. H., BANNISTER, A., ROBSON, S., KUMAR, U., PARR, N., LEE, K., LUGO, D., JEFFREY, P., TAYLOR, S., VECELLIO, M. L., BOUNTRA, C., BRENNAN, P. E., O'MAHONY, A., VELICHKO, S., MUELLER, S., HAY, D., DANIELS, D. L., URH, M., LA THANGUE, N. B., KOUZARIDES, T., PRINJHA, R., SCHWALLER, J. & KNAPP, S. 2015. Generation of a Selective Small Molecule Inhibitor of the CBP/p300 Bromodomain for Leukemia Therapy. *Cancer Research,* 75**,** 5106-5119.

PIERRE, S., ESCHENHAGEN, T., GEISSLINGER, G. & SCHOLICH, K. 2009. Capturing adenylyl cyclases as potential drug targets. *Nature Reviews Drug Discovery,* 8**,** 321-335.

RAHMAN, S., LI, P. P., YOUNG, L. T., KOFMAN, O., KISH, S. J. & WARSH, J. J. 1997. Reduced H-3 cyclic AMP binding in postmortem brain from subjects with bipolar affective disorder. *Journal of Neurochemistry,* 68**,** 297-304.

RALL, T. W. & SUTHERLAND, E. W. 1958. Formation of a cyclic adenine ribonucleotide by tissue particles. *Journal of Biological Chemistry,* 232**,** 1065-1076.

REN, X. G., RIZAVI, H. S., KHAN, M. A., BHAUMIK, R., DWIVEDI, Y. & PANDEY, G. N. 2014. Alteration of cyclic-AMP response element binding protein in the postmortem brain of subjects with bipolar disorder and schizophrenia. *Journal of Affective Disorders,* 152**,** 326-333.

REPPERT, S. M. & WEAVER, D. R. 2002. Coordination of circadian timing in mammals. *Nature,* 418**,** 935-941.

SADANA, R. & DESSAUER, C. W. 2009. Physiological Roles for G Protein-Regulated Adenylyl Cyclase Isoforms: Insights from Knockout and Overexpression Studies. *Neurosignals,* 17**,** 5-22.

SANABRA, C. & MENGOD, G. 2011. Neuroanatomical distribution and neurochemical characterization of cells expressing adenylyl cyclase isoforms in mouse and rat brain. *Journal of Chemical Neuroanatomy,* 41**,** 43-54.

SEIFERT, R. 2014. Vidarabine is neither a potent nor a selective AC5 inhibitor. *Biochemical Pharmacology,* 87**,** 543-546.

SHEARMAN, L. P., ZYLKA, M. J., WEAVER, D. R., KOLAKOWSKI, L. F. & REPPERT, S. M. 1997. Two period homologs: Circadian expression and photic regulation in the suprachiasmatic nuclei. *Neuron,* 19**,** 1261-1269.

SHIMIZU, K., KOBAYASHI, Y., NAKATSUJI, E., YAMAZAKI, M., SHIMBA, S., SAKIMURA, K. & FUKADA, Y. 2016. SCOP/PHLPP1 beta mediates circadian regulation of long-term recognition memory. *Nature Communications,* 7**,** 12926.

SU, Y., DOSTMANN, W. R. G., HERBERG, F. W., DURICK, K., XUONG, N. H., TENEYCK, L., TAYLOR, S. S. & VARUGHESE, K. I. 1995. Regulatory subunit of protein-kinase-A - structure of deletion mutant with cAMP binding domains. *Science,* 269**,** 807-813.

SUTHERLAND, E. W. & RALL, T. W. 1958. Fractionation and characterization of a cyclic adenine ribonucleotide formed by tissue particles. *Journal of Biological Chemistry,* 232**,** 1077-1091.

TRAVNICKOVA-BENDOVA, Z., CERMAKIAN, N., REPPERT, S. M. & SASSONE-CORSI, P. 2002. Bimodal regulation of mPeriod promoters by CREB-dependent signaling and CLOCK/BMAL1 activity. *Proceedings of the National Academy of Sciences of the United States of America,* 99**,** 7728-7733.

TZAVARA, E. T., POUILLE, Y., DEFER, N. & HANOUNE, J. 1996. Diurnal variation of the adenylyl cyclase type 1 in the rat pineal gland. *Proceedings of the National Academy of Sciences of the United States of America,* 93**,** 11208-11212.

VATNER, S. F., PARK, M., YAN, L., LEE, G. J., LAI, L., IWATSUBO, K., ISHIKAWA, Y., PESSIN, J. & VATNER, D. E. 2013. Adenylyl cyclase type 5 in cardiac disease, metabolism, and aging. *American Journal of Physiology-Heart and Circulatory Physiology,* 305**,** H1-H8.

VERIN, A. D., LIU, F., BOGATCHEVA, N., BORBIEV, T., HERSHENSON, M. B., WANG, P. Y. & GARCIA, J. G. N. 2000. Role of Ras-dependent ERK activation in phorbol ester-induced endothelial cell barrier dysfunction. *American Journal of Physiology-Lung Cellular and Molecular Physiology,* 279**,** L360-L370.

VISEL, A., ALVAREZ-BOLADO, G., THALLER, C. & EICHELE, G. 2006. Comprehensive analysis of the expression patterns of the adenylate cyclase gene family in the developing and adult mouse brain. *Journal of Comparative Neurology,* 496**,** 684-697.

WONG, S. T., ATHOS, J., FIGUEROA, X. A., PINEDA, V. V., SCHAEFER, M. L., CHAVKIN, C. C., MUGLIA, L. J. & STORM, D. R. 1999. Calcium-stimulated adenylyl cyclase activity is critical for hippocampus-dependent long-term memory and late phase LTP. *Neuron,* 23**,** 787-798.

WONG, S. T., TRINH, K., HACKER, B., CHAN, G. C. K., LOWE, G., GAGGAR, A., XIA, Z. G., GOLD, G. H. & STORM, D. R. 2000. Disruption of the type III adenylyl cyclase gene leads to peripheral and behavioral anosmia in transgenic mice. *Neuron,* 27**,** 487-497.

WONG, W. & SCOTT, J. D. 2004. AKAP signalling complexes: Focal points in space and time. *Nature Reviews Molecular Cell Biology,* 5**,** 959-970.

XUE, W., WANG, W., GONG, T., ZHANG, H., TAO, W., XUE, L., SUN, Y., WANG, F. & CHEN, G. 2016. PKA-CREB-BDNF signaling regulated long lasting antidepressant activities of Yueju but not ketamine. *Scientific Reports,* 6**,** 26331.

YAN, L., VATNER, D. E., O'CONNOR, J. P., IVESSA, A., GE, H., CHEN, W., HIROTANI, S., ISHIKAWA, Y., SADOSHIMA, J. & VATNER, S. F. 2007. Type 5 adenylyl cyclase disruption increases longevity and protects against stress. *Cell,* 130**,** 247-258.

Chapter 7: General Discussion

7. General Discussion

7.1 The Broad View of Bipolar Disorder

The overall aims of this DPhil thesis were to gain a deeper understanding of the mechanistic basis of circadian dysfunctions and the role of chronomodulatory drugs in BPD. This chronic neuropsychiatric disorder greatly impairs quality of life and effects 1-2% of the population worldwide, totalling approximately 70-140million people (Merikangas et al., 2011). As most patients require long-term care plans, the economic burden associated is substantial, highlighting the need to further research and identify the causal neurobiology of BPD (Young et al., 2011).

Lithium has proven effective at reducing suicidality and stabilising symptoms of both mania and depression, rendering it a true mood-stabiliser (Cipriani et al., 2013, Severus et al., 2014). Aside from the knowledge built from understanding lithium's polypharmacological actions, very little is known about the fundamental pathophysiology of BPD. Therefore, treatment options rarely target the underlying issues, but normalise the overt behavioural abnormalities. As a further consequence, BPD has been difficult to accurately model *in vitro*, thereby slowing down drug discovery efforts. There is now a wealth of evidence outlining the intimate association between sleep and circadian rhythm disruptions in neuropsychiatric disorders, including BPD (Jagannath et al., 2013). Given the overlapping nature of these systems, pharmacologically targeting circadian disruptions may provide an alternative means for stabilising mood as a novel treatment paradigm.

7.2 The Major Investigative Outcomes

Fibroblasts from well characterised patients suffering from BPD were cultured to assess *Bmal* and *Per2* periodicity using the largest number of patients to date. The patient's cells exhibited variability beyond the known influences of chronotype, suggesting the presence of additional unidentified disease traits. These patient-derived fibroblasts were found to be accurate *in vitro* models of lithium responses, presenting the known period lengthening and amplitude enhancing effects. Further, the additional compounds nobiletin and CGS-15943 modulated these circadian parameters *in vitro* and in wheel-running behavioural assays in wild-type mice. Thus, the fibroblasts accurately modelled *in vivo* drug responses, making them a valuable model for future drug discovery efforts. Furthermore, the observation that these structurally unrelated molecules, that act on distinctly different targets, exhibit common behavioural and chronomodulatory traits to lithium provides foundational evidence suggesting that pharmacological modulation of circadian rhythms may influence mood-related behaviours. The use of *Bmal::Luc* MMHD3 cells then revealed that lithium-induced perturbations of IMPase may be the mechanism via which period lengthening occurs. Finally, pharmacological inhibition of AC-CREB signalling induces period lengthening and could be an interesting route to explore novel mood modulating compounds.

7.3 Fibroblasts as Peripheral Clocks

Using healthy human samples it has previously been shown that fibroblasts contain an internal molecular clock and express rhythmic patterns of many genes including the core clock genes *PER2* and *BMAL* (Yang et al., 2009).

Indeed, mRNA analysis assessing rhythmicity in BPD patient fibroblasts have displayed amplitude dampening and luminometric studies found lengthening in *Per2* with similar trends identified for *Bmal* rhythms (Yang et al., 2009, McCarthy et al., 2013, Bamne et al., 2013). However, given the heterogeneity of BPD a broader characterisation of patient rhythmicity with known specific disease characteristics, such as lithium sensitivity has not been assessed. As examined in Chapter 3, all patient-derived cell lines displayed rhythmic *Bmal* or *Per2* oscillations, although with large inter-individual variability of up to 6h. Previous studies assessing healthy fibroblasts along with our healthy subject-derived cells exhibited variability by up to 4h (Brown et al., 2005, Brown et al., 2008). Thus, in addition to the variability resulting from the genetically pre-determined period lengths, patient cells exhibited additional, possibly disease-related variability. Using a larger number of patients, an intriguing experimental investigation would include identifying whether the degree of impairment to quality of life, societal problems, or specific compounds consumed by patients, could induce long-term genetic changes and account for this variability.

7.3.1 Fibroblasts in comparison to the SCN model

In order to be a valid and practical model of circadian rhythmicity, fibroblasts must display oscillatory patterns that would represent the activity of the SCN in that individual. Whilst in rodent studies, wheel-running activity is the most overt and accurate representation of the SCN, for obvious reasons, such experiments cannot be performed on humans with ease. Therefore, as discussed in Chapter 3, in healthy humans, endogenous rhythmicity has been assessed through behavioural questionnaire analysis or physiological melatonin assays

(Brown et al., 2008, Pagani et al., 2010). In line with previous human physiological findings, the average fibroblast period was also close to 24.5h in multiple studies, as summarised in Chapter 3, *Table 3.1* (Czeisler et al., 1999). Our healthy fibroblasts revealed an average endogenous period slightly shorter at 24.03±0.20 for *Bmal* and 23.48±0.27 for *Per2*. However, as luminescence studies have also found control cells to contain an average period which deviates from 24.5h by 1h, and as the half life of luciferase could differ from gene to gene, this is within the acceptable range of variability (Chapter 3, *Table 3.1*). Furthermore, our fibroblasts displayed ~24h oscillations lasting multiple days, in line with other *ex vivo* neural and non-neural tissues (Yoo et al., 2004, Guilding et al., 2010). However, as well as others, we have shown in Chapter 5 that *ex vivo* preparations of the SCN from PER2::LUC mice can oscillate for over a week, where the fibroblasts show rapid rates of dampening within 4 days (Yoo et al., 2004). This therefore limits their use in understanding long-term rhythmicity but does not impact their use as an alternative means for screening biochemical compounds, assays which require ~4 days. Moreover, it should be appreciated that fibroblasts do not mimic the SCN as they lack the fundamental SCN network properties and homeostatic feedback mechanisms. The fibroblasts do however provide strong indications regarding the state of the master molecular clock, although cellular rhythmic changes are amplified relative to behavioural patterns, an effect we and others have observed (Brown et al., 2005).

The number of viral integrations per fibroblast dictated amplitude in our circadian assays. Therefore, basal amplitude could not be accurately assessed in our cell lines. Phase also cannot be assessed accurately using plate reader based

assays as typically plates are read every 30min-1h. Therefore, within this timeframe phase within replicates would exhibit variability. Period on the other hand is independent of these factors and was therefore our primary parameter of interest. Indeed, trends for lengthening were apparent in our cell lines in accordance with previous molecular assays (Chapter 3, *Table 3.1*) and animal models of mania-like behaviour. For example, the *Clock*Δ19, *Afh,* and *Myshkin* mice all exhibited behavioural abnormalities akin to human mania and display period lengthening by 1-3h (King et al., 1997, Godinho et al., 2007, Timothy et al., 2017). Hence fibroblasts show strong correlations to circadian rhythmicity present within the master clock. They may therefore also provide indications of the circadian disturbances associated with BPD and may prove to be a more practical model of: 1) understanding the circadian rhythms of patients and 2) understanding drug-induced perturbations to rhythmicity and their mechanisms of action.

7.3.2 The 3R's objective

It is widely appreciated that animal models do not recapitulate all aspects of a disorder, but modelling neuropsychiatric disorders adds a further layer of complexity. In doing so one is trying to model seemingly unique human behaviours. Whilst behaviour is used as a reasonable correlate, its interpretations must be assessed with caution, as animal models have not proved to be the best system for evaluating drug outcomes. Decades of research requiring investment in the billions has culminated in limited mechanistically novel neuropsychiatric drugs (Fibiger, 2012). As such the development of novel therapeutics by pharmaceutical companies has declined, suggesting that a

greater push for translational research is required from an academic perspective.

Immortalised cell lines are frequently used to understand basic biology as well as pathophysiology. Problems arise in translational efforts as such cells do not accurately model the true phenomena. The U2OS cell line for example is frequently used as a cellular model of the molecular clock (Hoffmann et al., 2014). However, this non-neuronal model posses multiple chromosomal aberrations and, as such, does not serve as an accurate model for this disease. As discussed in Chapter 5, the U2OS cell line did not present any period changes following the application of LiCl, a well-validated drug effect, underscoring its limited applicability as a BPD model.

Whilst screening compounds for the identification of novel clock modulators has been performed on U2OS cells (Vasudevan Lab*, unpublished*), use of our patient-derived fibroblasts have several advantages above animal models and immortalised cell lines. It is known that at the time of cell division, fibroblasts pass on circadian timing to daughter cells, thus making them a valid and sensible tool to research patient clocks (Nagoshi et al., 2004). The further benefits of fibroblasts are that they provide a biological representation of the human genetic makeup, which could therefore help identify patient-relevant pharmacological treatments in the future. Furthermore, unlike previous studies, the patients from whom our fibroblasts originated were extensively evaluated such that each cell line is accompanied by a wealth of phenotypic information. Thus, along with our analysis of cell line specific basal circadian period, drug-induced amplitude and period changes are also available for future investigative

use. This makes such a model appealing as all 39 fibroblast lines could be utilised, or certain cell lines could be selected based on the research needs of the investigator.

This DPhil was funded by the NC3Rs, where one of the research goals was to identify a novel cellular model of BPD and validate whether fibroblasts could replace animal models in the early stages of drug discovery. We found correlations between *in vitro* and *in vivo* drug-induced circadian changes (Chapter 4). Therefore, this model could provide a valid insight into abnormalities in rhythmicity associated with BPD and could further deliver a means of high throughput screening for novel clock modulators, in addition to acting as a valuable tool for the BPD research community as a whole.

7.4 How Chronomodulation can Lead to Mood Modulation

Our current understanding of circadian rhythms and mood led to the model depicted in Chapter 1, *Figure 1.3A*. The model suggests that a dysfunctional clock causes escalating impairments as: 1) sleep is disrupted, 2) mood systems are disrupted, 3) sleep issues negatively impacts mood, and 4) mood disturbances negatively impact sleep (Jagannath et al., 2013). This bidirectional augmentation of pathophysiological states is so profound that sleep disruptions are frequently observed and included in the BPD diagnosis criteria (American Psychiatric Association, 2013, World Health Organisation, 2014).

As highlighted in Chapter 4, we found that the novel chronomodulatory drugs nobiletin and CGS-15943 also reduced rearing and anxiety-related behaviours, where light acts as an aversive stimulus. This provided preliminary

evidence to suggest that drugs that modulate circadian rhythms may impact behaviour. Evidence from previous investigations also suggest this may be the case, where key examples include the fact that the melatonergic agonist agomelatine, bright light therapy, or scheduled routines of sleep could normalise extreme behavioural irregularities such as depression, mania, and delusions, whilst synergistically improving sleep quality (Olie and Kasper, 2007, Rosenthal et al., 1984, Myers et al., 2011, Barbini et al., 2005). Of the mechanisms via which the circadian system can impact mood in BPD, the role of ipRGCs, the HPA axis, neurotransmitter systems, and receptor-coupled signalling pathways show potential as future therapeutic targets.

7.4.1 Neurotransmitter systems

The circadian regulation of neurotransmitter systems could denote where mood and circadian systems overlap. Indeed, synthesis and metabolism enzymes such as *Maoa* exhibit rhythmic expression patterns, where *Per2* mutant mice display reduced *Maoa* expression with increased dopamine levels in key dopaminergic limbic regions, thus highlighting the role of the clock in controlling neurotransmitter functions (Hampp et al., 2008). Additionally, a subset of BPD patients are known to present exacerbated behavioural abnormalities in altered light environments, either naturally due to photoperiodic changes associated with summer and winter, or artificially via transmeridian travel (Akhter et al., 2013, Inder et al., 2016). In line with this, Dulcis and colleagues found that under winter-like days, mice displayed reduced anxiety, behaviour that correlated with elevated *Th* and dopamine levels. Moreover, the increases in dopamine were correlated with reduced somatostatin, thus neurones of the adult rat brain were

changing transmitter expression following exposure to different photoperiods (Dulcis et al., 2013). Therefore, a malfunctional circadian system could impair this switch, exacerbating dopamine neurotransmission in the summer, when mania is high, with diminished expression during the winter months when depression is more prominent.

To take this one step further, this suggests that pharmacological modulation of circadian rhythms modulates neurotransmitter expression. Indeed, 56% of the top selling drugs in the USA impact targets with circadian oscillatory patterns, including aripiprazole and quetiapine, both of which are prescribed for BPD. The overlapping transcripts that were being modulated included the 5-HT and dopamine receptor isoforms (Zhang et al., 2014). This could suggest that pharmacologically modulating the molecular clock directly would restore the functioning of all its outputs, including neurotransmission systems, each of which can then trigger their own receptor-coupled signalling pathways, emphasising the potentially pleiotropic benefits of correcting the circadian clock.

As highlighted in Chapter 4, LiCl, nobiletin, and CGS-15943 impacted behaviour and circadian rhythms. Lithium modulates multiple neurotransmitter systems including dopamine and 5-HT (Can et al., 2014). Tangeritin, an alternative polymethoxylated flavone, induces chronomodulatory effects akin to nobiletin in mouse embryonic fibroblasts and elevated 5-HT and dopamine expression in multiple brain regions (Shinozaki et al., 2017, Lee et al., 2018). Similarly, chronic caffeine consumption is known to increase brain 5-HT levels

(Berkowitz and Spector, 1971). Therefore, it would be interesting to explore the effects of our compounds on brain dopamine and 5-HT expression.

7.4.2 Receptor-coupled signalling pathways

One approach employed to investigate the pathophysiology of BPD has stemmed from trying to comprehend how lithium is so effective at stabilising mood. Thus, two-major receptor coupled systems which have been highly investigated include the PI and the AC signalling pathways. Indeed, lithium, the gold standard mood-stabiliser, also lengthens period and amplitude (Li et al., 2012). As well as validating these findings using our patient-derived cells, this investigation uncovered in Chapters 5 and 6, that modulation of both these pathways can induce changes to circadian rhythmicity. It would therefore be interesting to assess whether nobiletin and CGS-15943 indirectly target IMPase or AC as part of their extended mechanisms of action.

Whilst the dominant mechanism via which lithium induces period lengthening and modulation of rearing behaviours is likely via IMPase, cAMP may be the common overlapping target between the 3 compounds assessed (Singh et al., 2013). Nobiletin has been shown to inhibit phosphodiesterase activity and thereby augment cAMP-PKA signalling in models of Alzheimer's disease, where the author's believed the ultimate target was ERK. As outlined in Chapter 6, our findings suggest that modulation of ERK does not modulate period, although amplitude effects were becoming apparent and augmentation of ERK has also been identified with lithium, potentially due to PKA influencing both the AC and MAPK pathways (Yan et al., 2007). Furthermore, CGS-15943 is a potent non-specific adenosine receptor antagonist, where the G_i coupled A_1

subtype is dominant within the SCN (Jagannath et al., *manuscript in preparation*). Therefore, much like lithium, it is likely that CGS-15943 reduces cAMP-PKA-CREB signalling, and indeed this is what has been found (Jagannath et al., *manuscript in preparation*). Pharmacologically increasing or reducing cAMP both impact circadian rhythms by inducing amplitude dampening on SCN explants (Aton et al., 2006, O'Neill et al., 2008). This suggests that augmentation or inhibition of the cAMP signalling pathway may induce pleiotropic effects that impact mood. In light of the evidence suggesting that cAMP signalling shows potential mechanistic similarities between our novel chronomodulators, this signalling pathway as well as others may be implicated in the overlap between such regulatory systems and may prove vital in the search for future mood-stabilising therapeutics.

7.5 The Mechanistic Pathways of Lithium-Induced Period Lengthening

7.5.1 Pre-hepatocytes in comparison to the SCN as model system

The cellular MMHD3 model was derived from liver explants of 3-day-old transgenic mice. This model expresses constitutively active cyto-Met, a human hepatocyte growth factor receptor which reduces the cells apoptotic abilities, introduces immortalisation characteristics, but does not form tumours like typical cancer cell lines. The cells are in their untransformed pre-hepatocyte form and can be differentiated, making them a prominent model for analysing hepatocellular functions (Bellovino et al., 1999). It has previously been shown that the liver exhibits robust expression of many clock genes, where up to 16% of the protein coding transcriptome also presents 24h oscillatory patterns (Atwood et al., 2011, Ramanathan et al., 2014, Zhang et al., 2014). The presence

of these functional cell-autonomous clocks therefore makes the liver, and specifically the MMHD3 cells an excellent model to study rhythmic processes.

Much like our fibroblasts, in order for the model to be applicable and insightful, it must behave in a comparable manner to the SCN. Although the MMHD3 cells lack important SCN coupling mechanisms, network properties, and homeostatic feedback mechanisms, similarities following perturbation to the molecular clock *in vivo* have been observed. Much like knockout mice, Ramanathan and colleagues found that in the MMHD3 cells, *Bmal1* knockdown resulted in arrythmicity, *Bmal2* knockdown had no effect, *Cry1* knockdown dampened amplitude, and *Cry2* knockdown induced a longer period (Ramanathan et al., 2014). Furthermore, as outlined in Chapter 5, unlike the cancerous U2OS cell line, the MMHD3 cells presented dose-dependent chronomodulatory changes in response to LiCl, in line with lithium's *in vivo* effects (Li et al., 2012, Kripke and Wyborney, 1980, Welsh and Mooreede, 1990, Johnsson et al., 1979). Therefore, not only has the circadian phenotype of the MMHD3 cells been explored but changes to the molecular clock also translate with *in vivo* rhythmicity, suggesting they may be an ideal model to study the mechanisms behind pharmacological drug targets. Indeed, the use of such cells allowed us to suggest that the PI system could be responsible for lithium-induced period lengthening.

7.5.2 Lithium concentration in vitro and in vivo

It should be appreciated that lithium has a narrow therapeutic index, ranging between 0.6-1.5mM, with lithium toxicity associated with higher concentrations (Timmer and Sands, 1999). Whilst period lengthening and

amplitude enhancement are observed *in vivo* within this therapeutic range, use of models other than whole animals requires higher concentrations. Interestingly, the pattern emerging suggests that the further we move away from the *in vivo* model systems, the higher the concentration required to induce the same effect, a pattern we and others have observed. For example, Li et al., found that use of SCN explant tissues required the addition of 2mM LiCl to induce a 1h period change. However to see a ~45min change using peripheral explants, 5mM LiCl was required, and taken one step further 20mM LiCl was required to see a 1h change in cultured fibroblasts (Li et al., 2012). As displayed in Chapter 4 and 5, we also found that period was lengthened by ~2h with 4mM LiCl on SCN explants, whereas 20mM concentrations and higher were required to observe significant lengthening by 2.5h or more in culture cell lines.

Whilst the causes of this have not been explored, one possibility could be associated with differences in the basal activity of signalling cascades with different model systems. Many receptors display constitutive, low level activity independent of ligand binding, actions that are believed to enable rapid responses upon stimulation, inverse agonism, and cell survival (Khilnani and Khilnani, 2011). For example, it is known that the PI cycle is constitutively active within the brain, suggesting that the basal turnover may be lower in the MMHD3 cells and thus higher concentrations are required to induce circadian changes (Li et al., 1993). Indeed, differences in pharmacological responses have been observed when receptor-coupled signalling cascades were stimulated or assessed at basal levels (Niepel et al., 2013). Given that lithium is an uncompetitive inhibitor of IMPase, it appears sensible to hypothesise that

greater inhibition would be observed when a pathway is more active and thus a lower concentration of lithium would be required to deplete myo-inositol and induce period lengthening. Consequently, one possible factor implicated in the variability in drug doses could be overcome by assessing compounds on overstimulated networks, a hypothesis for future investigations to consider.

Alternatively, it may simply be that lithium displays variable rates of accumulation, retention, and efflux in different cells and tissues, and therefore varying extracellular concentrations are needed to maintain the required intracellular concentrations. Indeed, lithium has been shown to display varying concentrations in different tissues and different regions of the brain. For example, lithium shows high rates of accumulation in the bones, muscle, and large intestine, followed by the brain and kidneys (Ebadi, 1974, Edelfors, 1975). Interestingly, the bones contained triple the concentration of lithium relative to the liver, where our ICP-MS study in Chapter 5, *Figure 5.17* supported these findings. When looking at the MMHD3 cells, the addition of 30mM LiCl resulted in 100ng of intracellular lithium in $4x10^5$ cells, a concentration which equates to approximately 2.2mM. Therefore, as well as displaying tissue-to-tissue variability, the intracellular concentrations required to see a chronomodulatory effect may not be as high as the extracellular concentrations.

7.5.3 IMPase over adenylate cyclase

Initially, we set out to explore whether IMPase or AC was primarily responsible for lithium-induced period lengthening. As outlined in Chapter 5, our investigations led us to believe that IMPase was the principal target through which these effects were occurring, as targeted inositol depletion induced the

actions of C/EBPα, a transcription factor capable of increasing *Per2* gene transcription and reducing *Rev-erbα,* thereby indirectly elevating *Bmal* expression. We went on to demonstrate that lithium inhibited AC at concentrations where period lengthening occurred, and that specific inhibition of the AC-cAMP-PKA-CREB pathway also induced period lengthening (Chapter 6). This led us to believe that AC plays a contributory but subordinate role in mediating these effects in the MMHD3 cells. The reasons for this are multi-fold. Firstly, we had established in Chapter 5 that a great portion of lithium's period lengthening effects occur due to specific IMPase inhibition. Further, the MMHD3 cells were the preferred cell line over the U2OS cells, as the U2OS cells did not induce any significant period lengthening upon application of LiCl. However, the U2OS cells still displayed dose-dependent cAMP and CREB reductions, in a similar manner to the MMHD3 cells following pharmacological inhibition. Thus, the AC pathway is unaltered and fully functional in the U2OS cells. Therefore, if this was the dominant target via which lithium induced period lengthening, then lengthening should have been observed in the U2OS cells. This suggests that AC signalling may stimulate period lengthening, but this is not the main pathway via which lithium induces such effects, as the true period lengthening target should be absent or muted in the U2OS cells. Indeed, IMPA1 expression was found to be considerably lower in the U2OS cells over the MMHD3 cells, further suggesting that IMPase may be the more dominant target.

7.6 Future Research Directions

Our data suggests that targeting the circadian system may be a viable alternative solution in the treatment of BPD. As our fibroblasts presented

differences in drug responses based on phenotypic period length, pending future drug evaluations, this could act as a potential biomarker in identifying responders to mood-stabilising mediations. Such technology could be pivotal in rapidly identifying the correct pharmacological treatments for patients by minimising the currently implemented 'trial-and-error' targeted approach for prescribing medications. Moreover, having shown that chronomodulation can influence mood, narrowing down the target to IMPase and C/EBPα for example could help in the search for future lithium mimetics, drugs which induce mood stabilisation without undesirable side effects attached. This would also reduce issues with covert non-compliance and thereby improve overall patient care.

Additionally, given the knowledge that a subset of our patient fibroblasts did not respond to lithium with the expected chronomodulatory changes, it would be interesting to assess whether any differences are observable in their PI, AC, or GSK3β signalling components. For example, we could explore the impact of pharmacologically manipulating various targets in our patient cell lines to assess their roles in chronomodulation. Indeed, further studies overexpressing C/EBPα in the MMHD3 and U2OS cells could help elucidate lithium's mechanism of action. This could help understand differences in drug responses within our patient cell lines and may ultimately lead to more tailored and beneficial patient treatments in the future.

Further, as we found that patient-derived fibroblasts display similarities to *in vivo* chronomodulation, this could encourage other investigators to adopt our model for their research purposes, thus replacing and reducing the use of animals in BPD research. Such cells do not need to be limited to their use in

circadian assays, as previous studies have used patient cells to understand variations in gene and protein expression, and signalling pathways. Therefore, their increased translatability as well as the accompaniment of demographic and circadian characteristics make them an attractive model for future studies.

Given that sleep and circadian rhythm disruptions are common to neuropsychiatric disorders, our finding suggest that this cellular model could be translated to further understanding major depressive disorder, schizophrenia, and anxiety disorders to name a few (Wulff et al., 2010). This could help further achieve the 3R's aims, whilst providing researchers with more relevant human models which may help to identify more efficacious drugs in the future.

7.7 Final Overviews

Returning to the original aims we set out to investigate, the work presented contributes several novel findings to both the fields of circadian neurobiology and BPD research. We were one of the first groups that set out to try to understand whether circadian differences are apparent between Li-T and Li-NT patients, and in doing so identified chronomodulatory differences. We proceeded to demonstrate that patient-derived fibroblasts display similar drug-induced chronomodulatory changes to those observed *in vivo*, providing evidence that these cells can act as valuable models in future drug discovery programmes, whilst achieving the 3R's ambition of using fewer animals. Our *in vivo* experiments additionally provide preliminary evidence suggesting that pharmacological modulation of circadian rhythms may modulate mood-related behaviours. Following further validation, this could introduce a paradigmatic shift in the future treatment of BPD, transforming the importance that is placed

on circadian rhythms in neuropsychiatry. Furthermore, investigations into the mechanisms behind lithium-induced period lengthening led us to understand that pharmacological augmentation of C/EBP via the inhibition of IMPase is the predominant target through which lithium may induce period changes. Indeed, inhibition of AC also induced period lengthening, making both signalling pathways attractive targets for the discovery of novel chronomodulatory compounds. Overall, our work provides original insights into the use of disease relevant cellular models, as well as the signalling pathways associated with circadian neurobiology and neuropsychiatric disorders, which pave the way for future research into identifying mechanistically novel mood-stabilising agents.

7.8 References

AKHTER, A., FIEDOROWICZ, J. G., ZHANG, T., POTASH, J. B., CAVANAUGH, J., SOLOMON, D. A. & CORYELL, W. H. 2013. Seasonal variation of manic and depressive symptoms in bipolar disorder. *Bipolar Disorders,* 15**,** 377-384.

AMERICAN PSYCHIATRIC ASSOCIATION 2013. *Diagnostics and Statisitcal Manual of Mental Disorders (DSM) 5th edition,* Washington.

ATON, S. J., HUETTNER, J. E., STRAUME, M. & HERZOG, E. D. 2006. GABA and G(i/o) differentially control circadian rhythms and synchrony in clock neurons. *Proceedings of the National Academy of Sciences of the United States of America,* 103**,** 19188-19193.

ATWOOD, A., DECONDE, R., WANG, S. S., MOCKLER, T. C., SABIR, J. S. M., IDEKER, T. & KAY, S. A. 2011. Cell-autonomous circadian clock of hepatocytes drives rhythms in transcription and polyamine synthesis. *Proceedings of the National Academy of Sciences of the United States of America,* 108**,** 18560-18565.

BAMNE, M. N., PONDER, C. A., WOOD, J. A., MANSOUR, H., FRANK, E., KUPFER, D. J., YOUNG, M. W. & NIMGAONKAR, V. L. 2013. Application of an ex vivo cellular model of circadian variation for bipolar disorder research: a proof of concept study. *Bipolar Disorders,* 15**,** 694-700.

BARBINI, B., BENEDETTI, F., COLOMBO, C., DOTOLI, D., BERNASCONI, A., CIGALA-FULGOSI, M., FLORITA, M. & SMERALDI, E. 2005. Dark therapy for mania: a pilot study. *Bipolar Disorders,* 7**,** 98-101.

BELLOVINO, D., LANYAU, Y., GARACUSO, I., AMICONE, L., CAVALLARI, C., TRIPODI, M. & GAETANI, S. 1999. MMH cells: An in vitro model for the study of retinol-binding protein secretion regulated by retinol. *Journal of Cellular Physiology,* 181**,** 24-32.

BERKOWITZ, B. A. & SPECTOR, S. 1971. Effect of caffeine and theophylline on disposition of brain serotonin in rat. *European Journal of Pharmacology,* 16**,** 322-+.

BROWN, S. A., FLEURY-OLELA, F., NAGOSHI, E., HAUSER, C., JUGE, C., MEIER, C. A., CHICHEPORTICHE, R., DAYER, J. M., ALBRECHT, U. & SCHIBLER, U. 2005. The period length of fibroblast circadian gene expression varies widely among human individuals. *Plos Biology,* 3**,** 1813-1818.

BROWN, S. A., KUNZ, D., DUMAS, A., WESTERMARK, P. O., VANSELOW, K., TILMANN-WAHNSCHAFFE, A., HERZEL, H. & KRAMER, A. 2008. Molecular insights into human daily behavior. *Proceedings of the National Academy of Sciences of the United States of America,* 105**,** 1602-1607.

CAN, A., SCHULZE, T. G. & GOULD, T. D. 2014. Molecular actions and clinical pharmacogenetics of lithium therapy. *Pharmacology Biochemistry and Behavior,* 123**,** 3-16.

CIPRIANI, A., HAWTON, K., STOCKTON, S. & GEDDES, J. R. 2013. Lithium in the prevention of suicide in mood disorders: updated systematic review and meta-analysis. *Bmj-British Medical Journal,* 346**,** f3646.

CZEISLER, C. A., DUFFY, J. F., SHANAHAN, T. L., BROWN, E. N., MITCHELL, J. F., RIMMER, D. W., RONDA, J. M., SILVA, E. J., ALLAN, J. S., EMENS, J. S., DIJK, D. J. & KRONAUER, R. E. 1999. Stability, precision, and near-24-hour period of the human circadian pacemaker. *Science,* 284**,** 2177-2181.

DULCIS, D., JAMSHIDI, P., LEUTGEB, S. & SPITZER, N. C. 2013. Neurotransmitter Switching in the Adult Brain Regulates Behavior. *Science,* 340**,** 449-453.

FIBIGER, H. C. 2012. Psychiatry, The Pharmaceutical Industry, and The Road to Better Therapeutics. *Schizophrenia Bulletin,* 38**,** 649-650.

GODINHO, S. I. H., MAYWOOD, E. S., SHAW, L., TUCCI, V., BARNARD, A. R., BUSINO, L., PAGANO, M., KENDALL, R., QUWAILID, M. M., ROMERO, M. R., O'NEILL, J., CHESHAM, J. E., BROOKER, D., LALANNE, Z., HASTINGS, M. H. & NOLAN, P. M. 2007. The after-hours mutant reveals a role for Fbxl3 in determining mammalian circadian period. *Science,* 316**,** 897-900.

GUILDING, C., HUGHES, A. T. L. & PIGGINS, H. D. 2010. Circadian oscillators in the epithalamus. *Neuroscience,* 169**,** 1630-1639.

HAMPP, G., RIPPERGER, J. A., HOUBEN, T., SCHMUTZ, I., BLEX, C., PERREAU-LENZ, S., BRUNK, I., SPANAGEL, R., AHNERT-HILGER, G., MEIJER, J. H. & ALBRECHT, U. 2008. Regulation of monoamine oxidase a by circadian-clock components implies clock influence on mood. *Current Biology,* 18**,** 678-683.

HOFFMANN, J., SYMUL, L., SHOSTAK, A., FISCHER, T., NAEF, F. & BRUNNER, M. 2014. Non-Circadian Expression Masking Clock-Driven Weak Transcription Rhythms in U2OS Cells. *Plos One,* 9**,** e102238.

INDER, M. L., CROWE, M. T. & PORTER, R. 2016. Effect of transmeridian travel and jetlag on mood disorders: Evidence and implications. *Australian and New Zealand Journal of Psychiatry,* 50**,** 220-227.

JAGANNATH, A., PEIRSON, S. N. & FOSTER, R. G. 2013. Sleep and circadian rhythm disruption in neuropsychiatric illness. *Current opinion in neurobiology,* 23**,** 888-94.

JOHNSSON, A., PFLUG, B., ENGELMANN, W. & KLEMKE, W. 1979. Effect of lithium-carbonate on circadian periodicity in humans. *Pharmakopsychiatrie Neuro-Psychopharmakologie,* 12**,** 423-425.

KHILNANI, G. & KHILNANI, A. K. 2011. Inverse agonism and its therapeutic significance. *Indian Journal of Pharmacology,* 43**,** 492-501.

KING, D. P., ZHAO, Y. L., SANGORAM, A. M., WILSBACHER, L. D., TANAKA, M., ANTOCH, M. P., STEEVES, T. D. L., VITATERNA, M. H., KORNHAUSER, J. M., LOWREY, P. L., TUREK, F. W. & TAKAHASHI, J. S. 1997. Positional cloning of the mouse circadian Clock gene. *Cell,* 89**,** 641-653.

KRIPKE, D. F. & WYBORNEY, V. G. 1980. Lithium slows rat circadian activity rhythms. *Life Sciences,* 26**,** 1319-1321.

LEE, B., SHIM, I., LEE, H. & HAHM, D. H. 2018. The polymethoxylated flavone, Tangeretin improves cognitive memory in rats experiencing a single episode of prolonged post-traumatic stress. *Animal Cells and Systems,* 22**,** 54-62.

LI, J., LU, W.-Q., BEESLEY, S., LOUDON, A. S. I. & MENG, Q.-J. 2012. Lithium Impacts on the Amplitude and Period of the Molecular Circadian Clockwork. *Plos One,* 7**,** e33292.

LI, R., WING, L. L., WYATT, R. J. & KIRCH, D. G. 1993. Effects of haloperidol, lithium, and valproate on phosphoinositide turnover in rat-brain. *Pharmacology Biochemistry and Behavior,* 46**,** 323-329.

MCCARTHY, M. J., WEI, H., MARNOY, Z., DARVISH, R. M., MCPHIE, D. L., COHEN, B. M. & WELSH, D. K. 2013. Genetic and clinical factors predict lithium's effects on PER2 gene expression rhythms in cells from bipolar disorder patients. *Translational Psychiatry,* 3**,** e318.

MERIKANGAS, K. R., JIN, R., HE, J. P., KESSLER, R. C., LEE, S., SAMPSON, N. A., VIANA, M. C., ANDRADE, L. H., HU, C. Y., KARAM, E. G., LADEA, M., MEDINA-MORA, M. E., ONO, Y., POSADA-VILLA, J., SAGAR, R., WELLS, J. E. & ZARKOV, Z. 2011. Prevalence and Correlates of Bipolar Spectrum Disorder in the World Mental Health Survey Initiative. *Archives of General Psychiatry,* 68**,** 241-251.

MYERS, E., STARTUP, H. & FREEMAN, D. 2011. Cognitive behavioural treatment of insomnia in individuals with persistent persecutory delusions: A pilot trial. *Journal of Behavior Therapy and Experimental Psychiatry,* 42**,** 330-336.

NAGOSHI, E., SAINI, C., BAUER, C., LAROCHE, T., NAEF, F. & SCHIBLER, U. 2004. Circadian gene expression in individual fibroblasts: Cell-autonomous and self-sustained oscillators pass time to daughter cells. *Cell,* 119**,** 693-705.

NIEPEL, M., HAFNER, M., PACE, E. A., CHUNG, M., CHAI, D. H., ZHOU, L. L., SCHOEBERL, B. & SORGER, P. K. 2013. Profiles of Basal and Stimulated Receptor Signaling Networks Predict Drug Response in Breast Cancer Lines. *Science Signaling,* 6**,** ra84.

O'NEILL, J. S., MAYWOOD, E. S., CHESHAM, J. E., TAKAHASHI, J. S. & HASTINGS, M. H. 2008. cAMP-dependent signaling as a core component of the mammalian circadian pacemaker. *Science,* 320**,** 949-953.

OLIE, J. P. & KASPER, S. 2007. Efficacy of agomelatine, a MT1/MT2 receptor agonist with 5-HT2C antagonistic properties, in major depressive disorder. *International Journal of Neuropsychopharmacology,* 10**,** 661-673.

PAGANI, L., SEMENOVA, E. A., MORIGGI, E., REVELL, V. L., HACK, L. M., LOCKLEY, S. W., ARENDT, J., SKENE, D. J., MEIER, F., IZAKOVIC, J., WIRZ-JUSTICE, A., CAJOCHEN, C., SERGEEVA, O. J., CHERESIZ, S. V., DANILENKO, K. V., ECKERT, A. & BROWN, S. A. 2010. The Physiological Period Length of the Human Circadian Clock In Vivo Is Directly Proportional to Period in Human Fibroblasts. *Plos One,* 5**,** e13376.

RAMANATHAN, C., XU, H. Y., KHAN, S. K., SHEN, Y., GITIS, P. J., WELSH, D. K., HOGENESCH, J. B. & LIU, A. C. 2014. Cell Type-Specific Functions of Period Genes Revealed by Novel Adipocyte and Hepatocyte Circadian Clock Models. *Plos Genetics,* 10**,** e1004244.

ROSENTHAL, N. E., SACK, D. A., GILLIN, J. C., LEWY, A. J., GOODWIN, F. K., DAVENPORT, Y., MUELLER, P. S., NEWSOME, D. A. & WEHR, T. A. 1984. Seasonal Affective-Disorder - A description of the syndrome and preliminary findings with light therapy. *Archives of General Psychiatry,* 41**,** 72-80.

SEVERUS, E., TAYLOR, M. J., SAUER, C., PFENNIG, A., RITTER, P., BAUER, M. & GEDDES, J. R. 2014. Lithium for prevention of mood episodes in bipolar disorders: systematic review and meta-analysis. *International journal of bipolar disorders* 2**,** 15.

SHINOZAKI, A., MISAWA, K., IKEDA, Y., HARAGUCHI, A., KAMAGATA, M., TAHARA, Y. & SHIBATA, S. 2017. Potent Effects of Flavonoid Nobiletin on Amplitude, Period, and Phase of the Circadian Clock Rhythm in PER2::LUCIFERASE Mouse Embryonic Fibroblasts. *Plos One,* 12**,** e0170904.

SINGH, N., HALLIDAY, A. C., THOMAS, J. M., KUZNETSOVA, O. V., BALDWIN, R., WOON, E. C. Y., ALEY, P. K., ANTONIADOU, I., SHARP, T., VASUDEVAN, S. R. & CHURCHILL, G. C. 2013. A safe lithium mimetic for bipolar disorder. *Nature Communications,* 4**,** 1332.

TIMMER, R. T. & SANDS, J. M. 1999. Lithium intoxication. *Journal of the American Society of Nephrology,* 10**,** 666-674.

TIMOTHY, J. W., KLAS, N., SANGHANI, H. R., AL-MANSOURI, T., HUGHES, A. T., KIRSHENBAUM, G. S., BRIENZA, V., BELLE, M. D., RALPH, M. R., CLAPCOTE, S. J. & PIGGINS, H. D. 2017. Circadian disruptions in the Myshkin mouse model of mania are independent of deficits in suprachiasmatic molecular clock function. *Biological psychiatry*.

WELSH, D. K. & MOOREEDE, M. C. 1990. Lithium lengthens circadian period in a diurnal primate, Saimiri-sciureus. *Biological Psychiatry,* 28**,** 117-126.

WORLD HEALTH ORGANISATION 2014. *ICD-10 classification of mental and behavioural disorders: clinical descriptions and diagnostic guidelines; 10th Revision,* Geneva.

WULFF, K., GATTI, S., WETTSTEIN, J. G. & FOSTER, R. G. 2010. Sleep and circadian rhythm disruption in psychiatric and neurodegenerative disease perspectives. *Nature Reviews Neuroscience,* 11**,** 589-+.

YAN, L., VATNER, D. E., O'CONNOR, J. P., IVESSA, A., GE, H., CHEN, W., HIROTANI, S., ISHIKAWA, Y., SADOSHIMA, J. & VATNER, S. F. 2007. Type 5 adenylyl cyclase disruption increases longevity and protects against stress. *Cell,* 130**,** 247-258.

YANG, S., VAN DONGEN, H. P. A., WANG, K., BERRETTINI, W. & BUCAN, M. 2009. Assessment of circadian function in fibroblasts of patients with bipolar disorder. *Molecular Psychiatry,* 14**,** 143-155.

YOO, S. H., YAMAZAKI, S., LOWREY, P. L., SHIMOMURA, K., KO, C. H., BUHR, E. D., SIEPKA, S. M., HONG, H. K., OH, W. J., YOO, O. J., MENAKER, M. & TAKAHASHI, J. S. 2004. PERIOD2 :: LUCIFERASE real-time reporting of circadian dynamics reveals persistent circadian oscillations in mouse peripheral tissues. *Proceedings of the National Academy of Sciences of the United States of America,* 101**,** 5339-5346.

YOUNG, A. H., RIGNEY, U., SHAW, S., EMMAS, C. & THOMPSON, J. M. 2011. Annual cost of managing bipolar disorder to the UK healthcare system. *Journal of Affective Disorders,* 133**,** 450-456.

ZHANG, R., LAHENS, N. F., BALLANCE, H. I., HUGHES, M. E. & HOGENESCH, J. B. 2014. A circadian gene expression atlas in mammals: Implications for biology and medicine. *Proceedings of the National Academy of Sciences of the United States of America,* 111**,** 16219-16224.